8612411

Shin, Joong-Ho

AN ITERATIVE TRANSFER MATRIX APPROACH TO THE KINETO-ELASTO STATIC AND DYNAMIC ANALYSES OF GENERAL PLANAR FLEXIBLE MECHANISMS

The Ohio State University PH.D. 1986

University Microfilms International 300 N. Zeeb Road, Ann Arbor, MI 48106

AN ITERATIVE TRANSFER MATRIX APPROACH
TO
THE KINETO-ELASTO STATIC AND DYNAMIC ANALYSES
OF
GENERAL PLANAR FLEXIBLE MECHANISMS

DISSERTATION

Presented in Partial Fulfillment of the Requirements for the Degree Doctor of Philosophy in the Graduate School of The Ohio State University

By

Joong-Ho Shin, B.S.M.E., M.S.M.E.

* * * * * * * *

The Ohio State University

1986

Dissertation Committee:

G. L. Kinzel

K. J. Waldron

H. R. Busby

N. Berme

Approved by

Gary L. Kinzel

Adviser

Department of Mechanical Engineering

To My Parents

ACKNOWLEDGEMENT

Many individuals and organizations have helped either directly or indirectly to the author's study; he should like to express his appreciations to some of them by name:

Adviser Dr. Gary L. Kinzel, of the Department of Mechanical Engineering, for his continued interests and helpful suggestions throughout the course of this study.

Dr. K. J. Waldron, Dr. H. R. Busby, and Dr. N. Berme, of the Department of Mechanical Engineering, for their assistances as members of the dissertation committee.

Dr. J. K. Lee, of the Department of Engineering Mechanics, for his comments and encouragements.

The Machine-Design Program Group made up of the following companies, such as Allis Chalmers, Borg Wanner, Cummins Engine, F. Jos. Lamb, Ford, General Motors, McDonnell Douglas, Pitney Bowes, Westinghouse Electric, Kodak, and ITI, in studying the graphics-oriented, interactive, computer-aided design of mechanical elements.

Okrye, his wife, Mitchell (Myungcheol), his son, and Jeanney (Myungjin), his daughter, for their patient acceptance as part-time husband and father.

His family members for their encouragements and financial help during this study.

VITA

January 17, 1953	....	Born Youngcheon, Kyungsangbuk-Do, Korea
1974	....	B.S.M.E. Mechanical Engineering Yonsei University Seoul, Korea
1974 - 1976	....	Research Lieutenant Hongneung Machinery Company Seoul, Korea
1976 - 1979	....	Researcher Hongneung Machinery Company Seoul, Korea
1981	....	M.S.M.E. Mechanical Engineering The Ohio State University Columbus, Ohio, U.S.A.
1979 - Present	....	Research Associate Mechanical Engineering The Ohio State University Columbus, Ohio, U.S.A.

FIELDS OF STUDY

Computer-Aided Design

Kineto-Elasto Static and Dynamic Analyses of Mechanisms and Structures

PUBLICATIONS

1. "The Development of An Interactive Fatigue Analysis Program for General Machine Elements", Master's Thesis, Department of Mechanical Engineering, The Ohio State University, Columbus, Ohio, 1981.

2. "The Development of An Interactive Procedure for Fatigue Analysis Using Computer Graphics", (with G. L. Kinzel), Paper published in Proceedings of The 2nd International Computer Engineering Conference and Exhibit, San Diego, CA, Aug. 14-17, 1982, published by ASME.

3. "An Interactive Procedure for Curve Fitting By Three-Variable Approximations", (with G. L. Kinzel), Paper published in Proceedings of The 2nd International Computer Engineering Conference and Exhibit, San Diego, CA, Aug. 14-17, 1982, published by ASME.

4. "Theoretical Manual for Interactive Fatigue Analysis Program to Machine-Design Programs Group", (with G. L. Kinzel), Dept. of Mechanical Engineering, The Ohio State University, Columbus, Ohio, 1981.

5. "User's Manual for Interactive Fatigue Analysis Program to Machine-Design Programs Group", (with G. L. Kinzel), Dept. of Mechanical Engineering, The Ohio State University, Columbus, Ohio, 1981.

6. "Programmer's Manual for Interactive Fatigue Analysis Program to Machine-Design Programs Group", (with G. L. Kinzel), Dept. of Mechanical Engineering, The Ohio State University, Columbus, Ohio, 1981.

7. "Theoretical and User's Manual for Cross-Section Property Program to Machine-Design Programs Group", (with M. Lamantia and G. L. Kinzel), Dept. of Mechanical Engineering, The Ohio State University, Columbus, Ohio, 1982.

8. "Programmer's Manual for Cross-Section Property Program to Machine-Design Programs Group", (with M. Lamantia and G. L. Kinzel), Dept. of Mechanical Engineering, The Ohio State University, Columbus, Ohio, 1982.

9. "Theoretical Manual for V-belt Design Program to Machine-Design Programs Group", (with G. L. Kinzel), Dept. of Mechanical Engineering, The Ohio State University, Columbus, Ohio, 1983.

10. "User's Manual for V-belt Design Program to Machine-Design Programs Group", (with G. L. Kinzel), Dept. of Mechanical Engineering, The Ohio State University, Columbus, Ohio, 1983.

11. "Programmer's Manual for V-belt Design Program to Machine-Design Programs Group", (with G. L. Kinzel), Dept. of Mechanical Engineering, The Ohio State University, Columbus, Ohio, 1983.

12. "Sample Output from Programs Developed to Design and Analyze Machine Elements", (with G. L. Kinzel and T. Walliser), Dept. of Mechanical Engineering, The Ohio State University, Columbus, Ohio, 1983.

13. "Manual for Fillet and Spot Welded Connections Design and Analysis Program", (with G. L. Kinzel), Dept. of Mechanical Engineering, The Ohio State University, Columbus, Ohio, 1984.

14. "A Comprehensive Analysis Procedure for V-belt System", (with G. L. Kinzel), Paper presented in *The 3rd International Computer Engineering Conference and Exhibit*, Las Vegas, NV, Aug. 12-16, 1984.

ABSTRACT

This study is concerned with the development of a transfer-matrix method for the static and dynamic analyses of general planar flexible-body mechanisms where the deflections may be large or small. The study includes the development of the necessary transfer matrices (field matrix, point matrix, transformation matrix, spring matrix, branch matrix, rigid-body inertial matrix, and elastic-body inertial matrix) for the analyses. These transfer matrices having 7 X 7 elements give three degrees-of-freedom per node by representing one degree-of-freedom in the longitudinal direction with two degrees-of-freedom in the transverse direction. In the dynamic analysis of flexible-body mechanisms, the rigid-body inertial effects caused by rigid-body accelerations are considered in a quasi-static sense. The elastic-body inertial forces due to the elastic vibrations are considered in a time-domain sense. An iteration method for the nonlinear analysis is based on the successive solutions of linear systems. For the dynamic stress analysis, the fatigue stress analysis is carried out for non-zero mean stress levels in the structure/mechanism members using Soderberg's linear failure line. The kinematic position and acceleration analyses of multiloop planar mechanisms are based on the component module approach using closed-form equations. Finally, an interactive, computer-aided analysis program CASDAM (Computer-Aided Static and Dynamic Analyses of Flexible Mechanisms/Structures) is developed.

TABLE OF CONTENTS

LIST OF FIGURES

LIST OF TABLES

CHAPTER I

INTRODUCTION

1.1 Introduction

In rigid body analyses, whether static or dynamic, the links of a mechanism or structure are assumed rigid. The complexity of the mathematical analysis of mechanisms with elastic links has been a deterrent against giving up the rigidity assumption. Vibrations in the mechanism links are often disregarded by the designers, because the body is assumed to be quasi-static. This is done for relative simplicity. However, omitting link deformations under dynamic conditions may contribute to a machine's failure to perform adequately at high speeds. The area of study pertaining to the motion of mechanisms, with link elasticity and mass distribution taken into account, has been called the <u>kineto-elastodynamics</u> (<u>KED</u>) of mechanisms.

The effects of mass distribution and elasticity in mechanisms become significant at high speed. One interpretation of <u>high-speed</u> may be the speed at which the deformations due to inertial forces becomes so large that they cannot be ignored. The resulting deflections caused by the inertial forces may render the performance of the machine unacceptable. High stress levels together with the large number of cyclic stresses may cause early failure from fatigue. Other problems associated with high-speed operation are difficulties in balancing and problems with stability.

This study proposes the development of a new technique for the kineto-elastostatic and dynamic analyses of general planar flexible mechanisms. Research in the following areas is addressed:

1) Kineto-elastostatic and dynamic analyses of flexible systems in general multiloop-planar mechanisms by an iterative transfer matrix method.

   1. The static analysis of flexible systems.

   2. The dynamic analysis of quasi-static systems.

   3. The time domain analysis of flexible systems.

2) An approximate method for large, elastic-deflection analyses.

3) A computer program CASDAM for the static and dynamic analyses of general multiloop planar mechanisms and structures under either the small- or large-deflection assumptions.

In addition, the necessary transfer matrices (field matrices, point matrix, spring matrix, transformation matrix, branch matrix, rigid-body inertial matrix, and elastic-body inertial matrix) are developed to give three degrees-of-freedom per node in the system. Finally, the kinematic position and acceleration equations of the component modules are derived by using a closed-form solution procedure.

1.2 Literature Review

In recent years, great emphasis has been placed on studying multi-body systems, and many analytical and numerical techniques have been developed for solving systems that consist of interconnected rigid components. In many industrial applications, however, the assumption of rigidity in mechanical elements does not represent a realistic condition, especially, if high precision and alignment are required. The demand for an accurate mathematical model that accounts for flexibility effects has been a motivation for various analytical and numerical investigations.

In this section, the literature for three areas will be reviewed. These include: the dynamic analysis of flexible mechanisms, the computer-aided kinematic/dynamic analysis/synthesis programs for rigid-link mechanisms, and the transfer matrix method.

1.2.1 Dynamic Analysis of Flexible Mechanisms

The study of the motion of linkages consisting of elastic members has been the subject of extensive research in recent years. In many present-day industrial applications, mechanisms are required to operate at high speeds and under large dynamic loads. In such cases, it is often necessary to consider the elastic behavior of links, since a rigid body analysis does not provide an adequate description of mechanism performance. A comprehensive bibliography of this field may be found in the review articles by Erdman and Sandor [1] and Lowen and Jandrasits [2]. A brief overview of the literature will be given here.

In 1969, Shoup [55] investigated analytically large deflections of flexible beam springs, and Kinzel [56] derived analytical formulations for a flexible slider-crank mechanism. In 1972, Erdman, Sandor, and Oakberg [3] proposed to use the flexibility approach for the structural analysis to study an elastic four-bar linkage. Winter and Shoup [4] considered the displacement of a four-bar mechanism in which at least one link is capable of undergoing large elastic bending deflections. They dealt with the displacement analysis of a partially flexible mechanism for purposes of path generation and defined the spring characteristics of the flexible member in an attempt to prevent the deformation which is followed by immediate structural failure due to a temporary overload.

In 1973, Imam, Sandor, and Kramer [5] applied the permutation vector approach of structural analysis to an elastic four-bar linkage and a six-bar multiloop mechanism. They included in their analysis the rate of change of eigenvalues and eigenvectors to reduce the required computer time. Also, they found dynamic stresses much higher than static stresses on the members at high operating speeds. In 1973, Sadler and Sandor [6] analyzed a slider-crank mechanism with a rigid crank and an elastic connecting rod using the Euler-Bernoulli theory for beams. In 1974, the same authors [8] analyzed a crank-rocker mechanism with rotational inertia in the output; they modeled the crank link as a cantilever beam, and the coupler and rocker links as simply supported beams.

The experimental investigations of the dynamic response of elastic mechanisms that were conducted by Alexander and Lawrence [7,9] have provided the opportunity for the verification of analytical studies of an elastic four-bar mechanism. They presented the steady-state elastic response of a planar four-bar, quick-return mechanism and gave strain data at points on the coupler and output link for several different input rotational speeds. Sadler [11] in 1975 compared these experimental results and his analytical results from a lumped-parameter model [8]. The analytical and experimental results matched satisfactorily. Chu and Pan [10] investigated the longitudinal transient dynamic response of an elastic connecting rod in a slider-crank mechanism. Their results included the fundamental natural frequency as a function of the ratios of the length of crank to the length of connecting rod and the viscous damping for different rotating speeds of the crank. In their results, they found the crank-connecting rod length ratio had a large effect on the amplitude of the response.

In 1976, Bahgat and Willmert [12] examined the vibration analysis of multiloop planar mechanisms using a finite element approach. They considered both axial and lateral vibrations using a high-order hermite polynomial approximation which conserves moment compatibility between elements. They obtained the steady-state solution for the resulting differential equations using a harmonic series technique and the stresses from the resulting deformations. Golebiewski and Sadler [13] obtained experimental data for a slider-crank mechanism with a rigid crank and an elastic connecting rod, and analyzed the system using lumped-parameter Euler-Bernoulli beam theory. Results included dynamic steady-state bending stresses for the midpoint of the connecting rod and the effects of crank speed, crank length, and slider offset on the maximum stress levels. The measured data showed that the maximum measured stresses were lower in magnitude than the maximum computed stresses. Sutherland [14] examined a completely elastic four-bar linkage by employing an assumed-modes analytical approach, and measured the follower angles at given crank angles. Thompson and Barr [15] developed a variational approach and applied it to a flexible slider-crank mechanism.

In 1977, Kohli, Hunter, and Sandor [16] used the Euler-Lagrange equations of motion for the vibration analysis of an offset slider-crank mechanism consisting of elastic links, elastic supports, and shafts. Midha, Erdman, and Frohrib [17] used an iterative technique to solve an elastic four-bar linkage which was treated as a series of single degree-of-freedom problems. However, comparisons with experimental data showed poor agreement. In 1978, Midha, Erdman, and Frohrib [18] used a displacement based finite-element method to develop the mass and stiffness properties of an elastic four-bar linkage. In 1979, they developed a numerical algorithm for the transient [19] and periodic response [20] of high-speed elastic four-bar linkages. A single degree-of-freedom system with time-dependent periodic parameters can be solved by discretizing the forcing period into a number of intervals and by assuming the system parameters to be constant over each interval. Their algorithm is employed to solve an elastic linkage problem via modal superposition.

Badlani and Kleinhenz [21] in 1979 studied the dynamic stability of a slider-crank mechanism with an undamped elastic connecting rod using the Euler-Bernoulli and Timoshenko beam theories. The results indicated new regions of instability when rotary inertia and shear deformation effects were included. Bagci and Kalaycioglu [22-23] used the stiffness based finite-element method with planar finite-line elements and lumped mass systems to calculate the elastodynamic responses and critical operating speeds of planar four-bar, slider-crank, and Stephenson's six-bar mechanisms. Jandrasits and Lowen [24-25] used Hamilton's integral, a novel elastic mechanism constraint equation, and Kantorovich method for a counter-weighted rocker link with an overhanging endmass in a four-bar linkage.

In 1980, Badlani and Midha [26] investigated the dynamic behavior of a slider-crank mechanism with an initially curved connecting rod using the Euler-Bernoulli beam theory, and showed that a very small initial curvature caused a significantly greater steady-state response. Nath and Ghosh [27] developed a systematic finite element method which eliminated the singularity in the stiffness matrices for mechanisms with Coriolis, tangential, and normal components of acceleration for a moving link. Also, they [28] used a harmonic series expressions for the element displacements in terms of the crank angle to obtain directly the steady-state displacements and stresses within the elastic links of a mechanism. Sadler, Mayne, and Fan [29-30] investigated the influence of system parameters, including both motor properties and mechanism properties, on various performance characteristics. They performed simulation studies on two different four-bar mechanisms using separately excited d.c. motors for actuation and carried out dynamic time-response analyses. They presented nondimensional graphs which give generalized, quantitative information for the design of actuator-mechanism systems.

In 1981, Cleghorn, Fenton, and Tabarrok [31] presented a refined mathematical, finite-element model of a four-bar mechanism by assuming axial rigidity in the elements to reduce the number of global equations. Means and Neon [32] dealt with studies of longitudinal, transverse, and rotary responses of a non-uniform elastic coupler for various speeds of a rigid crank of a slider-crank mechanism. Their study indicated that the rotary inertia did not have any notable effect on the dynamic response, but shear deformation could be a factor in the transverse deformation at a high crank speed. Zuccaro, Bengisu, and Thompson [33] examined the dynamic response of a four-bar mechanism fabricated from a graphite-epoxy composite with a unidirectional ply, and presented the variations of dynamic strain with crank angles for constant crank rotation. Sutherland [34] proposed a general procedure for the dynamic analysis of flexible mechanisms, based on the superposition of elastic-body motions on the gross rigid-body motions.

In 1982, Ardayfio [35], and Zhu and Chen [47] studied the dynamic stability of an eccentric slider crank mechanism with elastic effects at both joints of the coupler and illustrated the unstable frequency region with respect to crank speed. Badlani and Midha [36] presented the effect of internal material damping on the dynamic response of a slider-crank mechanism. They assumed a linear viscoelastic model for the connecting rod and demonstrated that the viscoelastic material damping could have significant influence, both favorable and adverse. Constantinou and Tadjbakhsh [38-39] investigated the dynamic instability of the elastic coupler of a four-bar mechanism and presented the unstable regions for a variety of geometric parameters.

Jaskie and Kohli [40] in 1982 solved the non-linear equations for the support vibrations of a slider-crank mechanism. They found that the support deflections predicted by linear and nonlinear theories differed by less than 5 percent and an increase in the flexibility of the supports decreased the velocity variation of the crank. Means [41] studied the dynamic bearing loads and the slider wall reaction of a slider-crank mechanism with an elastic coupler. The results showed that the bearing loads with an elastic coupler might be considerably higher in both magnitude and frequency than those computed using rigid body analyses. Shabana and Wehage [42] presented a method for the transient, dynamic analysis of mechanical systems composed of interconnected rigid- and flexible-bodies under large angular displacements, and simulated a flexible mechanical linkage and a tracked vehicle.

Stamps and Bagci [43] investigated, analytically and experimentally, the dynamic behavior of planar mechanisms with offset geometry for dynamic stress and critical speed levels. The experimental and analytical results showed that at the critical speeds the mechanism was subjected to shock loading depending on the acceleration history of the links. Sunada and Dubowsky [44] presented a method for analyzing the complete dynamic behavior of industrial robotic manipulators with complex-shaped flexible links, including effects of manipulators control systems and actuators. They demonstrated that link flexibility has a significant impact on system performance and stability. Sung and Thompson [45] examined the effect of sinusoidal foundation motion upon the response of a flexible four-bar mechanism. They used a displacement based finite-element model for the analytical solution, and obtained experimental data for a system fabricated from aluminum links and also links fabricated from a graphite-epoxy composite. These simulations demonstrated the undesirable effects of support motion on the response of the system as evidenced by the larger amplitudes of vibration with higher stress levels. Thompson, Zuccaro, Gamache, and Gandhi [46] examined a flexible planar four-bar linkage fabricated from a fiber-reinforced material, using the same experimental apparatus as was used in Reference [33]. The studies showed that an elastic continuum model might be employed to predict the dynamic response of a linkage made from a unidirectional fiber-reinforced material.

In 1983, Cleghorn and Konzelman [48] compared the effects of various beam elements on finite-element models used in flexible mechanisms. The results showed that the convergence was more rapid when quintic rather than cubic polynomials were employed for free vibrational responses of a stationary mechanism. In 1984, Bagci [49] presented a flexural finite-line element method for kineto-elastodynamic as well as kineto-elastostatic studies of industrial, planar, and three-dimensional linkages and robots. Garcia-Reynoso and Seering [50] developed a mathematical model for the linearized vibrations of a four-bar linkage with a flexible rocker-link and flexible input and output shafts. They found that the flexibility in the driving- and driven-shafts had a significant influence on the system response. Shabana [51] modeled inertia properties of flexible components with large angular rotations for a slider-crank mechanism. He evaluated the flexibility mass matrix based on a distributed-parameter approach and inertia coupling based on a lumped-mass technique.

Thompson, Sung, and McGrath in 1984 presented a variational method for the coupled thermoelastic response of planar flexible mechanism system subjected to both mechanical and thermal loadings [52] and for the nonlinear finite element analysis of multiloop planar mechanisms comprised of elastic bodies connected by revolute or slider joints [54]. And Thompson, Sung, Crouley, and Cuccio [53] used a commercial composite laminate as a coupler link of a flexible four-bar linkages in their experimental comparative study. The experimental results demonstrated that composite-linked mechanisms had responses superior to those of comparable mechanisms manufactured from commercial metals, and that the dynamic behavior is governed by the stiffness to density ratio of the link material.

1.2.2 Computer-Aided Kinematic/Dynamic Analysis and Synthesis Programs for Rigid Body Mechanisms

The kinematic analysis of a mechanical system is achieved by solving the kinematic equations of constraint. The equations of constraint may be established in matrix or vector form, either from the types of rigid constraints at the connecting joints, or from the conditions of closure for each of the connecting loops. For a dynamic analysis, the second-order differential equations can be easily obtained by taking derivatives of the algebraic equations of constraint.

The dynamic analysis of a given system of several interconnected rigid bodies involves the determination of the unknown accelerations, forces, and torques. Generally there are two basic classes of dynamic problems: <u>dynamic motion analysis</u> and <u>dynamic force analysis</u>. The dynamics of a system of rigid bodies connected by kinematic pairs may, in general, be described by a set of nonlinear ordinary differential equations consisting of the dynamic equations of motion and the kinematic equations of constraint.

In the case of a dynamic motion analysis, the externally applied forces are specified, the reaction forces and the accelerations are calculated, and the accelerations are then integrated to determine the required velocities and displacements. Conversely, in the case of a dynamic force analysis, the necessary input motions are specified; the kinematic analysis of the system determines the displacements, velocities, and accelerations of the moving members as a function of the input motion; and the equations of motion determine the active and reactive unknown forces.

Interactive computer-aided analysis/design of mechanical systems has recently been undergoing an evolution due to highly efficient computer graphics. The industrial implementation of state-of-the-art analytical developments in mechanisms has been facilitated by computer-aided design packages because these rigid-body mechanism analysis/synthesis programs dramatically reduce the time required for linkage design. A comprehensive bibliography of these programs may be found in the articles by Ardayfio [65] in 1981 and Ardayfio, Mittler, and Park [77] in 1984. In the U.S.A., these computer-aided analysis/synthesis programs are ADAMS [61-62], DRAM [58], IMP [57], KINSYN [63], KINANL [67], RECSYN [68-69], KADAM [64], DADS [79], and FORSS [66, 71-72, 75]. Also packages from the international literature, such as KOGEAN and KOGEOP (Germany), LINKE (Canada), TADSOL (Netherland), KIDYAN (Czechoslovakia), and MLINK (Italy), have been described [65, 77].

Orlandea, Chace, and Calahan [61-62] developed sparse matrix and stiff integrated numerical algorithms, which can be used for the simulation of electrical circuits and three-dimensional mechanical dynamic system. These algorithms can efficiently solve large sets of sparse linear equations and avoid the numerical instability associated with widely separated eigenvalues. Thus, the computer program ADAMS (Automatic Dynamic Analysis of Mechanical Systems) developed by implementing the algorithms can be used for simulation of three-dimensional mechanical systems. Advantages of ADAMS include the conditions that the necessary equations can be formulated directly from the connection data, and all angular and displacement variables are retained as solution variables. Also all joint reaction forces are explicit solution variables, and therefore the formulation is compatible with the continuum mechanics approach to internal stress analysis. As disadvantages, time is wasted in solving for variables of no interest to the designer.

In DRAM (Dynamic Response of Articulated Machinery), Smith, Chace, and Rubens [58] developed a technique for automatically generating a mathematical model for a planar mechanical system with Lagrange's equation. The technique used the elements of graph theory which were developed for electrical networks. The program DRAM requires three basic identifications to automate the generation of the differential equations appropriate to the physical system being modeled. These are the paths from ground to the center of mass of each part, the independent closed loops of the parts and the contacts, and the line of action of each applied force. Once, the solution procedure is formulated in matrix form; the system of equations is solved for the second-order acceleration terms and the Lagrange multipliers; the reaction forces are then computed; the second-order terms are integrated using initial conditions which are part of the input data. The loop is cycled through until the time specified by the user has been reached.

Sheth and Uicker [57] developed the computer program IMP (Integrated Mechanisms Program) which can be used for automating the kinematic, static, and dynamic analysis of planar or spatial and multiloop kinematic chains using a technique based on network theory and matrix methods. However, the program IMP requires a mechanism to be made entirely of rigid bodies (except for ideal springs) connected by kinematic pairs forming a closed kinematic chain. Also, one of the rigid bodies must remain fixed relative to some set of reference axes.

KADAM (Kinematic And Dynamic force Analysis of planar Mechanism) developed by Williams and Rupprecht [64] used a procedure based on three equations of equilibrium for each link in the mechanism. The free body diagrams included inertial forces based on D'Alembert's principle. The technique automatically formulates these equations into matrix form. Gaussian elimination is used for the joint constraint forces and driving input force or torque. The vector-loop equation approach is also used for the kinematic analysis.

FORSS [66, 71-72, 75] is an interactive computer program for structurally and dimensionally synthesizing force systems to drive a mechanism for a desired motion time response and input-output forces. The program can be used for any planar one degree-of-freedom linkage, but a force analysis program and a kinematic analysis program must be used as a host to generate pre and post synthesis data.

Haug, Wehage, and Barman [79] developed the computer program DADS (Dynamic Analysis and Design Systems) used a method of formulating and automatically integrating the equations of motion for dynamic analysis of general constrained systems, and a state space adjoint variable method for design sensitivity analysis extensively in optimal control and structural design optimization. Both dynamic analysis and design sensitivity formulations are automated and solved using a stiff numerical integration method for mixed differential equations. The program DADS can treat mechanical systems with intermittent motion to simulate jump conditions.

KINANL developed by Kinzel et al. [67] is a graphics-oriented, interactive computer program for the kinematic analysis of planar mechanisms using a modular approach. This approach was developed by Suh and Radcliff [105] to obtain position, velocity, and acceleration equations for the component modules: rigid body, oscillating slider, two-link dyad, and rotating guide for driving crank input. In KINANL, the technique is extended by incorporating dual-slider, slider-crank, and inverted slider-crank modules, permitting mechanisms to be analyzed when a slider input is involved. Also KINANL uses an extension of

Goodman's inversion technique to make the component approach applicable to most planar mechanisms with lower pairs.

KINSYN developed by Rubel and Kaufman [63] has both synthesis and analysis capabilities for planar, rigid four-bar linkages. An important capability of KINSYN is the post processor which gives the Grashof type, transmission angle, change points, the need for reassembly, and the ability to alter a mechanism's dimensions while animating its motion. Using synthesis capabilities coupled with the man-computer graphical interaction, planar four-bar, motion-generating mechanisms can be directly synthesized to guide a body through two, three, four, or five coplanar design positions. Also, all possible slider-crank inversions, and double-slide devices such as the scotch yokes and Cardanic mechanisms are designed at the same time. Immediately following the synthesizing of the mechanism, KINSYN analyzes the mechanism using a closed-form solution procedure for kinematic analysis, and animates the mechanism on the display screen.

RECSYN developed by Waldron [68-69] is a graphics-oriented, interactive computer program for the kinematic synthesis of planar mechanisms. It can design a four-bar linkage with its coupler passing through two, three, four, or five non-parallel positions while rectifying spurious and otherwise undesirable solutions. The program RECSYN uses numerical techniques eliminating solution failures due to numerical error or non-convergence and a closed-form solution procedure. An important feature of RECSYN is the automatic rectification of cursor selected points to the nearest actual points of linear, circular, and cubic loci to improve solution accuracy, and to reduce user strain.

In addition, as a technique for the kinematic analysis of planar mechanisms, Benedetto and Pennestri [73] proposed a numerical method for approximate calculations of angular velocities and accelerations in planar mechanisms. Fallahi and Ragsdell [74] presented a numerical approach to the planar kinematic analysis. Sharma [76] formulated and analyzed kinematically general four-bar mechanisms and elliptical mechanisms on the microcomputer. Sparis and Mouroutsos [78] presented an iterative matrix method for the kinematic analysis and the determination of the velocities and accelerations for planar mechanisms incorporating rolling, sliding, and pivoting members with a single or multiple degrees of freedom.

Also the vector graphical, vector analytical, and matrix approaches are presented in most textbooks for the dynamic analysis of rigid-body mechanisms [101-106]. Gupta [59] formulated the Newton-Euler equations of motion for the dynamic analysis of multiloop systems. Bagci [60] investigated the dynamic motion analysis of planar mechanisms with coulomb and viscous damping, via the joint force analysis. Bogci and Abounassif [70] developed an automated technique using irregular line elements for the dynamic force, torque, stress and deflection analysis of single degree-of-freedom, multiloop, planar mechanisms. They also developed a finite-element based method for determining the gross-motion response of planar mechanisms.

1.2.3 Transfer Matrix Methods

Toward the middle of this century, very powerful analog and digital computers were developed, and engineers were encouraged to establish the methods that would reduce the number of simplifying assumptions required to model and analyze mechanical systems. As part of this effort, the so-called matrix method of analysis of structures was introduced.

The ideas behind the matrix method are not new; they are closely associated with the principles set by Castigliano, Maxwell, and Muller-Breslau [95]. The only reason that the matrix methods were not fully developed and utilized in the last century is because they involve the solution of large simultaneous equations. Even for a fairly small structure, the number of simultaneous equations may reach a point where their solutions without computers would be totally impractical.

Basically there are three different types of matrix methods for analyzing structures, namely, stiffness (displacement), flexibility (force), and mixed matrix methods [89-95, 97-100]. Each method eventually involves the solution of simultaneous equations. The joint displacements are the unknown quantities in the stiffness method, member forces in the flexibility method, and both joint displacements and forces in the mixed method. The flexibility method is associated with the degree-of-indeterminacy of the structure and requires the solution of as many simultaneous equations as the number of unknowns.

The stiffness method, on the other hand, does not depend on whether the structure is determinate or indeterminate, but on the total number of state variables in the system.

In addition to the previous classification of matrix methods, the transfer-matrix method and the finite-element method are commonly used for structural analyses. These are based on the idea of breaking up a complicated system into component parts which have simple elastic and dynamic properties that can be readily expressed in matrix form. These component matrices are considered as building blocks which, when fitted together according to a set of predetermined rules, include the static and dynamic properties of the entire system. The matrix formulation of these rules is superbly adapted to digital computers.

A common type of structural system occuring in engineering practice consists of a number of elements linked together, end to end, in the form of a chain. The transfer matrix method is ideally suited for such systems, because only successive matrix multiplications are necessary to couple the elements together. Intermediate conditions and the number of degrees-of-freedom present no difficulty since they have no effect on the order of the transfer matrix required. In fact, the size is dependent only on the order of the differential equations governing the behavior of the elements of the system.

A type of transfer matrix method, called the Holzer transfer matrix method [95], can effectively carry out the dynamic analysis of one-dimensional system. This system involves one degree-of-freedom per node. The matrices used in the transfer-matrix method represent the forces and displacements at one section of a chain-type structure in terms of the corresponding forces and displacements at the adjacent section. Thus, the complete force and displacement profile of the structure can be obtained from a sequence of transfer matrix multiplications. A second type of transfer matrix method is an extension of the Holzer method to the analysis of flexible systems which have two degree-of-freedom per node. This method was first suggested by Myklestad [95], and is usually called the Holzer-Myklestad method. In this method, the mass is assumed to be concentrated at a series of points along the axis, and the degrees of freedom of the structure are the lateral translation and the rotation at these points. The beam segments connecting the mass points are assumed to be weightless and of constant stiffness.

Of the present-day transfer matrix methods for the simple systems requiring a vibration analysis or beam deflection analysis, the mixed transfer matrix method is most commonly used. The mixed transfer matrix method consists of single degree-of-freedom systems and two degrees-of-freedom systems. A single degree-of-freedom system allows only one directional displacement, usually in the longitudinal direction, and a two degrees-of-freedom system allows a displacement in the transverse direction and a rotational displacement.

In the transfer matrix methods for structure analysis, two methods, a stiffness (displacement) matrix method and a flexibility (force) matrix method, are most commonly used. Both methods satisfy the force equilibrium equations and the displacement compatibility conditions, but not in the same order. In the stiffness method, force-equilibrium is satisfied first, and in the flexibility method, displacement-compatibility is satisfied first. The choice of one method over the other depends upon the structure as well as the analyst's preference. Each method eventually involves the solution of simultaneous equations in which the nodal displacements are the unknown quantities in the stiffness method and the member forces in the flexibility method.

1.2.4 Discussion of Review

Generally, most of the available computer programs for dynamic analyses have been established for rigid-body mechanisms, and they use specific techniques to automately determine the equilibrium equations and to reformulate them into matrix form. Also they include inertia forces due to the rigid-body motions of the mechanism by applying D'Alembert's principle.

As a common dynamic analysis method for rigid-body mechanisms, the traditional vector graphical method can give poor accuracy. The vector analytical method gives accurate results using vectorial calculations instead of graphical manipulations for the resultant forces and moments. However, many of the vectorial calculations are tedious and can induce calculation errors, and they do not easily lend themselves to the analysis of flexible linkages. In the "free-body" diagram approach, three (or six for the spatial case) equilibrium equations including the inertia forces and moments are written for each link. Then, all of the equations for the system are expressed in matrix form. The advantage of this approach is that the equations of motion are quickly derived; however, the disadvantage is the need for a large number of matrix manipulations in order to solve the equations, and the total number of elements of the matrix is greatly increased by the number of links and degrees-of-freedom.

In addition, although no method can fully analyze the kineto-elastodynamic effects of general flexible mechanisms, during the last decade, the finite element method has been the most popular for the dynamic analysis of high-speed flexible mechanisms. For a flexible-body dynamic analysis, a mechanism can be thought of as an instantaneous structure, which is frozen at a particular instant by removing its degrees-of-freedom through the application of added mechanical constraints. Then, the same finite-element procedures used in structural analysis are applied. But, the finite-element method has a distinct disadvantage; the storage requirements for the system matrix rapidly increases with the numbers of nodes and degrees-of-freedom per node.

The transfer matrix method does not appear to have been generally applied to mechanisms for static and/or dynamic force analyses. However, it has a number of advantages over the other methods, especially when system flexibilities are concerned. The method is very compact making it ideally suited to microcomputers. It can also involve fewer calculations than does the finite-element method, and nonlinearities are easy to incorporate.

The purpose of the research described in this dissertation is to apply the transfer matrix method to multiloop flexible mechanisms and structures. This will include developing an iterative procedure to accomodate nonlinearities and the necessary transfer matrices to accomodate the special geometries arising in mechanisms. Also, a semiautomatic procedure will be established for applying the procedure to mechanisms. This will involve the development of the algorithms necessary for incorporating the procedure into an interactive analysis program.

1.3 Overview of Dissertation

In Chapter 2, the kinematic modular approach is presented for position and acceleration analyses, and eight types of components are identified. All of the formulations for the rigid-body kinematic analysis of the components are given in Appendix A.

Chapter 3 derives the transfer matrices required in an iterative transfer-matrix method; field, point, transformation, spring, rigid-body inertial, elastic-body inertial, and branch matrices. Chapter 4 presents an approximate method for large-deflection analyses and gives comparisons with exact solutions.

Chapter 5 derives the transfer matrix loop equations for the main loop systems and subloop systems. Chapter 6 explains the fundamental procedure for applying the iterative transfer-matrix method to kineto-elastostatic and dynamic analyses of flexible mechanisms and structures.

Chapter 7 briefly discusses the structure of the program CASDAM. Tree structure and storage requirements for each routine in the program CASDAM are presented in Appendix E. Six samples are analyzed in Chapter 8. The samples include a multiloop mechanism for static analyses under small- and large-deflection assumptions; a mechanism for a quasi-static analysis and for a time-domain analysis; a caltilever beam with end loads; and a stepped beam on elastic supports for structural analysis. The solution details for the static analysis under small-deflection assumption are presented in Appendix B; the solutions for the quasi-static analysis are given in Appendix C; the solutions for the stepped beam analysis are given in Appendix D. Finally, Chapter 9 presents the summary from the dissertation.

CHAPTER II

FUNDAMENTALS FOR THE KINEMATIC LOOP ANALYSES

2.1 Introduction

A mechanism is a mechanical device that has the purpose of transferring motion and/or force from a source to an output, and consists of links which are connected by joints (revolutes or prismatic joints). The rigid-body configuration of the mechanism can be considered as an '<u>instantaneous</u> <u>structure</u>' capable of undergoing both rigid-body and elastic motions. Because the mechanism forces are a function of the link accelerations, a kinematic analysis must be considered prior to any force analysis. This involves determining the positions, velocities, and accelerations of every important point in the mechanism.

Most multiloop mechanisms can be decomposed into several components. The kinematic properties (position, velocity, and acceleration) of every node can then be determined from the kinematic analyses of the corresponding component modules by a closed-form solution procedure.

In Section 2.2 of this chapter, eight types of component modules are identified for the kinematic analyses. Section 2.3 gives the positions and accelerations of every node in an example multiloop mechanism. All formulations for the kinematic analyses of the component modules are presented in Appendix A.

2.2 Types of Kinematic Component Modules

Most planar mechanisms which have lower pairs and which can be analyzed directly using classical graphical techniques can be shown to be assembled from one or more of the eight basic components shown in Fig. (2.1). The first component as shown in Fig. (2.1-1) is a simple crank with one end completely defined. The pivot point and all other points of interest on the components are called nodes. The crank has two nodes (1 and 2). This component is always a driver so that the angular position and velocity are assumed to be known.

Component 2 shown in Fig. (2.1-2) is a dyad made up of two links connected together by a revolute joint. This component together with the crank forms a four-bar linkage. For the dyad, it is assumed that the kinematic properties of node 1 are known. The kinematic properties for nodes 2 and 3 can then be computed directly if the configuration is specified and the lengths of links are given.

The third component shown in Fig. (2.1-3) is a slider which consists of a slider moving on a rod or ground. Here, it is assumed that the kinematic properties of node 1 are known and the azimuth angle of the sliding line is given. Then, the kinematic properties for node 2 can be calculated directly.

The fourth component shown in Fig. (2.1-4) is a rigid body defined by nodes 1, 2, and 3. Given the kinematic properties for nodes 1 and 2, the kinematic properties for node 3 can be determined from the configuration of the rigid body.

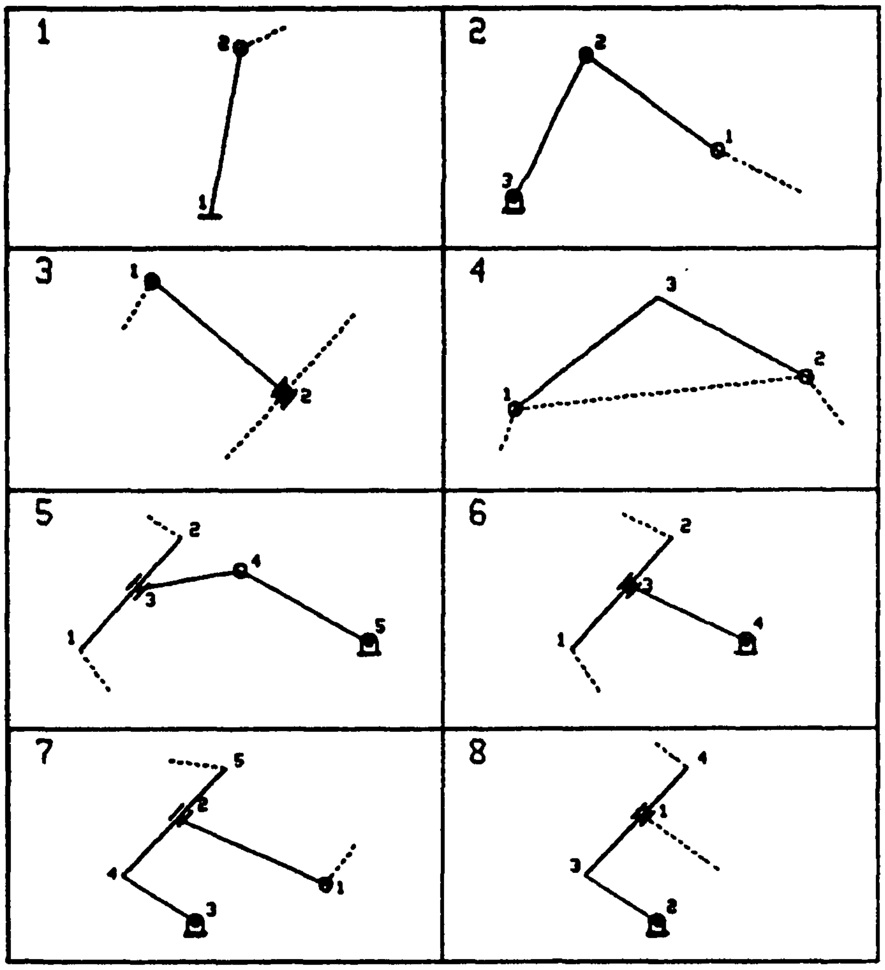

FIGURE 2.1 Types of Component Modules

The fifth component shown in Fig. (2.1-5) is an oscillating slider which consists of a dyad and a slider moving on a rod. Here, it is assumed that the kinematic properties of nodes 1 and 2 are known. Given the known kinematic quantities for these nodes and the configuration of the component, the kinematic properties of nodes 3, 4, and 5 are calculated directly.

The sixth component shown in fig. (2.1-6) is a special case of the fifth component. Here, a slider and a revolute are coincident at node 3. Given the kinematic quantities for nodes 1 and 2, the kinematic properties of nodes 3 and 4 can be computed.

The seventh component given in Fig. (2.1-7) is an oscillating slider which consists of a slider moving on a rod which has an eccentricity. Here, it is assumed that the kinematic properties of node 1 are known. The kinematic quantities of nodes 2, 3, 4, and 5 are directly calculated from the known configuration of the component.

The final component in Fig. (2.1-8) is a special case of the seventh component and is the standard slider crank with a slider input. The slider moves on the link and the kinematic quantities of the slider are assumed known. The kinematic properties of nodes 2, 3, and 4 can be determined. The formulations for the kinematic analyses of each module are given in Appendix A.

2.3 An Example of The Kinematic Analysis

A mechanism can be decomposed into several components as shown in Fig. (2.2). If the link between nodes 1 and 2 is an input link, the kinematic properties (position, velocity, and acceleration) of node 2 in Fig. (2.2b) can be determined from the given geometry and angular velocity. A component involving nodes 2, 4, and 6 forms a dyad in Fig. (2.2c), and the kinematic properties of nodes 4 and 6 are also determined from the known position of node 2. As one rigid body in Fig. (2.2d), the kinematic properties of node 3 are calculated from the conditions of nodes 2 and 4. After the kinematic properties of node 3 are determined, the properties of nodes 7 and 8 are calculated from the dyad connected by nodes 3, 7, and 8 in Fig. (2.2e). Finally, a dyad with a slider formed by nodes 4, 5, 6, 9, and 10 in Fig. (2.2f) can be analyzed from the known properties of nodes 4 and 6. Thus, all of the kinematic properties of every node in the mechanism in Fig. (2.2a) can be determined from the corresponding component modular analyses.

The mechanism in Fig. (2.2a) consists of five components. Fig. (2.3) shows the procedure for selecting each component module in the computer program CASDAM. Table 2.1 gives the positions and accelerations of every node for each position, and Table 2.2 shows the angular accelerations of the links.

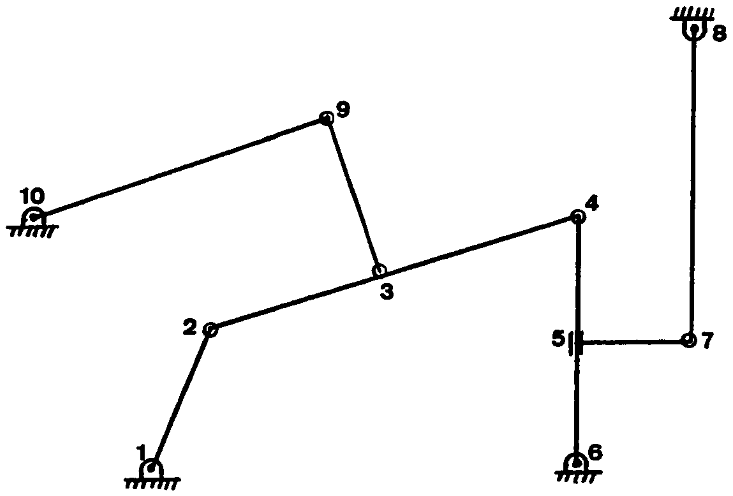

(a) A General Multiloop Mechanism

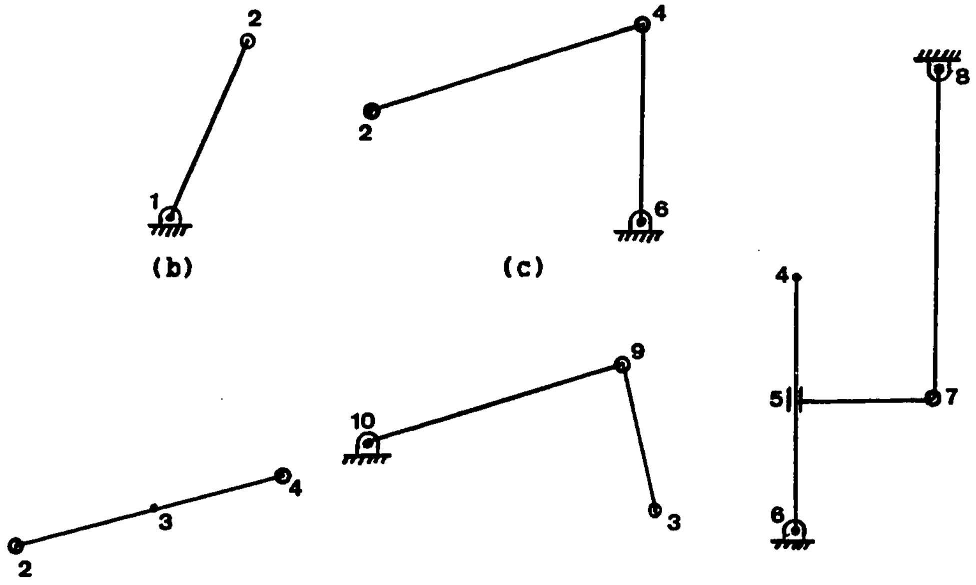

(d) (e) (f)

FIGURE 2.2 Components of A Multiloop Mechanism

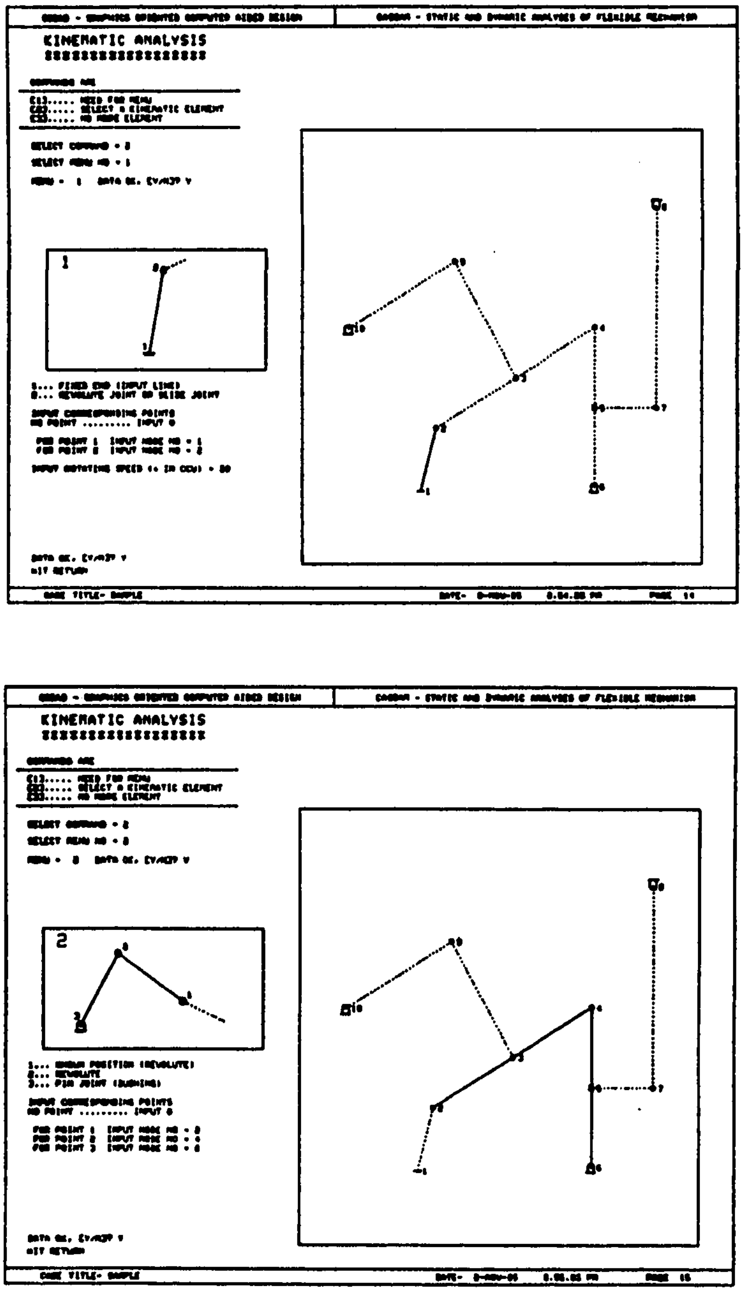

FIGURE 2.3 Procedure for Kinematic Analysis in CASDAM

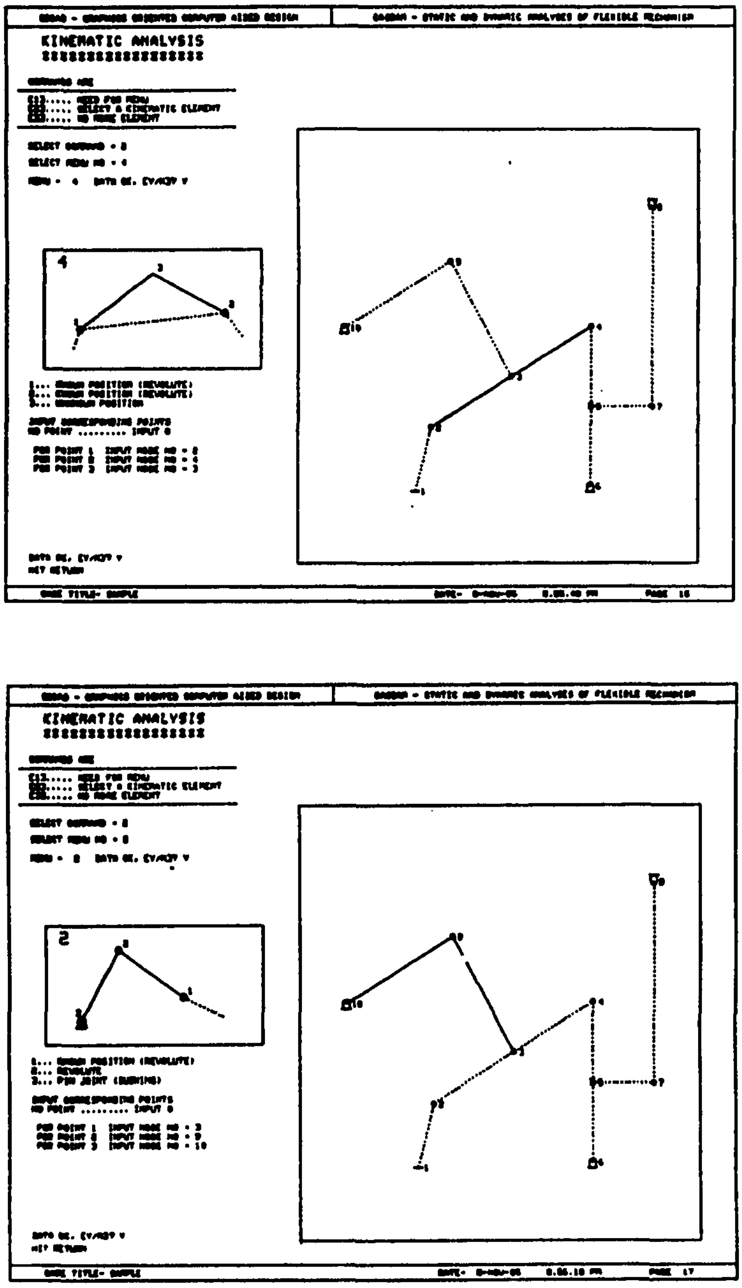

FIGURE 2.3 Procedure for Kinematic Analysis (Continued)

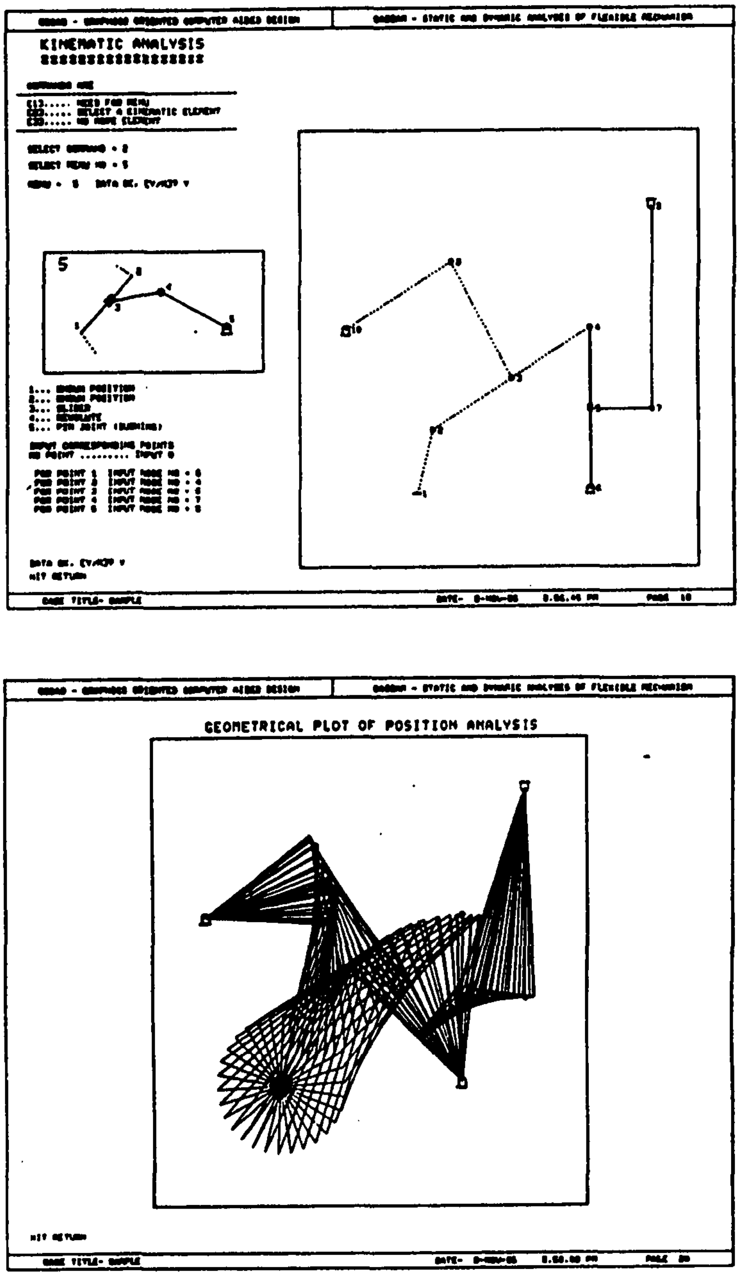

FIGURE 2.3 Procedure for Kinematic Analysis (Continued)

TABLE 2.1 Positions and Accelerations of nodes in Fig. (2.2)

TOTAL NODES	=	10	
ROTATING SPEED	=	0.2000E+02	rad/sec
INPUT-LINK ANGLE	=	0.7500E+02	degrees
UNITS	=	BRITISH (inches, inch/sec/sec)	

NODE	POSITIONS		ACCELERATIONS		SLIDING ACC.	
NO	HORZ.	VERT.	HORZ.	VERT.	HORZ.	VERT.
1	0.0000E+00	0.0000E+00	0.0000E+00	0.0000E+00		
2	0.1294E+01	0.4830E+01	-.5176E+03	-.1932E+04		
3	0.7789E+01	0.8580E+01	-.9894E+03	-.1174E+04		
4	0.1428E+02	0.1233E+02	-.1381E+04	-.5556E+03		
5	0.1428E+02	0.6330E+01	-.6905E+03	-.2778E+03	-.2275E+03	-.4643E+03
6	0.1428E+02	0.3296E+00	0.0000E+00	0.0000E+00		
7	0.1928E+02	0.6330E+01	-.4590E+03	0.1111E+03		
8	0.1928E+02	0.2133E+02	0.0000E+00	0.0000E+00		
9	0.2789E+01	0.1724E+02	0.3700E+03	-.7748E+03		
10	-.5871E+01	0.1224E+02	0.0000E+00	0.0000E+00		

TABLE 2.2 Angular Accelerations of Links in Fig. (2.2)

LINK BETWEEN NODE	NODE	ANGULAR ACC.
1	2	0.0000E+00
2	3	0.9755E+02
3	4	0.9755E+02
4	5	0.1151E+03
5	6	0.1151E+03
5	7	0.1151E+03
7	8	-0.3060E+02
3	9	-0.1377E+03
9	10	-0.8560E+02

CHAPTER III

FUNDAMENTALS OF ITERATIVE TRANSFER MATRIX METHOD

3.1 Introduction

The transfer-matrix method requires that a system be modeled as an assembly of elements in the same manner as does the finite-element method. The elements are connected together at nodes. The forces and displacements at one end of an element are related to those at the other end by a matrix of elastic properties called a field matrix. The forces and displacements between adjacent elements and the external forces at the node are related through a second matrix called a point matrix. The forces at nodes connected to a spring are related to the kinematic displacements and elastic displacements by a spring matrix. The element inertial properties due to the rigid-body kinematic accelerations are included in a rigid-body inertial matrix, which is used to analyze quasi-static responses. The inertial properties due to the link elastic vibrations are incorporated in an elastic-body inertial matrix. It is used to determine time-domain responses of flexible systems. If more than two elements come together at a point as is the case with multiloop mechanisms, the forces and displacements among the nodes are related through a branch matrix. Each element will have its own coordinate system relative to which the elastic properties and force-displacement relationships are defined. To transfer quantities from one coordinate system to another, a coordinate transformation matrix is required. Therefore, for the procedure developed here, a total of seven different transfer matrices (field, point, spring, rigid-body inertial, elastic-body inertial, branching, and transformation) must be developed. For a planar model, three degree-of-freedom (two translations, one rotation) per node are required

All of the necessary transfer matrices used in the iterative transfer matrix method have only 7X7 elements. Thus, the method requires much less storages than those of the finite-element techniques or finite-difference techniques. Also this method is simple and efficient to program on minicomputers and does not need any transformation of the developed transfer matrices into either stiffness matrices or flexibility matrices for a structural analysis. Previous transfer matrix methods in References [89-95] and finite element methods in References [96-100] must derive the matrices corresponding to either the force-matrix method or the displacement-matrix method.

The necessary transfer matrices for the iterative transfer-matrix method are derived in Section 3.3. Then, the solutions determined from the developed method are compared with previous published solutions [7, 9, 11-12, 17] in Section 3.4.

3.2 Nomenclature

A	Area of a given cross section
E	Modulus of elasticity
I	Area moment of inertia
K	Coefficient = $\sqrt{P/EI}$
L	Length of a section
m	Mass of a lumped-mass
M	Moment
N	Internal force in the axial direction
V	Internal force in the transverse direction
θ	Slope
P	Average axial force on a segment
t	Time
u	Displacement in the axial direction
w	Displacement in the transverse direction
x	Position axially along the section
ρ	Mass per unit length
ν	Poisson's ratio
[B]	Branch matrix
[F]	Field matrix
[M]	Inertial matrix
[P]	Point matrix
[S]	Spring matrix
[T]	Transformation matrix
{S}	State vector = $[u, w, \theta, M, V, N]^T$

3.3 Derivation of Transfer Matrices

The governing differential equations of motion are discussed in this section. The field matrix, the point matrix, the spring matrix, the rigid-body and elastic-body inertial matrices, and the transformation matrix are derived. Types of branches commonly used in mechanisms are given and the branch matrix is discussed.

The equations developed are based on the following assumptions:

1. The links of the mechanism move in one plane (planar mechanisms).
2. Beam-shaped links in a mechanism correspond to Euler-Bernoulli beams theory, where rotary inertia effects are neglected.
3. Plate-shaped links in a mechanism correspond to rigid bodies, because the elastic deflections of the links are negligible.
4. Deflections (slopes) of an element relative to its own local coordinate system are small.
5. Axial displacements due to the transverse loads are negligible.
6. No temperature gradients exist in members.
7. Homogeneous and isotropic elastic materials are used.
8. Friction is negligible.

3.3.1 Field Matrices

A system can be discretized into many elements connected together at the nodes. The forces and displacements at one node of an element are related to those at the other node by an elastic field matrix. Thus, the elastic field matrix contains the geometrical dimensions and elastic properties of the element. Furthermore, the elastic field matrices are different depending on the axial forces on the elements. There may be no axial force, or the force may be compressive or tensile.

For small-deflection analyses, a system is assumed to be linear, so that it can be solved by superposing the axial displacements due to the axial forces on the transverse displacements due to the transverse forces. The small-deflection analyses can be used when the maximum change in slope at any point in the system is less than about 10 degrees relative to local coordinate system. Then, the longitudinal displacement due to the transverse deflection is negligible and the system is linear. Fig. (3.1a) shows a massless beam relative to the local coordinate system. The local coordinate system is inclined with an angle Φ relative to the global X-axis, and a distributed loading (q) is present in the vertical direction of the global coordinate system.

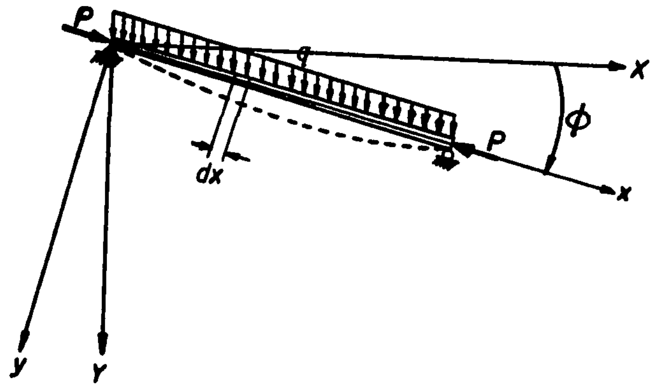

(a) A Beam Relative to The Local Coordinate System

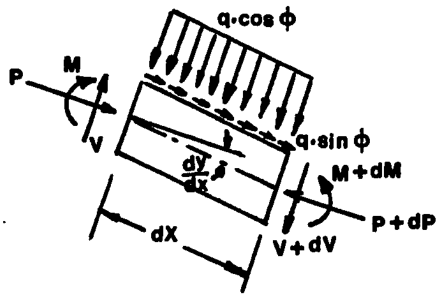

(b) Forces on A Element

FIGURE 3.1 A Beam on Two Simple Supports

The relationship among the loads, internal forces, and bending moments are obtained from the equilibrium of the element in Fig. (3.1b). Summing forces in the y-direction gives

$$- V + q \cdot \cos\phi \cdot dx + (V + dV) = 0$$

or

$$q \cdot \cos\phi = - \frac{dV}{dx} \qquad \text{(a)}$$

Taking moment about a center point at the right side gives

$$M + q \cdot \cos\phi \cdot dx \cdot \frac{dx}{2} + V \cdot dx - (M + dM) + P \cdot \frac{dy}{dx} \cdot dx - q \cdot \sin\phi \cdot dx \cdot \frac{dx}{2} = 0$$

If second order terms are neglected, the equation becomes

$$V = \frac{dM}{dx} - P \cdot \frac{dy}{dx} \qquad \text{(b)}$$

Here, the directions for V and P are perpendicular and parallel, respectively, to the local x-axis.

If the effects of shortening deformations and shortening of the beam axis are neglected, the moment curvature relationship can be written as

$$EI \frac{d^2y}{dx^2} = - M \qquad \text{(c)}$$

Combining Eqs. (a), (b), and (c), the differential equation of the beam gives

$$EI \frac{d^4y}{dx^4} + P \frac{d^2y}{dx^2} = q \cdot \cos\phi \tag{3.1}$$

The general solution to the equation depends on the sign of the axial force (P). If P is tensile (P > 0), the solution is

$$y = C1 \cdot \sinh Kx + C2 \cdot \cosh Kx + C3 \cdot x + C4 + \frac{Q \cdot x^2}{2 \cdot |P|} \tag{3.2}$$

where C1, C2, C3, and C4 are constants to be determined from the boundary conditions.

If P is compressive (P < 0), the solution becomes

$$y = C1 \cdot \sin Kx + C2 \cdot \cos Kx + C3 \cdot x + C4 + \frac{Q \cdot x^2}{2 \cdot |P|} \tag{3.3}$$

and if P is zero (P = 0), the solution becomes

$$y = C1 \cdot \frac{x^3}{6} + C2 \cdot \frac{x^2}{2} + C3 \cdot x + C4 + \frac{Q \cdot x^4}{24 \cdot E \cdot I} \tag{3.4}$$

In each case,

$$K = \sqrt{\frac{|P|}{E \cdot I}}$$

and

$$Q = q \cdot \cos\phi \tag{3.5}$$

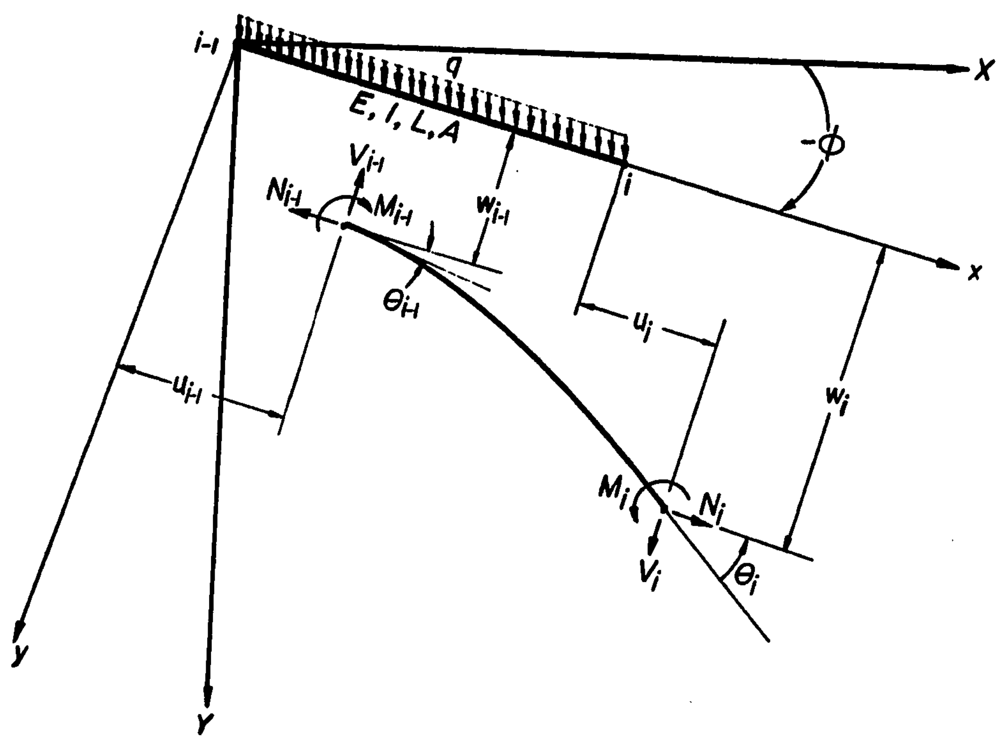

FIGURE 3.2 End Forces and Displacements for A massless Beam with Axial Forces

Note that Eqs. (3.2), (3.3), and (3.4) involve a separate set of C's. Based on Fig. (3.2), the boundary conditions at the left end of the segment (x = 0) can be written as

$$y = w_{i-1} \tag{3.6}$$

$$\frac{dy}{dx} = -\theta_{i-1} \tag{3.7}$$

$$EI\frac{d^2y}{dx^2} = -M_{i-1} \tag{3.8}$$

$$EI\frac{d^3y}{dx^3} = -V_{i-1} \tag{3.9}$$

If these conditions are substituted into Eqs. (3.2), (3.3), and (3.4), and the results are simplified to eliminate the constants, expressions for the deflection, slope, moment, and shear force at the right point of the segment (x = L) can be written as follows:

For a tensile force (P > 0), the state equations are:

$$w_i = w_{i-1} - \frac{\sinh KL}{K}\cdot\theta_{i-1} + \frac{1 - \cosh KL}{P}\cdot M_{i-1} + \left(\frac{L}{P} - \frac{\sinh KL}{KP}\right)\cdot V_{i-1} + \frac{Q}{EIK^4}\cdot\left(\cosh KL - 1 - \frac{K^2 \cdot L^2}{2}\right)$$

$$\theta_i = \cosh KL\cdot\theta_{i-1} + \frac{K\cdot\sinh KL}{P}\cdot M_{i-1} + \left(\frac{\cosh KL - 1}{P}\right)\cdot V_{i-1} + \frac{Q}{EIK^3}\cdot(KL - \sinh KL) \tag{3.10}$$

$$M_i = \frac{P\cdot\sinh KL}{K}\cdot\theta_{i-1} + \cosh KL\cdot M_{i-1} + \frac{\sinh KL}{K}\cdot V_{i-1} - \frac{Q}{K^2}\cdot(\cosh KL - 1)$$

$$V_i = V_{i-1} - QL$$

For compressive force (P < 0), the equations are:

$$w_i = w_{i-1} - \frac{\sin KL}{K}\cdot\theta_{i-1} + \frac{\cos KL - 1}{P}\cdot M_{i-1} + \left(\frac{\sin KL}{KP} - \frac{L}{P}\right)\cdot V_{i-1} - \frac{Q}{EIK^4}\cdot\left(1 - \cos KL - \frac{K^2 L^2}{2}\right)$$

$$\theta_i = \cos KL\cdot\theta_{i-1} + \frac{K\cdot\sin KL}{P}\cdot M_{i-1} + \left(\frac{1 - \cos KL}{P}\right)\cdot V_{i-1} - \frac{Q}{EIK^3}\cdot(KL - \sin KL) \qquad (3.11)$$

$$M_i = \frac{P\cdot\sin KL}{K}\cdot\theta_{i-1} + \cos KL\cdot M_{i-1} + \frac{\sin KL}{K}\cdot V_{i-1} - \frac{Q}{K^2}\cdot(1 - \cos KL)$$

$$V_i = V_{i-1} - QL$$

Finally, the state equations for no axial force (P = 0) are as follows:

$$w_i = w_{i-1} - L\cdot\theta_{i-1} - \frac{L^2}{2EI}\cdot M_{i-1} - \frac{L^3}{6EI}\cdot V_{i-1} + \frac{QL^4}{24EI}$$

$$\theta_i = \theta_{i-1} + \frac{L}{E\cdot I}\cdot M_{i-1} + \frac{L^2}{2EI}\cdot V_{i-1} - \frac{QL^3}{6EI} \qquad (3.12)$$

$$M_i = M_{i-1} + L \cdot V_{i-1} - \frac{QL^2}{2}$$

$$V_i = V_{i-1} - QL$$

Next, the force-displacement relationships for the axial direction can be determined as follows:

$$u_i = u_{i-1} + \frac{L}{EA} \cdot N_{i-1} - \frac{qL^2 \cdot \sin\phi}{EA}$$

$$N_i = N_{i-1} + qL \cdot \sin\phi \tag{3.13}$$

where u = displacement in the x-direction,

w = displacement in the y-direction,

θ = slope relative to the local coordinate system,

M = moment,

V = internal force in the y-direction,

N = internal force in the x-direction,

q = uniform distributed load on a segment,

ϕ = angle between the two coordinate systems,

and L = length of a segment.

These equations can be represented in matrix form as given in the following section.

3.3.1.1 Elastic Field Matrices

When no axial force is loaded on the section (P = 0), the elastic field matrix equation is:

$$\begin{bmatrix} u \\ w \\ \theta \\ M \\ V \\ N \\ 1 \end{bmatrix}_i = \begin{bmatrix} 1 & 0 & 0 & 0 & 0 & L/EA & F1 \\ 0 & 1 & -L & -L/2EI & -L/6EI & 0 & F2 \\ 0 & 0 & 1 & L/EI & L/2EI & 0 & F3 \\ 0 & 0 & 0 & 1 & L & 0 & F4 \\ 0 & 0 & 0 & 0 & 1 & 0 & F5 \\ 0 & 0 & 0 & 0 & 0 & 1 & F6 \\ 0 & 0 & 0 & 0 & 0 & 0 & 1 \end{bmatrix} \cdot \begin{bmatrix} u \\ w \\ \theta \\ M \\ V \\ N \\ 1 \end{bmatrix}_{i-1} \qquad (3.14)$$

When the axial force in a segment is tensile (P > 0), the elastic field matrix equation is

$$\begin{bmatrix} u \\ w \\ \theta \\ M \\ V \\ N \\ 1 \end{bmatrix}_i = \begin{bmatrix} 1 & 0 & 0 & 0 & 0 & L/EA & F1 \\ 0 & 1 & -\dfrac{\sinh KL}{K} & \dfrac{1-\cosh KL}{P} & \dfrac{L}{P} - \dfrac{\sinh KL}{K\,P} & 0 & F2 \\ 0 & 0 & \cosh KL & \dfrac{K \cdot \sinh KL}{P} & \dfrac{\cosh KL - 1}{P} & 0 & F3 \\ 0 & 0 & \dfrac{P \cdot \sinh KL}{K} & \cosh KL & \dfrac{\sinh KL}{K} & 0 & F4 \\ 0 & 0 & 0 & 0 & 1 & 0 & F5 \\ 0 & 0 & 0 & 0 & 0 & 1 & F6 \\ 0 & 0 & 0 & 0 & 0 & 0 & 1 \end{bmatrix} \cdot \begin{bmatrix} u \\ w \\ \theta \\ M \\ V \\ N \\ 1 \end{bmatrix}_{i-1} \qquad (3.15)$$

and the elastic field matrix equation for a compressive axial force $(P < 0)$ is

$$\begin{bmatrix} u \\ w \\ \theta \\ M \\ V \\ N \\ 1 \end{bmatrix}_i = \begin{bmatrix} 1 & 0 & 0 & 0 & 0 & L/EA & F1 \\ 0 & 1 & -\dfrac{\sin KL}{K} & \dfrac{\cos KL - 1}{P} & \dfrac{\sin KL}{KP} - \dfrac{L}{P} & 0 & F2 \\ 0 & 0 & \cos KL & \dfrac{K \cdot \sin KL}{P} & \dfrac{1 - \cos KL}{P} & 0 & F3 \\ 0 & 0 & -\dfrac{P \cdot \sin KL}{K} & \cos KL & \dfrac{\sin KL}{K} & 0 & F4 \\ 0 & 0 & 0 & 0 & 1 & 0 & F5 \\ 0 & 0 & 0 & 0 & 0 & 1 & F6 \\ 0 & 0 & 0 & 0 & 0 & 0 & 1 \end{bmatrix} \begin{bmatrix} u \\ w \\ \theta \\ M \\ V \\ N \\ 1 \end{bmatrix}_{i-1} \quad (3.16)$$

where $K = \sqrt{|P|/(EI)}$ and $|P|$ is the magnitude of the force in the longitudinal direction determined from the previous iteration. For a wide cross-section (plane strain), $K = \sqrt{|P| \cdot (1-\nu^2)/(EI)}$ is used.

The seventh column for no axial force (P = 0) in the segment becomes

$$\begin{bmatrix} F1 \\ F2 \\ F3 \\ F4 \\ F5 \\ F6 \end{bmatrix} = \begin{bmatrix} -\dfrac{qL^2\cdot\sin\phi}{EA} \\ \dfrac{qL^4\cdot\cos\phi}{24\ EI} \\ -\dfrac{qL^3\cdot\cos\phi}{6\ EI} \\ -\dfrac{qL^2\cdot\cos\phi}{2} \\ -\ qL\cdot\cos\phi \\ qL\cdot\sin\phi \end{bmatrix} \qquad (3.17)$$

the seventh column for the tensile axial force (P > 0) in the segment is

$$\begin{bmatrix} F1 \\ F2 \\ F3 \\ F4 \\ F5 \\ F6 \end{bmatrix} = \begin{bmatrix} -\dfrac{qL^2\cdot\sin\phi}{EA} \\ \dfrac{q\cdot\cos\phi}{EIK^4}\cdot(\cosh KL - 1 - \dfrac{K^2\cdot L^2}{2}) \\ \dfrac{q\cdot\cos\phi}{EIK^3}\cdot(KL - \sinh KL) \\ -\dfrac{q\cdot\cos\phi}{K^2}\cdot(\cosh KL - 1) \\ -\ qL\cdot\cos\phi \\ qL\cdot\sin\phi \end{bmatrix} \qquad (3.18)$$

and the seventh column for the compressive axial force ($P < 0$) in the segment is

$$\begin{bmatrix} F1 \\ F2 \\ F3 \\ F4 \\ F5 \\ F6 \end{bmatrix} = \begin{bmatrix} -\dfrac{qL^2 \cdot \sin\phi}{EA} \\ -\dfrac{q \cdot \cos\phi}{EIK^4} \cdot \left(1 - \cos KL - \dfrac{K^2 L^2}{2}\right) \\ -\dfrac{q \cdot \cos\phi}{EIK^3} \cdot (KL - \sin KL) \\ -\dfrac{q \cdot \cos\phi}{K^2} (1 - \cos KL) \\ -qL \cdot \cos\phi \\ qL \cdot \sin\phi \end{bmatrix} \tag{3.19}$$

3.3.1.2 Initial Field Matrix

When the system in Fig. (3.1) is analyzed, axial forces on every element must be known or estimated initially because the field matrices depend on the axial forces. Since the axial forces on the elements are unknown during the initial iteration, initial values for the axial forces must be estimated in order to use the successive iteration method for the flexible-body analysis. For the first iteration, all of the axial forces are set to zero, i.e., no effects due to the axial forces are included in the field matrix. The initial field matrices can then be determined from Eq. (3.14). Then, a transfer matrix equation can be built using the initial field matrices and solved for the internal forces at every node of the member. For the next iteration, the elastic field matrices can be calculated from Eqs. (3.14) through (3.19) using the axial forces determined at the previous iteration.

3.3.1.3 Field Matrix for Rigid-Body Element

Frequently plate-shaped elements are connected with beam-shaped links in a mechanism as shown in Fig. (3.3a). In a flexible-body analysis, the elastic deflections in the plate-shaped links can be neglected, because the in-plane stiffnesses of the plates are usually much higher than those of the beams under in-plane forces.

A plate-element ABC in Fig. (3.3a) has three rigid-body beam elements as shown in Fig. (3.3b), where point D is the center of mass of the plate. The motion of rigid-body links can be represented by the rigid-body translational displacements followed by a rotation as shown in Fig. (3.3b).

To derive the field matrix for a rigid-body element, let link AD rotate an angle θ about point A as shown in Fig. (3.3c). The local coordinate system is set and then u and w is the displacements due to the rotation of the rigid-body element with small deflections. From the geometric relationships, the displacements are as follows:

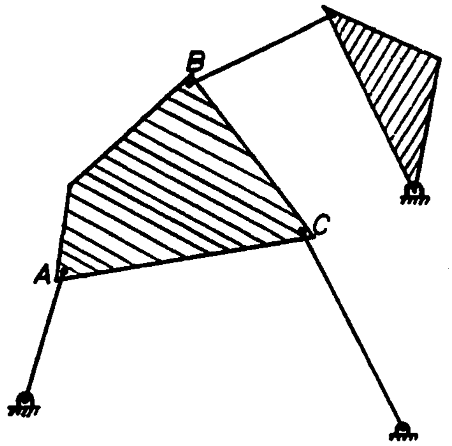

(a) A mechanism with Two Plate-Shaped Elements

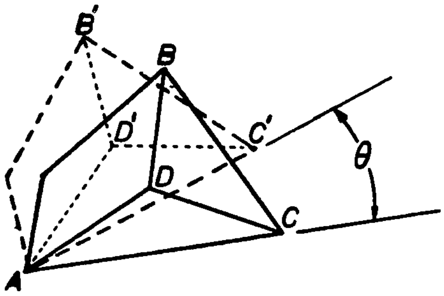

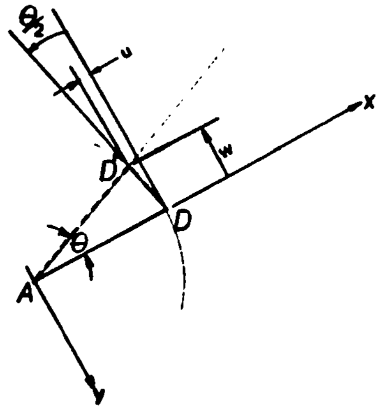

(b) Rotation of Plate-Shaped Link through an Angle θ

(c) Displacements of A Rigid-Body Element

FIGURE 3.3 A Mechanism with Plate-Shaped Links

$$u = \pm\ L\theta \cdot \sin\theta/2$$

$$w = \pm\ L\theta \cdot \cos\theta/2$$

The field matrix for a rigid-body element is given as follow in its local coordinate system:

$$[F] = \begin{bmatrix} 1 & 0 & -\delta L \cdot \sin\theta/2 & 0 & 0 & 0 & 0 \\ 0 & 1 & -\delta L \cdot \cos\theta/2 & 0 & 0 & 0 & 0 \\ 0 & 0 & 1 & 0 & 0 & 0 & 0 \\ 0 & 0 & 0 & 1 & L & 0 & 0 \\ 0 & 0 & 0 & 0 & 1 & 0 & 0 \\ 0 & 0 & 0 & 0 & 0 & 1 & 0 \\ 0 & 0 & 0 & 0 & 0 & 0 & 1 \end{bmatrix} \quad (3.20)$$

where θ is the rotational angle of the plate determined from the previous iteration and must be updated during the iterations. δ has a magnitude of 1 and has the same sign as the sign of the angle θ.

3.3.2 Point Matrix

The point matrix contains the effects of the external loads and moments applied at a specific point of a member. The transfer matrix equation at a specific point A as shown in Fig. (3.4a) is

$$\{S\}_A^R = [P]\cdot\{S\}_A^L$$

where $\{S\}_A^R$ = state vector at the right side of point A,

$\{S\}_A^L$ = state vector at the left side of point A,

and $[P]$ = point matrix at point A.

For a positive axial force (N), a positive transverse force (V), and a positive moment (M) applied in the coordinate system as shown in Fig. (3.4a), the equilibrium equations at point A shown in Fig. (3.4b) are as follows :

$$N_A^R = N_A^L - N$$
$$V_A^R = V_A^L - V$$
$$M_A^R = M_A^L - M$$

where R means the right side of point A,

L means the left side of point A,

N is a force in the axial direction,

V is a force in the transverse direction,

and M is a moment.

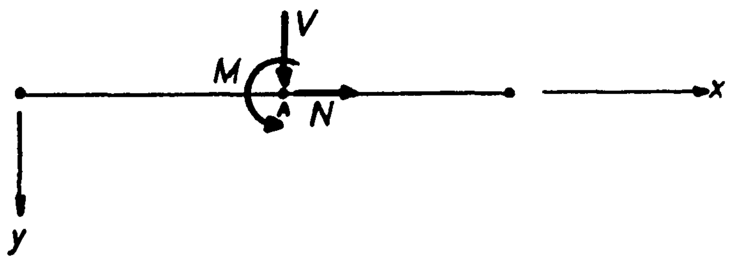

(a) External Forces at A Point for Point Matrix

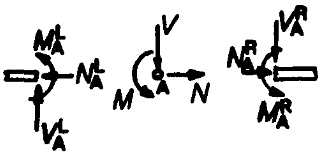

(b) Forces at Point A

FIGURE 3.4 Forces for Point Matrix

Then, the point matrix at point A becomes

$$[P] = \begin{bmatrix} 1 & 0 & 0 & 0 & 0 & 0 & 0 \\ 0 & 1 & 0 & 0 & 0 & 0 & 0 \\ 0 & 0 & 1 & 0 & 0 & 0 & 0 \\ 0 & 0 & 0 & 1 & 0 & 0 & -M \\ 0 & 0 & 0 & 0 & 1 & 0 & -V \\ 0 & 0 & 0 & 0 & 0 & 1 & -N \\ 0 & 0 & 0 & 0 & 0 & 0 & 1 \end{bmatrix} \quad (3.21)$$

3.3.3 Transformation Matrix

The transformation matrix transforms the geometric properties and state vector from one coordinate system to another rotated by the angle ϕ relative to the first coordinate system. The matrix equation at a point A in Fig. (3.5a) is

$$\{S\}_i = [T]\cdot\{S\}_{i-1}$$

where $\{S\}_i$ = state vector at A in the ith coordinate system,

$\{S\}_{i-1}$ = state vector at A in the (i-1) coordinate system,

and $[T]$ = transformation matrix at point A.

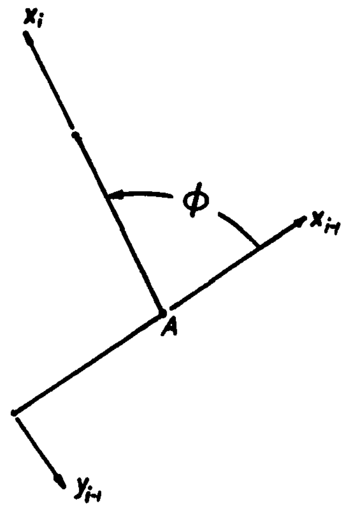

(a) Local Coordinate system in Each Segment

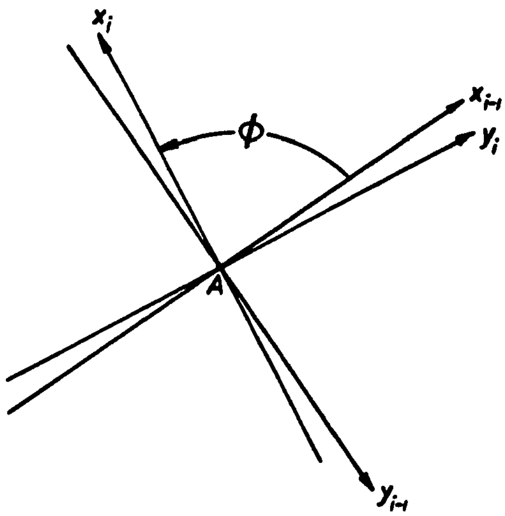

(b) Two Coordinate Systems at Point A

FIGURE 3.5 Coordinates for Transformation Matrix

The state variables of node A in the (i-1)th coordinate system are defined to those in the ith coordinate system as shown in Fig. (3.5b).

$$
\begin{aligned}
u_i &= u_{i-1}\cdot\cos\phi - w_{i-1}\cdot\sin\phi \\
w_i &= u_{i-1}\cdot\sin\phi + w_{i-1}\cdot\cos\phi \\
\theta_i &= \theta_{i-1} \\
M_i &= M_{i-1} \\
V_i &= V_{i-1}\cdot\cos\phi + N_{i-1}\cdot\sin\phi \\
N_i &= -V_{i-1}\cdot\sin\phi + N_{i-1}\cdot\cos\phi
\end{aligned}
$$

where u = displacement in the axial direction,

w = displacement in the transverse direction,

θ = slope,

M = moment,

V = force in the transverse direction,

and N = force in the axial direction.

The transformation matrix at the point is a simple rotation matrix as follows:

$$
[T] = \begin{bmatrix}
\cos\phi & -\sin\phi & 0 & 0 & 0 & 0 & 0 \\
\sin\phi & \cos\phi & 0 & 0 & 0 & 0 & 0 \\
0 & 0 & 1 & 0 & 0 & 0 & 0 \\
0 & 0 & 0 & 1 & 0 & 0 & 0 \\
0 & 0 & 0 & 0 & \cos\phi & \sin\phi & 0 \\
0 & 0 & 0 & 0 & -\sin\phi & \cos\phi & 0 \\
0 & 0 & 0 & 0 & 0 & 0 & 1
\end{bmatrix} \tag{3.22}
$$

3.3.4 Spring Matrix

The spring matrix contains the forces generated by a spring from the rigid-body kinematic displacements and elastic displacements. The matrix at a point A in Fig. (3.6a) is

$$\{S\}_A^R = [S]\cdot\{S\}_A^L$$

where $\{S\}_A^R$ = state vector at the right side of point A,

$\{S\}_A^L$ = state vector at the left side of point A,

and $[S]$ = spring matrix at point A.

Springs may be connected between the links in a mechanism or to the ground. Here, the spring forces of translational springs are considered. In Fig. (3.6a), the original positions of a mechanism (O P Q R) moves to the position (O P'Q'R) and the spring attachment point moves from A to A' for a ground-attached spring, and from C and D to C' and D', respectively, for a spring attached between two links. There are two types of spring forces in the mechanisms: one is developed from the displacements due to the kinematic motions (A to A' or line CD to C'D' in Fig. 3.6a) and the other comes from the elastic displacements (A' to A" or line C'D' to C"D" in Fig. 3.6b). Also, there are two types of spring end constraints: Pinned ends and sliding ends as shown in Fig. (3.6a). Sliding ends are connected to the frame only.

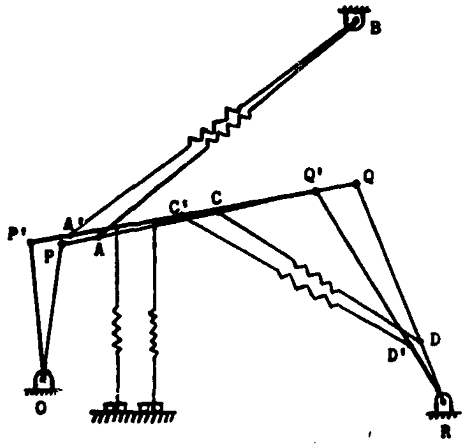

(a) Displacements due to The Kinematic Motions

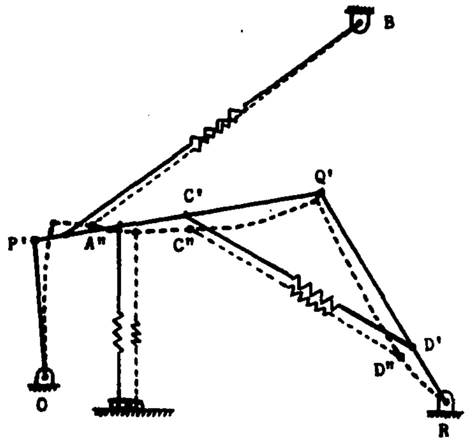

(b) Displacements due to The Elastic Deflections

FIGURE 3.6 Displacements for The Spring Matrix

3.3.4.1 Spring Forces Due To The Rigid-Body Kinematic Motion

The coordinates at Point A and A′ shown in Fig. (3.7) are assumed known from the rigid-body kinematic analysis. Thus, the length of OA′ (L) is

$$L = \sqrt{(x_o - x_{A'})^2 + (y_o - y_{A'})^2}$$

The generated force (F) along the OA′ axis is

$$F = -K\cdot(FL - L) = K\cdot(L - FL)$$

where FL is the free length of the spring.

The force components in the x- and y-directions are

$$\begin{aligned} Fx &= F\cdot\cos\theta = K\cdot(L - FL)\cdot\cos\theta \\ Fy &= -F\cdot\sin\theta = -K\cdot(L - FL)\cdot\sin\theta \end{aligned} \tag{3.23}$$

where K = spring stiffness,

θ = angle between the spring axis and the global x-axis,

and FL = free length of the spring.

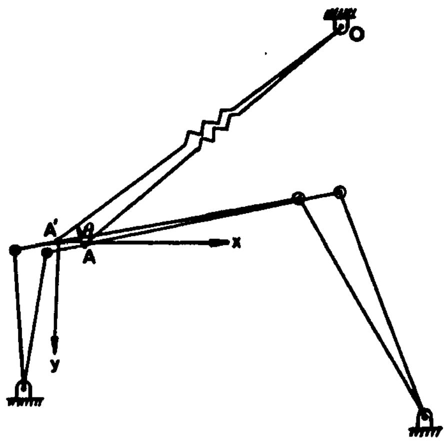

FIGURE 3.7 Rigid-Body Motion of A Mechanism

3.3.4.2 Spring Forces Due To The Elastic Displacements

Fig. (3.8a) shows the elastic displacements of a mechanism. Here, the angle θ is the angle between the spring axis and the global x-axis at point A'. The angle θ' is the angle between the spring axis and the global x-axis at point A". If Point A' moves to B, there is no additional spring force generated, because the lengths of OA' and OB are equal. But, when Point A' moves to A", there is a force reduction because of the elastic displacements.

To derive approximate relationships between the spring forces and elastic displacements, the coordinate system (x and y) is transformed into a new coordinate system (x' and y') located at Point A as shown in Fig. (3.8b). The displacement in y'-direction (w' in Fig. 3.8b) is the displacement involved to the spring force. This force is then decomposed into the x- and y-directions of the original coordinate system. The transformation angle between the two coordinate systems is $\theta s = \theta' + 90^\circ$. Thus, the transverse displacement (w') in the y'-direction as A moves from A' to A" becomes

$$W' = -u \cdot \sin \theta s + w \cdot \cos \theta s$$

The generated force (F) along the y'-direction is

$$F = -K \cdot w' = K \cdot u \cdot \sin \theta s - K \cdot w \cdot \cos \theta s$$

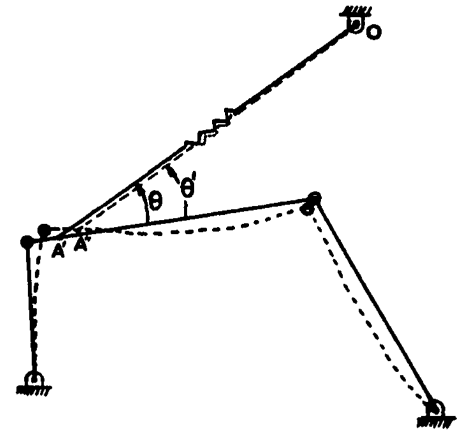

(a) Elastic Displacements of A Mechanism

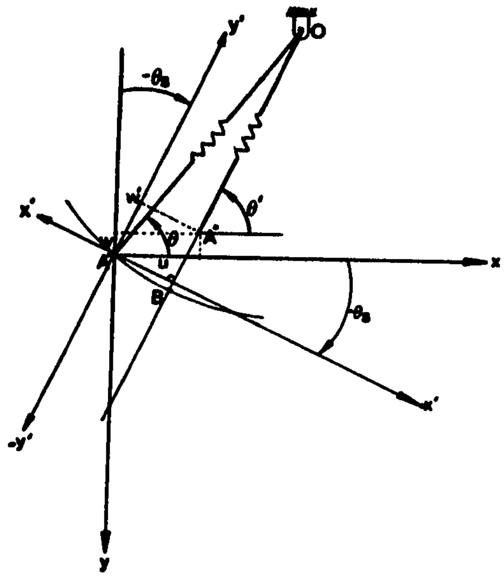

(b) Forces Due To The Elastic Displacements

FIGURE 3.8 Spring Forces Due To The Elastic Displacements

If the y'-axis has small deviations relative to the line OA" as shown in Fig. (3.8b), the angle θ' can be used to decompose the spring force into the components in the x- and y-directions as follows:

$$Fx = K \cdot \sin \theta s \cdot \cos \theta' \cdot u - K \cdot \cos \theta s \cdot \cos \theta' \cdot w$$

$$Fy = - K \cdot \sin \theta s \cdot \sin \theta' \cdot u + K \cdot \cos \theta s \cdot \sin \theta' \cdot w$$

Thus, these forces are rearranged in each displacement direction as follows:

$$\begin{aligned} Fxu &= K \cdot \sin \theta s \cdot \cos \theta' \cdot u \\ Fxw &= - K \cdot \cos \theta s \cdot \cos \theta' \cdot w \\ Fyu &= - K \cdot \sin \theta s \cdot \sin \theta' \cdot u \\ Fyw &= K \cdot \cos \theta s \cdot \sin \theta' \cdot w \end{aligned} \tag{3.24}$$

where Fxu = spring force in the x-direction due to the elastic displacement in the axial direction,

Fxw = spring force in the x-direction due to the elastic displacement in the transverse direction,

Fyu = spring force in the y-direction due to the elastic displacement in the axial direction,

and Fyw = spring force in the y-direction due to the elastic displacement in the transverse direction.

Finally, the spring matrix at a location of any spring is determined by combining Eqs. (3.23) and (3.24) as follows:

$$[S] = \begin{bmatrix} 1 & 0 & 0 & 0 & 0 & 0 & 0 \\ 0 & 1 & 0 & 0 & 0 & 0 & 0 \\ 0 & 0 & 1 & 0 & 0 & 0 & 0 \\ 0 & 0 & 0 & 1 & 0 & 0 & 0 \\ Syx & Syy & 0 & 0 & 1 & 0 & Syk \\ Sxx & Sxy & 0 & 0 & 0 & 1 & Sxk \\ 0 & 0 & 0 & 0 & 0 & 0 & 1 \end{bmatrix} \tag{3.25}$$

and

$$\begin{aligned} Syx &= K \cdot \sin\theta s \cdot \sin\theta' \\ Syy &= -K \cdot \cos\theta s \cdot \sin\theta' \\ Sxx &= -K \cdot \sin\theta s \cdot \cos\theta' \\ Sxy &= K \cdot \cos\theta s \cdot \cos\theta' \\ Syk &= K \cdot (L - FL) \cdot \sin\theta \\ Sxk &= -K \cdot (L - FL) \cdot \cos\theta \end{aligned} \tag{3.26}$$

where K = stiffness of a translational spring,

FL = free length of the spring,

L = spring length from rigid-body kinematics,

θs = angle between the spring axis and the global x-axis and $\theta s = \theta' + 90^\circ$,

θ = angle between the spring axis and the horizontal axis for rigid-body displacements alone,

θ' = angle between the spring axis and the horizontal axis for both rigid-body and elastic displacements,

Sxx = spring force intensity (force/length) in the x-direction due to the displacement in the x-direction,

Sxy = spring force intensity (force/length) in the x-direction due to the displacement in the y-direction,

Syx = spring force intensity (force/length) in the y-direction due to the displacement in the x-direction,

Syy = spring force intensity (force/length) in the y-direction due to the displacement in the y-direction,

Syk = spring force in the y-direction due to the pre-load and to the rigid-body displacements in the mechanism,

and Sxk = spring force in the x-direction due to the pre-load and to the rigid-body displacements in the mechanism.

3.3.4.3 Spring forces for A Spring Connected Between Links

For a spring interconnected between links, both connecting points move with the spring. As shown in Fig. (3.9a), Point C' moves to C" and Point D' moves to D". When the spring forces at Point C are calculated, Point D' is set to coincident to Point D" as shown in Fig. (3.9b) and then the same procedure in Section 3.3.4.2 are used to determine the spring forces due to the elastic displacements of Points C and D. For the spring forces at Point D, Point C' is coincident to Point C". Here, the total displacements used in Eq. (3.26) are the sum of the elastic displacements of both nodes.

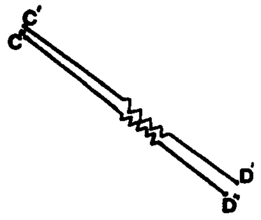

(a) Displacements of Both ends

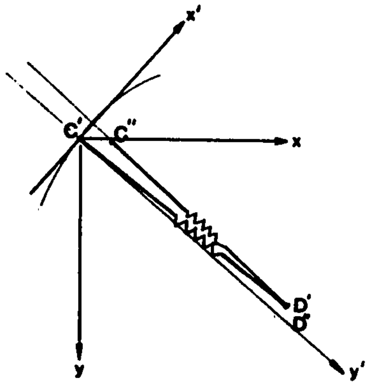

(b) Displacements of Point C For The Coincident Point D

FIGURE 3.9 Spring Forces For A Spring Connected Between Links

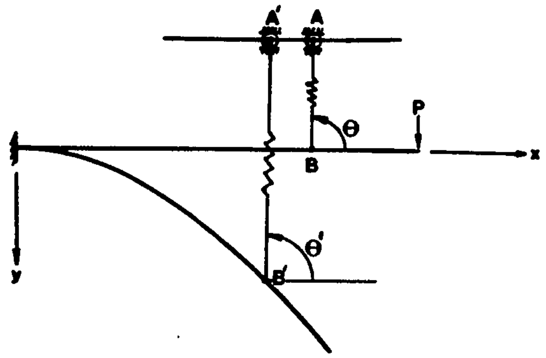

FIGURE 3.10 A Spring with A Sliding End

3.3.4.4 Spring Forces for A Spring with A Sliding End

Fig. (3.10) shows a spring with a sliding end. As the system deforms, Point A moves to A', and Point B moves to B'. Thus, the angle θ' remains the same angle as θ as shown in figure. A spring force is generated in only one direction and is calculated from the spring matrix given in Eqs. (3.25) and (3.26).

For example, the spring forces generated at point B in Fig. (3.10) are calculated from the condition of the angles $\theta = \theta' = 90^\circ$ as follows:

$$\theta s = \theta' + 90^\circ = 180.0^\circ$$

and from Eq. (3.24),

$$Syu = 0.0$$

$$Syw = - K \cdot w$$

$$Sxu = 0.0$$

$$Sxw = 0.0$$

It means that the spring force at node B is generated in the negative y-direction only due to the displacement in the positive y-direction.

3.3.5 Branch Systems

3.3.5.1 Types of Branch Systems

Several types of branches may be connected to the main system (loop) in multiloop mechanisms. Thus, the properties of these branch systems must be incorporated into the main loop. Generally, four types of one degree-of-freedom branches are considered in this research. These types are given in Fig. (3.11). The detail procedures for the subloop matrix equations are presented in Chapter 5.

3.3.5.2 Branch Matrix

The branch matrix contains the properties of a branch system. At any branch point in the system, the transfer matrix equation becomes

$$\{S\}_A^R = [B]\cdot\{S\}_A^L$$

where $\{S\}_A^R$ = state vector at the right side of point A,

$\{S\}_A^L$ = state vector at the left side of point A,

and $[B]$ = branch matrix at point A.

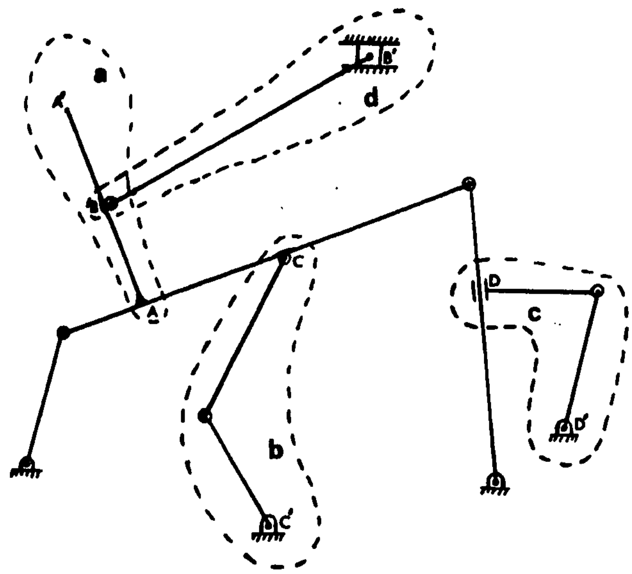

FIGURE 3.11 Four Types of Sub-Loop Systems

(a) A Fixed Branch with A Free End

(b) A Revolute Branch with A Pin End

(c) A Slide Branch with A Pin End

(d) A Revolute Branch with A Slide End

The general transfer matrix equation for any of the subloop systems in Fig. (3.11) is

$$\begin{bmatrix} u \\ w \\ \theta \\ M \\ V \\ N \\ 1 \end{bmatrix}_P = \begin{bmatrix} U(1,1) & U(1,2) & U(1,3) & U(1,4) & U(1,5) & U(1,6) & U(1,7) \\ U(2,1) & U(2,2) & U(2,3) & U(2,4) & U(2,5) & U(2,6) & U(2,7) \\ U(3,1) & U(3,2) & U(3,3) & U(3,4) & U(3,5) & U(3,6) & U(3,7) \\ U(4,1) & U(4,2) & U(4,3) & U(4,4) & U(4,5) & U(4,6) & U(4,7) \\ U(5,1) & U(5,2) & U(5,3) & U(5,4) & U(5,5) & U(5,6) & U(5,7) \\ U(6,1) & U(6,2) & U(6,3) & U(6,4) & U(6,5) & U(6,6) & U(6,7) \\ 0 & 0 & 0 & 0 & 0 & 0 & 1 \end{bmatrix} \cdot \begin{bmatrix} u \\ w \\ \theta \\ M \\ V \\ N \\ 1 \end{bmatrix}_{P'} \qquad (3.27)$$

From the end conditions of the subloop system, three components in the state variables must be zero, and the other three are unknown. For the subloop from A to A′, an end at Point A′ is free so that $M = V = N = 0$ and three displacements are unknown. Thus, the transfer matrix equation of the branch system simplifies to

$$\begin{bmatrix} u \\ w \\ \theta \\ M \\ V \\ N \\ 1 \end{bmatrix}_A = \begin{bmatrix} U(1,1) & U(1,2) & U(1,3) & U(1,7) \\ U(2,1) & U(2,2) & U(2,3) & U(2,7) \\ U(3,1) & U(3,2) & U(3,3) & U(3,7) \\ U(4,1) & U(4,2) & U(4,3) & U(4,7) \\ U(5,1) & U(5,2) & U(5,3) & U(5,7) \\ U(6,1) & U(6,2) & U(6,3) & U(6,7) \\ 0 & 0 & 0 & 1 \end{bmatrix} \cdot \begin{bmatrix} u \\ w \\ \theta \\ 1 \end{bmatrix}_{A'} \qquad (3.28)$$

Then, Eq. (3.28) can be partitioned into two matrices as follows:

$$\begin{bmatrix} u \\ w \\ \theta \\ 1 \end{bmatrix}_A = [\ Z1\ ] \cdot \begin{bmatrix} u \\ w \\ \theta \\ 1 \end{bmatrix}_{A'} \tag{3.29}$$

and

$$\begin{bmatrix} M \\ V \\ N \\ 1 \end{bmatrix}_A = [\ Z2\ ] \cdot \begin{bmatrix} u \\ w \\ \theta \\ 1 \end{bmatrix}_{A'} \tag{3.30}$$

From Eqs. (3.29) and (3.30), the forces must be functions of the displacements at the branch point as follows:

$$\begin{bmatrix} M \\ V \\ N \\ 1 \end{bmatrix}_A = [Z2]\cdot[Z1]^{-1} \cdot \begin{bmatrix} u \\ w \\ \theta \\ 1 \end{bmatrix}_A = [ZZ] \cdot \begin{bmatrix} u \\ w \\ \theta \\ 1 \end{bmatrix}_A \tag{3.31}$$

Rewriting Eq. (3.31) gives

$$M_A = ZZ(1,1)\cdot u_A + ZZ(1,2)\cdot w_A + ZZ(1,3)\cdot \theta_A + ZZ(1,4)$$

$$V_A = ZZ(2,1)\cdot u_A + ZZ(2,2)\cdot w_A + ZZ(2,3)\cdot \theta_A + ZZ(2,4)$$

$$M_A = ZZ(3,1)\cdot u_A + ZZ(3,2)\cdot w_A + ZZ(3,3)\cdot \theta_A + ZZ(3,4)$$

Finally, a branch matrix can be derived from Eq. (3.31) as follows:

$$[B] = \begin{bmatrix} 1 & 0 & 0 & 0 & 0 & 0 & 0 \\ 0 & 1 & 0 & 0 & 0 & 0 & 0 \\ 0 & 0 & 1 & 0 & 0 & 0 & 0 \\ ZZ(1,1) & ZZ(1,2) & ZZ(1,3) & 1 & 0 & 0 & ZZ(1,4) \\ ZZ(2,1) & ZZ(2,2) & ZZ(2,3) & 0 & 1 & 0 & ZZ(2,4) \\ ZZ(3,1) & ZZ(3,2) & ZZ(3,3) & 0 & 0 & 1 & ZZ(3,4) \\ 0 & 0 & 0 & 0 & 0 & 0 & 1 \end{bmatrix} \qquad (3.32)$$

The branch matrix in Eq. (3.32) can be determined from the same procedure from Eq. (3.27) to Eq. (3.31) for all types of subloop systems. However, the ZZ(i,j)'s in Eq. (3.32) are different depending on a subloop system. The formulation details for each subloop system are given in Section 5.4.

3.3.6 Inertial Matrices for Dynamic Analyses

To get quasi-static and time-domain responses from a dynamic analysis, the effects of the lumped mass of the links must be considered. In dynamic analyses of flexible mechanism, the inertial forces from the rigid-body kinematic accelerations acting on the members are sometimes treated as external forces at the locations of the lumped masses. But, the elastic-body accelerations from the axial and transverse vibrations of the members can not be determined directly. To account for the effects of these elastic-body vibrations from the lumped masses, the Houbolt difference direct integration method is used since this method is one of the most effective and stable methods available [96-97].

At node A of a lumped mass as shown in Fig. (3.12a), the transfer matrix equation becomes

$$\{S\}_A^R = [M]\cdot\{S\}_A^L$$

where $\{S\}_A^R$ = state vector at the right side of point A,

$\{S\}_A^L$ = state vector at the left side of point A,

and $[M]$ = inertial matrix for the lumped mass at point A.

The rigid-body inertial matrix for the quasi-static analysis is derived in Section 3.3.6.1. The elastic-body inertial matrix for the time-domain analysis is given in Section 3.3.6.2. The procedure for the dynamic analysis is briefly explained in Section 3.3.6.3.

(a) A Lumped Mass at Point A

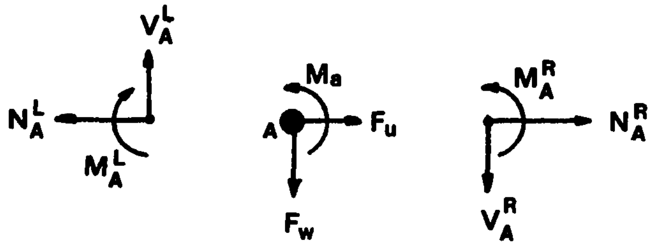

(b) Rigid-Body Inertial Forces

FIGURE 3.12 A Lumped Mass with Rigid-Body Kinematic Accelerations

3.3.6.1 Rigid-Body Inertial Matrix for Quasi-Static Analysis

The rigid-body inertial forces in the global coordinate system as shown in Fig. (3.12b) can be calculated from the rigid-body accelerations due to the kinematic motions:

$$
\begin{aligned}
Fu &= -\, m \cdot Au \\
Fw &= -\, m \cdot Aw \\
Ma &= -\, I \cdot Aa
\end{aligned}
\tag{3.33}
$$

where Fu = inertial force in the longitudinal direction,

Fw = inertial force in the transverse direction,

M = inertial moment due to the angular acceleration,

m = lumped-mass,

I = mass moment of inertia about the center of mass,

Au = rigid-body linear accelerations in the longitudinal direction,

Aw = rigid-body linear accelerations in the transverse direction,

Aa = angular acceleration of the rigid-body links.

The rigid-body inertial matrix including the inertial effects due to the rigid-body kinematic accelerations is analogous to the point matrix discussed earlier. The result becomes:

$$[M] = \begin{bmatrix} 1 & 0 & 0 & 0 & 0 & 0 & 0 \\ 0 & 1 & 0 & 0 & 0 & 0 & 0 \\ 0 & 0 & 1 & 0 & 0 & 0 & 0 \\ 0 & 0 & 0 & 1 & 0 & 0 & I\cdot Aa \\ 0 & 0 & 0 & 0 & 1 & 0 & m\cdot Aw \\ 0 & 0 & 0 & 0 & 0 & 1 & m\cdot Au \\ 0 & 0 & 0 & 0 & 0 & 0 & 1 \end{bmatrix} \tag{3.34}$$

3.3.6.2 Elastic-Body Inertial Matrix For Time-Domain Analysis

3.3.6.2.1 Governing Equations of Motion

The fundamental equations of motion in first order form are as follows: For the transverse direction,

$$\frac{\partial w}{\partial x} = -\theta \tag{3.35}$$

$$\frac{\partial \theta}{\partial x} = \frac{M}{EI} \tag{3.36}$$

$$\frac{\partial M}{\partial x} = V \tag{3.37}$$

$$\frac{\partial V}{\partial x} = -\rho\cdot\frac{\partial^2 w}{\partial t^2} \tag{3.38}$$

and also for the axial direction,

$$\frac{\partial u}{\partial x} = \frac{N}{EA} \tag{3.39}$$

$$\frac{\partial N}{\partial x} = -\rho \cdot \frac{\partial^2 u}{\partial t^2} \tag{3.40}$$

where u = displacement in the axial direction,

w = displacement in the transverse direction,

θ = slope,

M = bending moment,

V = internal force in the transverse direction,

N = internal force in the axial direction,

x = position axially along the shaft,

A = area of cross-section,

E = modulus of elasticity,

I = area moment of inertia,

ρ = mass per unit length,

and

t = time.

3.3.6.2.2 Houbolt Difference Direct Integration Scheme

For a system of ordinary differential equations with constant coefficients, any convenient finite difference expressions to approximate the accelerations and velocities in terms of displacements can be used. Theoretically, a large number of different finite difference expressions could be employed. However, the solution scheme should be effective, and it follows that only a few schemes need to be considered.

For elastic-body inertial forces for the time-domain analyses, the Houbolt difference scheme is used. The method is based on a third-order interpolation of displacements. In the Houbolt integration scheme, multi-step implicit formulas for velocity and acceleration are derived in terms of displacements using backward differences shown in Fig. (3.13). The difference formulas in the Houbolt difference method has the following relationships [96-97]:

$$q_t = q_{t+\Delta t} - \Delta t \dot{q}_{t+\Delta t} + \frac{\Delta t^2}{2} \ddot{q}_{t+\Delta t} - \frac{\Delta t^3}{6} \dddot{q}_{t+\Delta t}$$

$$q_{t-\Delta t} = q_{t+\Delta t} - (2\,\Delta t)\dot{q}_{t+\Delta t} + \left(\frac{2\,\Delta t}{2}\right)^2 \ddot{q}_{t+\Delta t} - \left(\frac{2\,\Delta t}{6}\right)^3 \dddot{q}_{t+\Delta t}$$

$$q_{t-2\Delta t} = q_{t+\Delta t} - (3\,\Delta t)\dot{q}_{t+\Delta t} + \left(\frac{3\,\Delta t}{2}\right)^2 \ddot{q}_{t+\Delta t} - \left(\frac{3\,\Delta t}{6}\right)^3 \dddot{q}_{t+\Delta t}$$

Solving the above equations for acceleration and velocity gives the following difference formulas:

$$\begin{aligned} \ddot{q}_{t+\Delta t} &= \frac{1}{\Delta t^2}(2q_{t+\Delta t} - 5q_t + 4q_{t-\Delta t} - q_{t-2\Delta t}) \\ \dot{q}_{t+\Delta t} &= \frac{1}{6\,\Delta t}(11q_{t+\Delta t} - 18q_t + 9q_{t-\Delta t} - 2q_{t-2\Delta t}) \end{aligned} \tag{3.41}$$

The inertial forces from the elastic vibrations of the links in Eqs. (3.38) and (3.40) can be formulated using the Houbolt difference algorithm. Eq. (3.38) is changed at the time t+Dt as follows:

$$\frac{\partial V_{t+\Delta t}}{\partial x} = -\rho \frac{\partial^2 w_{t+\Delta t}}{\partial t^2} \tag{3.42}$$

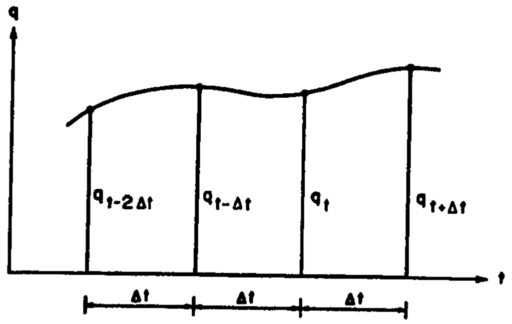

FIGURE 3.13 Displacement Versus Time

Substituting Eq. (3.41) into Eq. (3.42) gives

$$\frac{dV_{t+\Delta t}}{dx} = - \frac{\rho}{Dt^2} [2 w_{t+\Delta t} - 5 w_t + 4 w_{t-\Delta t} - w_{t-2\Delta t}] \tag{3.43}$$

and Eq. (3.40) becomes:

$$\frac{dN_{t+\Delta t}}{dx} = - \frac{\rho}{Dt^2} [2 w_{t+\Delta t} - 5 w_t + 4 w_{t-\Delta t} - w_{t-2\Delta t}] \tag{3.44}$$

From Eqs. (3.43) and (3.44) the elastic-body inertial forces at any time t+Dt are as follows:

$$\begin{aligned} Ve &= - \frac{2m}{Dt^2} w_{t+\Delta t} - \frac{m}{Dt^2} [- 5 w_t + 4 w_{t-\Delta t} - w_{t-2\Delta t}] \\ Ne &= - \frac{2m}{Dt^2} u_{t+\Delta t} - \frac{m}{Dt^2} [- 5 u_t + 4 u_{t-\Delta t} - u_{t-2\Delta t}] \end{aligned} \tag{3.45}$$

where Ve = elastic-body inertial force in the transverse direction,

Ne = elastic-body inertial force in the axial direction,

m = mass of a lumped-mass,

u = displacements of the lumped-mass in the axial direction,

and w = displacements of the lumped-mass in the transverse direction.

3.3.6.2.3 Elastic-body Inertial Matrix

Fig. (3.13a) shows the rigid-body inertial forces due to the rigid-body accelerations. Fig. (3.13b) gives the elastic-body inertial forces due to the elastic vibrations of the members. At a lumped-mass of Point A, the total of the inertial forces are determined by summing the rigid-body inertial forces (Fig. 3.13a) and the elastic-body inertial forces (Fig. 3.13b) as follows:

$$
\begin{aligned}
M_A^R &= M_A^L - Ma \\
V_A^R &= V_A^L - Ve - Fw \\
N_A^R &= N_A^L - Ne - Fu
\end{aligned}
\qquad (3.46)
$$

where

M = moment,

V = force in the transverse direction,

N = force in the axial direction,

Ma = moment due to the rigid-body angular acceleration,

Fw = transverse force due to the rigid-body acceleration,

Fu = axial force due to the rigid-body acceleration,

Ve = transverse force due to the elastic vibrations at a time,

Ne = axial force due to the elastic vibrations at a time.

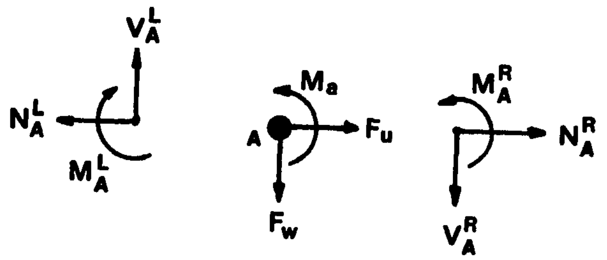

(a) Rigid-Body Inertial Forces

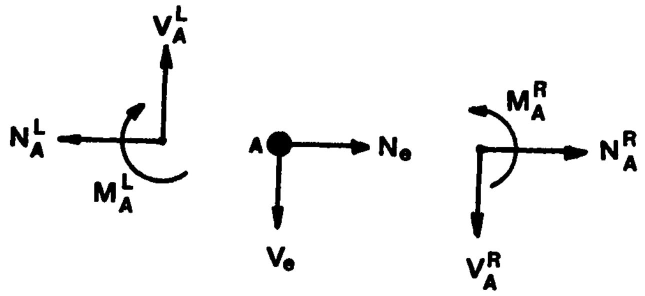

(b) Elastic-Body Inertial Forces

FIGURE 3.14 Inertial Forces of A Lumped-Mass at Point A

By substituting Eqs. (3.33) and (3.45) into Eq. (3.46), the elastic-body inertial matrix is derived as follows:

$$[M] = \begin{bmatrix} 1 & 0 & 0 & 0 & 0 & 0 & 0 \\ 0 & 1 & 0 & 0 & 0 & 0 & 0 \\ 0 & 0 & 1 & 0 & 0 & 0 & 0 \\ 0 & 0 & 0 & 1 & 0 & 0 & Fmm \\ 0 & Fmw & 0 & 0 & 1 & 0 & Fww \\ Fmu & 0 & 0 & 0 & 0 & 1 & Fuu \\ 0 & 0 & 0 & 0 & 0 & 0 & 1 \end{bmatrix} \quad (3.47)$$

and

$$\begin{aligned} Fmw &= 2m/Dt^2 \\ Fmu &= 2m/Dt^2 \\ Fmm &= I\ Aa \\ Fww &= \frac{m}{Dt^2}\left[-5\, w_t + 4\, w_{t-\Delta t} - w_{t-2\Delta t} \right] + m \cdot Aw \\ Fuu &= \frac{m}{Dt^2}\left[-5\, u_t + 4\, u_{t-\Delta t} - u_{t-2\Delta t} \right] + m \cdot Au \end{aligned} \quad (3.48)$$

where m = mass of a lumped-mass,

Dt = time interval,

I = mass moment of inertia,

Aa = rigid-body angular acceleration of link,

Au = rigid-body acceleration in the axial direction,

Aw = rigid-body acceleration in the transverse direction,

u = displacements of the lumped-mass in the axial direction,

and w = displacements of the lumped-mass in the transverse direction.

3.3.6.3 Procedure for The Inertial Matrices

In a dynamic analysis for quasi-static responses, the rigid-body accelerations of lumped masses are required to be calculated from the kinematic acceleration analysis. These inertial forces due to the rigid-body kinematic accelerations acting on the members can be treated as external forces at the locations of the lumped masses. Thus, Eq. (3.34) can be used directly for the dynamic analysis for the quasi-static responses of mechanisms.

However, the elastic-body accelerations due to the elastic vibrations of the members can not be calculated directly. To account for the effects of the elastic-body vibrations, a direct integration method is used. The direct integration method is that static equilibrium, which includes the effects of inertial forces, is sought at discrete time points within the interval of solution. Therefore, all solution techniques employed in the static analysis can also be used effectively in direct integration. The second point is that a specific variation of displacements, velocities, and accelerations within each time interval is assumed.

Displacements, velocities, and accelerations of elastic members due to the elastic vibrations are zero at the initial position (initial conditions). Time interval is calculated from the angular velocity of an input-link in a mechanism and the angle interval to the next position to be analyzed as follow [27-28]:

$$Dt = \frac{\pi \cdot \Delta\theta}{\Omega} \tag{3.49}$$

where Dt = time interval in Eq. (3.48),

$\Delta\theta$ = angular difference to each position of the mechanism,

and Ω = angular velocity of the input-link.

Thus, all of the displacements of every node in the system are calculated from the rigid-body inertial forces and the elastic-body inertial forces at each position. The elastic-body inertial forces of every lumped-mass due to the elastic vibrations are computed from Eq. (3.45) using the displacements at three positions. The inertial matrix at next position of the mechanism can be evaluated from Eq. (3.48) using the displacements determined at the previous positions of the mechanism.

3.4 Comparison with The Solutions of Flexible Mechanisms

As a first comparative study, a four-bar crank-rocker mechanism shown in Fig. (3.15) is analyzed. This mechanism is examined by Buhgat and Willmert [12] using a displacement-based finite element method and a high-order hermite polynomial approximation.

The data for the mechanism shown in Fig. (3.15) are:

Length of input crank (AB) = 5.0 inches.
Length of coupler (BC) = 11.0 inches.
Length of follower (CD) = 10.5 inches.
Fixed distance (AD) = 10.0 inches.

The initial position of the crank at t = 0 coincides with the ground link as shown in Fig. (3.15). The angular speed of the crank is constant at 125 rad/sec, and each bar is considered to be a steel rod with 0.25 inch wide and 1.0 inch high.

The results are compared with the solutions presented in Reference [12] and given in Figs. (3.16) - (3.19). Figs. (3.16) and (3.17) give the displacements in the horizontal direction and slopes at node B, respectively, as a function of crank angle. Fig. (3.18) shows the horizontal displacements at node C, and Fig. (3.19) gives the stresses at the mid-point of the coupler. The comparative study shows that both solutions are in good agreement.

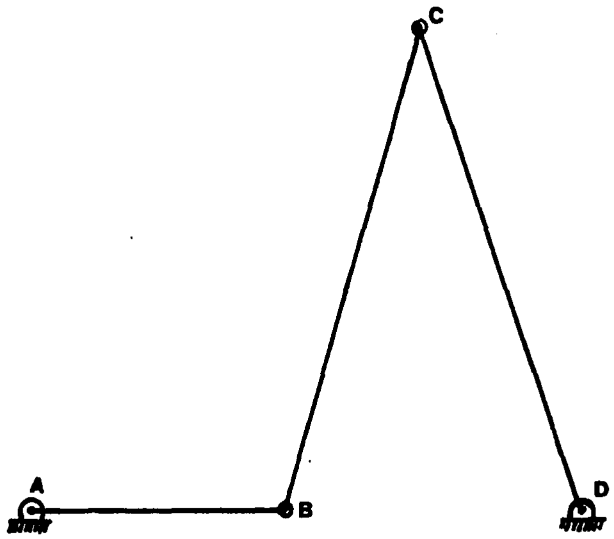

FIGURE 3.15 Four-Bar Mechanism

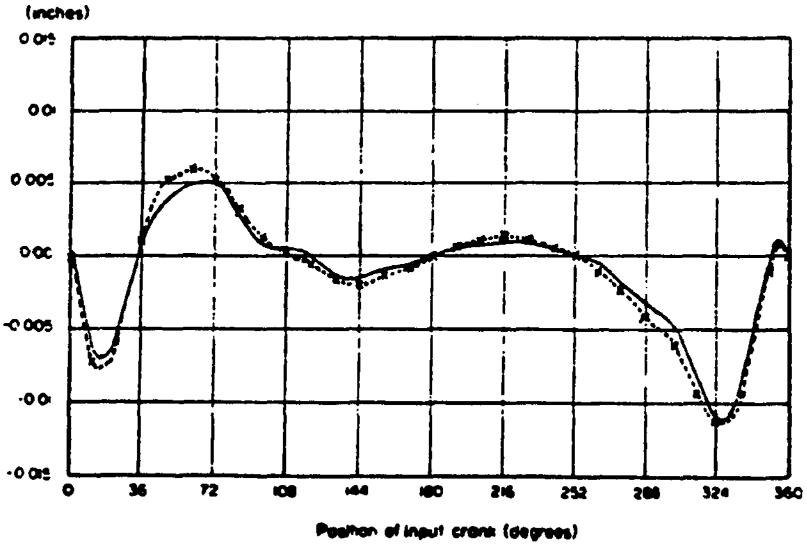

——————— Solution from Reference [12]

-- ★ --- ★ --- Solution from the developed method

FIGURE 3.16 Horizontal Displacements at Node B

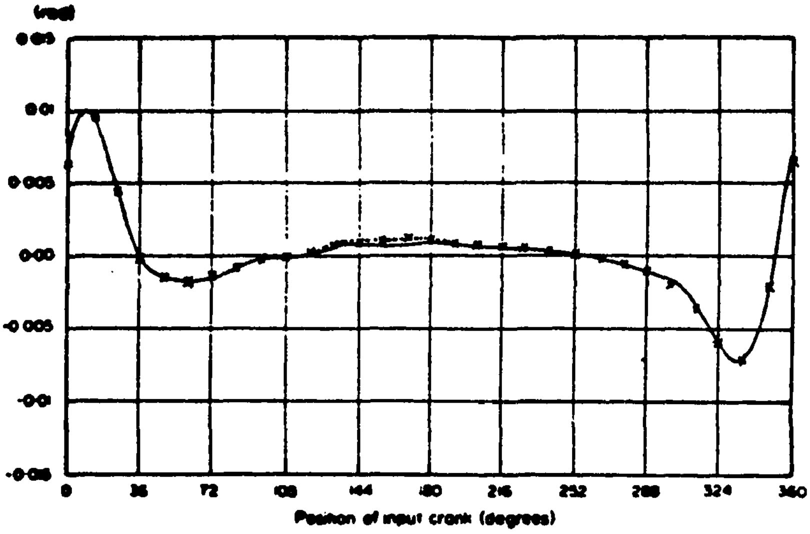

———————— Solution from Reference [12]

-- ★ --- ★ --- Solution from the developed method

FIGURE 3.17 Slopes at Node B

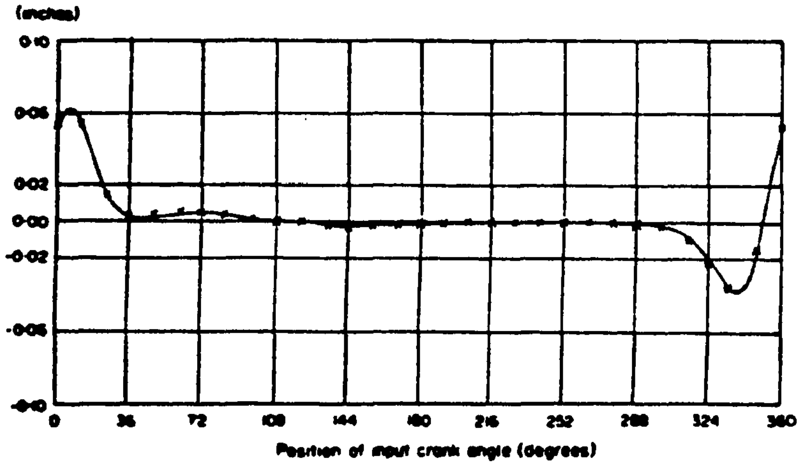

———————— Solution from Reference [12]

-- ★ --- ★ --- Solution from the developed method

FIGURE 3.18 Horizontal Displacement at Node C

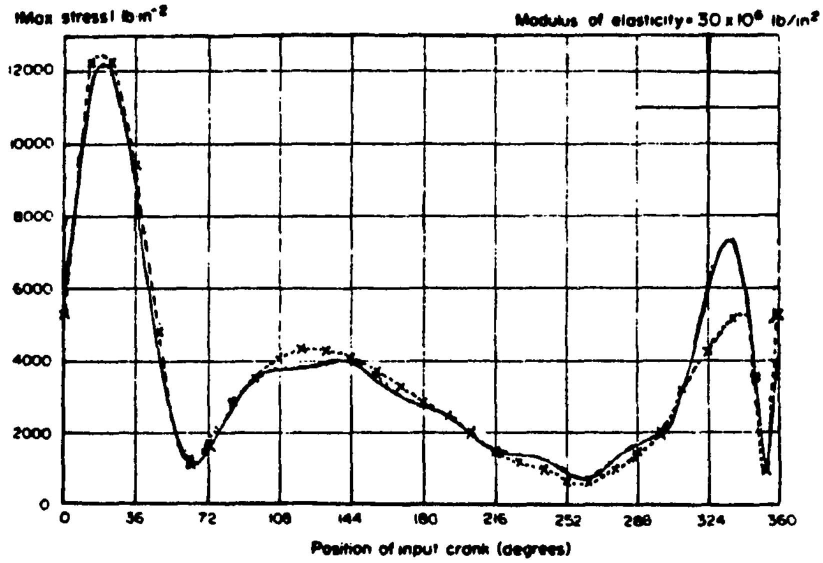

——————— Solution from Reference [12]

— * --- * --- Solution from the developed method

FIGURE 3.19 Stresses at Mid-Point of the Coupler

As a second study, a four-bar crank-rocker mechanism as given in References [7, 9, 11, 17] is studied. The geometry of the mechanism shown in Fig. (3.20) has the following dimensions:

Length of crank	=	4.0 inches.
Length of coupler	=	11.0 inches.
Length of Follower	=	10.5 inches.
Ground link	=	10.0 inches.

The model in [7, 9] was constructed of aluminum strip 1.0 inch wide. The crank was 0.167 inch thick. The coupler and follower links were 0.063 inch thick. The coupler was connected to the crank and the follower by means of pins and small ball bearings mounted in sleeves. The total weight of the bearing and the sleeve at each end was 0.06 lb. Other apparatus details may be found in [7, 9]. In References [11, 17], the total weight of the bearing and the sleeve was assumed to be distributed equally to lumped masses on the crank and follower.

The input-link is rotated at 400 rpm in the clockwise direction. Fig. (3.21) gives the nomalized rigid-body angular acceleration of the follower plotted against the crank rotation angle. The results are the quasi-static strains at mid-point of the follower. These strains are illustrated in Fig. (3.22) and show in good agreement. Finally, Fig. (3.23) shows the steady-state strains at the mid-point of the follower determined from the time-domain analysis. The solution details are given in Section 8.3 and Appendix C.

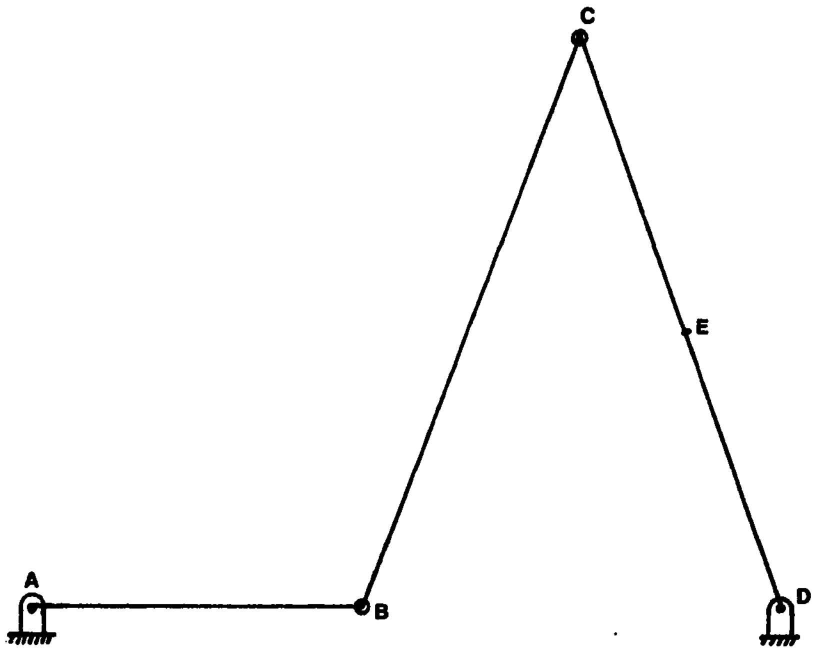

FIGURE 3.20 Four-Bar Crank-Rocker Mechanism

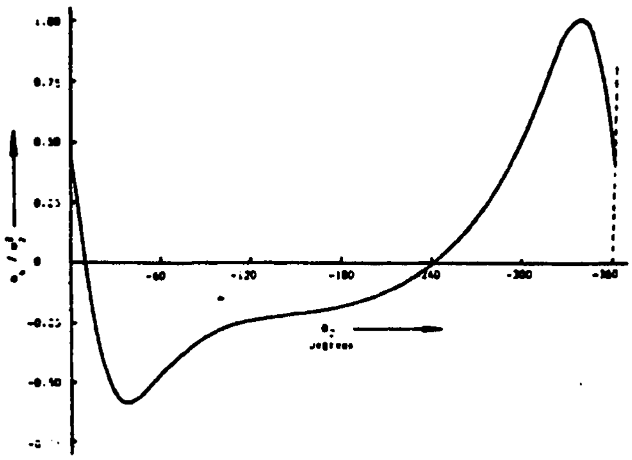

FIGURE 3.21 Nomalized Rigid-Body Angular Acceleration of Follower

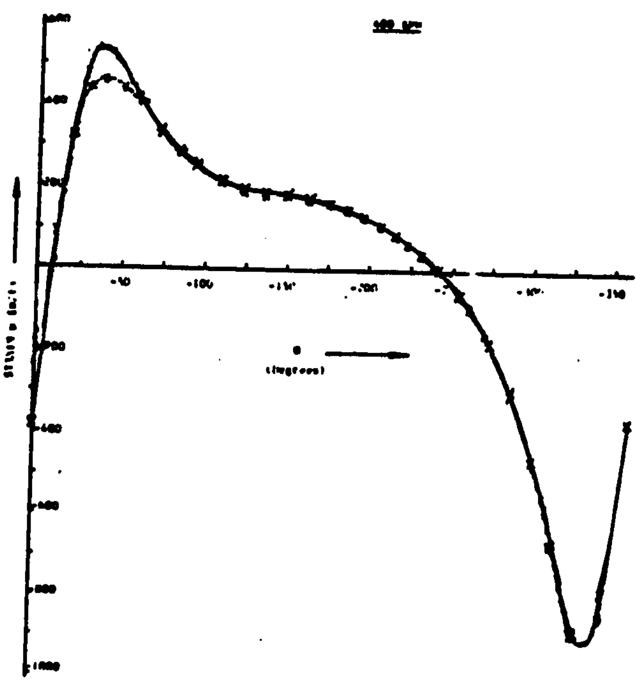

——————— Solution from Reference [17]

-- * --- * --- Solution from the developed method

FIGURE 3.22 Quasi-Static Strains at Mid-Point of Follower

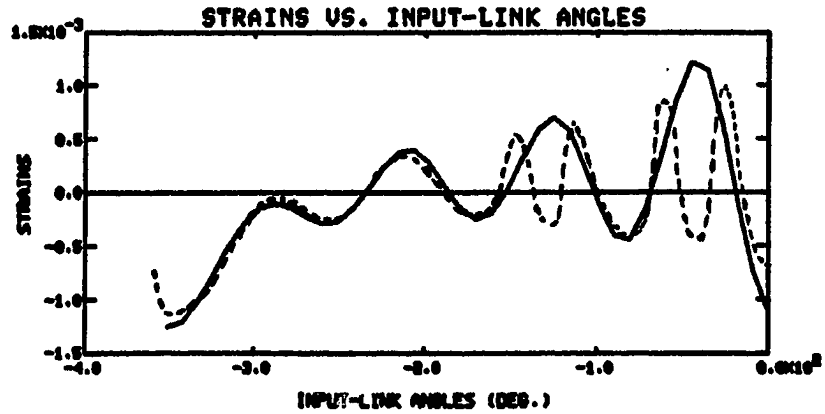

- - - - - - - - Solution from Reference [7, 9]

——————— Solution from the developed method

FIGURE 3.23 Steady-State Strains at Mid-Point of Follower

CHAPTER IV

APPROXIMATE METHOD FOR LARGE-DEFLECTION ANALYSIS

4.1 Introduction

In Section 3.3.1, the elastic field matrices for the small-deflection analyses are derived by assuming a linear system. However, large-deflection problems can not be solved by superposition of the displacements, because the system is nonlinear. Thus, the solutions for the large-deflection problems can not be obtained directly from elementary beam theory for linearized systems since the basic assumptions are no longer valid. Specifically, elementary theory neglects the square of the first derivative in the beam curvature formula and provides no correction for the shortening of the moment-arm caused by transverse deflections. Thus, for large loads elementary theory for a linearized system can give deflections greater than the length of the system.

The objective of this chapter is to develop an approximate method for the large-deflection analyses. Then, the solutions determined from the approximate method developed are compared with exact solutions [86-88].

4.2 Fundamentals for Large-Deflection Analysis

As mentioned earlier, large-deflection problems cannot be solved directly from elementary beam theory for the linearized systems, because the theory neglects both the square of the first derivative in the denominator of the beam curvature formula and the shortening of the moment-arm. However, if these effects are evaluated approximately and involved iteratively, the large-deflection problems may be analyzed using linearized equations. Hence, from the state equations given by Eqs. (3.14)-(3.19) for the linearized system, the displacements are corrected by a geometric relationship. Then, an updated average axial force in each segment is determined from equilibrium conditions. The corrections for the displacements and average axial force are updated at every iteration.

A general beam subjected to external loadings is represented in Fig. (4.1). Regardless of the beam loading, the beam can be accurately modeled as a series of discrete segments so that each segment is subjected to the internal forces at both ends as shown in Fig. (4.2). Each segment has its own local coordinate system oriented at an angle with respect to the fixed global system. The position of the local coordinate system must be updated as the member deforms.

A typical beam segment can be represented as shown in Fig. (4.3). The internal forces at both ends are present in the local coordinate system. As the segment deflects, the moment-arm is shortened by the transverse displacement due to the transverse loading.

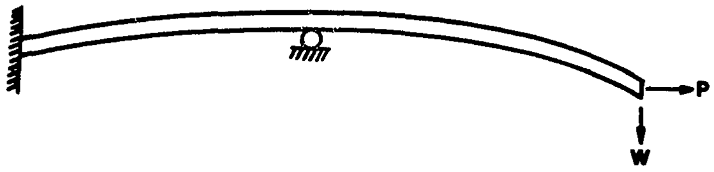

FIGURE 4.1 A General Beam Subjected to External Loadings

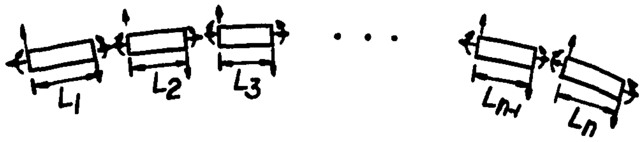

FIGURE 4.2 Beam Divided into Finite Segments

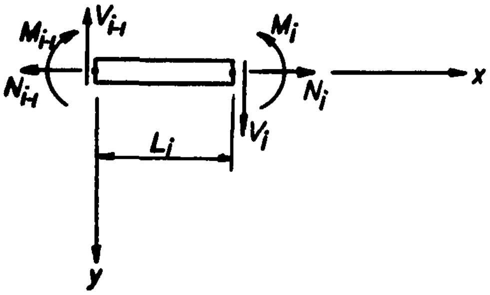

FIGURE 4.3 Internal Forces in A Segment

The relationships among the displacements and internal forces at both ends of segment under axial tension can be determined from Eqs. (3.15) and (3.18) as follows:

$$u'_i = u'_{i-1} + \frac{L}{EA} \cdot N_{i-1} - \frac{q \cdot L^2 \cdot \sin\phi}{EA} \tag{4.1}$$

$$\begin{aligned} w'_i = {} & w'_{i-1} - \frac{\sinh KL}{K} \cdot \theta_{i-1} + \frac{1 - \cosh KL}{P} \cdot M_{i-1} \\ & + \left(\frac{L}{P} - \frac{\sinh KL}{KP}\right) \cdot V_{i-1} + \frac{q \cdot \cos\phi}{EIK^4} \cdot \left(\cosh KL - 1 - \frac{K^2 L^2}{2}\right) \end{aligned} \tag{4.2}$$

$$\begin{aligned} \theta_i = {} & \cosh KL \cdot \theta_{i-1} + \frac{K \cdot \sinh KL}{P} \cdot M_{i-1} + \frac{\cosh KL - 1}{P} \cdot N_{i-1} \\ & + \frac{q \cdot \cos\phi}{EIK^3} \cdot (KL - \sinh KL) \end{aligned} \tag{4.3}$$

$$\begin{aligned} M_i = {} & \frac{P \cdot \sinh KL}{K} \cdot \theta_{i-1} + \cosh KL \cdot M_{i-1} + \frac{\sinh KL}{K} \cdot N_{i-1} \\ & - \frac{q \cdot \cos\phi}{K^2} \cdot (\cosh KL - 1) \end{aligned} \tag{4.4}$$

$$V_i = V_{i-1} - q \cdot L \cdot \cos\phi \tag{4.5}$$

$$N_i = N_{i-1} + q \cdot L \cdot \sin\phi \tag{4.6}$$

where u' = longitudinal displacement in the local coordinate system,

w' = transverse displacement in the local coordinate system,

θ = slope,

M = moment,

V = internal force in the transverse direction,

N = internal force in the longitudinal direction,

P = axial force on the segment,

L = length of the segment,

K = $\sqrt{P/EI}$,

q = uniform distributed load on a segment,

and ϕ = angle between the local x-axis and the global X-axis.

Here, the displacements u' and w' in Eqs. (4.1) and (4.2) are values in the local coordinate system for the small deflection analysis. But, for the large deflection analysis, the displacements are related to each other and to the total length of the segment $(L + \Delta L)$, which L is the original length of the segment and ΔL is the elongation due to the axial (tensile) force. The angle is the rotation angle between the current and original local coordinate systems. This angle is updated iteratively as the segment deforms. In a kinematic analysis, the position corresponding to $\alpha = 0$ would be the position determined in a rigid-body kinematic analysis. Fig. (4.4) shows the displacements of the end of the segment in the inclined axes, where the inclined axes are dependent on the deflected position of a node.

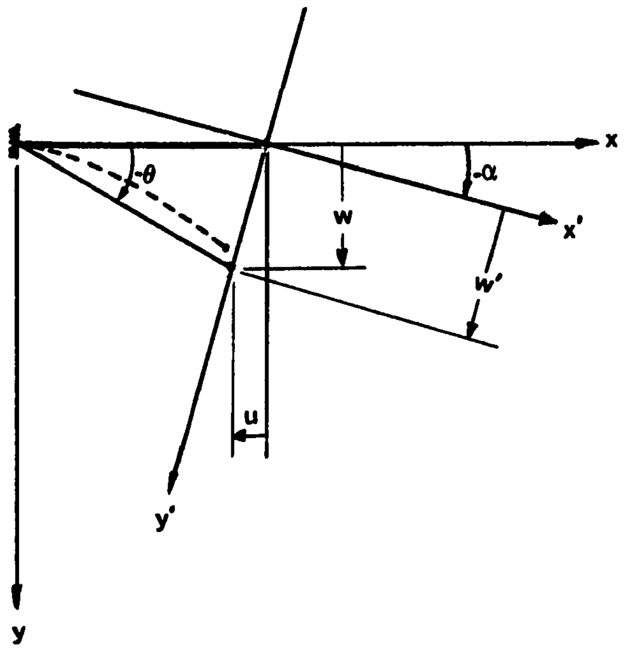

FIGURE 4.4 Transverse Displacement in An Inclined Axes

Then, the displacements in the local coordinate system can be determined from the geometric relationship as follows:

$$u = u' \cdot \cos\alpha + w' \cdot \sin\alpha \tag{4.7}$$

$$w = -u' \cdot \sin\alpha + w' \cdot \cos\alpha \tag{4.8}$$

and

$$\alpha = \theta / 2 \tag{4.9}$$

where θ is the average slope of the deflected segment. In real situation, α is not exactly $\theta/2$, because the deflected segment is not a straight line as shown in Fig. (4.4). But, if the length of the segment is short enough to be approximately straight, the relationship can be used for the formulations.

Substituting Eqs. (4.1) and (4.2) into Eqs. (4.7) and (4.8) gives

$$\begin{aligned} u_i = u_{i-1} &- \frac{\sinh KL}{K} \cdot \sin\alpha \cdot \theta_{i-1} + \frac{1 - \cosh KL}{P} \cdot \sin\alpha \cdot M_{i-1} \\ &+ \left(\frac{L}{P} - \frac{\sinh KL}{K\,P} \right) \cdot \sin\alpha \cdot V_{i-1} + \frac{L}{EA} \cdot N_{i-1} \\ &- \frac{qL^2 \cdot \sin\phi}{EA} + \frac{q \cdot \cos\phi}{EIK^4} \cdot \left(\cosh KL - 1 - \frac{K^2 L^2}{2}\right) \cdot \sin\alpha \end{aligned} \tag{4.10}$$

$$w_i = w_{i-1} - \frac{\sinh KL}{K}\cdot\cos\alpha\cdot\theta_{i-1} + \frac{1-\cosh KL}{P}\cdot\cos\alpha\cdot M_{i-1}$$

$$+ \left(\frac{L}{P} - \frac{\sinh KL}{K\,P}\right)\cdot\cos\alpha\cdot V_{i-1} \qquad (4.11)$$

$$+ \frac{q\cdot\cos\phi}{EIK^4}\cdot\left(\cosh KL - 1 - \frac{K^2L^2}{2}\right)\cdot\cos\alpha$$

The other components of the state vector (θ, M, V, and N) are not changed.

4.3 Determination of The Average Axial Forces from The Equilibrium Conditions

Let us consider the equilibrium conditions of the segment as shown Fig. (4.5) to determine a way of iteratively updating the average axial forces (P) in each beam segment. The average axial force in the segment is determine so that equilibrium conditions at the end nodes can be satisfied.

Fig. (4.5) shows a beam segment under large deflection. The relationships of the state variables between nodes i and i-1 are given in Eqs. (4.3)-(4.6) and Eqs. (4.10)-(4.11). Here, the equilibrium condition for the moments in the beam segment is investigated. From the summation of moment about the right end the following condition is given:

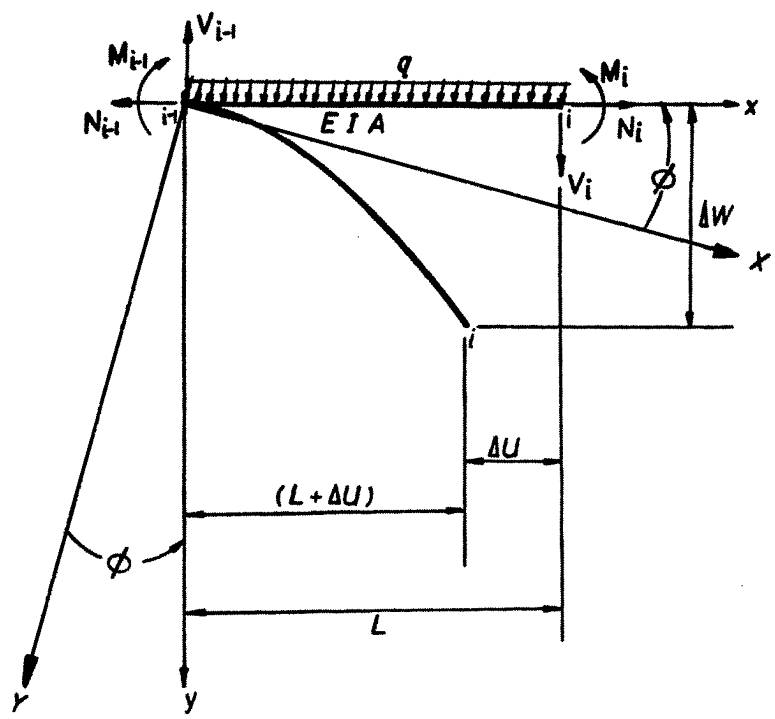

FIGURE 4.5 A Beam Segment Under Large Deflection

$$\sum M = 0 = M_{i-1} - M_i + (L + \Delta u)\cdot V_{i-1} - (\Delta w)\cdot N_{i-1} - q\cdot L\cdot \cos\phi \cdot (L + \Delta u)/2 - q\cdot L\cdot \sin\phi \cdot (\Delta w)/2 \tag{4.12}$$

Here, the last two terms in Eq. (4.12) correspond to the moments due to the distributed load. Δu and Δw are the net displacements in the axial and transverse directions.

The net displacements in each direction can be calculated from Eqs. (4.10) and (4.11) as follows:

$$\begin{aligned}\Delta u &= u_i - u_{i-1} \\ &= -\frac{\sinh KL}{K}\cdot \sin\alpha \cdot \theta_{i-1} + \frac{1 - \cosh KL}{P}\cdot \sin\alpha \cdot M_{i-1} \\ &\quad + \left(\frac{L}{P} - \frac{\sinh KL}{K\cdot P}\right)\cdot \sin\alpha \cdot V_{i-1} + \frac{L}{EA}\cdot N_{i-1} \\ &\quad - \frac{qL^2\cdot \sin\phi}{EA} + \frac{q\cdot \cos\phi}{EIK^4}\cdot\left(\cosh KL - 1 - \frac{K^2\cdot L^2}{2}\right)\cdot \sin\alpha\end{aligned}$$

and

$$\begin{aligned}\Delta w &= w_i - w_{i-1} \\ &= -\frac{\sinh KL}{K}\cdot \cos\alpha \cdot \theta_{i-1} + \frac{1 - \cosh KL}{P}\cdot \cos\alpha \cdot M_{i-1} \\ &\quad + \left(\frac{L}{P} - \frac{\sinh KL}{K\cdot P}\right)\cdot \cos\alpha \cdot V_{i-1} \\ &\quad + \frac{q\cdot \cos\phi}{EIK^4}\cdot\left(\cosh KL - 1 - \frac{K^2\cdot L^2}{2}\right)\cdot \cos\alpha\end{aligned}$$

Here, the elongation or shortening of the segment length due to the axial force is very small relative to the displacement due to the transverse deflection.

$$\left[\frac{L}{EA}\cdot N_{i-1} - \frac{qL^2\sin\phi}{EA}\right] \ll \left[-\frac{\sinh KL}{K}\cdot\sin\alpha\cdot\theta_{i-1} + \frac{1-\cosh KL}{p}\cdot\sin\alpha\cdot M_{i-1} + \left(\frac{L}{P} - \frac{\sinh KL}{K\cdot P}\right)\cdot\sin\alpha\cdot V_{i-1} + \frac{q\cdot\cos\phi}{EIK^4}\cdot\left(\cosh KL - 1 - \frac{K^2L^2}{2}\right)\cdot\sin\alpha\right]$$

Thus, the terms of the left side in the above equation can be neglected.

Let us calculate each term in Eq. (4.12).

$$\begin{aligned}(L + \Delta u)\cdot[V_{i-1} - (qL\cdot\cos\phi)/2] &= L\cdot V_{i-1} - \frac{qL^2\cos\phi}{2} + (\sin\alpha)\cdot\left[-\frac{\sinh KL}{K}\cdot\theta_{i-1}\right.\\ &\quad + \frac{1-\cosh KL}{p}\cdot M_{i-1} + \left(\frac{L}{P} - \frac{\sinh KL}{K\cdot P}\right)\cdot V_{i-1}\\ &\quad \left.+ \frac{q\cdot\cos\phi}{EIK^4}\cdot\left(\cosh KL - 1 - \frac{K^2L^2}{2}\right)\right]\cdot\left[V_{i-1} - (qL\cdot\cos\phi)/2\right]\end{aligned} \tag{4.13}$$

$$(\Delta W)\cdot[N_{i-1} + (qL\cdot\sin\phi)/2]$$

$$= (\cos\alpha)\cdot\left[-\frac{\sinh KL}{K}\cdot\theta_{i-1} + \frac{1-\cosh KL}{P}\cdot M_{i-1} + \left(\frac{L}{P} - \frac{\sinh KL}{K\cdot P}\right)\cdot V_{i-1} + \frac{q\cdot\cos\phi}{EIK^4}\cdot\left(\cosh KL - 1 - \frac{K^2L^2}{2}\right)\right]\cdot\left[N_{i-1} + (qL\cdot\sin\phi)/2\right] \tag{4.14}$$

Substituting Eqs. (4.4) for M_i, Eqs. (4.13) and (4.14) into Eq. (4.12) and rearrangement of the equation gives

$$\left[-\frac{\sinh KL}{K}\cdot\theta_{i-1} + \frac{1-\cosh KL}{P}\cdot M_{i-1} + \left(\frac{L}{P} - \frac{\sinh KL}{KP}\right)\cdot V_{i-1} + \frac{q\cdot\cos\phi}{EIK^4}\cdot\left(\cosh KL - 1 - \frac{K^2L^2}{2}\right)\right]\cdot\left[P + \left(V_{i-1} - \frac{qL\cdot\cos\phi}{2}\right)\cdot\sin\alpha - \left(N_{i-1} + \frac{qL\cdot\sin\phi}{2}\right)\cdot\cos\alpha\right] = 0 \tag{4.15}$$

The first square bracket in Eq. (4.15) corresponds to W' in Eq. (4.2) and this term can not be zero. Thus, the average axial force in a segment can be derived from the terms in the second bracket in Eq. (4.15) as follows:

$$P = \left(N_{i-1} + \frac{qL\cdot\sin\phi}{2}\right)\cdot\cos\alpha - \left(V_{i-1} - \frac{qL\cdot\cos\phi}{2}\right)\cdot\sin\alpha \tag{4.16}$$

4.4 Field Matrices for Large-Deflection Analysis

Field matrices for the large-deflection analyses can be derived from Eqs. (3.14) - (3.19) in Section 3.3.1 and Eqs. (4.7) - (4.9). The average axial force in a segment is given by Eq. (4.16).

$$P = \left(N_{i-1} + \frac{qL\cdot\sin\phi}{2}\right)\cdot\cos\alpha - \left(V_{i-1} - \frac{qL\cdot\cos\phi}{2}\right)\cdot\sin\alpha$$

where P = total axial force present in a segment,

N_{i-1} = longitudinal force at the (i-1)th node,

V_{i-1} = transverse force at the (i-1)th node,

α = angle in Eq. (4.9).

q = force intensity on a segment (force/length),

and ϕ = angle between the horizontal axis and the global x-axis.

When there is no axial force (P = 0) in the segment, the field matrix becomes

$$[F] = \begin{bmatrix} 1 & 0 & -L\cdot\sin\alpha & -\frac{L^2}{2EI}\cdot\sin\alpha & -\frac{L^3}{6EI}\cdot\sin\alpha & \frac{L}{EA} & F1 \\ 0 & 1 & -L\cdot\cos\alpha & -\frac{L^2}{2EI}\cdot\cos\alpha & -\frac{L^3}{6EI}\cdot\cos\alpha & 0 & F2 \\ 0 & 0 & 1 & \frac{L}{EI} & \frac{L^2}{2EI} & 0 & F3 \\ 0 & 0 & 0 & 1 & L & 0 & F4 \\ 0 & 0 & 0 & 0 & 1 & 0 & F5 \\ 0 & 0 & 0 & 0 & 0 & 1 & F6 \\ 0 & 0 & 0 & 0 & 0 & 0 & 1 \end{bmatrix} \qquad (4.17)$$

for a tensile force (P > 0), the field matrix is

$$
[F] = \begin{bmatrix}
1 & 0 & \dfrac{-\sinh KL}{K}\cdot\sin\alpha & \dfrac{1-\cosh KL}{P}\cdot\sin\alpha & \left(\dfrac{L}{P} - \dfrac{\sinh KL}{KP}\right)\cdot\sin\alpha & \dfrac{L}{EA} & F1 \\
0 & 1 & \dfrac{-\sinh KL}{K}\cdot\cos\alpha & \dfrac{1-\cosh KL}{P}\cdot\cos\alpha & \left(\dfrac{L}{P} - \dfrac{\sinh KL}{KP}\right)\cdot\cos\alpha & 0 & F2 \\
0 & 0 & \cosh KL & \dfrac{K\cdot\sinh KL}{P} & \dfrac{\cosh KL - 1}{P} & 0 & F3 \\
0 & 0 & -\dfrac{P\cdot\sinh KL}{K} & \cosh KL & \dfrac{\sinh KL}{K} & 0 & F4 \\
0 & 0 & 0 & 0 & 1 & 0 & F5 \\
0 & 0 & 0 & 0 & 0 & 1 & F6 \\
0 & 0 & 0 & 0 & 0 & 0 & 1
\end{bmatrix} \qquad \text{.........(4.18)}
$$

and for a compressive force (P < 0), the field matrix is

$$
[F] = \begin{bmatrix}
1 & 0 & -\dfrac{\sin KL}{K}\cdot\sin\alpha & \dfrac{\cos KL - 1}{P}\cdot\sin\alpha & \left(\dfrac{\sin KL}{KP} - \dfrac{L}{P}\right)\cdot\sin\alpha & \dfrac{L}{EA} & F1 \\
0 & 1 & -\dfrac{\sin KL}{K}\cdot\cos\alpha & \dfrac{\cos KL - 1}{P}\cdot\cos\alpha & \left(\dfrac{\sin KL}{KP} - \dfrac{L}{P}\right)\cdot\cos\alpha & 0 & F2 \\
0 & 0 & \cos KL & \dfrac{K\cdot\sin KL}{P} & \dfrac{1 - \cos KL}{P} & 0 & F3 \\
0 & 0 & -\dfrac{P\cdot\sin KL}{K} & \cos KL & \dfrac{\sin KL}{K} & 0 & F4 \\
0 & 0 & 0 & 0 & 1 & 0 & F5 \\
0 & 0 & 0 & 0 & 0 & 1 & F6 \\
0 & 0 & 0 & 0 & 0 & 0 & 1
\end{bmatrix} \qquad \text{.........(4.19)}
$$

where $k = \sqrt{|P|/EI}$ and $|P|$ is the total axial force determined from Eq. (4.19) at the previous iteration. For a wide cross-section, $K = \sqrt{|P|\cdot(1-\nu^2)/(EI)}$ is used. The angle α is the displacement correction angle in Eq. (4.9) and must be updated during the iterations.

The seventh column for no axial force in the segment becomes

$$\begin{bmatrix} F1 \\ F2 \\ F3 \\ F4 \\ F5 \\ F6 \end{bmatrix} = \begin{bmatrix} -\dfrac{qL^2\cdot\sin\phi}{EA} + \dfrac{qL^4\cdot\cos\phi}{24\cdot EI}\cdot\sin\alpha \\ \dfrac{qL^4\cdot\cos\phi}{24\cdot EI}\cdot\cos\alpha \\ -\dfrac{qL^3\cdot\cos\phi}{6\cdot EI} \\ -\dfrac{qL^2\cdot\cos\phi}{2} \\ -\,qL\cdot\cos\phi \\ qL\cdot\sin\phi \end{bmatrix} \tag{4.20}$$

the seventh column for the tensile axial force in the segment is

$$\begin{bmatrix} F1 \\ F2 \\ F3 \\ F4 \\ F5 \\ F6 \end{bmatrix} = \begin{bmatrix} -\dfrac{qL^2\cdot\sin\phi}{EA} + \dfrac{q\cdot\cos\phi}{EIK^4}\cdot\left(\cosh KL - 1 - \dfrac{K^2\cdot L^2}{2}\right)\cdot\sin\alpha \\ \dfrac{q\cdot\cos\phi}{EIK^4}\cdot\left(\cosh KL - 1 - \dfrac{K^2\cdot L^2}{2}\right)\cdot\cos\alpha \\ \dfrac{q\cdot\cos\phi}{EIK^3}\cdot(KL - \sinh KL) \\ -\dfrac{q\cdot\cos\phi}{K^2}\cdot(\cosh KL - 1) \\ -qL\cdot\cos\phi \\ qL\cdot\sin\phi \end{bmatrix} \quad (4.21)$$

and the seventh column for the compressive axial force in the segment is

$$\begin{bmatrix} F1 \\ F2 \\ F3 \\ F4 \\ F5 \\ F6 \end{bmatrix} = \begin{bmatrix} -\dfrac{qL^2\cdot\sin\phi}{EA} - \dfrac{q\cdot\cos\phi}{EIK^4}\cdot\left(1 - \cos KL - \dfrac{K^2\cdot L^2}{2}\right)\cdot\sin\alpha \\ -\dfrac{q\cdot\cos\phi}{EIK^4}\cdot\left(1 - \cos KL - \dfrac{K^2\cdot L^2}{2}\right)\cdot\cos\alpha \\ -\dfrac{q\cdot\cos\phi}{EIK^3}\cdot(KL - \sin KL) \\ -\dfrac{q\cdot\cos\phi}{K^2}\cdot(1 - \cos KL) \\ -qL\cdot\cos\phi \\ qL\cdot\sin\phi \end{bmatrix} \quad (4.22)$$

4.5 Comparison with The Exact Solution

As the first comparative study, let us solve a large-deflection problem, which is a cantilever beam under transverse loading at the tip. Bisshopp and Drucker [87] obtained the relationships between the end loads and the displacements in the longitudinal and transverse directions for an inextensible caltilevered beam with the end loads as shown in Fig. (4.6a). In their analytical study, the exact expression for the beam curvature of the elastic line is related to the arc-length and the slope of the deflected beam. They assumed that the curvature of the beam is proportional to the bending moment, and that the curvature at the loaded end is zero. The solution was in terms of elliptic integrals which were evaluated numerically. The solution is given in Fig. (4.6b)

To investigate the proposed approximate method for the large-deflection analyses, a steel cantilevered beam subjected to the transverse loads at the end is considered. The beam has a 10 - inch length with a square cross-section of 0.1 X 0.1 ($inch^2$). The total number of elements is 10 with each element of equal length. The results are compared with the curves presented in References [86-87] and given in Fig. (4.6b). The comparative study shows that both curves for H/L and V/L are in good agreement. The solution details are given in Section 8.4.

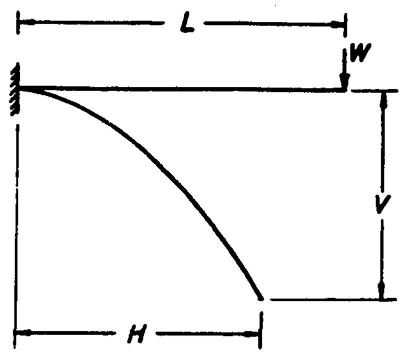

(a) A Cantilever Beam

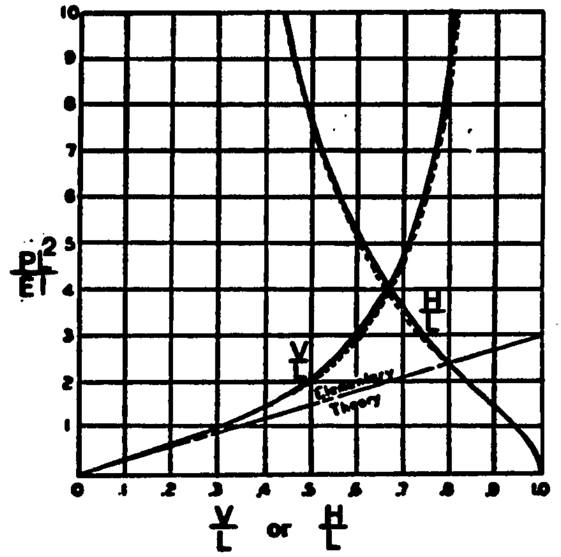

.... Solution from The Proposed Method

---- Exact Solution from Bisshopp and Drucker [87]

(b) Solutions of Large-Deflection Problem

FIGURE 4.6 Comparison of The Solutions

As a second study, a cantilever beam acted on by an end moment as shown in Fig. (4.7) is studied. This causes a tip rotation of 1.0 rad (57.295 degrees) which is considered a large rotation. De Arantes e Oliviera [88] solved the problem by sub-dividing the load into ten equal increments using an iteration approach. Thus, this problem has been solved in ten load steps with an unspecified number of iterations at each load step. But, the proposed method uses the entire load. The results shown in Table 4.1 are after only 8 iterations, and there is less than 2 percent error compared to the solutions given in [88].

TABLE 4.1 Tip Motion of The Cantilever Beam

Solution Method	X (cm)	Y (cm)	θ (Deg)
Linear Theory	100.0000	50.0000	57.295
Exact Solutions [88]	84.1471	45.9698	57.295
Solutions from The Developed Method	83.367	46.746	57.295
ERROR (Percent)	0.9	1.7	0.0

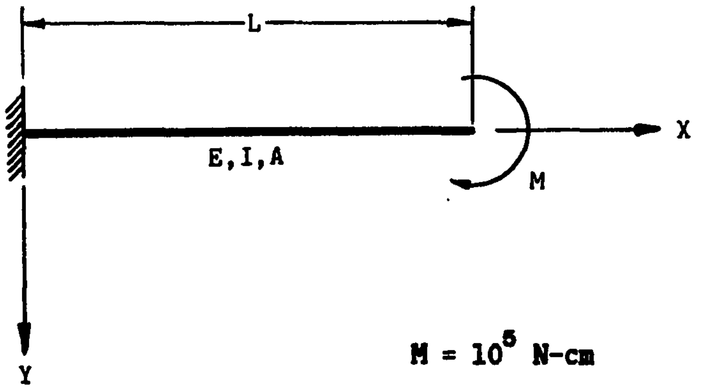

$M = 10^5$ N-cm

$L = 100$ cm

$A = 10.0\ cm^2$

$I = 5.0\ cm^4$

$E = 2.0 \times 10^6\ N/cm^2$

FIGURE 4.7 Cantilever Acted on by End Moment

CHAPTER V

TRANSFER MATRIX EQUATIONS FOR LOOPS

5.1 Introduction

Mechanisms have joints (revolutes and sliders). At the joints one of the state variables must be discontinuous. For example, at a revolute joints, the slopes of both sides at pre- and post-locations of the revolute are not continuous, because the moment at the location of the revolute must be zero. At a slider, a displacement in the sliding direction is discontinuous, because the force in the sliding direction must be zero. Thus, additions of the slopes (for the revolutes) and displacements (for the sliders) to compensate for the discontinuity must be determined from equilibrium conditions at the locations of the joints.

This chapter presents the derivation of the transfer matrix equations for linkages. As mentioned in Chapter 3, there are two types of loops: main loops and subloops (branch systems). The main loop systems consist of four-bar mechanisms and slider-crank mechanisms. In a mechanism, the support shaft for the input link must carry a torque so that the input-link is treated as fixed. The subloop systems are identified by four types as given in Section 3.3.5. The transfer matrix equations for each subloop system is derived in the following sections.

Section 5.2 identifies the boundary conditions. Sections 5.3 and 5.4 give the procedures for the derivations of the main loop and subloop systems, respectively.

5.2 Boundary Conditions

Each loop system has the typical boundary conditions corresponding to the end point. The state vector at the support (end point) consists of six components:

$$\{S\} = [u, w, \theta, M, V, N]^T$$

where u = displacement in the longitudinal direction,

w = displacement in the transverse direction,

θ = slope,

M = moment,

V = internal force in the transverse direction,

and N = internal force in the longitudinal direction.

Table 5.1 gives the types of supports considered and the corresponding boundary conditions.

TABLE 5.1 Types of Supports and The Boundary Conditions

Type of Supports		Boundary conditions	Unknown Values
Pinned	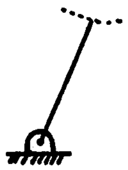	u = 0 w = 0 M = 0	S1 = θ S2 = V S3 = N
Fixed	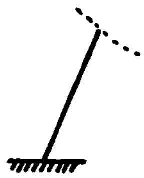	u = 0 w = 0 θ = 0	S1 = M S2 = V S3 = N
Free	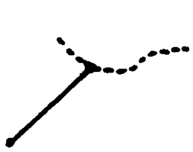	M = 0 V = 0 N = 0	S1 = u S2 = w S3 = θ
Slider	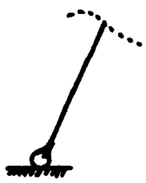	w = 0 θ = 0 N = 0	S1 = u S2 = M S3 = V
Simple Supported	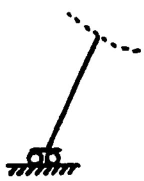	w = 0 M = 0 N = 0	S1 = u S2 = θ S3 = V

5.3 Transfer Matrix Equations of Main Loops

A mechanism is assumed to consist of the links and two types of kinematic joints (revolutes and sliders). For the revolutes, no moment is transmitted to the adjacent link(s) and the slopes are discontinuous. For sliders, the force in the sliding direction is zero and the displacements in the sliding direction are discontinuous. The transfer matrix equations for the main systems are derived in the following sections.

5.3.1 Transfer Matrix Equations for A Four-Bar Mechanism

Fig. (5.1a) shows a four-bar mechanism with two revolutes at points B and C, and grounded revolutes at points A and D. If link AB is the input link, the end types become fixed at point A and pinned at point D. Then, the transfer matrix equation for the overall system is

$$\{S\}_D = [T]_D \cdot [F] \ldots [F] \cdot \{R\}_C \cdot [T]_C \cdot [F] \ldots [P] \ldots [F] \cdot \{R\}_B \cdot [T]_B \cdot [F] \ldots [F] \cdot [T]_A \cdot \{S\}_A \qquad (5.1)$$

where $[T]_B [F] \ldots [F] \cdot [T]_A$ = loop matrix equation for link AB,

$[T]_C [F] \ldots [F]$ = loop matrix equation for link BC,

$[T]_D [F] \ldots [F]$ = loop matrix equation for link CD,

$[P]$ = point matrix,

$\{S\}_A$ and $\{S\}_D$ = state vectors at both end,

and $\{R\}$ = matrix reformulation for the revolutes.

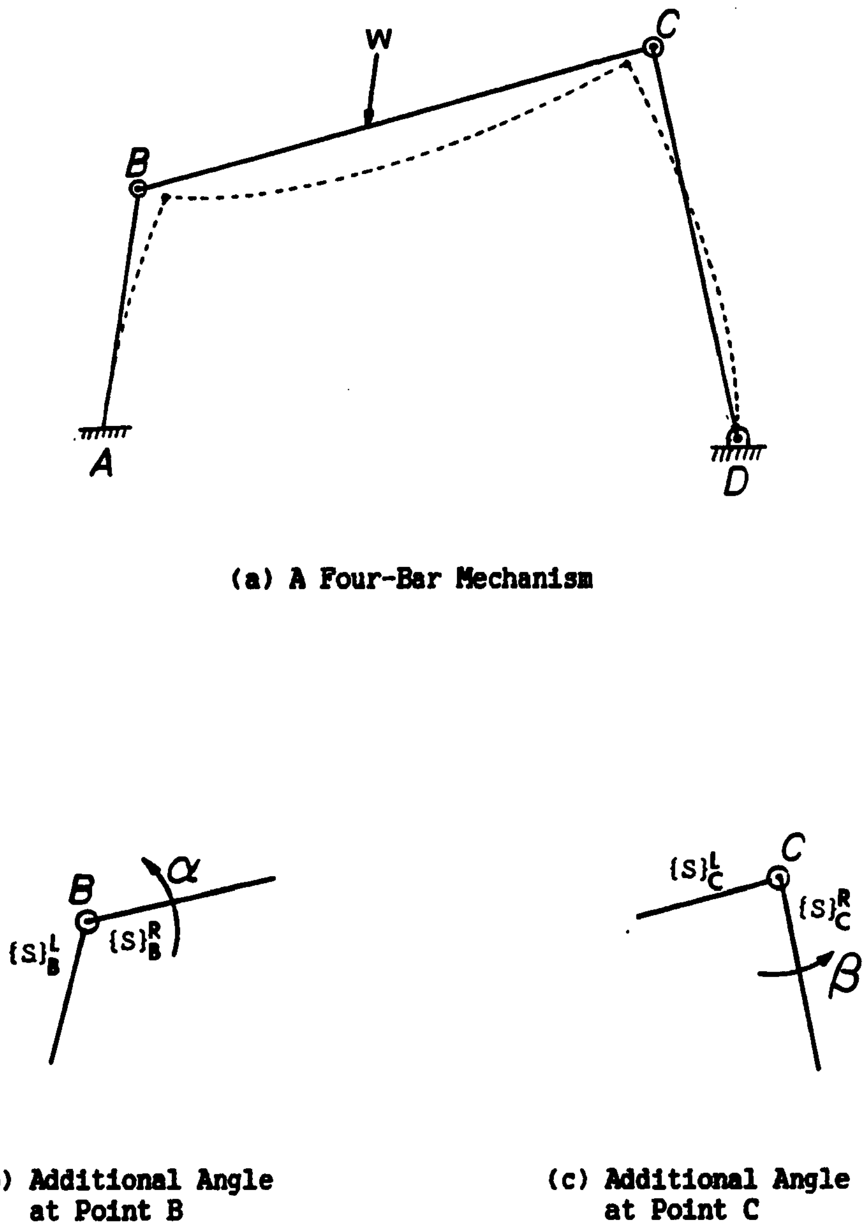

FIGURE 5.1 A Four-Bar Mechanism Model

Let us consider the transfer matrix equation of each link. A transfer matrix equation for a link AB is

$$\{S\}_B = [T]_B \cdot [F] \ldots [F] \cdot [T]_A \cdot \{S\}_A \tag{5.2}$$

Rewriting Eq. (5.2) gives

$$\begin{bmatrix} u \\ w \\ \theta \\ M \\ V \\ N \\ 1 \end{bmatrix}_B^L = \begin{bmatrix} U(1,1) & U(1,2) & U(1,3) & U(1,4) & U(1,5) & U(1,6) & U(1,7) \\ U(2,1) & U(2,2) & U(2,3) & U(2,4) & U(2,5) & U(2,6) & U(2,7) \\ U(3,1) & U(3,2) & U(3,3) & U(3,4) & U(3,5) & U(3,6) & U(3,7) \\ U(4,1) & U(4,2) & U(4,3) & U(4,4) & U(4,5) & U(4,6) & U(4,7) \\ U(5,1) & U(5,2) & U(5,3) & U(5,4) & U(5,5) & U(5,6) & U(5,7) \\ U(6,1) & U(6,2) & U(6,3) & U(6,4) & U(6,5) & U(6,6) & U(6,7) \\ 0 & 0 & 0 & 0 & 0 & 0 & 1 \end{bmatrix} \cdot \begin{bmatrix} u \\ w \\ \theta \\ M \\ V \\ N \\ 1 \end{bmatrix}_A \tag{5.3}$$

Here, three components of the state vector at point A are zero from Table 5.1. Thus, there are only three unknowns. The colummns in the matrix corresponding to the zero values of the state components can be eliminated from Eq. (5.3) as follows:

$$\begin{bmatrix} u \\ w \\ \theta \\ M \\ V \\ N \\ 1 \end{bmatrix}_B^L = \begin{bmatrix} P(1,1) & P(1,2) & P(1,3) & P(1,4) \\ P(2,1) & P(2,2) & P(2,3) & P(2,4) \\ P(3,1) & P(3,2) & P(3,3) & P(3,4) \\ P(4,1) & P(4,2) & P(4,3) & P(4,4) \\ P(5,1) & P(5,2) & P(5,3) & P(5,4) \\ P(6,1) & P(6,2) & P(6,3) & P(6,4) \\ 0 & 0 & 0 & 1 \end{bmatrix} \cdot \begin{bmatrix} S1 \\ S2 \\ S3 \\ 1 \end{bmatrix} \qquad (5.4)$$

where S1, S2, and S3 are the non-zero state components as given in Table 5.1. And $\{S\}_B^L$ is the state vector at the left side of point B as shown in Fig. (5.1b).

At point B, the kinematic conditions for a revolute joint are satisfied: No moment is transmitted and the slopes are discontinuous.

$$M_B = 0 = P(4,1)\cdot S1 + P(4,2)\cdot S2 + P(4,3)\cdot S3 + P(4,4) \qquad (5.5)$$

Rearrangement of Eq. (5.5) gives

$$S2 = -Z(1,2)\cdot S1 - Z(3,2)\cdot S3 - Z(4,2) \qquad (5.6)$$

where $Z(1,2) = P(4,1)/P(4,2)$,

$Z(3,2) = P(4,3)/P(4,2)$,

and $Z(4,2) = P(4,4)/P(4,2)$.

Substituting Eq. (5.6) into Eq. (5.4) gives

$$\begin{Bmatrix} u \\ w \\ \theta \\ M \\ V \\ N \\ 1 \end{Bmatrix}_B^L = \begin{bmatrix} (P(1,1)-P'(1,1)) & (P(1,3)-P'(1,3)) & (P(1,4)-P'(1,4)) \\ (P(2,1)-P'(2,1)) & (P(2,3)-P'(2,3)) & (P(2,4)-P'(2,4)) \\ (P(3,1)-P'(3,1)) & (P(3,3)-P'(3,3)) & (P(3,4)-P'(3,4)) \\ 0 & 0 & 0 \\ (P(5,1)-P'(5,1)) & (P(5,3)-P'(5,3)) & (P(5,4)-P'(5,4)) \\ (P(6,1)-P'(6,1)) & (P(6,3)-P'(6,3)) & (P(6,4)-P'(6,4)) \\ 0 & 0 & 1 \end{bmatrix} \begin{Bmatrix} S1 \\ S3 \\ 1 \end{Bmatrix} \qquad (5.7)$$

where $\quad P'(i,j) = P(i,2)\cdot Z(j,2)$

At point B, the slopes are discontinuous. Thus, an additional slope as shown in Fig. (5.1b) is present as follows:

$$\{S\}_B^R = \{S\}_B^L + \alpha \qquad (5.8)$$

where α is the additional angle between the two adjacent links at B, and can be determined from Eq. (5.18). Then, the matrix equation to the right side of point B from point A becomes

$$\begin{Bmatrix} u \\ w \\ \theta \\ M \\ V \\ N \\ 1 \end{Bmatrix}_B^R = \begin{bmatrix} (P(1,1)-P'(1,1)) & 0 & (P(1,3)-P'(1,3)) & (P(1,4)-P'(1,4)) \\ (P(2,1)-P'(2,1)) & 0 & (P(2,3)-P'(2,3)) & (P(2,4)-P'(2,4)) \\ (P(3,1)-P'(3,1)) & 1 & (P(3,3)-P'(3,3)) & (P(3,4)-P'(3,4)) \\ 0 & 0 & 0 & 0 \\ (P(5,1)-P'(5,1)) & 0 & (P(5,3)-P'(5,3)) & (P(5,4)-P'(5,4)) \\ (P(6,1)-P'(6,1)) & 0 & (P(6,3)-P'(6,3)) & (P(6,4)-P'(6,4)) \\ 0 & 0 & 0 & 1 \end{bmatrix} \begin{Bmatrix} S1 \\ \alpha \\ S3 \\ 1 \end{Bmatrix} \qquad (5.9)$$

Next, the matrix equation for the link BC is

$$\{S\}_C^L = [T]_C \cdot [F] \; \dots \; [P] \; \dots \; [F] \cdot \{S\}_B^R \tag{5.10}$$

Combining Eqs. (5.9) and (5.10) gives Eq. (5.11).

$$\begin{bmatrix} u \\ w \\ \theta \\ M \\ V \\ N \\ 1 \end{bmatrix}_C^L = \begin{bmatrix} Q(1,1) & Q(1,2) & Q(1,3) & Q(1,4) \\ Q(2,1) & Q(2,2) & Q(2,3) & Q(2,4) \\ Q(3,1) & Q(3,2) & Q(3,3) & Q(3,4) \\ Q(4,1) & Q(4,2) & Q(4,3) & Q(4,4) \\ Q(5,1) & Q(5,2) & Q(5,3) & Q(5,4) \\ Q(6,1) & Q(6,2) & Q(6,3) & Q(6,4) \\ 0 & 0 & 0 & 1 \end{bmatrix} \cdot \begin{bmatrix} S1 \\ \alpha \\ S3 \\ 1 \end{bmatrix} \tag{5.11}$$

At point C, $M_C = 0$. Thus, the moment equation from Eq. (5.11) is

$$M_C = 0 = Q(4,1) \cdot S1 + Q(4,2) \cdot \alpha + Q(4,3) \cdot S3 + Q(4,4)$$

and elimination of S3 gives

$$S3 = -ZZ(1,3) \cdot S1 - ZZ(2,3) \cdot \alpha - ZZ(4,3) \tag{5.12}$$

where $ZZ(1,3) = Q(4,1)/Q(4,3)$,

$ZZ(2,3) = Q(4,2)/Q(4,3)$,

and $ZZ(4,3) = Q(4,4)/Q(4,3)$.

Substituting Eq. (5.12) into Eq. (5.11) gives

$$\begin{Bmatrix} u \\ w \\ \theta \\ M \\ V \\ N \\ 1 \end{Bmatrix}_C^L = \begin{bmatrix} (Q(1,1)-Q'(1,1)) & (Q(1,2)-Q'(1,2)) & (Q(1,4)-Q'(1,4)) \\ (Q(2,1)-Q'(2,1)) & (Q(2,2)-Q'(2,2)) & (Q(2,4)-Q'(2,4)) \\ (Q(3,1)-Q'(3,1)) & (Q(3,2)-Q'(3,2)) & (Q(3,4)-Q'(3,4)) \\ 0 & 0 & 0 \\ (Q(5,1)-Q'(5,1)) & (Q(5,2)-Q'(5,2)) & (Q(5,4)-Q'(5,4)) \\ (Q(6,1)-Q'(6,1)) & (Q(6,2)-Q'(6,2)) & (Q(6,4)-Q'(6,4)) \\ 0 & 0 & 1 \end{bmatrix} \begin{Bmatrix} S1 \\ \alpha \\ 1 \end{Bmatrix} \quad (5.13)$$

where $\quad Q'(i,j) = Q(i,3)\cdot ZZ(j,3)$

At point C, the slope is discontinuous. Thus, an additional angle is present as shown in Fig. (5.1c). The state vector is as follows:

$$\{S\}_C^R = \{S\}_C^L + \beta \quad (5.14)$$

where β is the additional angle between the two adjacent links at C, and can be determined from Eq. (5.18). Then, the matrix equation to the right side of point C from point A becomes

$$\begin{Bmatrix} u \\ w \\ \theta \\ M \\ V \\ N \\ 1 \end{Bmatrix}_C^R = \begin{bmatrix} (Q(1,1)-Q'(1,1)) & (Q(1,2)-Q'(1,2)) & 0 & (Q(1,4)-Q'(1,4)) \\ (Q(2,1)-Q'(2,1)) & (Q(2,2)-Q'(2,2)) & 0 & (Q(2,4)-Q'(2,4)) \\ (Q(3,1)-Q'(3,1)) & (Q(3,2)-Q'(3,2)) & 1 & (Q(3,4)-Q'(3,4)) \\ 0 & 0 & 0 & 0 \\ (Q(5,1)-Q'(5,1)) & (Q(5,2)-Q'(5,2)) & 0 & (Q(5,4)-Q'(5,4)) \\ (Q(6,1)-Q'(6,1)) & (Q(6,2)-Q'(6,2)) & 0 & (Q(6,4)-Q'(6,4)) \\ 0 & 0 & 0 & 1 \end{bmatrix} \cdot \begin{Bmatrix} S1 \\ \alpha \\ \beta \\ 1 \end{Bmatrix} \quad (5.15)$$

Finally, the matrix equation for the link CD is

$$\{S\}_D = [T]_D \cdot [F] \ldots [F] \cdot \{S\}_C^R \tag{5.16}$$

Combining Eqs. (5.15) and (5.16) gives Eq. (5.17).

$$\begin{bmatrix} u \\ w \\ \theta \\ M \\ V \\ N \\ 1 \end{bmatrix}_D = \begin{bmatrix} R(1,1) & R(1,2) & R(1,3) & R(1,4) \\ R(2,1) & R(2,2) & R(2,3) & R(2,4) \\ R(3,1) & R(3,2) & R(3,3) & R(3,4) \\ R(4,1) & R(4,2) & R(4,3) & R(4,4) \\ R(5,1) & R(5,2) & R(5,3) & R(5,4) \\ R(6,1) & R(6,2) & R(6,3) & R(6,4) \\ 0 & 0 & 0 & 1 \end{bmatrix} \cdot \begin{bmatrix} S1 \\ \alpha \\ \beta \\ 1 \end{bmatrix} \tag{5.17}$$

Applying the boundary conditions at point D gives three simultaneous equations for the pinned support:

$$\begin{aligned} u_D &= 0 = R(1,1)\cdot S1 + R(1,2)\cdot \alpha + R(1,3)\cdot \beta + R(1,4) \\ w_D &= 0 = R(2,1)\cdot S1 + R(2,2)\cdot \alpha + R(2,3)\cdot \beta + R(2,4) \\ M_D &= 0 = R(4,1)\cdot S1 + R(4,2)\cdot \alpha + R(4,3)\cdot \beta + R(4,4) \end{aligned} \tag{5.18}$$

The solutions of Eq. (5.18) gives three values for S1, α, and β. Then, the unknown values of S2 and S3 can be calculated from Eqs. (5.6) and (5.12), respectively.

5.3.2 Transfer Matrix Equation for A Slider-Crank Mechanism

Fig. (5.2) shows a slider-crank mechanism with revolutes at points B and C, grounded by a fixed end at point A, and by a slider at point D. The procedures for the derivations of the transfer matrix equations are the same as those in Section 5.3.1.

The boundary conditions at the slider given in Table 5.1 are as follows:

$$\begin{aligned} w_D &= 0 \\ \theta_D &= 0 \\ N_D &= 0 \end{aligned} \qquad (5.19)$$

The same procedure up to Eq. (5.11) in Section 5.3.1 can be used. At points C and D, the kinematic conditions must be satisfied: No moment can be transmitted at point C, and no reaction force is present in the sliding direction. Thus, a displacement continuity at point D is present in the sliding direction as shown in Figs. (5.2a) and (5.2b). After the expressions in Eqs. (5.12) and (5.13) are used, the condition at points C and D becomes

$$\{S\}_D = \{S\}_C + u'' \qquad (5.20)$$

where u" is the additional displacement in the sliding direction as shown in Fig. (5.2b).

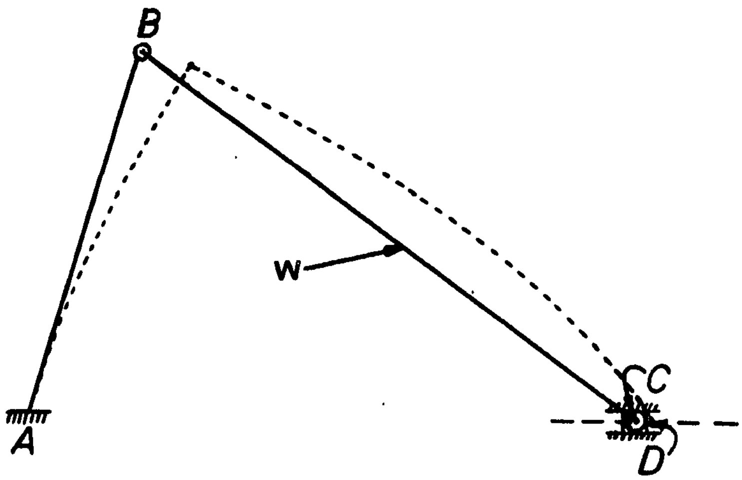

(a) A Slider-Crank Mechanism

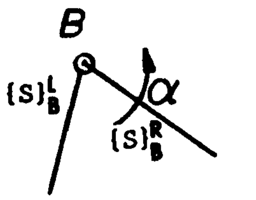

(b) Additional Angle at Point B

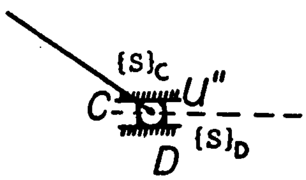

(c) Additional Displacement at Point D

FIGURE 5.2 A Slider-Crank Mechanism Model

Then, the equation to point D from point C becomes

$$\begin{bmatrix} u \\ w \\ \theta \\ M \\ V \\ N \\ 1 \end{bmatrix}_D = \begin{bmatrix} (Q(1,1)-Q'(1,1)) & (Q(1,2)-Q'(1,2)) & 1 & (Q(1,4)-Q'(1,4)) \\ (Q(2,1)-Q'(2,1)) & (Q(2,2)-Q'(2,2)) & 0 & (Q(2,4)-Q'(2,4)) \\ (Q(3,1)-Q'(3,1)) & (Q(3,2)-Q'(3,2)) & 0 & (Q(3,4)-Q'(3,4)) \\ 0 & 0 & 0 & 0 \\ (Q(5,1)-Q'(5,1)) & (Q(5,2)-Q'(5,2)) & 0 & (Q(5,4)-Q'(5,4)) \\ (Q(6,1)-Q'(6,1)) & (Q(6,2)-Q'(6,2)) & 0 & (Q(6,4)-Q'(6,4)) \\ 0 & 0 & 0 & 1 \end{bmatrix} \cdot \begin{bmatrix} S1 \\ \alpha \\ u'' \\ 1 \end{bmatrix} \qquad (5.21)$$

where $\quad Q'(i,j) = Q(i,3) \cdot ZZ(j,3).$

Finally, the matrix equation in Eq. (5.21) can be written in the same form as in Eq. (5.17) as follows:

$$\begin{bmatrix} u \\ w \\ \theta \\ M \\ V \\ N \\ 1 \end{bmatrix}_D = \begin{bmatrix} R(1,1) & R(1,2) & R(1,3) & R(1,4) \\ R(2,1) & R(2,2) & R(2,3) & R(2,4) \\ R(3,1) & R(3,2) & R(3,3) & R(3,4) \\ R(4,1) & R(4,2) & R(4,3) & R(4,4) \\ R(5,1) & R(5,2) & R(5,3) & R(5,4) \\ R(6,1) & R(6,2) & R(6,3) & R(6,4) \\ 0 & 0 & 0 & 1 \end{bmatrix} \cdot \begin{bmatrix} S1 \\ \alpha \\ u'' \\ 1 \end{bmatrix} \qquad (5.22)$$

Applying the conditions in Eq. (5.19) to Eq. (5.22) gives the following three equations:

$$
\begin{aligned}
u_D &= 0 = R(1,1)\cdot S1 + R(1,2)\cdot \alpha + R(1,3)\cdot u'' + R(1,4) \\
\theta_D &= 0 = R(3,1)\cdot S1 + R(3,2)\cdot \alpha + R(3,3)\cdot u'' + R(3,4) \qquad (5.23) \\
N_D &= 0 = R(6,1)\cdot S1 + R(6,2)\cdot \alpha + R(6,3)\cdot u'' + R(6,4)
\end{aligned}
$$

The solutions of Eq. (5.23) gives three values for S1, α, and u", where α is an additional angle at point B and u" is an additional displacement in the sliding direction at point D. Then, the unknown values of S2 and S3 can be calculated from Eqs. (5.6) and (5.12), respectively.

5.4 Transfer Matrix Equations for the Sub-loop (Branch) Systems

As shown in Fig. (3.11), there are four types of sub-loop systems. Combining the same procedures for the matrix equations as in Section 5.3 and for the branch matrices as in Section 3.3.5 gives the transfer matrix equations for each type of the sub-system. Figs. (5.3) through (5.6) give the sub-loop systems, and Tables (5.2) through (5.5) give the loop equations for each sub-loop system.

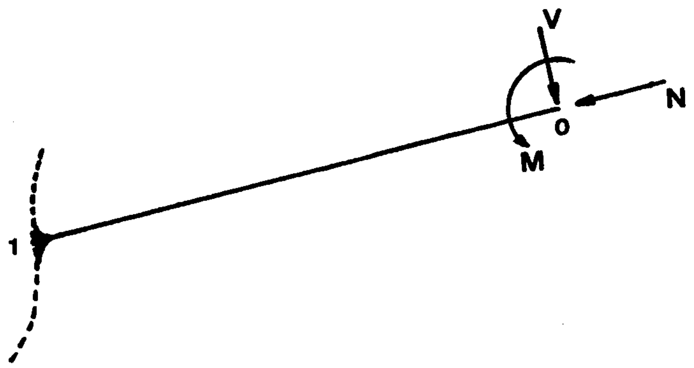

FIGURE 5.3 Sub-Loop with A Free End and A Fixed Branch Point (Case 1).

TABLE 5.2 Loop Equations for The Unknowns at Point 0 (Case 1)

$$u_0 = ZZ(1,1)\cdot u_1 + ZZ(1,2)\cdot w_1 + ZZ(1,3)\cdot \theta_1 + ZZ(1,4)$$

$$w_0 = ZZ(2,1)\cdot u_1 + ZZ(2,2)\cdot w_1 + ZZ(2,3)\cdot \theta_1 + ZZ(2,4)$$

$$\theta_0 = ZZ(3,1)\cdot u_1 + ZZ(3,2)\cdot w_1 + ZZ(3,3)\cdot \theta_1 + ZZ(3,4)$$

where u_0, w_0, θ_0 = displacements at node 0,

u_1, w_1, θ_1 = displacements at node 1,

and $ZZ(i,j)$ = components in the matrix of Eq. (3.32).

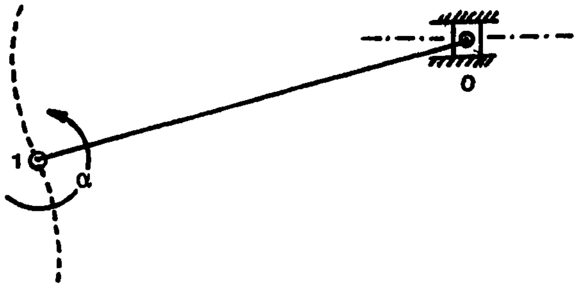

FIGURE 5.4 Sub-Loop with A Slider End and A Revolute Branch Point (Case 2).

TABLE 5.3 Loop Equations for The Unknowns at Point 0 (Case 2)

$u_0 = ZZ(1,1)\cdot u_1 + ZZ(1,2)\cdot w_1 + ZZ(1,3)\cdot \theta_1 + ZZ(1,4)$

$\alpha = ZZ(2,1)\cdot u_1 + ZZ(2,2)\cdot w_1 + ZZ(2,3)\cdot \theta_1 + ZZ(2,4)$

$\theta_0 = ZZ(3,1)\cdot u_1 + ZZ(3,2)\cdot w_1 + ZZ(3,3)\cdot \theta_1 + ZZ(3,4)$

w_0 is determined from Eq. (5.6)

where u_0, w_0, θ_0 = displacements at node 0,

u_1, w_1, θ_1 = displacements at node 1,

α = additional angle for point 1,

and ZZ(i,j) = components in the matrix of Eq. (3.32).

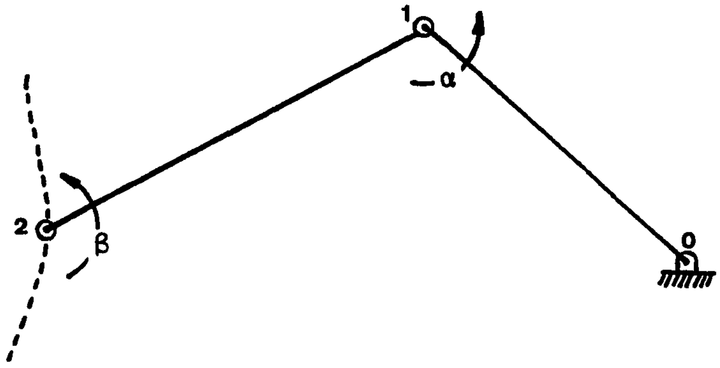

FIGURE 5.5 Sub-Loop with A Pin End and A Revolute Branch Point (Case 3).

TABLE 5.4 Loop Equations for The Unknowns at Point 0 (Case 3)

$$\theta_o = ZZ(1,1)\cdot u_2 + ZZ(1,2)\cdot w_2 + ZZ(1,3)\cdot \theta_2 + ZZ(1,4)$$

$$\alpha = ZZ(2,1)\cdot u_2 + ZZ(2,2)\cdot w_2 + ZZ(2,3)\cdot \theta_2 + ZZ(2,4)$$

$$\beta = ZZ(3,1)\cdot u_2 + ZZ(3,2)\cdot w_2 + ZZ(3,3)\cdot \theta_2 + ZZ(3,4)$$

V_o is determined from Eq. (5.6)

N_o is determined from Eq. (5.12)

where u_o, w_o, θ_o = displacements at node 0,

M_o, V_o, N_o = forces at node 0,

u_2, w_2, θ_2 = displacements at node 2,

α , β = additional angles for points 1 and 2,

and ZZ(i,j) = components in the matrix of Eq. (3.32).

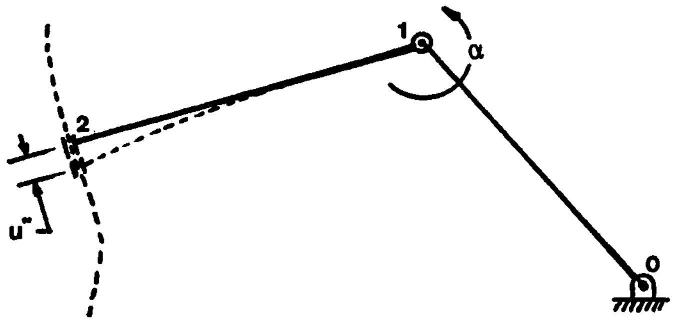

FIGURE 5.6 Sub-Loop with A Pin End and A Slider Branch Point (Case 4).

TABLE 5.5 Loop Equations for The Unknowns at Point 0 (Case 4)

u_0 = $ZZ(1,1)\cdot u_2 + ZZ(1,2)\cdot w_2 + ZZ(1,3)\cdot\theta_2 + ZZ(1,4)$

α = $ZZ(2,1)\cdot u_2 + ZZ(2,2)\cdot w_2 + ZZ(2,3)\cdot\theta_2 + ZZ(2,4)$

u'' = $ZZ(3,1)\cdot u_2 + ZZ(3,2)\cdot w_2 + ZZ(3,3)\cdot\theta_2 + ZZ(3,4)$

V_0 is determined from Eq. (5.6)

N_0 is determined from Eq. (5.12)

where u_0, w_0, θ_0 = displacements at node 0,

M_0, V_0, N_0 = forces at node 0,

u_2, w_2, θ_2 = displacements at node 2,

α = additional angle at point 1,

u'' = additional deflection in the sliding direction at point 2,

and $ZZ(i,j)$ = components in the matrix of Eq. (3.32).

CHAPTER VI

GENERAL PROCEDURES FOR ITERATIVE TRANSFER MATRIX METHOD FOR KINETO-ELASTODYNAMIC ANALYSIS OF GENERAL PLANAR MECHANISMS

6.1 Introduction

This chapter explains the basic ideas in the dynamic analysis method for flexible-body systems for general planar mechanisms. Since the mechanism forces are a function of the link accelerations, a kinematic analysis must be conducted prior to any force analysis. Section 6.2 gives the basic procedure for a closed-form, component approach for the rigid-body kinematic analysis.

Next, the basic procedures in the iterative transfer matrix method for a flexible-body dynamic analysis is explained in Section 6.3. Section 6.4 gives a model for the transfer matrix method.

6.2 Procedure of Component Approach for The Kinematic Analysis

As mentioned in Chapter 2, a multiloop mechanism can be decomposed into several components, which can be analyzed directly using a closed-form solution procedure. The rigid-body kinematic analysis involves determining the positions, velocities, and accelerations of every important point in the mechanism.

Fig. (6.1) shows a multiloop mechanism. Fig. (6.2) gives four components of the mechanism to calculate the kinematic properties (positions, velocities, and accelerations). For an input-link (Fig. 6.2a), the kinematic properties of node B can be directly determined from the given angular velocity and the length of the link. After determining the kinematic properties of node B, those of nodes C and D (Fig. 6.2b) are calculated from dyad equations. The kinematic properties of node E (Fig. 6.2c) are computed directly from the known properties of nodes B and C, which three nodes form a solid link. Finally, nodes E, F, and G (Fig. 6.2d) is a dyad so that the kinematic properties of nodes F and G can be determined from the known properties of node E.

Eight types of the basic components are identified in Section 2.2 for the kinematic analysis. All of the formulations for the rigid-body kinematic analyses of the components are presented in Appendix A.

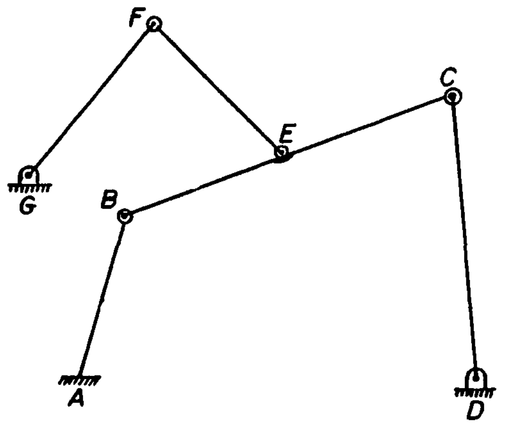

FIGURE 6.1 A Multiloop Mechanism

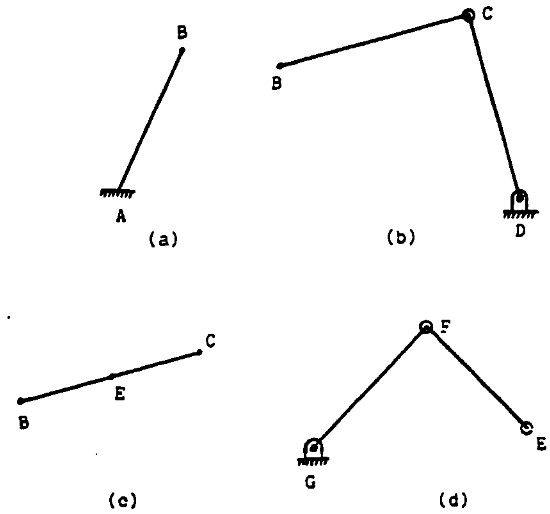

FIGURE 6.2 Components of The Mechanism In Fig. (6.1)

6.3 Procedures for The Proposed Iterative Transfer Matrix Methods for The Dynamic Analysis

6.3.1 Fundamentals for the Procedures

A planar mechanism can be thought of as an instantaneous-structure which is frozen at a particular instant by fixing the degree(s)-of-freedom associated with the mechanism input-link(s). At an instantaneous position the mechanism is modeled as a planar structure with several revolutes (moment-release joints), sliders (force-release joints), and branch systems (any sub-loop system connected with the main loop). The overall system has a global coordinate system, and each link has a local coordinate system usually defined in the axial and transverse directions.

Next, each link is divided into many sections with a lumped elastic stiffness and a lumped mass. The necessary transfer matrices at each section can be determined from the material properties, geometry, and external loads. The formulations for the transfer matrices are presented in Section 3.3.

6.3.2 Transfer Matrix Equation

After the transfer matrices for all of the sections and nodes are determined, a system equation is built by multiplying the matrices from the starting node to the end node. However, special formulations are required for the revolutes, prismatic joints, and branch points.

For the revolute, the moment about the turning axis must vanish, and the link angles are discontinuous; for the prismatic joint (slider), the sliding force must be zero, and the longitudinal displacement becomes discontinuous; and for the branch point, some of the displacements and forces at the branch points must be continuous depending on the type of branch.

6.3.3 Solution Procedures

In common boundary-value problems, there are three unknowns and three knowns in the state vectors at the starting point and the end point (usually supports). Three unknowns at the starting support can be easily determined by solving three linear simultaneous equations.

To illustrate the procedures, consider the multiloop planar mechanism shown in Fig. (6.3). A-B-C-D is a 4-bar mechanism with link AB as the input driver. It is assumed here that a rigid-body kinematic analysis has already been conducted so that nominal values for all of the linkage angles are known. For the mechanism analysis, the input link must accommodate a torque so that its support becomes a clamped condition. A branch E-F-G is connected to the main body at point E by a revolute joint. In Fig. (6.3), the driving link is at an angle θ_A from the horizontal axis in the global coordinate system. Thus, the state vector in the global coordinates at point A must be transformed by the angle θ_A into the state vector in the local coordinates at the same point. At point B, the state vector in the local coordinates of

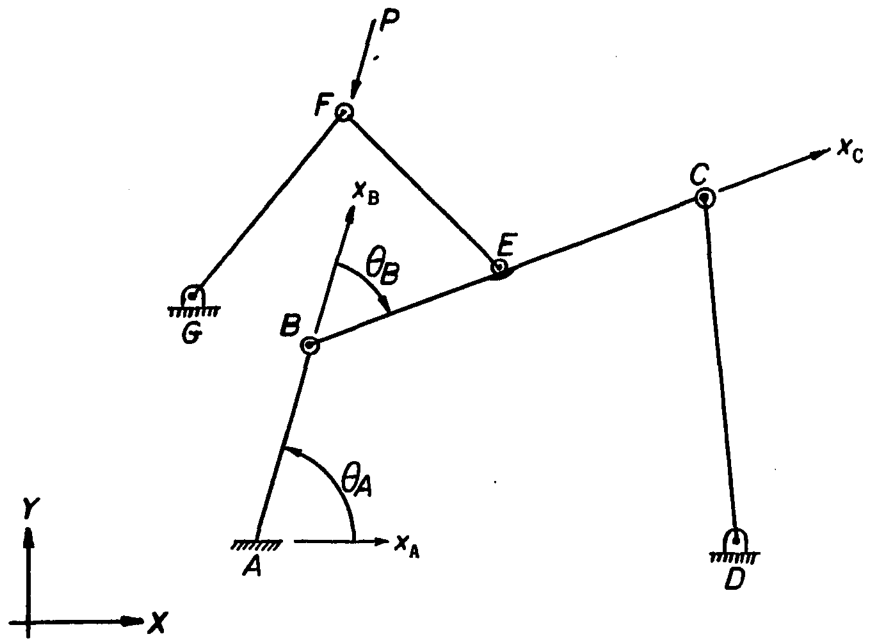

FIGURE 6.3 A Multiloop Planar Mechanism

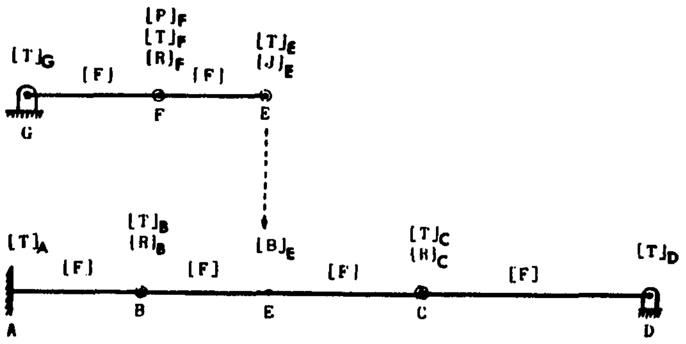

FIGURE 6.4 Schematic Plot of The Mechanism in Fig. (6.3)

link AB must be transformed by the angle Θ_B to those in the local coordinates of link BC in order to satisfy the continuity conditions. The mechanism in Fig. (6.3) can be mapped schematically as shown in Fig. (6.4). The detail numerical solutions for the system in Fig. (6.3) are given in Chapter 8 and Appendix C.

Fig. (6.4) shows the transformed main 4-bar linkage as well as the branch system of the mechanism given in Fig. (6.3), and shows the qualitative scheme used to analyze the mechanism. A transfer matrix equation for the main loop is given as follows:

$$\{S\}_D = [T]_D \cdot [F] \ldots [F] \cdot \{R\}_C \cdot [T]_C \cdot [F] \ldots [F] \cdot [B]_E$$
$$[F] \ldots [F] \cdot \{R\}_B \cdot [T]_B \cdot [F] \ldots [F] \cdot [T]_A \cdot \{S\}_A \qquad (6.1)$$

and for the branch loop,

$$\{S\}_E = \{J\}_E \cdot [T]_E \cdot [F] \ldots [F] \cdot [P]_F \cdot \{R\}_F \cdot [T]_F$$
$$[F] \ldots [F] \cdot [T]_G \cdot \{S\}_G \qquad (6.2)$$

Here, a branch matrix $[B]_E$ at point E can be determined from Eq. (6.4) using the procedures in Sections 3.3.5.2 and 5.4. $\{R\}$ and $\{J\}$ are not really matrices, but are operators which represent the matrix reformulation process to satisfy the kinematic conditions. These operators were presented in Chapter 5.

Rewriting Eq. (6.1) into a transfer matrix equation for the main loop gives

$$\{S\}_D = [TM] \{S\}_A \qquad (6.3)$$

where $\{S\}_D$ = state vector at the support D,

$\{S\}_A$ = state vector at the support A,

$\{S\}_E$ = state vector at the support E,

$\{S\}_G$ = state vector at the support G,

$[TM]$ = equivalent transfer matrix combined all elements,

$[T]$ = transformation matrix at each point,

$[F]$ = field matrix at each section,

$[B]_E$ = branch matric at point E due to a open branch E-F-G.

$[P]_F$ = point matrix at point F,

$\{J\}_E$ = branch connectivity operator,

and $\{R\}$ = revolute operator.

The state vector consists of the six variables (i.e. u, w, θ, M, V, and N). These state variables are

u = displacement in the axial direction,

w = displacement in the transverse direction,

θ = slope,

M = moment,

V = transverse force,

and N = axial force.

The boundary conditions at point A are $u_A = w_A = \theta_A = 0$ and M, V, and N as the unknowns. At point D, the pinned condition gives $u_D = w_D = M_D = 0$ and θ, V, and N as the unknowns. Thus, using the known conditions at point D, three simultaneous equations can be written and solved for the unknowns at point A.

Thus, Eq. (6.2) can be written as follows:

$$\begin{bmatrix} u \\ w \\ \theta \\ M \\ V \\ N \\ 1 \end{bmatrix}_D = \begin{bmatrix} U(1,1) & U(1,2) & U(1,3) & U(1,4) & U(1,5) & U(1,6) & U(1,7) \\ U(2,1) & U(2,2) & U(2,3) & U(2,4) & U(2,5) & U(2,6) & U(2,7) \\ U(3,1) & U(3,2) & U(3,3) & U(3,4) & U(3,5) & U(3,6) & U(3,7) \\ U(4,1) & U(4,2) & U(4,3) & U(4,4) & U(4,5) & U(4,6) & U(4,7) \\ U(5,1) & U(5,2) & U(5,3) & U(5,4) & U(5,5) & U(5,6) & U(5,7) \\ U(6,1) & U(6,2) & U(6,3) & U(6,4) & U(6,5) & U(6,6) & U(6,7) \\ 0 & 0 & 0 & 0 & 0 & 0 & 1 \end{bmatrix} \cdot \begin{bmatrix} u \\ w \\ \theta \\ M \\ V \\ N \\ 1 \end{bmatrix}_A$$

Then, applying the boundary conditions at each support

$$\begin{bmatrix} 0 \\ 0 \\ \theta \\ 0 \\ V \\ N \\ 1 \end{bmatrix}_D = \begin{bmatrix} U(1,1) & U(1,2) & U(1,3) & U(1,4) & U(1,5) & U(1,6) & U(1,7) \\ U(2,1) & U(2,2) & U(2,3) & U(2,4) & U(2,5) & U(2,6) & U(2,7) \\ U(3,1) & U(3,2) & U(3,3) & U(3,4) & U(3,5) & U(3,6) & U(3,7) \\ U(4,1) & U(4,2) & U(4,3) & U(4,4) & U(4,5) & U(4,6) & U(4,7) \\ U(5,1) & U(5,2) & U(5,3) & U(5,4) & U(5,5) & U(5,6) & U(5,7) \\ U(6,1) & U(6,2) & U(6,3) & U(6,4) & U(6,5) & U(6,6) & U(6,7) \\ 0 & 0 & 0 & 0 & 0 & 0 & 1 \end{bmatrix} \cdot \begin{bmatrix} 0 \\ 0 \\ 0 \\ M \\ V \\ N \\ 1 \end{bmatrix}_A$$

and finally three simultaneous equations are:

$$0 = U(1,4)\cdot M_A + U(1,5)\cdot V_A + U(1,6)\cdot N_A + U(1,7)$$
$$0 = U(2,4)\cdot M_A + U(2,5)\cdot V_A + U(2,6)\cdot N_A + U(2,7)$$
$$0 = U(4,4)\cdot M_A + U(4,5)\cdot V_A + U(4,6)\cdot N_A + U(4,7)$$

After solving for the unknowns (M_A, V_A, and N_A) at point A, the state vectors at every other points in the main body can be calculated, and the state vectors at every branch system can also be determined by applying the state vector, determined at the branched point. Eq. (6.4) is a typical transfer matrix equation for a segment, which shows the relationships between state vectors at the (i-1)th point and at the ith point; here, $\{S\}_i$ can be calculated from Eq. (6.4) if $\{S\}_{i-1}$ is known:

$$\{S\}_i = [TM]\cdot\{S\}_{i-1} \tag{6.4}$$

where $\{S\}_i$ = state vector at the ith position,

$\{S\}_{i-1}$ = state vector at the (i-1)th position,

and $[TM]$ = transfer matrix between the two points.

6.3.4 Iteration Procedures for Field Matrices

As mentioned earlier, the zero-axial force condition is used to determine the initial forces at any node of the flexible-body systems. Because the axial force at each section is unknown at the initial iteration, equilibrium cannot be represented explicitly so that the equations become non-linear. The moment at each segment depends on the transverse forces and displacements as well as on the unknown axial force. In addition, the displacements at the end of each segment is a function of the unknown internal forces. This means that a field matrix must incorporate the unknown axial loads which are part of the state variables. In the method presented here, the nonlinear problem is linearlized by first separating the interrelative elastic effects for the segment into the transverse and the longitudinal directions, and by calculating the internal forces in each direction. For subsequent iterations, the field matrices are calculated again by using the internal forces determined during the previous iteration.

Thus, the initial field matrix contains the elastic properties of a segment and those are independent of the elastic effects due to the internal forces. But, the elastic field matrix contains the elastic properties which are a function of the axial forces determined at the previous iteration. The accuracy of the matrix improves with each iteration. Convergence of this method is very fast, and usually only three or four iterations are required.

6.3.5 Dynamic Analyses

In dynamic analyses of flexible mechanisms, there are two types of inertial forces at the locations of lumped-masses: one is rigid-body inertial forces due to the rigid-body accelerations and the other is the elastic-body inertial forces due to the elastic vibrations of the flexible members.

The inertial forces from the rigid-body accelerations acting on the members are sometimes treated as external forces at the locations of the lumped masses. But, the elastic-body accelerations from the axial and transverse vibrations of the members can not be determined directly. To account for the inertial effects of the elastic-body vibrations, the Houbolt difference direct integration method is used as derived in Section 3.3.6.

Thus, two types of the inertial matrices are derived as given in Section 3.3.6: The rigid-body inertial matrix is used for the quasi-static analyses, and the elastic-body matrix is used for the time-domain analyses.

6.3.6 Considerations of the Fatigue Stress and Distortion Analyses

After determining all of the state variables at each point of interest in the members, stresses in each direction, combined stresses, distortions, and distortion-angles can be calculated. The stresses in each direction are determined from the forces, moments, and geometric properties. The combined stresses can also be calculated from the stresses determined. The distortion at any point is defined as the distance from the position determined by the rigid-body analysis to the position determined by the flexible-body analysis, and is easily calculated from the displacements in each direction. Finally, the distortion-angle at each point shows the direction of the distortion at the point. These stresses and distortions change with the rotation of the input link as shown in Fig. (6.5).

Here, a fatigue analysis for the dynamic stresses must be involved. The proposed ideas in the fatigue analysis are that the stresses at any segment in a member are determined for a period of one revolution of the input link as shown in Fig. (6.6). It is assumed that the segment is ideally subjected to the cyclic stresses with the maximum and minimum stresses given by the dotted line in the figure. Then, Soderberg's linear-failure line can be used for the fatigue failure analysis. This failure line is the most conservative of the non-zero mean stress fatigue failure lines [80-85]. Also it will be assumed that the mechanism can be used for infinite cycles, and therefore the endurance limit is used as the maximum allowable strength

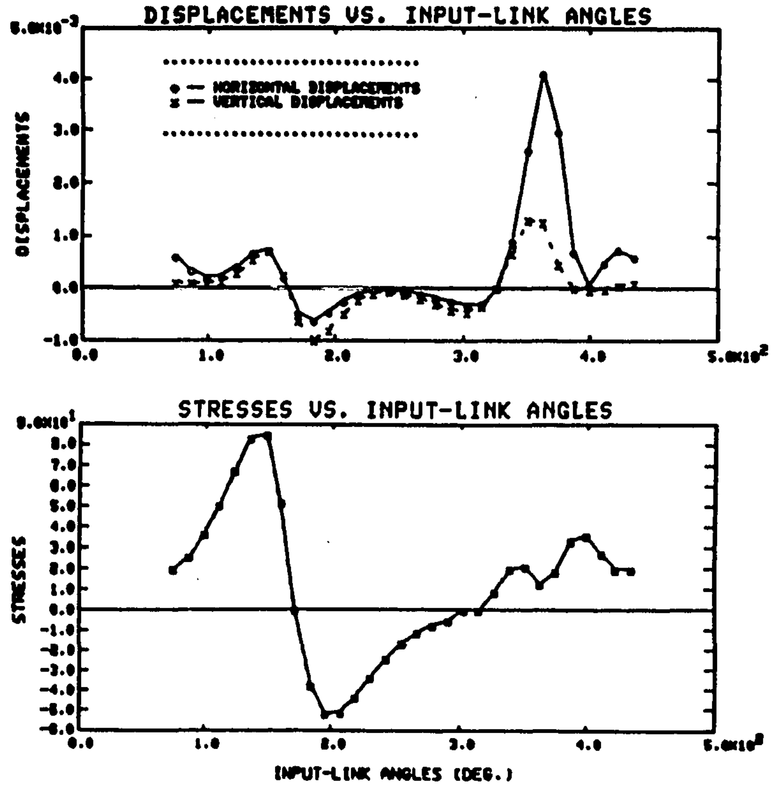

FIGURE 6.5 Stresses and Displacements of A Location in A Mechanism with The Rotation of Input Link

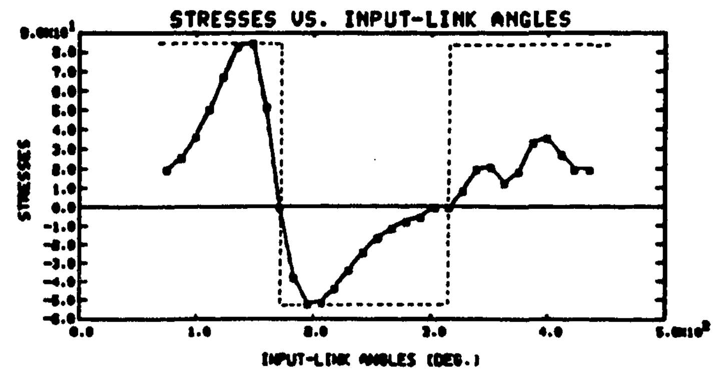

FIGURE 6.6 Stress State Assumed for The Fatigue Analysis

for stress analysis.

Applying Soderberg's linear line to the cyclic stresses, the safety factor for each link can be determined by the following relationships [80-83].

$$S_{mean} = (S_{max} + S_{min}) / 2$$
$$S_{altn} = (S_{max} - S_{min}) / 2 \qquad (6.5)$$

and

$$SF = \frac{1}{\dfrac{S_{mean}}{S_y} + \dfrac{S_{altn}}{S_n}} \qquad (6.6)$$

where SF = factor of safety,

Sn = fatigue endurance limit,

Sy = yielding strength,

Smean = mean stress,

Saltn = alternating stress,

Smax = maximum stress,

and Smin = minimum stress.

6.4 A Model for The Transfer Matrix Method for Flexible Systems

To fit into the methodology of the transfer matrix method, the following model of a mechanism is used. At an initial time $t = t_o$, the rigid-body configuration determined from a rigid-body kinematic analysis of the mechanism is considered as an 'instantaneous structure' capable of undergoing both rigid-body and elastic motions. A C D B is the position of the rigid-body system, and A C'D'B is the deformed position of the flexible linkage in Fig. (6.7). For this instantaneous structure, the inertial forces due to the rigid-body accelerations of the elements, the forces generated by springs, and the external forces acting on it are considered here. The mass and stiffness properties of the mechanism, treated as an elastic system, are derived for the rigid-body position and are assumed to remain unchanged during a chosen interval of time Dt.

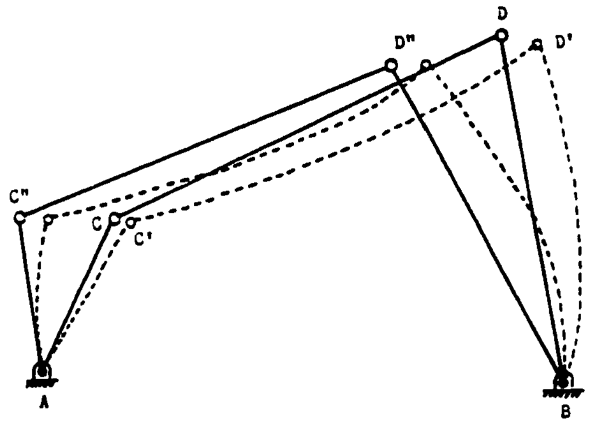

FIGURE 6.7 Model of A Mechanism for The Analyses

CHAPTER VII

OVERVIEW OF COMPUTER PROGRAM CASDAM

7.1 Introduction

The program CASDAM is a graphics-oriented, interactive, computer-aided program for static and dynamic analyses of flexible mechanisms and structures. The program incorporates the developed iterative transfer-matrix method and is intended for use with a graphics terminal such as the Tektronix 4014. The necessary transfer matrices used in the iterative transfer-matrix method have 7 X 7 elements so that the program requires much less storage than does the finite-element methods and other lumped-mass techniques. Thus, the program should be effective on mini/micro-computers.

The program CASDAM is developed on a Digital Equipment Corporation VAX 11/750 minicomputer installed in The Advance Design Method Laboratory, Department of Mechanical Engineering, The Ohio State University. There has been considerable effort made in trying to develop the program so that the program has minimal amounts of machine dependency. The program language used is 1977 ANSI FORTRAN IV.

In this chapter, the program CASDAM is discussed briefly. Section 7.2 explains the functional structure of CASDAM. The description of each routine, tree structure, and overall statistical data for the program are given in Appendix E.

7.2 Functional Structure of Program CASDAM

The program CASDAM consists of three processes given in Table 7.1: pre-process, process, and post-process. In the preprocess step, the necessary data are input interactively or in batch mode, and then data for processing are generated automatically. The kinematic analyses are carried out if a dynamic analysis is required.

In the process step, the displacements and internal forces are calculated by the iterative transfer-matrix method. The static stress analysis or dynamic stress analysis is also carried out. Then, the maximum displacements at every node and the safety factors for the system at the critical nodes are determined.

The postprocess gives the geometrical and graphical plots for the displacements, stresses, and safety factors. All of the results are given by the graphics-oriented plots on the terminal screen and in the tabular forms.

TABLE 7.1 Functional Structure of CASDAM

STEP	FUNCTIONS
PREPROCESS	Input Data ↓ Kinematic Analyses ****************** Calculate positions and accelerations ↓ Data Generation ↓
PROCESS	ANALYSES ******** Calculate displacements, internal forces, stresses, and safety factors. ↓
POSTPROCESS	Geometrical Plots for Displacements and Safety Factors of The System ↓ Graphical Plots for Displacements and Stresses of A Node

CHAPTER VIII

DEMONSTRATION AND APPLICATION

8.1 Introduction

In this chapter, six problems are analyzed for demonstration of the iterative transfer-matrix method. Section 8.2 gives a multiloop mechanism for static analyses under small- and large-deflection assumptions, and Section 8.3 shows a mechanism for dynamic analyses (quasi-static and steady-state responses), when the input-link can rotate a full 360 degrees. Section 8.4 gives a cantilever beam with end loads, and Section 8.5 gives a stepped beam on elastic supports under static loads. The complete solutions for these problems are given in Appendices.

8.2 Static Analyses of A Multiloop Mechanism

8.2.1 Static Analysis for Small-Deflection Problem

A planar multiloop mechanism shown in Fig. (8.1) consists of seven beam elements and a triangular plate connected with two springs. A link between nodes 1 and 2 is set as the input-link so that the end condition at node 1 becomes fixed: The end conditions at nodes 6, 8, and 12 are pinned: The sliding condition is used at node 13. All of the nodes have revolute joints except for node 5, where a sliding joint is used. Each beam is uniform and made from AISI 4340 CD steel. There are two springs in the system: A spring is connected between nodes 4 and 11, and the other spring is connected from node 3 to ground.

At node 13, an external force is loaded horizontally in the negative direction and is 100 pounds. For the geometry of the spring, the free lengths of the springs are set as 5 inches, and the distance of the grounded spring at node 3 is about 7.5 inches so that a force due to the spring is generated. The spring constant is $K = 100$ lb/in. The cross-sectional area is 0.5 X 0.5 (inch^2), and the thickness of the plate is 0.5 inch.

Fig. (8.2) shows the mechanism generated with a number of elements for each link. Figs. (8.3) and (8.4) give the deflected system under small-deflections and the safety factors, respectively. Table 8.1 gives the displacements at every node. Table 8.2 shows the internal forces and stresses at each node. The reaction forces at the supports are given in Table 8.3. Finally, the safety factors for nodes are shown in Table 8.4.

The mechanism link deflections are assumed to be small. The maximum distortion, which is the distance from the original position to the deflected position, is 0.0787 inch at node 11. The minimum safety factor for the system is 1.86 at node 3 for the given steel based on a yield strength of 100,000 psi. The analysis details are given in Appendix B.

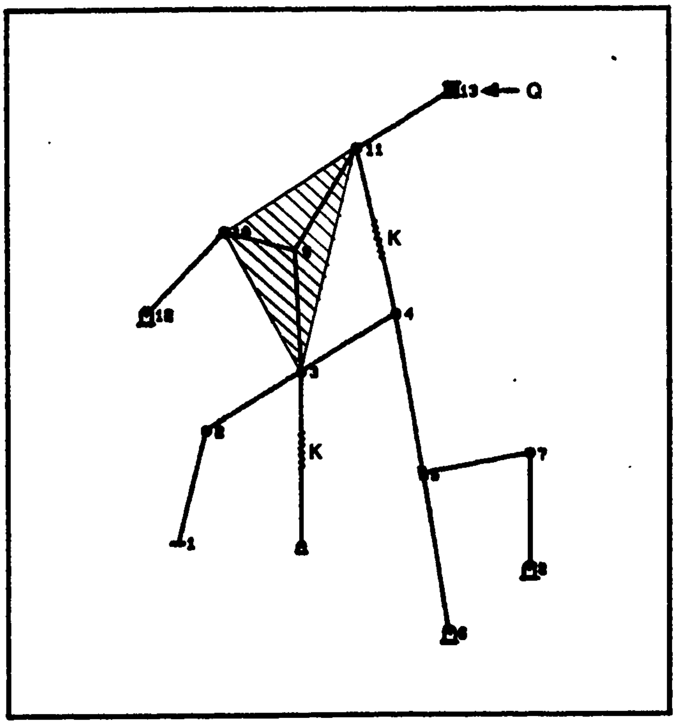

FIGURE 8.1 A Multiloop Mechanism for Static Analysis

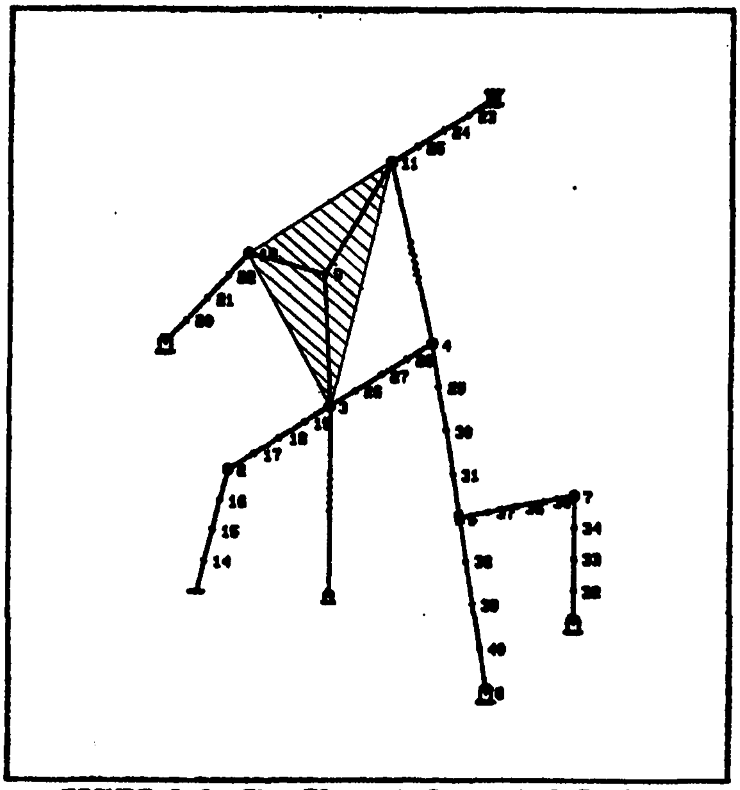

FIGURE 8.2 The Element-Generated System

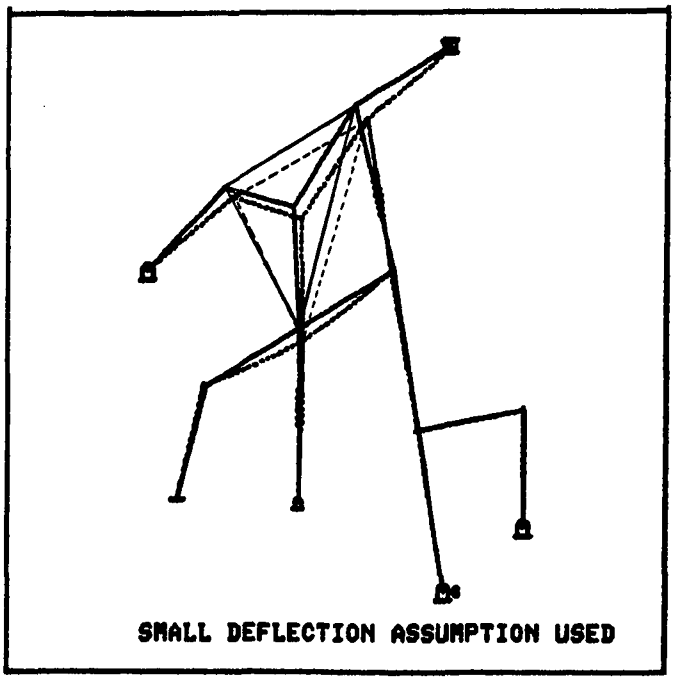

FIGURE 8.3 The Deflected System under Small-Deflections

TABLE 8.1 Displacements of Nodes

SMALL-DEFLECTION ASSUMPTION USED
UNITS ARE BRITISH (INCHES)

NODE NO	LOCATION X	LOCATION Y	DISPLACEMENTS HORIZ	DISPLACEMENTS VERTI	SLOPE DEG
1	0.0000E+00	0.0000E+00	0.0000E+00	0.0000E+00	0.0000E+00
2	0.1294E+01	0.4830E+01	-0.1077E-01	0.2627E-02	-0.1053E+01
3	0.5624E+01	0.7330E+01	0.1964E-01	-0.5131E-01	-0.2393E-01
4	0.9954E+01	0.9830E+01	-0.9424E-02	-0.1674E-02	0.3917E-01
5	0.1117E+02	0.2936E+01	-0.4712E-02	-0.8368E-03	0.3917E-01
6	0.1239E+02	-.3958E+01	0.0000E+00	0.0000E+00	0.3917E-01
7	0.1609E+02	0.3804E+01	-0.4860E-02	-0.2363E-05	0.3917E-01
8	0.1609E+02	-.1196E+01	0.0000E+00	0.0000E+00	0.5570E-01
9	0.5320E+01	0.1257E+02	0.3677E-01	-0.5032E-01	0.1873E+00
10	0.2124E+01	0.1339E+02	0.3946E-01	-0.3987E-01	0.1873E+00
11	0.8212E+01	0.1699E+02	0.5122E-01	-0.5977E-01	0.1873E+00
12	-.1411E+01	0.9856E+01	0.0000E+00	0.0000E+00	-0.6428E+00
13	0.1254E+02	0.1949E+02	0.1607E-01	0.0000E+00	0.7946E+00
14	0.3235E+00	0.1207E+01	-0.9330E-03	0.1889E-03	0.8319E-01
15	0.6470E+00	0.2415E+01	-0.3372E-02	0.7790E-03	0.1428E+00
16	0.9706E+00	0.3622E+01	-0.6818E-02	0.1636E-02	0.1787E+00
17	0.2377E+01	0.5455E+01	0.2682E-03	-0.1699E-01	-0.9885E+00
18	0.3459E+01	0.6080E+01	0.9939E-02	-0.3414E-01	-0.7951E+00
19	0.4542E+01	0.6705E+01	0.1686E-01	-0.4638E-01	-0.4732E+00
20	-.5274E+00	0.1074E+02	0.9865E-02	-0.9967E-02	-0.6428E+00
21	0.3565E+00	0.1162E+02	0.1973E-01	-0.1993E-01	-0.6428E+00
22	0.1240E+01	0.1251E+02	0.2960E-01	-0.2990E-01	-0.6428E+00
23	0.1146E+02	0.1886E+02	0.2486E-01	-0.1494E-01	0.7946E+00
24	0.1038E+02	0.1824E+02	0.3365E-01	-0.2989E-01	0.7946E+00
25	0.9295E+01	0.1761E+02	0.4243E-01	-0.4483E-01	0.7946E+00
26	0.6707E+01	0.7955E+01	0.1734E-01	-0.4732E-01	0.4245E+00
27	0.7789E+01	0.8580E+01	0.1080E-01	-0.3611E-01	0.7446E+00
28	0.8872E+01	0.9205E+01	0.1405E-02	-0.2009E-01	0.9365E+00
29	0.1026E+02	0.8106E+01	-0.8246E-02	-0.1464E-02	0.3917E-01
30	0.1056E+02	0.6383E+01	-0.7068E-02	-0.1255E-02	0.3917E-01
31	0.1087E+02	0.4659E+01	-0.5890E-02	-0.1046E-02	0.3917E-01
32	0.1609E+02	0.5422E-01	-0.1215E-02	0.0000E+00	0.5570E-01
33	0.1609E+02	0.1304E+01	-0.2430E-02	-0.1181E-05	0.5570E-01
34	0.1609E+02	0.2554E+01	-0.3645E-02	-0.1772E-05	0.5570E-01
35	0.1486E+02	0.3587E+01	-0.4712E-02	-0.8439E-03	0.3917E-01
36	0.1363E+02	0.3370E+01	-0.4563E-02	-0.1686E-02	0.3917E-01
37	0.1240E+02	0.3153E+01	-0.4414E-02	-0.2527E-02	0.3917E-01
38	0.1147E+02	0.1213E+01	-0.3534E-02	-0.6275E-03	0.3917E-01
39	0.1178E+02	-.5109E+00	-0.2356E-02	-0.4183E-03	0.3917E-01
40	0.1208E+02	-.2234E+01	-0.1178E-02	-0.2091E-03	0.3917E-01

TABLE 8.2 Internal Forces and Stresses

SMALL-DEFLECTION ASSUMPTION USED
UNITS ARE BRITISH (LBS, LBS-IN, AND PSI)

NODE NO	INTERNAL FORCES HORIZ	VERTI	MOMENT	STRESSES TOP	BOTTOM
1	-0.1304E+03	-0.3296E+03	0.2070E+03	0.9414E+04	-0.1046E+05
2	-0.1304E+03	-0.3296E+03	0.0000E+00	-0.5216E+03	-0.5216E+03
3	-0.5403E+02	0.2280E+03	0.1118E+04	0.5345E+05	-0.5388E+05
4	-0.7885E+00	0.4454E+01	0.0000E+00	-0.3154E+01	-0.3154E+01
5	-0.7885E+00	0.4454E+01	0.0000E+00	-0.3154E+01	-0.3154E+01
6	-0.7885E+00	0.4454E+01	0.0000E+00	-0.1810E+02	-0.1810E+02
7	0.0000E+00	0.0000E+00	0.0000E+00	0.0000E+00	0.0000E+00
8	0.0000E+00	0.0000E+00	0.0000E+00	0.0000E+00	0.0000E+00
9	0.7636E+02	0.3127E+03	0.4952E+03	0.0000E+00	0.0000E+00
10	0.3044E+02	0.2976E+02	0.0000E+00	0.1218E+03	0.1218E+03
11	0.4592E+02	0.2830E+03	0.0000E+00	0.1837E+03	0.1837E+03
12	0.3044E+02	0.2976E+02	0.0000E+00	0.1218E+03	0.1218E+03
13	0.1000E+03	0.5960E+02	0.0000E+00	0.4000E+03	0.4000E+03
14	-0.1304E+03	-0.3296E+03	0.1559E+03	0.6075E+04	-0.8892E+04
15	-0.1304E+03	-0.3296E+03	0.1042E+03	0.3593E+04	-0.6410E+04
16	-0.1304E+03	-0.3296E+03	0.5221E+02	0.1098E+04	-0.3914E+04
17	-0.1304E+03	-0.3296E+03	0.2816E+03	0.1241E+05	-0.1463E+05
18	-0.1304E+03	-0.3296E+03	0.5623E+03	0.2588E+05	-0.2810E+05
19	-0.1304E+03	-0.3296E+03	0.8416E+03	0.3929E+05	-0.4151E+05
20	0.3044E+02	0.2976E+02	0.0000E+00	0.1703E+03	0.1703E+03
21	0.3044E+02	0.2976E+02	0.0000E+00	0.1703E+03	0.1703E+03
22	0.3044E+02	0.2976E+02	0.0000E+00	0.1703E+03	0.1703E+03
23	0.1000E+03	0.5960E+02	0.0000E+00	-0.4656E+03	-0.4656E+03
24	0.1000E+03	0.5960E+02	0.0000E+00	-0.4656E+03	-0.4656E+03
25	0.1000E+03	0.5960E+02	0.0000E+00	-0.4656E+03	-0.4656E+03
26	-0.5403E+02	0.2280E+03	0.8382E+03	0.4050E+05	-0.3996E+05
27	-0.5403E+02	0.2280E+03	0.5585E+03	0.2708E+05	-0.2654E+05
28	-0.5403E+02	0.2280E+03	0.2791E+03	0.1367E+05	-0.1313E+05
29	-0.7885E+00	0.4454E+01	0.0000E+00	-0.1810E+02	-0.1810E+02
30	-0.7885E+00	0.4454E+01	0.0000E+00	-0.1810E+02	-0.1810E+02
31	-0.7885E+00	0.4454E+01	0.0000E+00	-0.1810E+02	-0.1810E+02
32	0.0000E+00	0.0000E+00	0.0000E+00	0.0000E+00	0.0000E+00
33	0.0000E+00	0.0000E+00	0.0000E+00	0.0000E+00	0.0000E+00
34	0.0000E+00	0.0000E+00	0.0000E+00	0.0000E+00	0.0000E+00
35	0.0000E+00	0.0000E+00	0.0000E+00	0.0000E+00	0.0000E+00
36	0.0000E+00	0.0000E+00	0.0000E+00	0.0000E+00	0.0000E+00
37	0.0000E+00	0.0000E+00	0.0000E+00	0.0000E+00	0.0000E+00
38	-0.7885E+00	0.4454E+01	0.0000E+00	-0.1810E+02	-0.1810E+02
39	-0.7885E+00	0.4454E+01	0.0000E+00	-0.1810E+02	-0.1810E+02
40	-0.7885E+00	0.4454E+01	0.0000E+00	-0.1810E+02	-0.1810E+02

TABLE 8.3 Reaction Forces of Supports

UNITS ARE BRITISH (LBS AND LBS-IN)

NODE NO	REACTION FORCES HORZ.	REACTION FORCES VERT.	MOMENT
1	0.1304E+03	0.3296E+03	-0.2070E+03
6	-0.7885E+00	0.4454E+01	0.0000E+00
8	0.0000E+00	0.0000E+00	0.0000E+00
12	-0.3044E+02	-0.2976E+02	0.0000E+00
13	0.0000E+00	-0.5960E+02	0.0000E+00

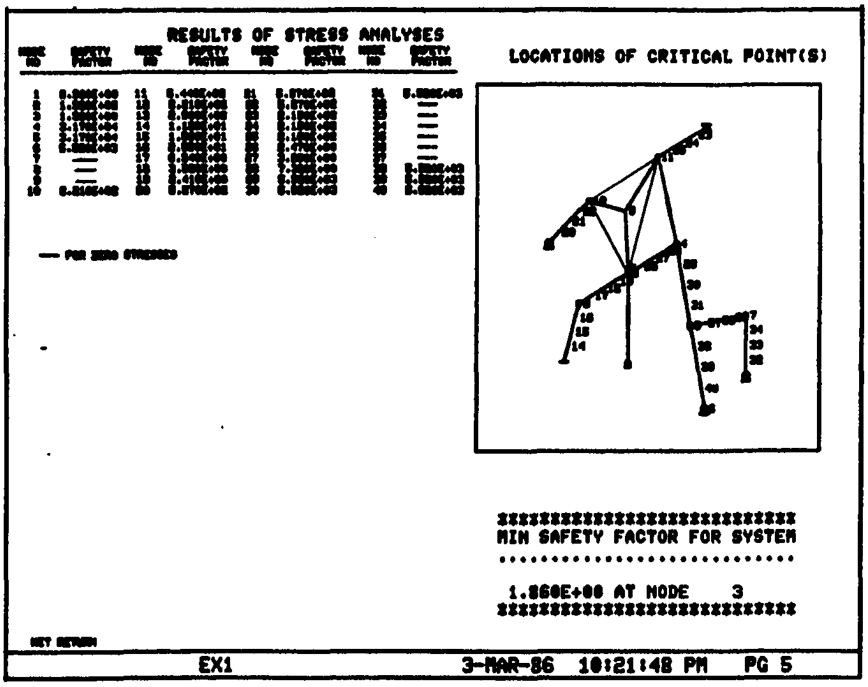

FIGURE 8.4 The Safety Factors for the Nodes

TABLE 8.4 Safety Factors of Nodes

SAFETY FACTOR DETERMINED FROM MAX. NORMAL STRESS THEORY
*** CORRESPONDS TO ZERO STRESS ON THE LINK OR RIGID LINK
UNITS ARE BRITISH (PSI FOR STRESSES)

NODE NO	YIELD STRENGTH	STRESSES TOP	STRESSES BOTTOM	SAFETY FACTOR
1	0.1000E+06	0.9414E+04	-.1046E+05	0.956E+01
2	0.1000E+06	-.5216E+03	-.5216E+03	0.192E+03
3	0.1000E+06	0.5345E+05	-.5388E+05	0.186E+01
4	0.1000E+06	-.3154E+01	-.3154E+01	0.317E+05
5	0.1000E+06	-.3154E+01	-.3154E+01	0.317E+05
6	0.1000E+06	-.1810E+02	-.1810E+02	0.552E+04
7	0.1000E+06	0.0000E+00	0.0000E+00	***
8	0.1000E+06	0.0000E+00	0.0000E+00	***
9	0.1000E+06	0.0000E+00	0.0000E+00	***
10	0.1000E+06	0.1218E+03	0.1218E+03	0.821E+03
11	0.1000E+06	0.1837E+03	0.1837E+03	0.544E+03
12	0.1000E+06	0.1218E+03	0.1218E+03	0.821E+03
13	0.1000E+06	0.4000E+03	0.4000E+03	0.250E+03
14	0.1000E+06	0.6075E+04	-.8892E+04	0.112E+02
15	0.1000E+06	0.3593E+04	-.6410E+04	0.156E+02
16	0.1000E+06	0.1098E+04	-.3914E+04	0.255E+02
17	0.1000E+06	0.1241E+05	-.1463E+05	0.684E+01
18	0.1000E+06	0.2588E+05	-.2810E+05	0.356E+01
19	0.1000E+06	0.3929E+05	-.4151E+05	0.241E+01
20	0.1000E+06	0.1703E+03	0.1703E+03	0.587E+03
21	0.1000E+06	0.1703E+03	0.1703E+03	0.587E+03
22	0.1000E+06	0.1703E+03	0.1703E+03	0.587E+03
23	0.1000E+06	-.4656E+03	-.4656E+03	0.215E+03
24	0.1000E+06	-.4656E+03	-.4656E+03	0.215E+03
25	0.1000E+06	-.4656E+03	-.4656E+03	0.215E+03
26	0.1000E+06	0.4050E+05	-.3996E+05	0.247E+01
27	0.1000E+06	0.2708E+05	-.2654E+05	0.369E+01
28	0.1000E+06	0.1367E+05	-.1313E+05	0.732E+01
29	0.1000E+06	-.1810E+02	-.1810E+02	0.552E+04
30	0.1000E+06	-.1810E+02	-.1810E+02	0.552E+04
31	0.1000E+06	-.1810E+02	-.1810E+02	0.552E+04
32	0.1000E+06	0.0000E+00	0.0000E+00	***
33	0.1000E+06	0.0000E+00	0.0000E+00	***
34	0.1000E+06	0.0000E+00	0.0000E+00	***
35	0.1000E+06	0.0000E+00	0.0000E+00	***
36	0.1000E+06	0.0000E+00	0.0000E+00	***
37	0.1000E+06	0.0000E+00	0.0000E+00	***
38	0.1000E+06	-.1810E+02	-.1810E+02	0.552E+04
39	0.1000E+06	-.1810E+02	-.1810E+02	0.552E+04
40	0.1000E+06	-.1810E+02	-.1810E+02	0.552E+04

*** MIN. SAFETY FACTOR FOR SYSTEM = 1.86 AT NODE 3 ***

8.2.2 Static Analysis for Large-Deflection Problem

External forces are applied -300 lbs horizontally and vertically at nodes 5 and 7, respectively, in the system shown in Fig. (8.5a). The cross-sectional area for the links is 0.3 X 0.3 ($inch^2$), and made from a steel. Fig. (8.5b) gives the deflected system under large-deflections.

Table 8.5 gives the displacements at every node. Table 8.6 shows the internal forces and stresses at the nodes. The reaction forces at the supports are given in Table 8.7. Fig. (8.6) gives the safety factors of every node in the system. The safety factors are tabulated in Table 8.8.

The mechanism link deflections are assumed to be large. The maximum distortion, which is the distance from the original position to the deflected position, is 4.097 inch at node 33. The safety factor for the system is 0.261 at node 3 for the given steel based on a yield strength of 100,000 psi.

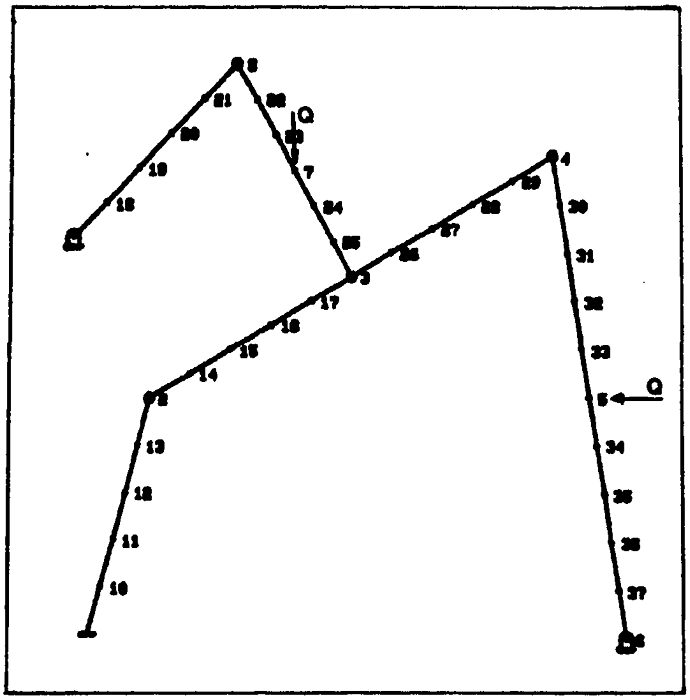

(a) Element-Generated System

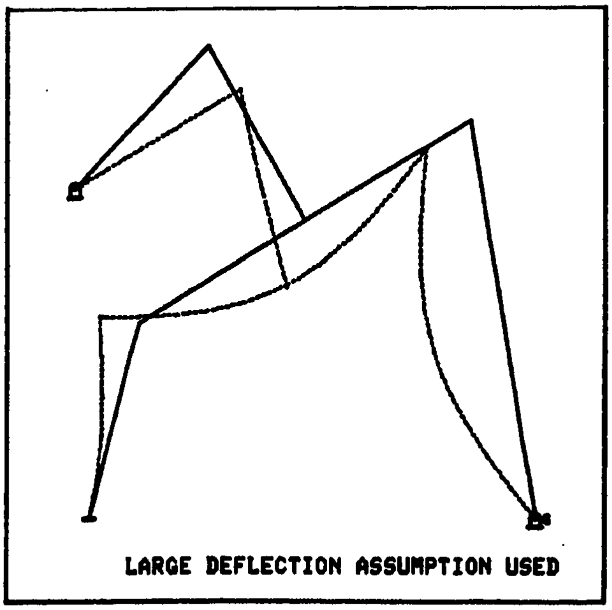

(b) Deflected system

FIGURE 8.5 A Mechanism For Large-Deflections Analysis

TABLE 8.5 Displacements of Nodes

LARGE-DEFLECTION ASSUMPTION USED
UNITS ARE BRITISH (INCHES)

NODE NO	LOCATION X	LOCATION Y	DISPLACEMENTS HORIZ	DISPLACEMENTS VERTI	SLOPE DEG
1	0.0000E+00	0.0000E+00	0.0000E+00	0.0000E+00	0.0000E+00
2	0.2588E+01	0.9659E+01	-0.2062E+01	0.2818E+00	-0.2991E+02
3	0.1125E+02	0.1466E+02	-0.9330E+00	-0.3194E+01	-0.3792E+01
4	0.1991E+02	0.1966E+02	-0.2325E+01	-0.1447E+01	-0.1567E+02
5	0.2165E+02	0.9811E+01	-0.3674E+01	-0.1519E+01	0.7776E+01
6	0.2338E+02	-.3690E-01	0.0000E+00	0.0000E+00	0.3031E+02
7	0.8748E+01	0.1899E+02	0.2736E+00	-0.2695E+01	-0.1589E+02
8	0.6248E+01	0.2332E+02	0.1638E+01	-0.2156E+01	-0.1726E+02
9	-.8226E+00	0.1625E+02	0.0000E+00	0.0000E+00	-0.1551E+02
10	0.5176E+00	0.1932E+01	-0.1080E+00	0.2557E-01	0.6194E+01
11	0.1035E+01	0.3864E+01	-0.4115E+00	0.8206E-01	0.1129E+02
12	0.1553E+01	0.5796E+01	-0.8710E+00	0.1492E+00	0.1508E+02
13	0.2071E+01	0.7727E+01	-0.1439E+01	0.2166E+00	0.1742E+02
14	0.4320E+01	0.1066E+02	-0.1794E+01	-0.7139E+00	-0.2880E+02
15	0.6052E+01	0.1166E+02	-0.1528E+01	-0.1630E+01	-0.2550E+02
16	0.7784E+01	0.1266E+02	-0.1274E+01	-0.2391E+01	-0.2011E+02
17	0.9516E+01	0.1366E+02	-0.1061E+01	-0.2930E+01	-0.1279E+02
18	0.5916E+00	0.1766E+02	0.3275E+00	-0.4312E+00	-0.1551E+02
19	0.2006E+01	0.1908E+02	0.6550E+00	-0.8625E+00	-0.1551E+02
20	0.3420E+01	0.2049E+02	0.9825E+00	-0.1294E+01	-0.1551E+02
21	0.4834E+01	0.2191E+02	0.1310E+01	-0.1725E+01	-0.1551E+02
22	0.7082E+01	0.2188E+02	0.1171E+01	-0.2339E+01	-0.1711E+02
23	0.7915E+01	0.2043E+02	0.7138E+00	-0.2519E+01	-0.1665E+02
24	0.9582E+01	0.1755E+02	-0.1434E+00	-0.2866E+01	-0.1512E+02
25	0.1042E+02	0.1610E+02	-0.5427E+00	-0.3031E+01	-0.1464E+02
26	0.1298E+02	0.1566E+02	-0.9469E+00	-0.3171E+01	0.5067E+01
27	0.1471E+02	0.1666E+02	-0.1119E+01	-0.2919E+01	0.1208E+02
28	0.1644E+02	0.1766E+02	-0.1433E+01	-0.2509E+01	0.1715E+02
29	0.1818E+02	0.1866E+02	-0.1851E+01	-0.2001E+01	0.2021E+02
30	0.2026E+02	0.1769E+02	-0.2860E+01	-0.1468E+01	-0.1470E+02
31	0.2060E+02	0.1572E+02	-0.3327E+01	-0.1495E+01	-0.1181E+02
32	0.2095E+02	0.1375E+02	-0.3660E+01	-0.1525E+01	-0.7031E+01
33	0.2130E+02	0.1178E+02	-0.3795E+01	-0.1544E+01	-0.4598E+00
34	0.2199E+02	0.7842E+01	-0.3272E+01	-0.1404E+01	0.1590E+02
35	0.2234E+02	0.5872E+01	-0.2641E+01	-0.1178E+01	0.2221E+02
36	0.2269E+02	0.3902E+01	-0.1846E+01	-0.8505E+00	0.2672E+02
37	0.2303E+02	0.1933E+01	-0.9481E+00	-0.4459E+00	0.2942E+02

TABLE 8.6 Internal Forces and Stresses of Nodes

LARGE-DEFLECTION ASSUMPTION USED
UNITS ARE BRITISH (LBS, LBS-IN, AND PSI)

NODE NO	INTERNAL FORCES HORIZ	VERTI	MOMENT	STRESSES TOP	BOTTOM
1	-0.1287E+03	-0.1957E+03	0.1177E+04	0.2601E+06	-0.2630E+06
2	-0.1287E+03	-0.1957E+03	0.0000E+00	-0.1430E+04	-0.1430E+04
3	-0.1638E+03	0.8453E+02	0.1719E+04	0.3802E+06	-0.3838E+06
4	-0.1638E+03	0.8453E+02	0.0000E+00	-0.1820E+04	-0.1820E+04
5	0.1362E+03	0.8453E+02	0.1592E+04	0.3553E+06	-0.3523E+06
6	0.1362E+03	0.8453E+02	0.0000E+00	-0.6621E+03	-0.6621E+03
7	-0.3507E+02	0.2802E+03	0.1933E+03	0.4257E+05	-0.4335E+05
8	-0.3507E+02	-0.1979E+02	0.0000E+00	-0.3897E+03	-0.3897E+03
9	-0.3507E+02	-0.1979E+02	0.0000E+00	-0.3897E+03	-0.3897E+03
10	-0.1287E+03	-0.1957E+03	0.1005E+04	0.2209E+06	-0.2258E+06
11	-0.1287E+03	-0.1957E+03	0.7907E+03	0.1732E+06	-0.1782E+06
12	-0.1287E+03	-0.1957E+03	0.5448E+03	0.1186E+06	-0.1235E+06
13	-0.1287E+03	-0.1957E+03	0.2777E+03	0.5924E+05	-0.6418E+05
14	-0.1287E+03	-0.1957E+03	0.3908E+03	0.8452E+05	-0.8917E+05
15	-0.1287E+03	-0.1957E+03	0.7710E+03	0.1690E+06	-0.1737E+06
16	-0.1287E+03	-0.1957E+03	0.1129E+04	0.2486E+06	-0.2532E+06
17	-0.1287E+03	-0.1957E+03	0.1450E+04	0.3199E+06	-0.3245E+06
18	-0.3507E+02	-0.1979E+02	0.0000E+00	-0.4310E+03	-0.4310E+03
19	-0.3507E+02	-0.1979E+02	0.0000E+00	-0.4310E+03	-0.4310E+03
20	-0.3507E+02	-0.1979E+02	0.0000E+00	-0.4310E+03	-0.4310E+03
21	-0.3507E+02	-0.1979E+02	0.0000E+00	-0.4310E+03	-0.4310E+03
22	-0.3507E+02	-0.1979E+02	0.6429E+02	0.1428E+05	-0.1429E+05
23	-0.3507E+02	-0.1979E+02	0.1287E+03	0.2860E+05	-0.2860E+05
24	-0.3507E+02	0.2802E+03	0.1331E+03	0.2669E+05	-0.3247E+05
25	-0.3507E+02	0.2802E+03	0.6788E+02	0.1219E+05	-0.1798E+05
26	-0.1638E+03	0.8453E+02	0.1407E+04	0.3116E+06	-0.3138E+06
27	-0.1638E+03	0.8453E+02	0.1070E+04	0.2367E+06	-0.2389E+06
28	-0.1638E+03	0.8453E+02	0.7190E+03	0.1587E+06	-0.1609E+06
29	-0.1638E+03	0.8453E+02	0.3609E+03	0.7909E+05	-0.8131E+05
30	-0.1638E+03	0.8453E+02	0.3420E+03	0.7476E+05	-0.7724E+05
31	-0.1638E+03	0.8453E+02	0.6791E+03	0.1497E+06	-0.1522E+06
32	-0.1638E+03	0.8453E+02	0.1005E+04	0.2221E+06	-0.2246E+06
33	-0.1638E+03	0.8453E+02	0.1313E+04	0.2905E+06	-0.2930E+06
34	0.1362E+03	0.8453E+02	0.1276E+04	0.2829E+06	-0.2842E+06
35	0.1362E+03	0.8453E+02	0.9557E+03	0.2117E+06	-0.2130E+06
36	0.1362E+03	0.8453E+02	0.6355E+03	0.1406E+06	-0.1419E+06
37	0.1362E+03	0.8453E+02	0.3171E+03	0.6980E+05	-0.7113E+05

TABLE 8.7 Reaction Forces at Supports

UNITS ARE BRITISH (LBS AND LBS-IN)

NODE NO	REACTION FORCES HORZ.	VERT.	MOMENT
1	0.1287E+03	0.1957E+03	-0.1177E+04
6	0.1362E+03	0.8453E+02	0.0000E+00
9	0.3507E+02	0.1979E+02	0.0000E+00

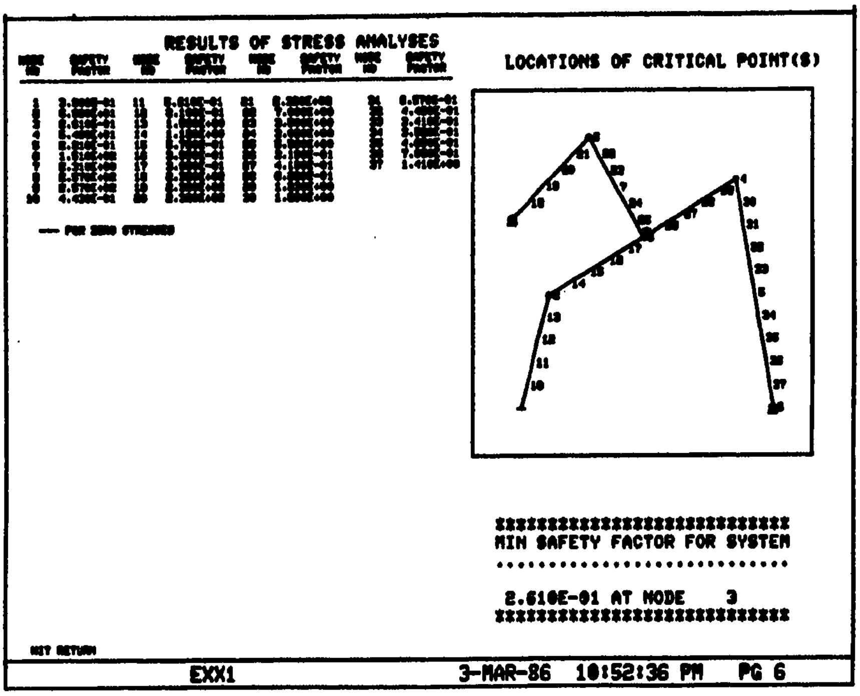

FIGURE 8.6 The Safety Factors of Nodes

TABLE 8.8 Safety Factors of Nodes

SAFETY FACTOR DETERMINED FROM MAX. NORMAL STRESS THEORY
*** CORRESPONDS TO ZERO STRESS ON THE LINK OR RIGID LINK
UNITS ARE BRITISH (PSI FOR STRESSES)

NODE NO	YIELD STRENGTH	STRESSES TOP	STRESSES BOTTOM	SAFETY FACTOR
1	0.1000E+06	0.2601E+06	-.2630E+06	0.380E+00
2	0.1000E+06	-.1430E+04	-.1430E+04	0.699E+02
3	0.1000E+06	0.3802E+06	-.3838E+06	0.261E+00
4	0.1000E+06	-.1820E+04	-.1820E+04	0.549E+02
5	0.1000E+06	0.3553E+06	-.3523E+06	0.281E+00
6	0.1000E+06	-.6621E+03	-.6621E+03	0.151E+03
7	0.1000E+06	0.4257E+05	-.4335E+05	0.231E+01
8	0.1000E+06	-.3897E+03	-.3897E+03	0.257E+03
9	0.1000E+06	-.3897E+03	-.3897E+03	0.257E+03
10	0.1000E+06	0.2209E+06	-.2258E+06	0.443E+00
11	0.1000E+06	0.1732E+06	-.1782E+06	0.561E+00
12	0.1000E+06	0.1186E+06	-.1235E+06	0.810E+00
13	0.1000E+06	0.5924E+05	-.6418E+05	0.156E+01
14	0.1000E+06	0.8452E+05	-.8917E+05	0.112E+01
15	0.1000E+06	0.1690E+06	-.1737E+06	0.576E+00
16	0.1000E+06	0.2486E+06	-.2532E+06	0.395E+00
17	0.1000E+06	0.3199E+06	-.3245E+06	0.308E+00
18	0.1000E+06	-.4310E+03	-.4310E+03	0.232E+03
19	0.1000E+06	-.4310E+03	-.4310E+03	0.232E+03
20	0.1000E+06	-.4310E+03	-.4310E+03	0.232E+03
21	0.1000E+06	-.4310E+03	-.4310E+03	0.232E+03
22	0.1000E+06	0.1428E+05	-.1429E+05	0.700E+01
23	0.1000E+06	0.2860E+05	-.2860E+05	0.350E+01
24	0.1000E+06	0.2669E+05	-.3247E+05	0.308E+01
25	0.1000E+06	0.1219E+05	-.1798E+05	0.556E+01
26	0.1000E+06	0.3116E+06	-.3138E+06	0.319E+00
27	0.1000E+06	0.2367E+06	-.2389E+06	0.419E+00
28	0.1000E+06	0.1587E+06	-.1609E+06	0.622E+00
29	0.1000E+06	0.7909E+05	-.8131E+05	0.123E+01
30	0.1000E+06	0.7476E+05	-.7724E+05	0.129E+01
31	0.1000E+06	0.1497E+06	-.1522E+06	0.657E+00
32	0.1000E+06	0.2221E+06	-.2246E+06	0.445E+00
33	0.1000E+06	0.2905E+06	-.2930E+06	0.341E+00
34	0.1000E+06	0.2829E+06	-.2842E+06	0.352E+00
35	0.1000E+06	0.2117E+06	-.2130E+06	0.469E+00
36	0.1000E+06	0.1406E+06	-.1419E+06	0.705E+00
37	0.1000E+06	0.6980E+05	-.7113E+05	0.141E+01

*** MIN SAFETY FACTOR FOR SYSTEM = 0.261 ***

8.3 Dynamic Analyses of A Mechanism Under Continuous Motions

For a mechanism under continuous motions, the kinematic analyses are carried out to determine the positions and accelerations of the nodes, and a fatigue stress analysis is conducted for the dynamic stresses in the elements. In the program CASDAM, the modular approach is used for the kinematic analyses at every 9 degrees of the input-link as given in Chapter 2. For the fatigue stress analyses, Soderberg's linear failure line is used.

A four-bar crank-rocker mechanism as given in Fig. (8.7) is studied (see References [7, 9, 11, 17]). The geometry of the mechanism shown in Fig. (8.7) has the following dimensions:

Length of crank	=	4.0 inches.
Length of coupler	=	11.0 inches.
Length of Follower	=	10.5 inches.
Ground link	=	10.0 inches.

The model in [7, 9] was constructed of aluminum strip 1.0 inch wide. The crank was 0.167 inch thick. The coupler and follower links were 0.063 inch thick. The coupler was connected to the crank and the follower by means of pins and small ball bearings mounted in sleeves. The total weight of the bearing and the sleeve at each end was 0.06 lb. Other apparatus details may be found in [7, 9]. As the same procedure as in References [11, 17], the total weight of the bearing and the sleeve was assumed to be distributed equally to lumped masses on the crank and follower.

The input-link is rotated at 400 rpm in the clockwise direction. Fig. (3.21) in Section 3.4 gives the nomalized rigid-body angular acceleration of the follower plotted against the crank rotation angle. Table 8.9 gives the positions and accelerations of the nodes, and Table 8.10 gives the angular accelerations of the links at the initial position. Fig. (8.8) shows the continuous motion of the mechanism.

TABLE 8.9 Positions and Accelerations of Nodes at Initial Position

TOTAL NODES	=	4
ROTATING SPEED	=	-41.87 RAD/SEC
INPUT-LINK ANGLE	=	0.0 DEGREES
UNITS	=	BRITISH

NODE NO	POSITIONS HORZ.	VERT.	ACCELERATIONS HORZ.	VERT.
1	0.0000E+00	0.0000E+00	0.0000E+00	0.0000E+00
2	0.4000E+01	0.0000E+00	-.7012E+04	0.0000E+00
3	0.7896E+01	0.1029E+02	-.5949E+04	-.9568E+04
4	0.1000E+02	0.2003E-04	0.0000E+00	0.0000E+00

TABLE 8.10 Angular Accelerations of Links at Initial Position

LINK BETWEEN NODE	NODE	ANGULAR ACCELERATIONS
1	2	0.0000E+00
2	3	-0.3984E+03
3	4	0.7377E+03

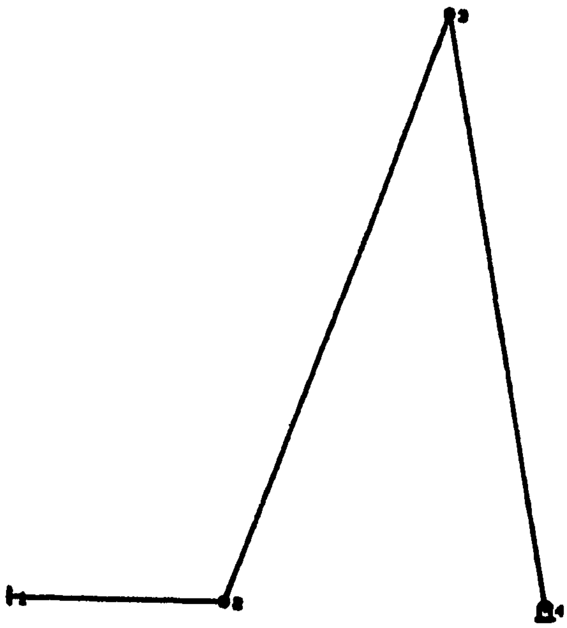

FIGURE 8.7 Initial Positions of A Mechanism

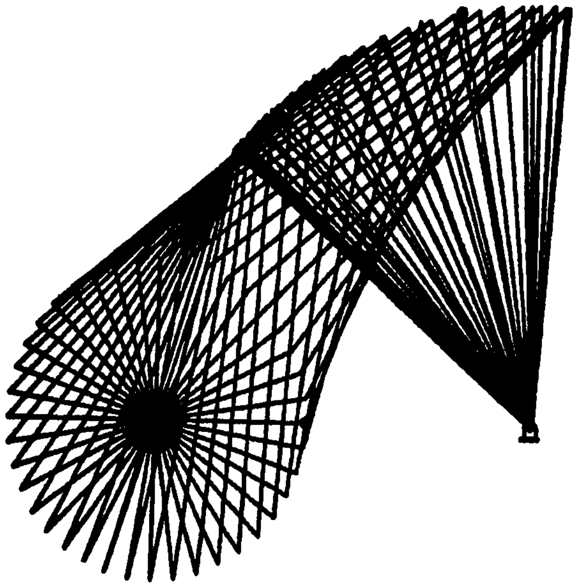

FIGURE 8.8 Continuous Motion of Mechanism

8.3.1 Quasi-Static Responses of A Mechanism

The maximum distortions at the nodes are shown in Fig. (8.9), and the safety factors from the dynamic stress analysis are given in Fig. (8.10) for a aluminum (yield strength = 90,000 psi and endurance limit = 45,000 psi). The maximum distortions at the nodes are given in Table 8.11, and the equivalent stresses and safety factors are given in Table 8.12. The minimum safety factor for the system is 5.44 at the critical point (node 12), and the maximum distortion in the system is 0.3443 inch at node 12.

Fig. (8.11) shows the displacements and stresses of node 12 in the global coordinate system. Fig. (8.12) gives the displacements and strains of node 12 in the local coordinate system. Fig. (8.13) shows the displacements and stresses of node 9 in the global coordinate system. Fig. (8.14) gives the displacements and strains of node 9 in the local coordinate system. Finally, when the angle of the input-link is -324 degrees, the positions of the rigid and deflected systems are given in Fig. (8.15). The analysis details are given in Appendix C.

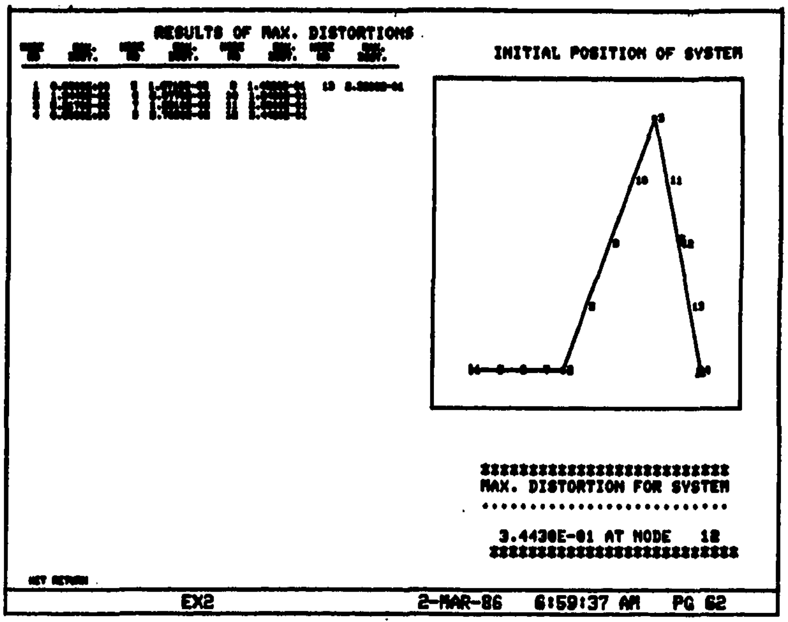

FIGURE 8.9 Maximum Distortions of Nodes

TABLE 8.11 Maximum Distortions of Nodes

UNITS ARE BRITISH (INCHES FOR DISTORTIONS)

NODE NO	MAXIMUM DISTORTIONS	
1	0.0000E+00	
2	0.1944E-01	
3	0.5217E-01	
4	0.0000E+00	
5	0.1671E-02	
6	0.6077E-02	
7	0.1231E-01	
8	0.8702E-01	
9	0.1402E+00	
10	0.1240E+00	
11	0.2690E+00	
12	0.3443E+00	***
13	0.2330E+00	

**** CORRESPONDS TO MAX. DISTORTION IN THE SYSTEM

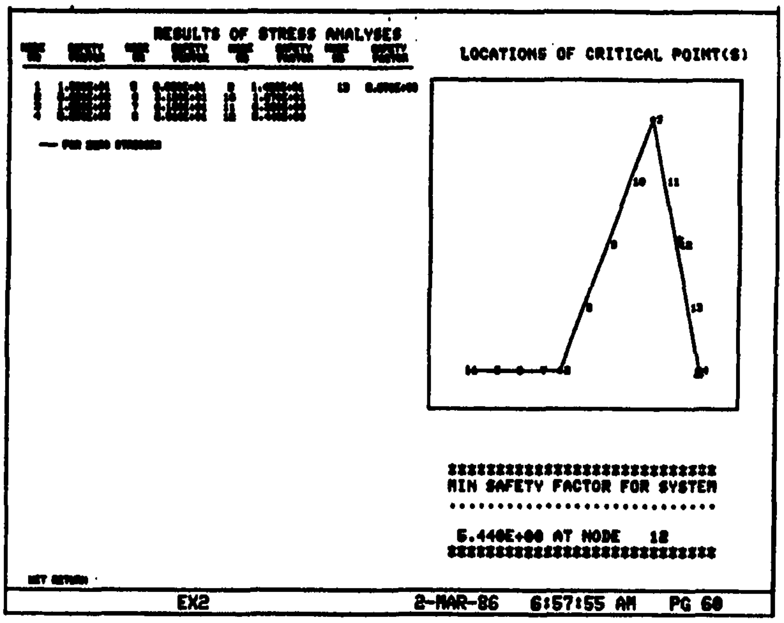

FIGURE 8.10 Safety Factors from Fatigue Stress Analysis

TABLE 8.12 Equivalent Stresses and Safety Factors of Nodes

SAFETY FACTOR DETERMINED FROM SODERBERG FAILURE LINE
UNITS ARE BRITISH (PSI FOR STRESSES)

NODE	STRENGTH		EQUIVALENT STRESSES		SAFETY	
NO	YIELD	ENDURANCE	MEAN.	ALTN.	FACTOR	
1	0.9000E+05	0.4500E+05	0.5655E+03	0.2597E+04	0.156E+02	
2	0.9000E+05	0.4500E+05	0.2455E+02	0.3989E+02	0.863E+03	
3	0.9000E+05	0.4500E+05	0.1441E+02	0.1554E+02	0.198E+04	
4	0.9000E+05	0.4500E+05	-.4585E+01	0.5226E+02	0.825E+03	
5	0.9000E+05	0.4500E+05	0.4335E+03	0.1945E+04	0.208E+02	
6	0.9000E+05	0.4500E+05	0.2930E+03	0.1298E+04	0.312E+02	
7	0.9000E+05	0.4500E+05	0.1518E+03	0.6521E+03	0.618E+02	
8	0.9000E+05	0.4500E+05	0.1780E+03	0.2149E+04	0.201E+02	
9	0.9000E+05	0.4500E+05	0.4705E+03	0.2932E+04	0.142E+02	
10	0.9000E+05	0.4500E+05	0.5520E+03	0.2420E+04	0.167E+02	
11	0.9000E+05	0.4500E+05	-.2249E+04	0.5994E+04	0.632E+01	
12	0.9000E+05	0.4500E+05	-.2752E+04	0.6900E+04	0.544E+01	**
13	0.9000E+05	0.4500E+05	-.1778E+04	0.4303E+04	0.867E+01	

*** MIN. SAFETY FACTOR FOR SYSTEM = 5.44 AT NODE 12 ***

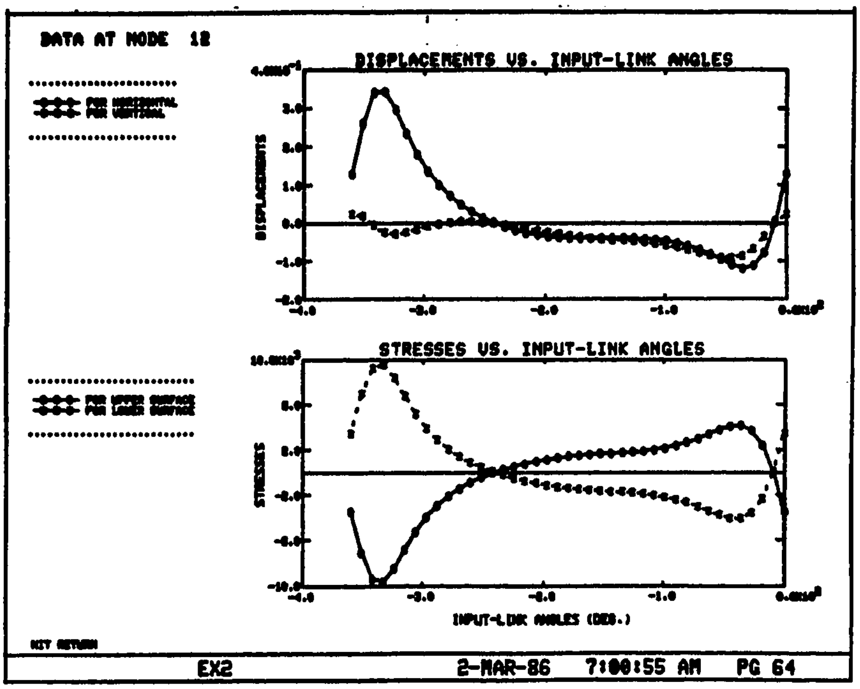

FIGURE 8.11 Displacements and Stresses of Node 12 in The Global Coordinate System

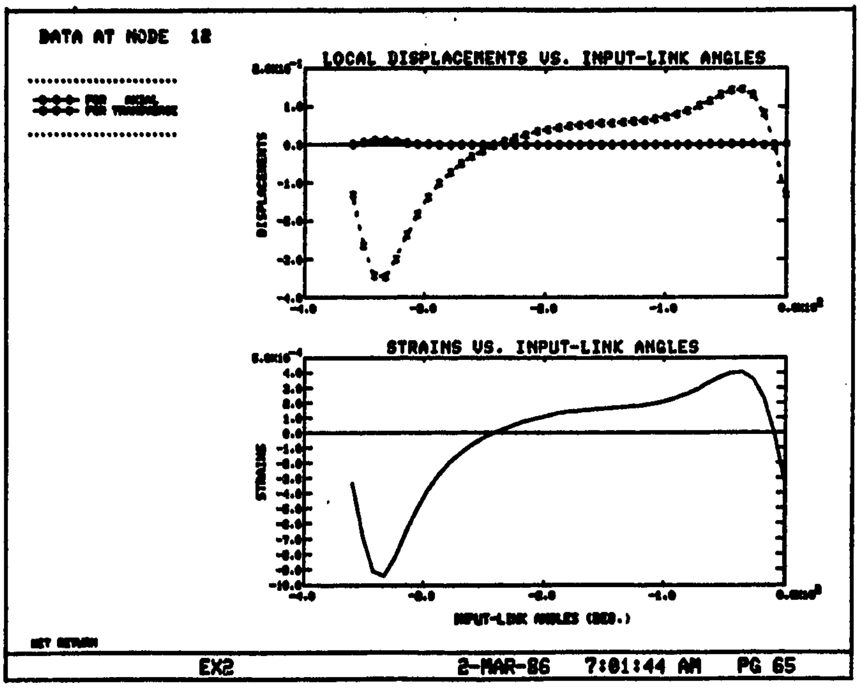

FIGURE 8.12 Displacements and Stresses of Node 12 in The Local Coordinate System

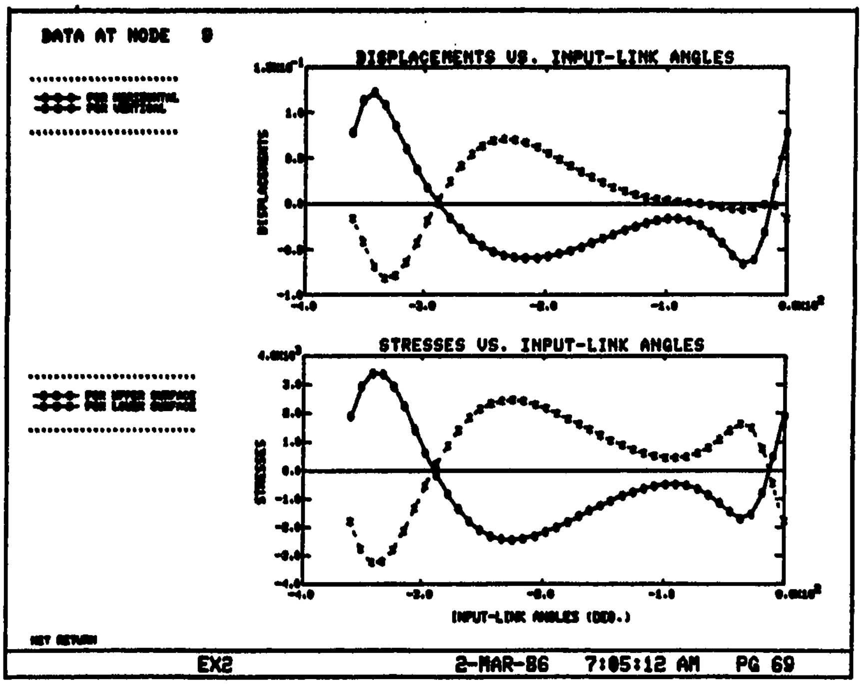

FIGURE 8.13 Displacements and Stresses of Node 9 in The Global Coordinate System

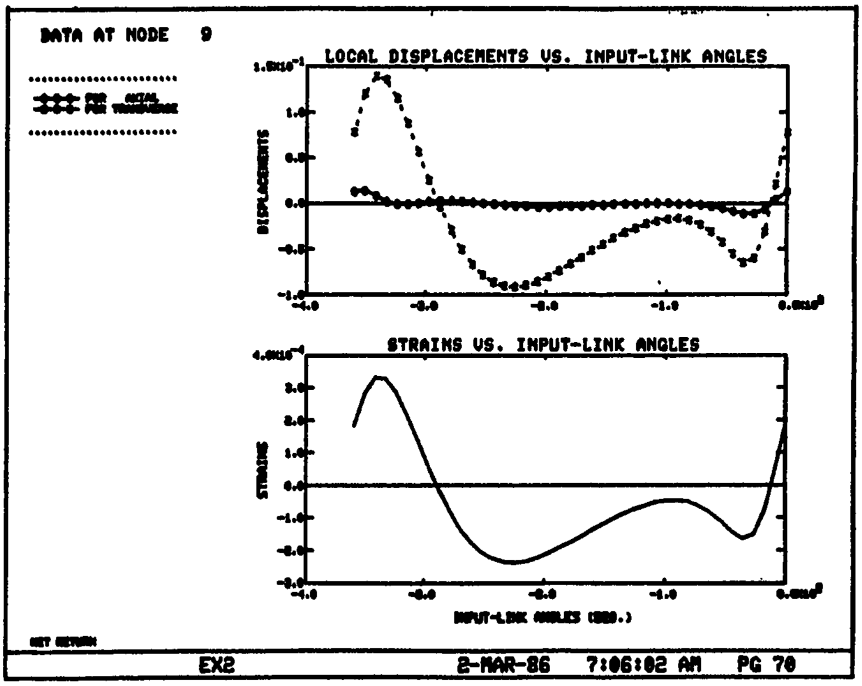

FIGURE 8.14 Displacements and Stresses of Node 9 in The Local Coordinate System

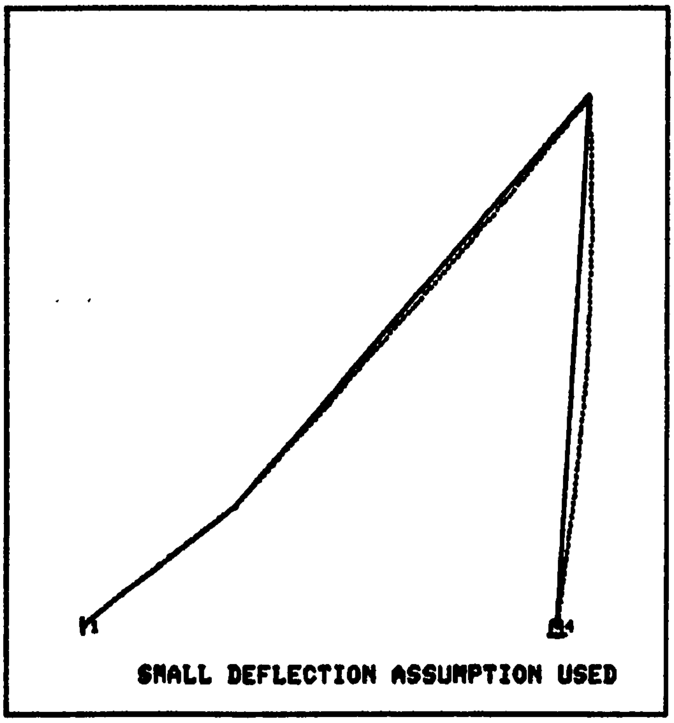

FIGURE 8.15 Deflected System at -324 Degrees of the Input-Link

8.3.2 Steady-State Responses of A Mechanism

The mechanism shown in Fig. (8.7) is used for time-domain analysis. At the initial position, velocities and accelerations of every node due to the elastic vibrations of the flexible members are set to zero. The steady-state responses of the mechanism are investigated.

The maximum distortions of the nodes are shown in Fig. (8.16) and the safety factors from the dynamic stress analysis are given in Fig. (8.17). The maximum distortions of the nodes are given in Table 8.13, and the equivalent stresses and safety factors are given in Table 8.14. The safety factor for the system is 3.50 at the critical point (node 12), and the maximum distortion in the system is 0.4845 inch at node 12.

Fig. (8.18) shows the displacements and stresses of node 12 in the global coordinate system. Fig. (8.19) gives the displacements and strains of node 12 in the local coordinate system. Fig. (8.20) shows the displacements and stresses of node 9 in the global coordinate system. Fig. (8.21) gives the displacements and strains of node 9 in the local coordinate system. Finally, the strains at mid-point of the follower (node 12) are given in Fig. (8.22) for each full cycle of the input-link: Fig. (8.22a) gives the strains for the first full cycle; Fig. (8.22b) shows the strains for the second full cycle; and Fig. (8.22b) gives for the third full cycle.

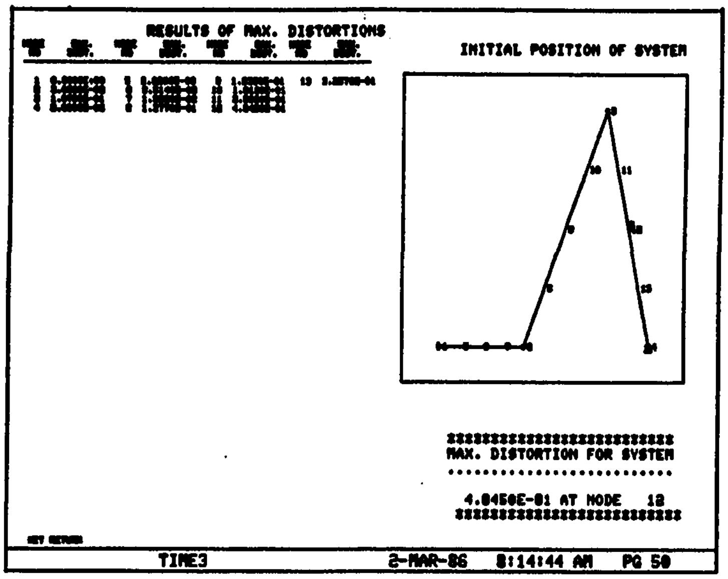

FIGURE 8.16 Maximum Distortions of Nodes

TABLE 8.13 Maximum Distortions of Nodes

UNITS ARE BRITISH (INCHES FOR DISTORTIONS)

NODE NO	MAXIMUM DISTORTIONS	
1	0.0000E+00	
2	0.3036E-01	
3	0.1079E+00	
4	0.2090E-05	
5	0.2620E-02	
6	0.9514E-02	
7	0.1923E-01	
8	0.1377E+00	
9	0.1835E+00	
10	0.1616E+00	
11	0.3903E+00	
12	0.4845E+00	***
13	0.3257E+00	

**** CORRESPONDS TO MAX. DISTORTION IN THE SYSTEM

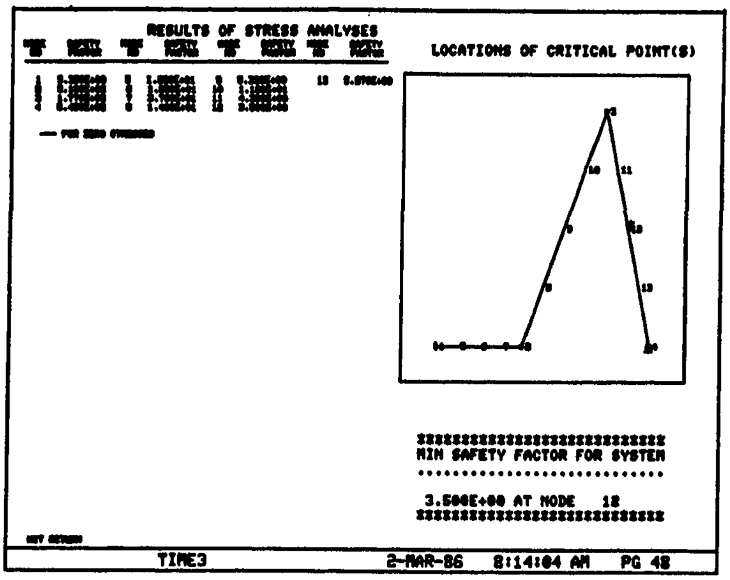

FIGURE 8.17 Safety Factors from Fatigue Stress Analysis

TABLE 8.14 Equivalent Stresses and Safety Factors of Nodes

SAFETY FACTOR DETERMINED FROM SODERBERG FAILURE LINE
UNITS ARE BRITISH (PSI FOR STRESSES)

NODE	STRENGTH		EQUIVALENT STRESSES		SAFETY	
NO	YIELD	ENDURANCE	MEAN.	ALTN.	FACTOR	
1	0.9000E+05	0.4500E+05	-.2250E+03	0.4699E+04	0.935E+01	
2	0.9000E+05	0.4500E+05	0.2256E+02	0.4415E+02	0.812E+03	
3	0.9000E+05	0.4500E+05	0.1256E+02	0.1911E+02	0.177E+04	
4	0.9000E+05	0.4500E+05	0.1132E+02	0.7624E+02	0.549E+03	
5	0.9000E+05	0.4500E+05	0.1960E+03	0.3503E+04	0.125E+02	
6	0.9000E+05	0.4500E+05	0.1315E+03	0.2324E+04	0.188E+02	
7	0.9000E+05	0.4500E+05	0.6900E+02	0.1154E+04	0.379E+02	
8	0.9000E+05	0.4500E+05	-.5145E+03	0.2955E+04	0.140E+02	
9	0.9000E+05	0.4500E+05	-.8370E+03	0.4407E+04	0.933E+01	
10	0.9000E+05	0.4500E+05	-.5185E+03	0.3555E+04	0.118E+02	
11	0.9000E+05	0.4500E+05	-.4955E+03	0.9995E+04	0.439E+01	
12	0.9000E+05	0.4500E+05	-.2100E+03	0.1276E+05	0.350E+01	**
13	0.9000E+05	0.4500E+05	0.5450E+02	0.8513E+04	0.527E+01	

*** MIN. SAFETY FACTOR FOR SYSTEM = 3.50 AT NODE 12 ***

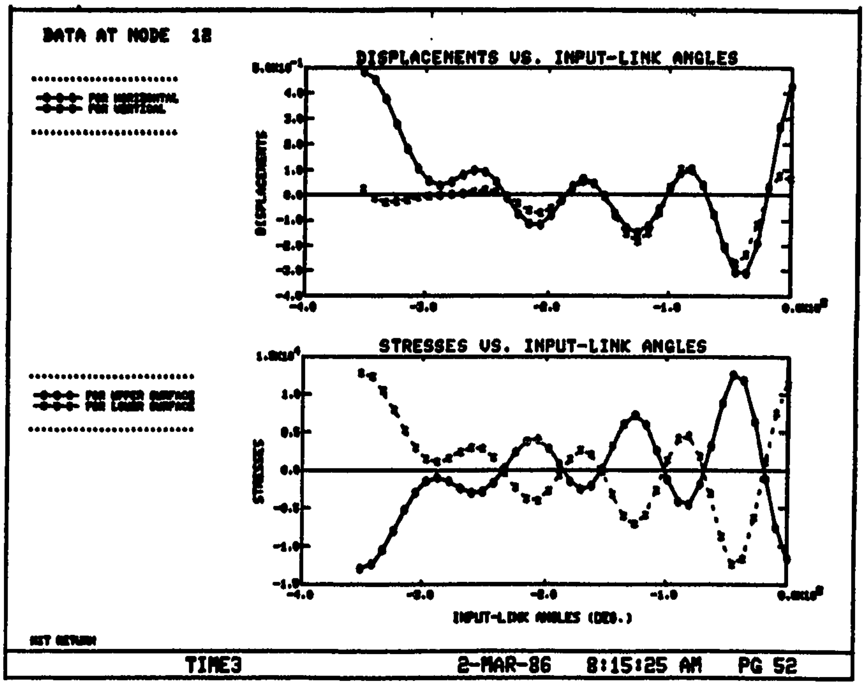

FIGURE 8.18 Displacements and Stresses of Node 12 in The Global Coordinate System

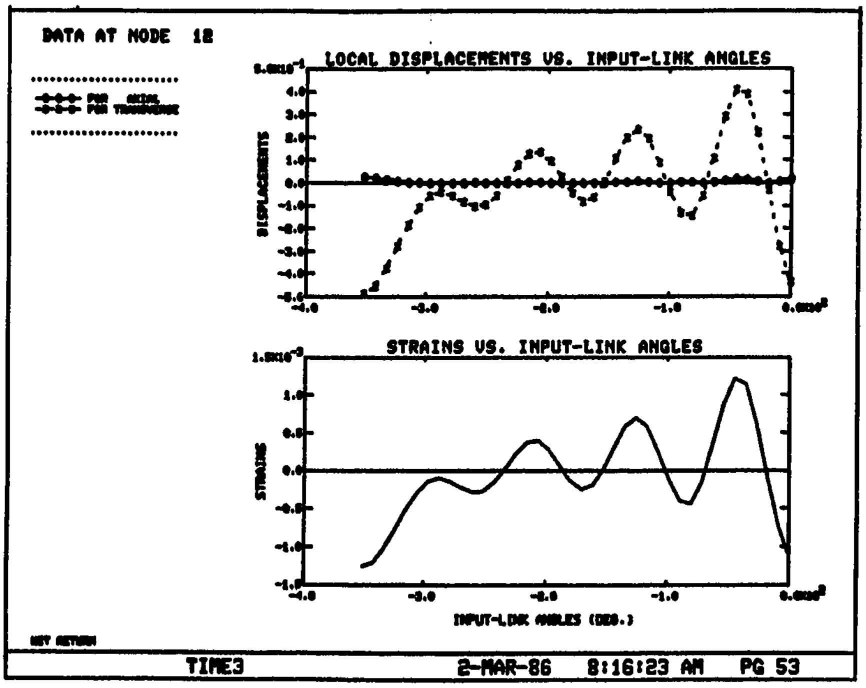

FIGURE 8.19 Displacements and Stresses of Node 12 in The Local Coordinate System

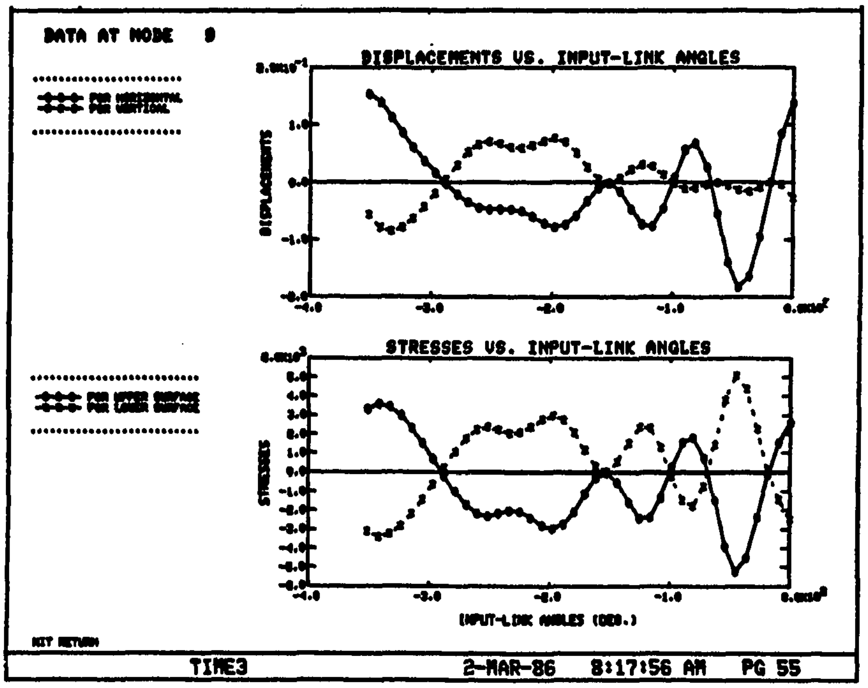

FIGURE 8.20 Displacements and Stresses of Node 9 in The Global Coordinate System

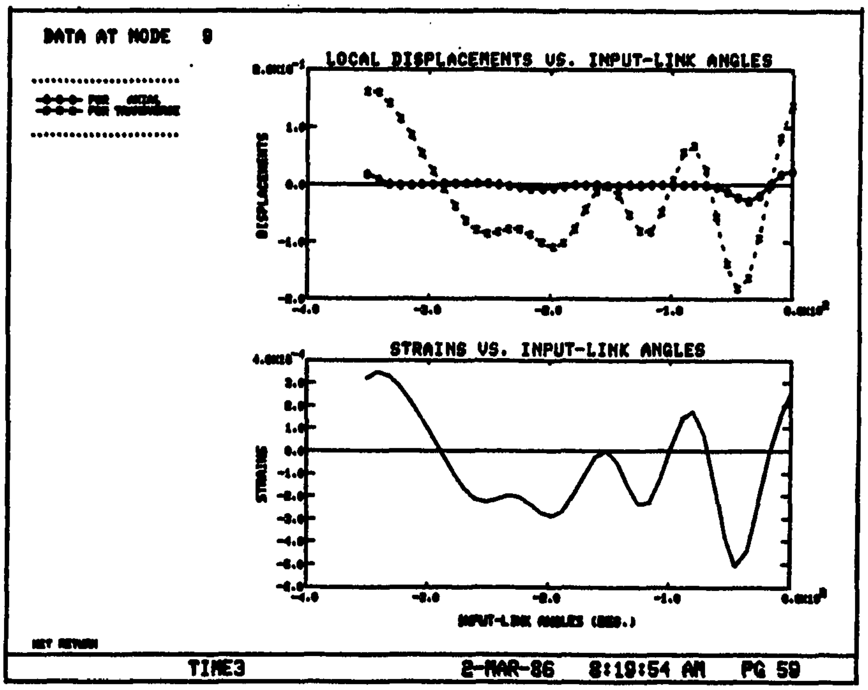

FIGURE 8.21 Displacements and Stresses of Node 9 in The Local Coordinate System

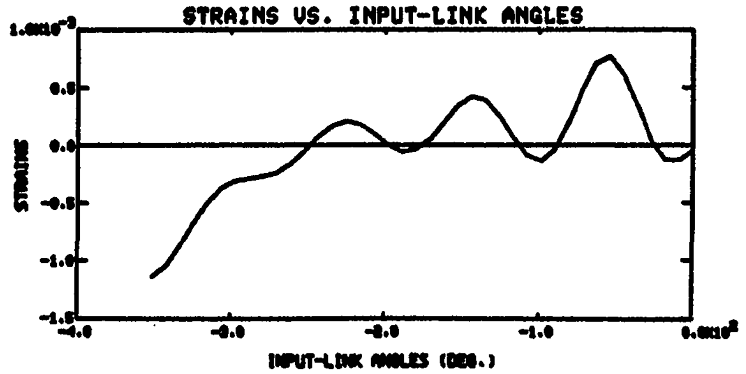

(a) For The First Full Cycle of The Input-Link

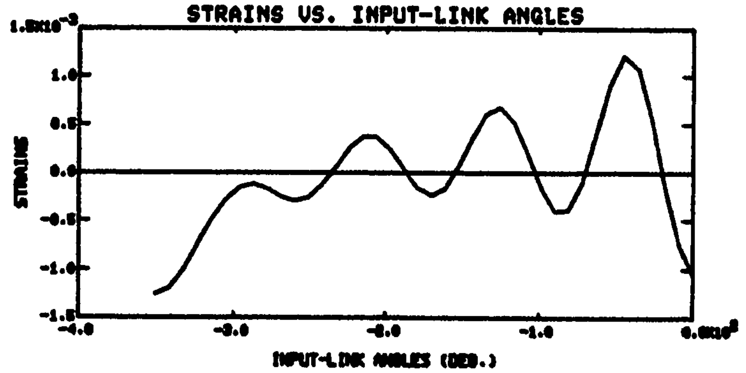

(b) For The Second Full Cycle of The Input-Link

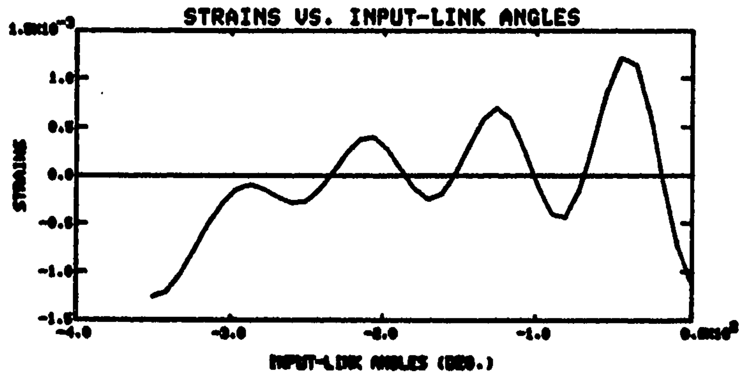

(c) For The Third Full Cycle of The Input-Link

FIGURE 8.22 Strains at Mid-Point of The Follower (Node 12)

8.4 Cantilever Beam with End Loads

The cantilever beam represented in Fig. (8.23) is loaded by end loads P and Q. Increasing the vertical load, the beam deflects in the large-deflection mode. Furthermore, the deflections of the beam will be changed by applying the horizontal (tensile or compressive) loads at the end point. In this section, the large-deflections of the cantilever beam are analyzed when a nondimensional parameter (PL^2/EI) ranges 0 from 10 and a loading factor (Q/P) ranges between -1 and 1.

Fig. (8.24) shows the displacement for the different values of the loading factor at -1.0, -0.2, 0.0, 0.2, and 1.0. Table 8.9 gives the displacements of an end point in the horizontal and vertical directions. Figs. (8.25) - (8.31) give the deflected beams for each loading factor. Fig. (8.32) shows the deflections of the beam when the parameter (PL^2/EI) is 5. The case of Q = 0 corresponds to the model given by Bisshopp and Drucker [87], and the solutions were verified in good agreement in Section 4.5.

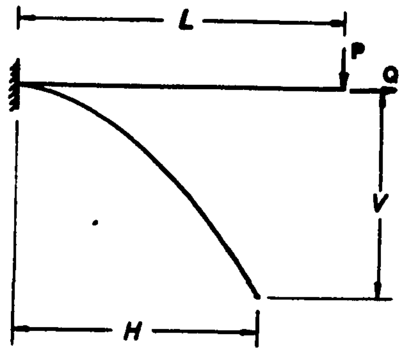

FIGURE 8.23 Cantilever Beam Loaded by End Loads

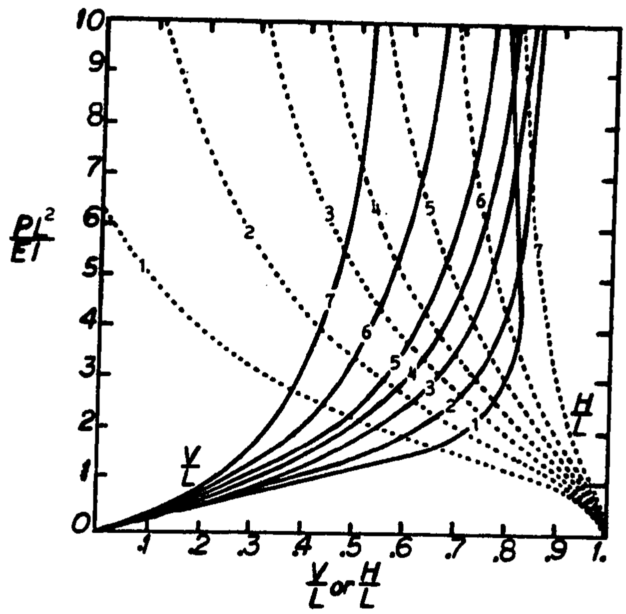

Curve No	Q/P
(1)	-1.0
(2)	-0.5
(3)	-0.2
(4)	0.0
(5)	0.2
(6)	0.5
(7)	1.0

FIGURE 8.24 Displacements of End Point of Beam

TABLE 8.15 Displacements of End Point of Cantilever Beam

PL^2/EI	Q/P	-1.0	-0.5	-0.2	0.0	0.2	0.5	1.0
0.5	H/L	0.9756	0.9805	0.9827	0.9841	0.9852	0.9867	0.9888
	V/L	0.1998	0.1793	0.1688	0.1624	0.1565	0.1484	0.1366
1.0	H/L	0.8761	0.9179	0.9344	0.9430	0.9501	0.9586	0.9688
	V/L	0.4351	0.3601	0.3241	0.3033	0.2847	0.2603	0.2274
2.0	H/L	0.5605	0.7276	0.7993	0.8356	0.8644	0.8966	0.9310
	V/L	0.7255	0.6140	0.5425	0.4981	0.4577	0.4048	0.3357
3.0	H/L	0.3295	0.5585	0.6755	0.7382	0.7887	0.8449	0.9026
	V/L	0.8031	0.7323	0.6608	0.6091	0.5584	0.4893	0.3972
4.0	H/L	0.1842	0.4348	0.5793	0.6613	0.7289	0.8048	0.8816
	V/L	0.8180	0.7866	0.7265	0.6754	0.6215	0.5437	0.4369
5.0	H/L	0.0862	0.3444	0.5057	0.6013	0.6818	0.7734	0.8657
	V/L	0.8168	0.8139	0.7663	0.7184	0.6640	0.5817	0.4648
6.0	H/L	0.0151	0.2760	0.4482	0.5537	0.6443	0.7483	0.8532
	V/L	0.8116	0.8292	0.7924	0.7483	0.6947	0.6098	0.4858
7.0	H/L	-.0400	0.2223	0.4022	0.5152	0.6137	0.7279	0.8431
	V/L	0.8058	0.8385	0.8108	0.7704	0.7180	0.6315	0.5022
8.0	H/L	-.0830	0.1789	0.3644	0.4834	0.5883	0.7109	0.8348
	V/L	0.8004	0.8447	0.8245	0.7874	0.7363	0.6490	0.5154
10.0	H/L	-.1490	0.1126	0.3060	0.4337	0.5484	0.6843	0.8218
	V/L	0.7914	0.8523	0.8438	0.8122	0.7637	0.6755	0.5357

where H and V are designated in Fig. (8.23),
and L is total length of beam.

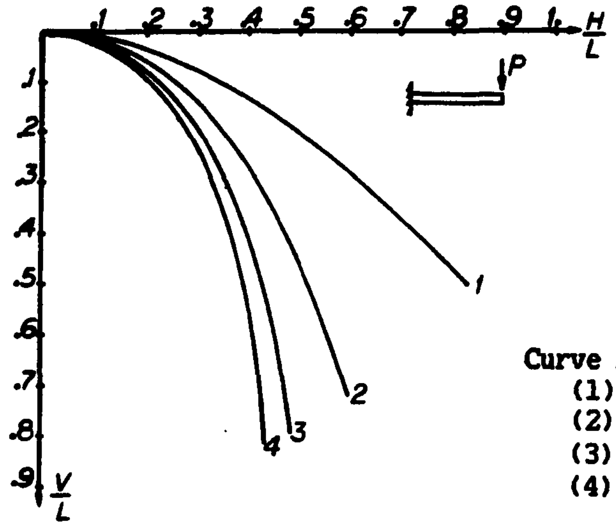

Curve No	PL^2/EI
(1)	2
(2)	5
(3)	8
(4)	10

FIGURE 8.25 Deflected Beams When Q/P = 0

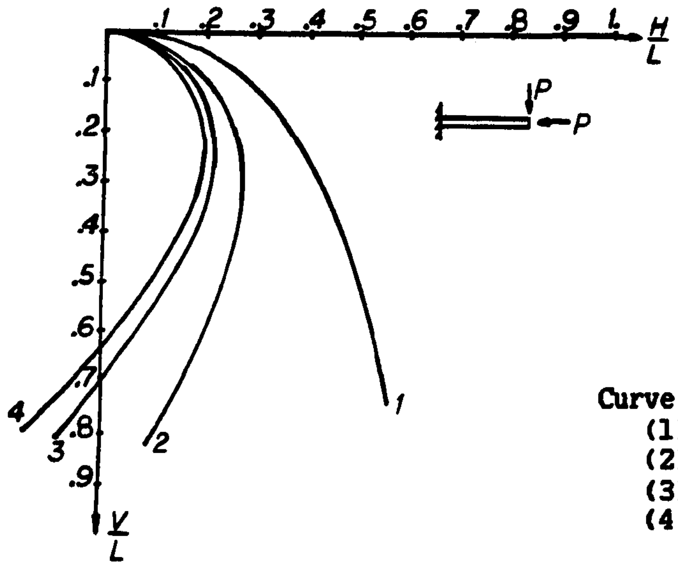

Curve No	PL^2/EI
(1)	2
(2)	5
(3)	8
(4)	10

FIGURE 8.26 Deflected Beams When Q/P = - 1.0

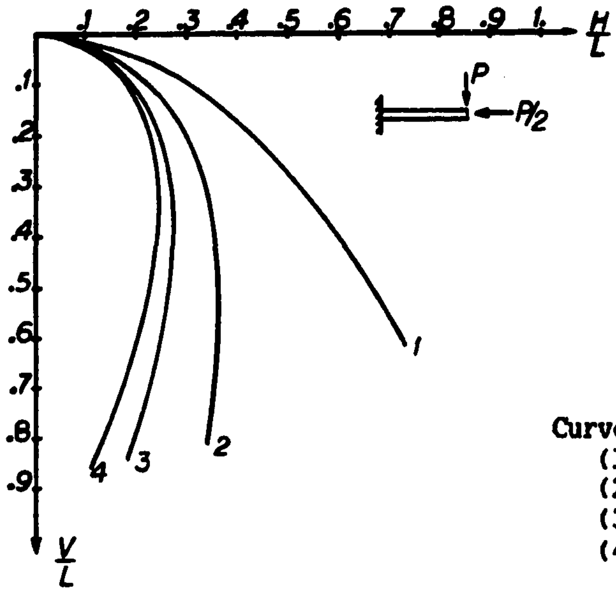

Curve No	PL^2/EI
(1)	2
(2)	5
(3)	8
(4)	10

FIGURE 8.27 Deflected Beams When Q/P = - 0.5

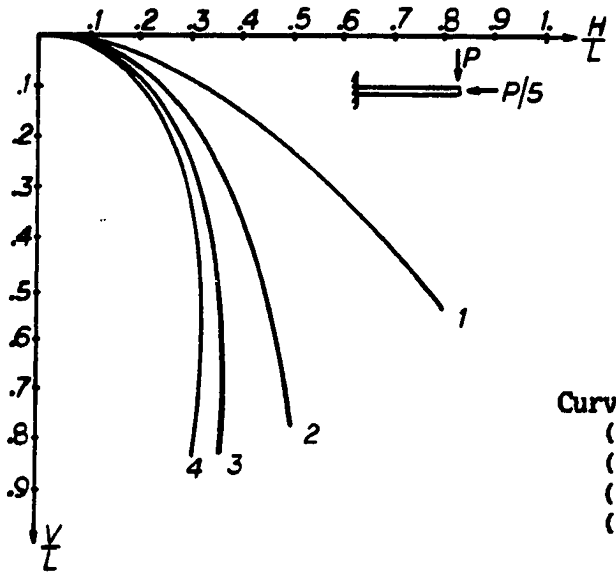

Curve No	PL^2/EI
(1)	2
(2)	5
(3)	8
(4)	10

FIGURE 8.28 Deflected Beams When Q/P = - 0.2

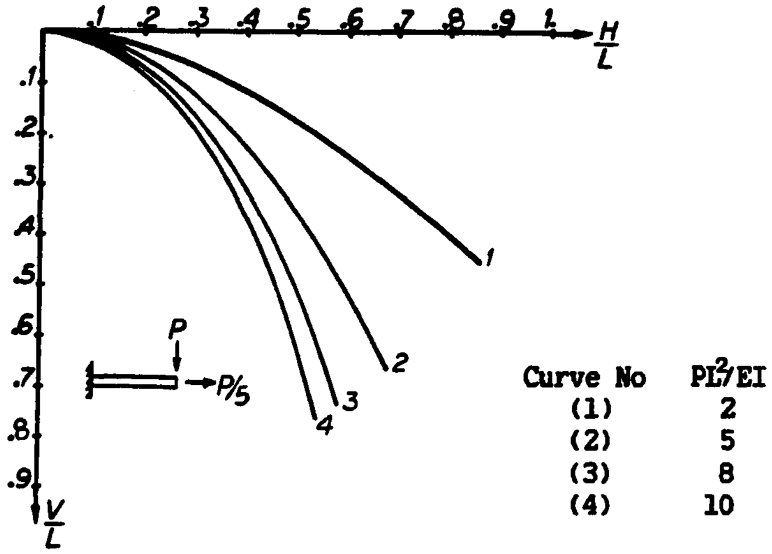

FIGURE 8.29 Deflected Beams When Q/P = 0.2

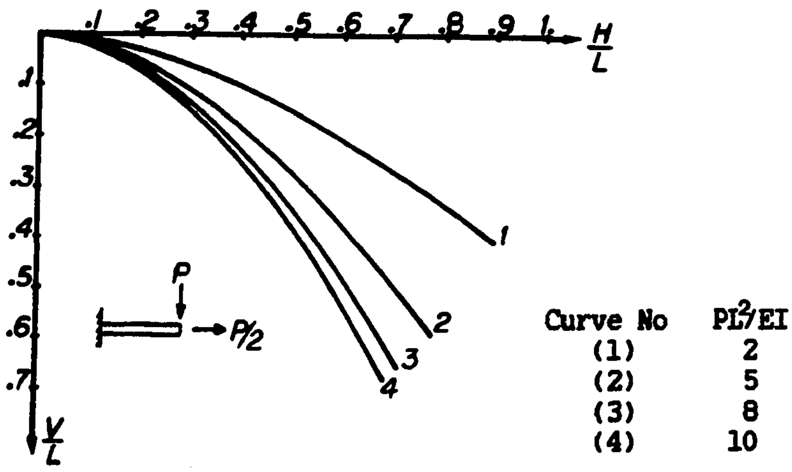

FIGURE 8.30 Deflected Beams When Q/P = 0.5

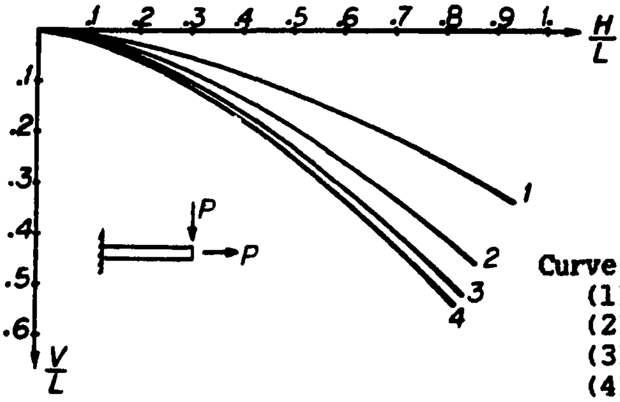

Curve No	PL^2/EI
(1)	2
(2)	5
(3)	8
(4)	10

FIGURE 8.31 Deflected Beams When Q/P = 1.0

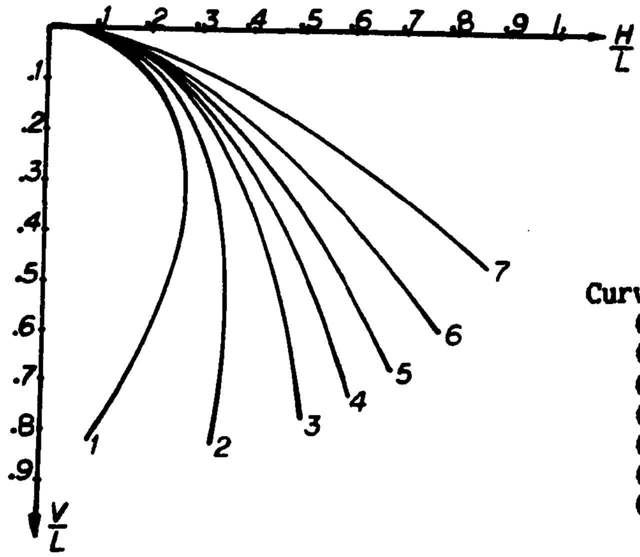

Curve No	Q/P
(1)	-1.0
(2)	-0.5
(3)	-0.2
(4)	0.0
(5)	0.2
(6)	0.5
(7)	1.0

FIGURE 8.32 Deflected Beams When PL^2/EI = 5

8.5 Stepped Beam on Elastic Supports

The system in Fig. (8.33) shows a stepped beam loaded by its own weight and a vertical end load (15N). The shaft is supported at three locations, the right two supports being elastic supports with a spring constant K = 2 N/mm. The springs are assumed to be unloaded when the beam is horizontal and the springs exert a vertical load only where the ends of springs are sliding. Numerical values for the system parameters are given in Fig. (8.33).

For the analysis, the beam is broken into 20 segments as shown in Fig. (8.34). The shaft is made from steel AISI 4340 (yield strength = 689 Mpa). The deflections of the system are given in Fig. (8.35), and the safety factors of the system are given in Fig. (8.36). Table 8.16 gives the displacements of the nodes. Table 8.17 gives the internal forces and stresses of the nodes. Table 8.18 gives the safety factors of the nodes and for the system.

The solution from the analysis gives -2.737 and -23.37 mm for the maximum displacements at the end point in the horizontal and vertical directions, respectively. The factor of safety in the system is 1.25 at node 4. The analysis details are presented in Appendix D.

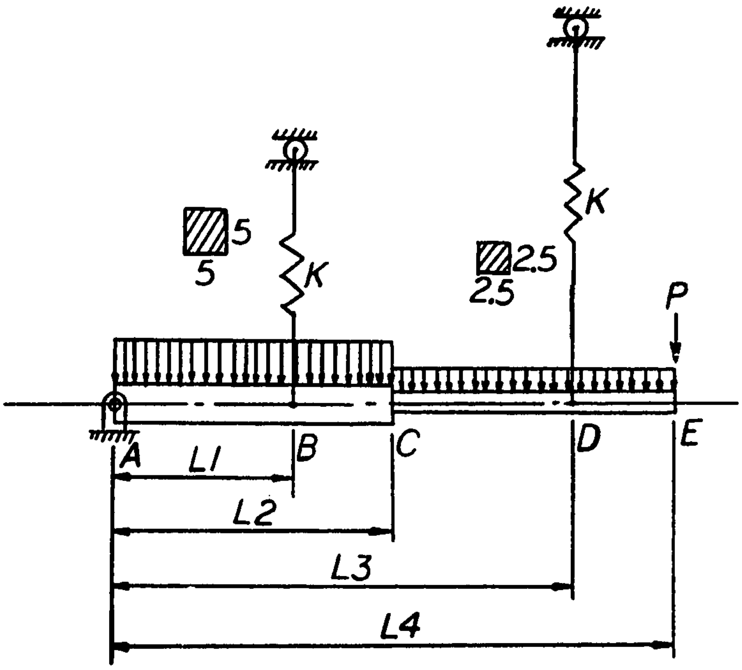

Lengths: L1 = 150 mm
L2 = 250 mm
L3 = 400 mm
L4 = 500 mm

Cross-Sections: Beam AC = 5 X 5 mm^2
Beam CE = 2.5 X 2.5 mm^2

Spring Length: at node B = 200 mm
at node E = 400 mm

Load at end point, P = 15 N

Weight per unit volume = 76.5 X 10^{-6} N/mm^3

FIGURE 8.33 Stepped Beam on Elastic Supports

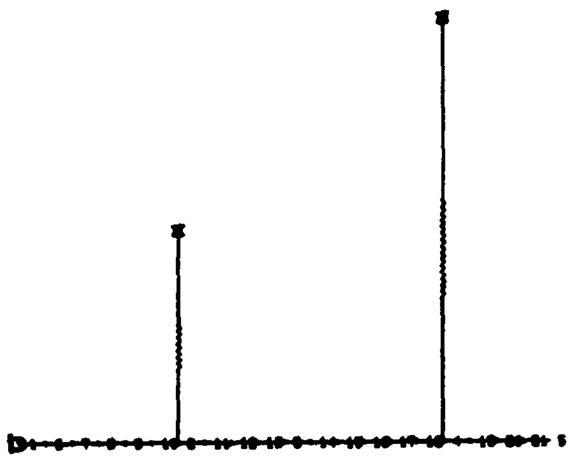

FIGURE 8.34 Element-Generated System

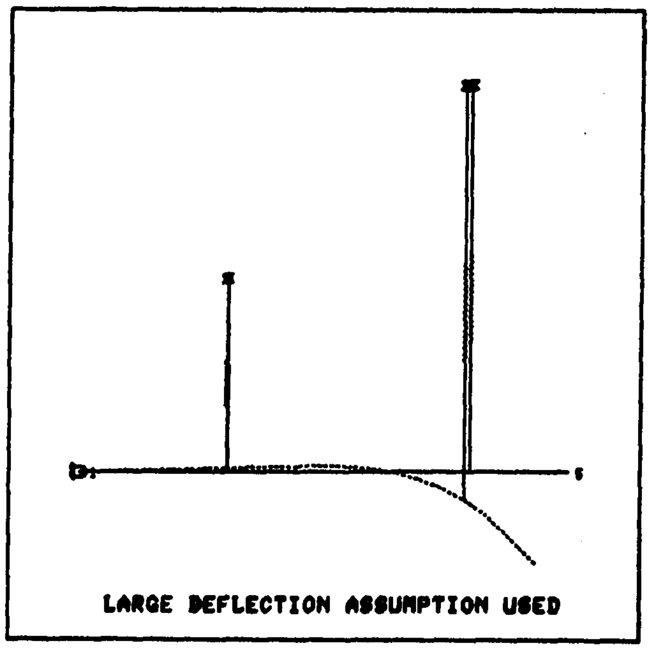

FIGURE 8.35 Deflected System

TABLE 8.16 Displacements of Nodes

LARGE-DEFLECTION ASSUMPTION USED
UNITS ARE SI (MM IN DISPLACEMENTS)

NODE NO	LOCATION X	LOCATION Y	DISPLACEMENTS HORIZ	DISPLACEMENTS VERTI	SLOPE DEG
1	0.0000E+00	0.0000E+00	0.0000E+00	0.0000E+00	0.8208E+00
2	0.1500E+03	0.0000E+00	-0.1488E-01	0.2113E+01	0.7778E+00
3	0.2500E+03	0.0000E+00	-0.2242E-01	0.3337E+01	0.5785E+00
4	0.4000E+03	0.0000E+00	-0.9664E+00	-0.1022E+02	-0.1267E+02
5	0.5000E+03	0.0000E+00	-0.5273E+01	-0.3909E+02	-0.1875E+02
6	0.2500E+02	0.0000E+00	-0.2563E-02	0.3580E+00	0.8198E+00
7	0.5000E+02	0.0000E+00	-0.5113E-02	0.7150E+00	0.8165E+00
8	0.7500E+02	0.0000E+00	-0.7635E-02	0.1070E+01	0.8108E+00
9	0.1000E+03	0.0000E+00	-0.1011E-01	0.1422E+01	0.8026E+00
10	0.1250E+03	0.0000E+00	-0.1253E-01	0.1770E+01	0.7916E+00
11	0.1750E+03	0.0000E+00	-0.1712E-01	0.2447E+01	0.7540E+00
12	0.2000E+03	0.0000E+00	-0.1918E-01	0.2768E+01	0.7129E+00
13	0.2250E+03	0.0000E+00	-0.2097E-01	0.3067E+01	0.6545E+00
14	0.2750E+03	0.0000E+00	-0.2250E-01	0.3272E+01	-0.9199E+00
15	0.3000E+03	0.0000E+00	-0.3467E-01	0.2493E+01	-0.2702E+01
16	0.3250E+03	0.0000E+00	-0.8712E-01	0.8741E+00	-0.4768E+01
17	0.3500E+03	0.0000E+00	-0.2205E+00	-0.1705E+01	-0.7118E+01
18	0.3750E+03	0.0000E+00	-0.4900E+00	-0.5366E+01	-0.9752E+01
19	0.4250E+03	0.0000E+00	-0.1720E+01	-0.1631E+02	-0.1534E+02
20	0.4500E+03	0.0000E+00	-0.2737E+01	-0.2337E+02	-0.1723E+02
21	0.4750E+03	0.0000E+00	-0.3953E+01	-0.3107E+02	-0.1837E+02

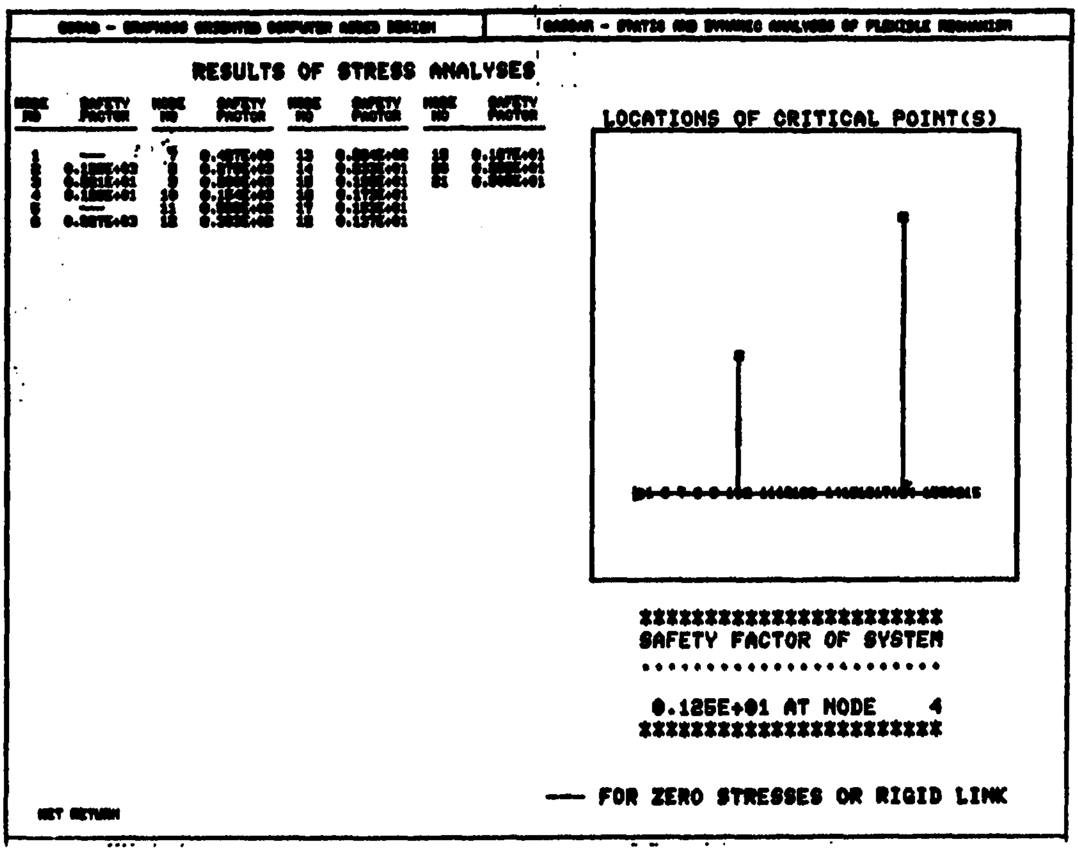

FIGURE 8.36 Safety Factors of System

TABLE 8.17 Internal Forces and Stresses of Nodes

LARGE-DEFLECTION ASSUMPTION USED
UNITS ARE SI (NEWTON, N-MM, AND MPA)

NODE NO	INTERNAL FORCES HORIZ	VERTI	MOMENT	STRESSES TOP	BOTTOM
1	0.0000E+00	0.6238E+00	0.0000E+00	0.0000E+00	0.0000E+00
2	0.0000E+00	0.5136E+01	-0.1151E+03	-0.5525E+01	0.5525E+01
3	0.0000E+00	0.5327E+01	-0.6382E+03	-0.2451E+03	0.2451E+03
4	0.0000E+00	-0.1505E+02	-0.1438E+04	-0.5522E+03	0.5522E+03
5	0.0000E+00	0.0000E+00	0.0000E+00	0.0000E+00	0.0000E+00
6	0.0000E+00	0.6716E+00	-0.1619E+02	-0.7771E+00	0.7771E+00
7	0.0000E+00	0.7194E+00	-0.3358E+02	-0.1612E+01	0.1612E+01
8	0.0000E+00	0.7672E+00	-0.5216E+02	-0.2504E+01	0.2504E+01
9	0.0000E+00	0.8150E+00	-0.7194E+02	-0.3453E+01	0.3453E+01
10	0.0000E+00	0.8628E+00	-0.9291E+02	-0.4460E+01	0.4460E+01
11	0.0000E+00	0.5184E+01	-0.2441E+03	-0.1172E+02	0.1172E+02
12	0.0000E+00	0.5231E+01	-0.3743E+03	-0.1797E+02	0.1797E+02
13	0.0000E+00	0.5279E+01	-0.5056E+03	-0.2427E+02	0.2427E+02
14	0.0000E+00	0.5339E+01	-0.7715E+03	-0.2963E+03	0.2963E+03
15	0.0000E+00	0.5351E+01	-0.9052E+03	-0.3476E+03	0.3476E+03
16	0.0000E+00	0.5363E+01	-0.1039E+04	-0.3990E+03	0.3990E+03
17	0.0000E+00	0.5375E+01	-0.1172E+04	-0.4500E+03	0.4500E+03
18	0.0000E+00	0.5387E+01	-0.1305E+04	-0.5011E+03	0.5011E+03
19	0.0000E+00	-0.1504E+02	-0.1073E+04	-0.4120E+03	0.4120E+03
20	0.0000E+00	-0.1502E+02	-0.7125E+03	-0.2736E+03	0.2736E+03
21	0.0000E+00	-0.1501E+02	-0.3553E+03	-0.1364E+03	0.1364E+03

TABLE 8.18 Safety Factors of Nodes

LARGE-DEFLECTION ASSUMPTION USED

SAFETY FACTOR DETERMINED FROM MAX. NORMAL STRESS THEORY
*** CORRESPONDS TO ZERO STRESS ON THE LINK OR RIGID LINK
UNITS ARE SI (MPA FOR STRESSES)

NODE NO	YIELD STRENGTH	STRESSES TOP	STRESSES BOTTOM	SAFETY FACTOR
1	0.6890E+03	0.0000E+00	0.0000E+00	***
2	0.6890E+03	-.5525E+01	0.5525E+01	0.125E+03
3	0.6890E+03	-.2451E+03	0.2451E+03	0.281E+01
4	0.6890E+03	-.5522E+03	0.5522E+03	0.125E+01
5	0.6890E+03	0.0000E+00	0.0000E+00	***
6	0.6890E+03	-.7771E+00	0.7771E+00	0.887E+03
7	0.6890E+03	-.1612E+01	0.1612E+01	0.427E+03
8	0.6890E+03	-.2504E+01	0.2504E+01	0.275E+03
9	0.6890E+03	-.3453E+01	0.3453E+01	0.200E+03
10	0.6890E+03	-.4460E+01	0.4460E+01	0.154E+03
11	0.6890E+03	-.1172E+02	0.1172E+02	0.588E+02
12	0.6890E+03	-.1797E+02	0.1797E+02	0.383E+02
13	0.6890E+03	-.2427E+02	0.2427E+02	0.284E+02
14	0.6890E+03	-.2963E+03	0.2963E+03	0.233E+01
15	0.6890E+03	-.3476E+03	0.3476E+03	0.198E+01
16	0.6890E+03	-.3990E+03	0.3990E+03	0.173E+01
17	0.6890E+03	-.4500E+03	0.4500E+03	0.153E+01
18	0.6890E+03	-.5011E+03	0.5011E+03	0.137E+01
19	0.6890E+03	-.4120E+03	0.4120E+03	0.167E+01
20	0.6890E+03	-.2736E+03	0.2736E+03	0.252E+01
21	0.6890E+03	-.1364E+03	0.1364E+03	0.505E+01

****
SAFETY FACTOR FOR SYSTEM = 1.25 AT NODE 4
****

CHAPTER IX

SUMMARY

9.1 Discussion

The <u>iterative</u> <u>transfer</u> <u>matrix</u> <u>method</u> presented here can be applied to the static and dynamic analyses of both general multiloop flexible-body mechanisms and structures.

The internal forces are interrelated elastically with the displacements at a node. Also, the field matrices for the flexible-body analysis must contain the elastic effects due to the internal forces, which are unknown. This complexity in the solution process can be reduced by using the iterations in order to update the internal forces at every node in the flexible-body systems. The initial field matrix is used only to determine the initial forces, and the elastic field matrix is used for both the force and displacement analyses of the flexible-body systems. The initial field matrix is determined from the elastic properties of the member with zero axial forces on each segment. The elastic field matrix is calculated from both the elastic properties of the member and the internal forces determined from the previous iteration.

In the solution procedure for the iterative transfer matrix method, the corresponding transfer matrices at every section and node can be calculated. Next, the first matrix equation can be built by manipulating the matrices from the starting node to the end node, and the unknowns can be solved at the starting node by applying the corresponding boundary conditions at both ends. Then, the state variables at each node in the system are calculated by manipulating the corresponding transfer matrices and the state vector at one end of the section.

After determining all of the internal forces at each node from the first matrix equation, the elastic field matrices can be obtained from the internal forces and used to make the second matrix equation. Then, the same solution procedures are used to solve the next matrix equation. For the third matrix equation, all procedures for the second matrix equation are repeated, where elastic field matrices for the third equation are updated by the internal forces determined from the second equation.

In addition, there are two types of elastic field matrices. One is for solving small-deflection problems, and the other is for large-deflection problems. Since the iterative transfer matrix method converges rapidly to the solution, three iterations of the solution procedures for the small-deflection analysis are usually enough. But, for the large-deflection analysis, the solution procedures are continued until all state variables are essentially unchanged, and this usually requires about 10 iterations.

The iterative transfer matrix method requires much less storage than does the finite-element methods and the other lumped-mass techniques because all necessary matrices used in the method are 7X7.

9.2 Research Contributions

The following is a list of specific contributions to the field of general multiloop-planar flexible mechanisms from this research.

1. The iterative-transfer matrix method developed here can be used for the static and dynamic analyses of general planar flexible mechanisms and structures.

2. The necessary transfer matrices are developed. These transfer matrices consist of seven different types of matrices (field matrices, a point matrix, a transformation matrix, a spring matrix, a branch matrix, a inertial matrix, and a frequency matrix). All of these transfer matrices have three degrees-of-flexibility per node. These transfer matrices are applied directly to the analysis without any transformations, which must be done in the traditional transfer-matrix methods.

3. In the dynamic analysis of flexible mechanisms, the inertial effects caused by rigid-body accelerations due to the kinematic motions are incorporated in the rigid-body inertial matrix. This rigid-body inertial matrix is used for quasi-static analyses. The

inertial forces caused by the elastic vibrations are formulated from the Houbolt direct integration method and incorporated in the elastic-body matrix. The elastic-body inertial matrix is used for time-domain dynamic analyses.

4. The iteration method is developed based on the successive solutions of linear systems and can be used for both small-deflection and large-deflection analyses.

5. The approximate method for the large-deflection analysis is developed by correcting the geometry of a deformed beam and the internal forces in the beam segment. The geometric correction is derived from the relationships between the beam length and the geometry of the deformed beam. The average axial force in a beam segment is derived from equilibrium condition in the segment.

6. A computer program CASDAM (Computer-Aided Static and Dynamic Analyses of Flexible Mechanisms) was developed. CASDAM is the graphics-oriented, interactive, computer-aided analysis program for the static and dynamic analyses of general multiloop planar mechanisms.

9.3 Recommendations

There are areas in which extension of the present research would be beneficial. The iterative transfer-matrix method is developed for the planar systems. One possible improvement is to extend the procedure to analyze spatial mechanisms.

As a direct integration method for the time-domain analyses, the Houbolt method is used to evaluate the elastic-body inertial effects due to the elastic vibrations. However, the solutions are not in good agreement with the experiment data from References [7, 9]. A possible improvement is to develop a method to evaluate the inertial effects due to the elastic vibrations of the members.

To effectively design a high-speed mechanism, kineto-elastodynamic design must be considered. This is normally achieved by first performing the kinematic synthesis of the rigid-body mechanism, and then proportioning the areas of cross-section of the links optimally to account for kineto-elastodynamic effects. The computer program CASDAM can be used for kineto-elastodynamic design by interconnecting with the programs KINANL [67] and RECSYN [67-68]. They are developed for the rigid-body kinematic analysis and synthesis, and installed in The Advanced Design Method Laboratory, Department of Mechanical Engineering, The Ohio State University.

There are cases where the procedure does not work, because the system matrix equation becomes singular. These cases are as follows:

1. The angular velocity of the input-link of a mechanism is near the natural frequency of elastic links.

2. Two links connected by a revolute joint are on a straight line.

3. The axial compressive force is equal to or greater than the buckling load of a beam segment.

REFERENCES

GENERAL SURVEY FOR FLEXIBLE MECHANISMS ANALYSES

1. ERDMAN, A. G., and SANDOR, G. N., "Kineto-Elastodynamic - A Review of the State of the Art and Trends," Mechanism and Machine Theory, 1972, Vol. 7, PP. 19-33.

2. LOWEN, G. G., and JANDRASITS, W. G., "Survey of Investigations into the Dynamic Behavior of Mechanisms containing Links with Distributed Mass and Elasticity," Mechanism and Machine Theory, 1972, Vol. 7, PP. 3-17.

ANALYSIS, VIBRATION, AND EXPERIMENT FOR FLEXIBLE MECHANISMS

3. ERDMAN, A. G., SANDOR, G. N., and OAKBERG, R. G., "A General Method for Kineto-Elastodynamic Analysis and Synthesis of Mechanisms," Trans. ASME, Journal of Engineering for Industry, Nov. 1972, PP. 1193-1205.

4. WINTER, S. J., and SHOUP, T. E., "The Displacement Analysis of Path-Generating Flexible-Link Mechanisms," Mechanism and Machine Theory, 1972, Vol. 7, PP. 443-451.

5. IMAM, I., SANDOR, G. N., and KRAMER, S. N, "Deflection and Stress Analysis in High Speed Planar Mechanisms with Elastic Links," Trans. ASME, Journal of Engineering for Industry, May 1973, PP. 541-548.

6. SADLER, J. P., and SANDOR, G. N., "A Lumped Parameter Approach to Vibration and Stress Analysis of Elastic Linkages," Trans. ASME, Journal of Engineering for Industry, May 1973, PP. 549-557.

7. ALEXANDER, R. M., and LAWRENCE, K. L., "An Experimental Investigation of the Dynamic Response of an Elastic Mechanism," Trans. ASME, Journal of Engineering for Industry, Feb. 1974, PP. 268-274.

8. SADLER, J. P., and SANDOR, G. N., "Nonlinear Vibration Analysis of Elastic Four-Bar Linkages," Trans. ASME, Journal of Engineering for Industry, May 1974, PP. 411-419.

9. ALEXANDER, R. M., and LAWRENCE, K. L., "Experimentally Determined Dynamic Strains in an Elastic Mechanism," Trans. ASME, Journal of Engineering for Industry, Aug. 1975, PP. 791-794.

10. CHU, S.-C., and PAN, K. C.,"Dynamic Response of a High-Speed Slider-Crank Mechanism with an Elastic Connecting Rod," Trans. ASME, Journal of Engineering for Industry, May 1975, PP. 542-550.

11. SADLER, J. P., "On the Analytical Lumped-Mass Model of an Elastic Four-bar Mechanism," Trans. ASME, Journal of Engineering for Industry, May 1975, PP. 561-565.

12. BAHGAT, B. M., and WILLMERT, K. D., "Finite Element Vibrational Analysis of Planar Mechanisms," Mechanism and Machine Theory, 1976, Vol. 11, PP. 47-71.

13. GOLEBIEWSKI, E. P., and SADLER, J. P., "Analytical and Experimental Investigation of Elastic Slider-Crank Mechanisms," Trans. ASME, Journal of Engineering for Industry, Nov. 1976, PP. 1266-1271.

14. SUTHERLAND, G. H., "Analytical and Experimental Investigation of a High-Speed Elastic-Membered Linkage," Trans. ASME, Journal of Engineering for Industry, Aug. 1976, PP. 788-794.

15. THOMPSON, B. S., and BARR, A. D. S., "A Variational Principle for the Elastodynamic Motion of Planar Linkage," Trans. ASME, Journal of Engineering for Industry, Nov. 1976, PP. 1306-1312.

16. KOHLI, D., HUNTER, D., and SANDOR, G. N., "Elastodynamic Analysis of a Completely Elastic System," Trans. ASME, Journal of Engineering for Industry, Aug. 1977, PP. 604-609.

17. MIDHA, A., ERDMAN, A. G., and FROHRIB, D. A., "An Approximate Method for the Dynamic Analysis of Elastic Linkages," Trans. ASME, Journal of Engineering for Industry, May 1977, PP. 449-455.

18. MIDHA, A., ERDMAN, A. G., and FROHRIB, D. A., "Finite Element Approach to Mathematical Modeling of High-Speed Elastic Linkages," Mechanism and Machine Theory, Vol. 13, PP. 603-618, 1978.

19. MIDHA, A., ERDMAN, A. G., and FROHRIB, D. A., "A Computational Efficient Numerical Algorithm for the Transient Response of High-Speed Elastic Linkages," Trans. ASME, Paper No. 78-DET-54, Journal of Mechanical Design, Jan. 1979, Vol. 101, PP. 138-148.

20. MIDHA, A., ERDMAN, A. G., and FROHRIB, D. A., "A Closed-Form Numerical Algorithm for the Periodic Response of High-Speed Elastic Linkages," Trans. ASME, Paper No. 78-DET-15, Journal of Mechanical Design, Jan. 1979, Vol. 101, PP. 154-162.

21. BADLANI, M., and KLEINHENZ, N., "Dynamic Stability of Elastic Mechanisms," Trans. ASME, Paper No. 78-DET-17, Journal of Mechanical Design, Jan. 1979, Vol. 101, pp. 149-153.

22. BAGCI, C., and KALAYCIOGLU, S., "Elastodynamics of Planar Mechanisms Using Planar Actual Finite Line Elements, Lumped Mass Systems, Matrix-Exponential Method, and the Method of 'Critical-Geometry-kineto-elasto-statics' (CGKES)," Trans. ASME, Paper No. 78-DET-26, Journal of Mechanical Design, July 1979, Vol. 101, PP. 417-427.

23. KALAYCIOGLU, S., and BAGCI, C., "Determination of the Critical Operating Speeds of Planar Mechanisms by the Finite Element Method Using Planar Actual Line Elements and Lumped Mass Systems," Trans. ASME, Paper No. 78-DET-37, Journal of Mechanical Design, April 1979, Vol. 101, PP. 210-223.

24. JANDRASITS, W. G., and LOWEN G. G, "The Elastic-Dynamic Behavior of a Counterweighted Rocker Link with an Overhanging Endmass in a Four-Bar Linkage, Part I: Theory," Trans. ASME, Paper No. 78-DET-23, Journal of Mechanical Design, Jan. 1979, Vol. 101, PP. 77-88.

25. JANDRASITS, W. G., and LOWEN, G. G, "The Elastic-Dynamic Behavior of a Counterweighted Rocker Link with an Overhanging Endmass in a Four-Bar Linkage, Part II: Application and Experiment," Trans. ASME, Paper No. 78-DET-24, Journal of Mechanical Design, Jan. 1979, Vol. 101, PP. 89-98.

26. BADLANI, M., and MIDHA, A., "Member Initial Curvature Effects on the Elastic Slider-Crank Mechanism Response," Trans. ASME, Paper No. 80-DET-72, Journal of Mechanical Design, Jan. 1980, Vol. 104, PP. 159-167.

27. NATH, P. K., and GHOSH, A., "Kineto-Elastodynamic Analysis of Mechanisms by Finite Element Method," Mechanism and Machine theory, Vol. 15, PP. 179-197, 1980.

28. NATH, P. K., and GHOSH, A., "Steady state Response of Mechanisms with Elastic Links by Finite Element Method," Mechanism and Machine theory, Vol. 15, PP. 179-197, 1980.

29. SADLER, J. P., MAYNE, R. W., and FAN, K. C., "Generalized Study of Crank-Rocker Mechanisms Driven by a d.c. Motor; Part I. Mathematical Model," Mechanism and Machine theory, Vol. 15, PP. 447-461, 1980.

30. MAYNE, R. W., SADLER, J. P., and FAN, K. C., "Generalized Study of Crank-Rocker Mechanisms Driven by a d.c. Motor; Part II. Applications," Mechanism and Machine theory, Vol. 15, PP. 447-461, 1980.

31. CLEGHORN, W. L., FENTON, R. G., and TABARROK, B., "Finite Element Analysis of High-Speed Flexible Mechanisms," Mechanism and Machine theory, Vol. 16, PP. 407-424, 1981.

32. MEANS, K. H. and NEOU, I. M., "Elasto-Dynamic Responses of a Non-uniform Elastic Coupler of a Slider-Crank Mechanism," proceedings of The 7th Applied Mechanisms Conference, at OSU, Kansas City, Mo., 1981, PP. XXXV.1-16.

33. ZUCCARO, D., Bengisu, M. T., and Thompson, B. S., "An Experimental Investigation of a Four-Bar Mechanism with Links Fabricated from a Graphite-Epoxy Composite Material," proceedings of The 7th Applied Mechanisms Conference, at OSU, Kansas City, Mo., 1981, PP. XI.1-6.

34. SUTHERLAND, G. H., "Elastic-Member Mechanism Dynamics," proceedings of The 7th Applied Mechanisms Conference, at OSU, Kansas City, Mo., 1981, PP. XLVIII.1-3.

35. ARDAYFIO, D. D., "Dynamic Stability of a Slider-Crank Mechanism with Elastic Effects at Both Coupler Joints," ASME Paper No. 82-DET-19, 1982.

36. BADLANI, M., and MIDHA, A., "Effect of Internal Material Damping on the Dynamics of a Slider-Crank Mechanism," Trans. ASME, Paper No. 82-DET-2, Journal of Mechanical Design, 1982.

37. CHU, F. H., and PILKEY, W. D., "A Direct Integration Technique for the Transient Analysis of Rotating Shafts," Trans. ASME, Paper No. 81-DET-56, Journal of Mechanical Design, April 1982, Vol. 104, PP. 384-388.

38. CONSTANTINOU, M. C., and TADJBAKHSH, I. G., "Dynamic Instability of the Elastic Coupler of a Four-Bar Mechanism," ASME Paper No. 82-DET-6, 1982.

39. TADJBAKHSH, I. G., "Stability of Motion of Elastic Planar Linkages with Application to Slider Crank Mechanism," Trans. ASME, Paper No. 81-DET-6, Journal of Mechanical Design, Oct. 1982, Vol. 104, PP. 698-703.

40. JASKIE, J. E., and KOHLI, D., "A Note on Support Vibrations of a Slider-Crank Mechanism," ASME Paper No. 82-DET-76, 1982.

41. MEANS, K. H., "Bearing Loads in an Elastic Slider Crank Mechanism," ASME Paper No. 82-DET-36, 1982.

42. SHABANA, A., and WEHAGE, R. A., "Variable Degree-of-Freedom Component Mode Analysis of Inertia Variant Flexible Mechanical Systems," Trans. ASME, Paper No. 82-DET-93, Journal of Mechanical Design, 1982.

43. STAMPS, F. R., and BOGCI, C., "Dynamics of Planar, Elastic, High-Speed Mechanisms Considering Three-Dimensional Offset Geometry: Analytical and Experimental Investigations," Trans.

ASME, Paper No. 82-DET-34, Journal of Mechanical Design, 1982.

44. SUNADA, W. H., and DUBOWSKY, S., "On the Dynamic Analysis and Behavior of Industrial Robotic Manipulators with Elastic Members," Trans. ASME, Paper No. 82-DET-45, Journal of Mechanical Design, 1982.

45. SUNG, C. K., and THOMPSON, B. S., "A Note on the Effect of Foundation Motion upon the Response of Flexible Linkages," ASME Paper No. 82-DET-26, 1982.

46. THOMPSON, B. S., ZUCCARO, D., GAMACHE, D., and GANDHI, M. V., "An Experimental and Analytical Study of the Dynamic Response of a Linkage Fabricated from a Unidirectional Fiber-Reinforced Composite Laminate," Trans. ASME, Paper No. 82-DET-67, Journal of Mechanical Design, 1982.

47. ZHU, Z. G., and CHEN, Y., "The Stability of the Motion of a Connecting Rod," Trans. ASME, Paper No. 82-DET-84, Journal of Mechanical Design, 1982.

48. CLEGHORN, W. L., and KONZELMAN, C. J., "Comparative Analysis of Finite Element Types used in Flexible Mechanism Models," Proceedings of The 8th Applied Mechanisms Conference, at OSU, Saint Louis, Mo, 1983.

49. BAGCI, C., "Observations on Analytical and Experimental Kinetoelastodynamic response of Mechanisms Involving Flexural Line Elements, Lumped Mass Systems, and Dynamic Damping Factors, and Applications to Kinetoelastodynamics of Industrial Robots," Trans. ASME, Paper No. 84-DET-141, 1984.

50. GARCIA-REYNOSO, A., and SEERING, W. P., "Vibration Characteristics of an Elastic Linkage with Elastic Input and Output Shafts," ASME Paper No. 84-DET-1, 1984.

51. SHABANA, A. A., "Dynamics of Constrained Flexible Systems Using Consistent, Lumped and Hybrid Mass Formulation," Trans. ASME, Paper No. 84-DET-125, 1984.

52. SUNG, C. K., THOMPSON, B. S., and MCGRATH, J. J., "A Variational Principle for the Linear Coupled Thermoelastodynamic Analysis of Mechanism Systems," Trans. ASME, Paper No. 84-DET-39, 1984.

53. SUNG, C. K., THOMPSON, B. S., CROULEY, P., and CUCCIO, J., "An Experimental Comparative Study of Flexible Four Bar Linkages and Slider Crank Mechanisms Fabricated in Commercial Metals and Composite Laminate," Trans. ASME, Paper No. 84-DET-52, 1984.

54. THOMPSON, B. S., and SUNG, C. K., "A Variational Formulation for the Nonlinear Finite Element Analysis of Flexible Linkages : Theory, Implementation, and Experimental Results," Trans. ASME, Paper No. 84-DET-15, 1984.

55. SHOUP, T. E., "An Analytical Investigation of the Large Deflections of Flexible Beam Springs," Ph.D. Dissertation, The Ohio State University, 1969.

56. KINZEL, G. L., "An Analytical Kinetostatic Study of a Flexible Slider-Crank Mechanism with from One to Four Degrees of Flexibility," Thesis, The Ohio State University, 1969.

COMPUTER-AIDED KINEMATIC/DYNAMIC ANALYSIS PROGRAMS FOR RIGID MECHANISMS

57. SHETH, P. N., and UICKER, J. J. Jr., "IMP (Integral Mechanisms Program), A Computer-Aided Design Analysis System for Mechanisms and Linkage," Journal of Engineering for Industry, PP. 454-464, 1972.

58. SMITH, D. A., CHACE, M. A., and RUBENS, A. C., "The Automatic Generation of a Mathematical Model for Machinery Systems," Journal of Engineering for Industry, PP. 629-635, 1973.

59. GUPTA, V. K., "Dynamic Analysis of Multi-Rigid-Body Systems," Trans. ASME, Paper No. 73-WA/DE-12, Journal of Engineering for Industry, Aug. 1974.

60. BAGCI, C., "Dynamic Motion Analysis of Plane Mechanisms With Columb and Viscous Damping via the Joint Force Analysis," Trans. ASME, Paper No. 74-DET-37, Journal of Engineering for Industry, May 1975.

61. ORLANDEA, N., CHACE, M. A., and CALAHAN, D. A., "A Sparsity-Oriented Approach to the Dynamic Analysis and Design of Mechanical Systems: Part I," Trans. ASME, Paper No. 76-DET-19, Journal of Engineering for Industry, Aug. 1977.

62. ORLANDEA, N., CHACE, M. A., and CALAHAN, D. A., "A Sparsity-Oriented Approach to the Dynamic Analysis and Design of Mechanical Systems: Part II," Trans. ASME, Paper No. 76-DET-20, Journal of Engineering for Industry, Aug. 1977.

63. RUBEL, A. J. and KAUFMAN, R. E., "KINSYN III: A New Human-Engineered System for Interactive Computer-Aided Design of Planar Linkages," Journal of Engineering for Industry, Trans. ASME, 76-DET-48, PP 440-448, May 1977.

64. WILLIAMS, R. J., and RUPPRECHT, S., "Dynamic Force Analysis of Planar Mechanisms," Mechanism and Machine theory, Vol. 16, PP. 425-440, 1981.

65. ARDAYFIO, D. D., "Design of Kinematic Mechanisms using CAD Technology," proceedings of The 7th Applied Mechanisms Conference, at OSU, Kansas City, Mo., 1981, PP. XXI.1-5.

66. CARSON, W. L., and OLADIRAN, O. B., "An Interactive Computer Program for Force System Structural and Dimensional Synthesis," proceedings of The 7th Applied Mechanisms Conference, at OSU, Kansas City, Mo., 1981, PP. XXII.1-15.

67. KINZEL, G. L., and CHANG, C., "The Analysis of Planar Linkages Using a Modular Approach," proceedings of The 7th Applied Mechanisms Conference, at OSU, Kansas City, Mo., 1981, PP. XLVII.1-7.

68. WALDRON, K. J., "Graphical Solution of the Branch and Order Problems of Linkage Synthesis for Multiply Separated Positions," Journal of Engineering for Industry, Trans. ASME, 76-DET-16, PP 591-597, Aug. 1977.

69. WALDRON, K. J. and SONG, S. M., "Theoretical and Numerical Improvements to an Interactive Linkage Design Program - RECSYN," proceedings of The 7th Applied Mechanisms Conference, at OSU, Kansas City, Mo., 1981, PP. VIII.1-8.

70. BAGCI, C., and Abounassif, J. A.-N., "Computer Aided Dynamic Force, Stress and Gross-Motion Response Analysis of Planar Mechanism Using Finite Line Element Technique," ASME Paper No. 82-DET-11, 1982.

71. CARSON, W. L., and LEE, C.-S. I., "A Force System Synthesis Algorithm for Use as a Companion to Mechanism Dynamic Analysis Programs," Trans. ASME, Paper No. 82-DET-72.

72. CARSON, W. L., and LEE, C.-S. I., "An Interactive Force System Synthesis Program for Use with A Host Mechanism Dynamic Analysis Program," Trans. ASME, Paper No. 82-DET-74

73. BENEDETTO, A. D., and PENNESTRI, E., "Analysis of Angular Velocities and Accelerations in Plane Linkages by Means of Numerical Procedure," Trans. ASME, Paper No. 82-DET-82.

74. FALLAHI, B., and RAGSDELL, K. M., "A Compact Approach to Planar Kinematic Analysis," Trans. ASME, Journal of Mechanisms, Transmissions, and Automation Design, Vol. 105, PP. 434-440, Sep. 1983.

75. CARSON, W. L., MUENKS, J., and POURMAND, B., "Examples of Force System Structural and Dimensional Synthesis by Use of Interactive Computer Graphics," Proceedings of The 8th Applied Mechanisms Conference, at OSU, Saint Louis, Mo., 1983.

76. SHARMA, R. P., "Mechanism Analysis on Microcomputers," proceedings of The 8th Applied Mechanisms Conference, at OSU, Saint Louis, Mo., 1983.

77. ARDAYFIO, D. D., MITTLER, J. P., and PARK, A. S., "Interactive Microcomputer Package for the Dynamic Analysis of Machines," Trans. ASME, Paper No. 84-DET-9, 1984.

78. SPARIS, P. D., and MOUROUTSOS, S. G., "A new Matrix Method for the Kinematic Analysis and Motion Simulation of Planar Mechanisms with Lower Pairs," Trans. ASME, Paper No. 84-DET-193, 1984.

79. HAUG, E. J., WEHAGE, E., and BARMAN, N. C., "Design Sensitivity Analysis of Planar Mechanism and Machine Dynamics," Trans. ASME, Paper No 80-DET-6, Journal of Mechanical Design, July 1981, Vol. 103, PP. 560-570.

FATIGUE AND LARGE ELASTIC DEFORMATION ANALYSES

80. SHIN, J. H., "The Development of an Interactive Fatigue Analysis Program for Machine Elements," Thesis, The Ohio State University, 1981.

81. SHIN, J. H., and KINZEL, G. L., "The Development of An Interactive Procedure for Fatigue Analysis Using Computer Graphics," Proceedings of the 2nd International Computer Engineering Conference and Exhibit," San Diego, CA., 1982.

82. SHIN, J. H., and KINZEL, G. L., "Manual for Fillet and Spot Welding Connections Design and Analysis Program," Dept. of Mechanical Engineering, The Ohio State University, 1984.

83. COLLINS, J. A., "Failure of Materials in Mechanical Design," John Wiley and Sons, Inc., N.Y., 1981.

84. JUVINALL, R. C., "Stress, Strain, and Strength," McGraw-Hill Book Comp., N.Y., 1967.

85. SHIGLEY, J. E., "Mechanical Engineering Design," rd Edit., McGraw-Hill Book Comp., N.Y., 1977.

86. FAUPEL, J. H., and FISHER, F. E., "Engineering Design," 2nd Edition, John Wiley and Sons, Inc., N.Y., 1981.

87. BISSHOPP, K. E., and DRUCKER, D. C., "Large Deflections of Cantilever Beams," Quarterly of Applied Mathematics, Vol. 3, 1945, PP 272-275.

88. de ARANTESE OLIVEIRA, E. R.,"A Method of Fictitious Forces for The Geometrically Nonlinear Analysis of Structures," in Computational Method in Nonlinear Mechanics, The Texas Institute for Computational Mechanics, 1974.

MATRIX METHODS AND DYNAMIC ANALYSIS

89. PESTEL, E. C., and LECKIE, F. A., "Matrix Methods in Elasto Mechanics," McGraw-Hill Book Comp., N.Y., 1963.

90. PILKEY, R. B., and PILKEY, O. H., "Mechanics of Solid," Quantum Publishers, Inc., N.Y., 1974.

91. PILKEY, W. D., and CHANG, P. Y., "Modern Formulas for Statics and Dynamics, A Stress-and-Strain Approach," McGraw-Hill Book Comp., N.Y., 1978.

92. PRZEMIENIECKI, J. S., "Theory of Matrix Structure Analysis," McGraw-Hill Book Comp., N.Y., 1968.

93. KARDESTUNCER, H., "Elementary Matrix Analysis of Structures," McGraw-Hill Book Comp., N.Y., 1974.

94. LIVESLEY, R. K., "Matrix Methods of Structural Analysis," 2nd Edit., Pergamon Press, Inc., Elmsford, N.J., 1975.

95. CLOUGH, R. W., and PENZIEN, J., "Dynamics of Structures," McGraw-Hill Book Comp., N.Y., 1982.

96. D'SOUZA, A. F. and GARG, V. K., "Advanced Dynamics, Modeling and Analysis," McGraw-Hill Book Comp., N.Y., 1984.

97. BATHE, K. J., and WILSON, E. L., "Numerical Methods in Finite Element Analysis," Prentice-Hall,Inc., Englewood Cliffs, N.J., 1976.

98. BECKER, E. B., CAREY, G. F., and ODEN, J. T., "Finite Elements, An Introduction," Vol. I, Prentice-Hall,Inc., Englewood Cliffs, N.J., 1981.

99. SEGERLIND, L. J., "Applied Finite Element Analysis," John Wiley and Sons, Inc., N.Y., 1976.

100. ZIENKIEWICZ, O. C., "The Finite Element Analysis," Mcgraw-Hill Book Comp., N.Y., 1977.

MECHANISM ANALYSIS

101. SHIGLEY, J. E., "Kinematic Analysis of Mechanisms," 2nd Edit., McGraw-Hill Book Comp., N.Y., 1969.

102. SHIGLEY, J. E., "Dynamic Analysis of Machines," McGraw-Hill Book Comp., N.Y., 1961.

103. SHIGLEY, J. E. and UICKER, J. J., "Theory of Machines and Mechanisms," McGraw-Hill Book Comp., N.Y., 1980.

104. MARTIN, G. H., "Kinematic and Dynamics of Machines," McGraw-Hill Book Comp., N.Y., 1982.

105. SUH, C. H. and RADCLIFF, C. W., "Kinematics and Mechanism Design," John Wiley and Sons, Inc., N.Y., 1978.

106. SANDOR, G. N., and ERDMAN, A. G., "Advanced Mechanism Design: Analysis and Synthesis," Vol. 2, Prentice-Hall,Inc., Englewood Cliffs, N.J., 1984.

APPENDICES A - E

APPENDIX A

FORMULATIONS FOR THE RIGID-BODY KINEMATIC ANALYSES BY A CLOSED-FORM COMPONENT APPROACH

A.1 Nomenclatures

A, B, C	Parameters
L	Length of a link
$\dot{L}$	Linear velocity of a slider
$\ddot{L}$	Linear acceleration of a slider
X, $\dot{X}$, $\ddot{X}$	Position,velocity, and acceleration in the horizontal direction
Y, $\dot{Y}$, $\ddot{Y}$	Position, velocity, and acceleration in the vertical direction
θ, $\dot{\theta}$, $\ddot{\theta}$	Slope-angle, angular velocity, and acceleration of a link from the horizontal axis
XX	Initial position of a slider in the horizontal direction
Xs, $\dot{X}s$, $\ddot{X}s$	Position, velocity, and acceleration of a slider in the X-axis
YY	Initial position of a slider in the vertical direction
Ys, $\dot{Y}s$, $\ddot{Y}s$	Position, velocity, and acceleration of a slider in the Y-axis
θs	Azimuth angle of the sliding axis
α and β	Angles between two solid elements

A.2 Equations of The Component Modules

This section presents the equations of the kinematic loop components for the position and acceleration analyses of the multiloop mechanisms. Node 1 is assigned as the point of which the kinematic properties are known.

A.2.1 Input-Link Component Module (Type 1)

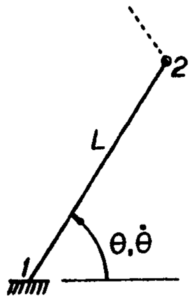

FIGURE A.1 Input-Link Component Module

The positions of node 2 are

$$X2 = X1 + L \cdot \cos\theta$$

$$Y2 = Y1 + L \cdot \sin\theta$$

the velocity components of node 2 are

$$\dot{X}2 = -L \cdot \dot{\theta} \cdot \sin\theta$$

$$\dot{Y}2 = L \cdot \dot{\theta} \cdot \cos\theta$$

and the acceleration components are

$$\ddot{X}2 = -L \cdot \dot{\theta}^2 \cdot \cos\theta$$

$$\ddot{Y}2 = -L \cdot \dot{\theta}^2 \cdot \sin\theta$$

where L = length of the input-link,

θ = angle of the input-link,

and $\dot{\theta}$ = angular velocity of the input-link.

A.2.2 Dyad component module (Type 2)

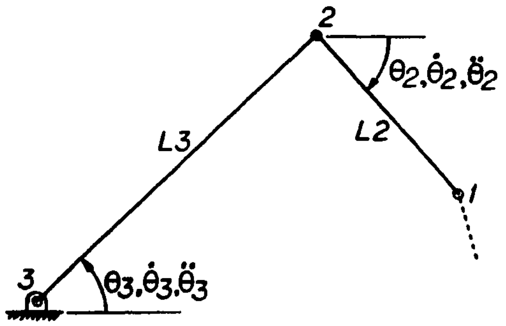

FIGURE A.2 Dyad Component Module

The parameters to determine the angle $\theta 3$ are

$$A = 2 \cdot L3 \cdot (X3 - X1)$$

$$B = 2 \cdot L3 \cdot (Y3 - Y1)$$

$$C = (X3 - X1)^2 + (Y3 - Y1)^2 + L3^2 - L2^2$$

where L2 = length of the link between nodes 1 and 2,

L3 = length of the link between nodes 2 and 3,

$\theta 2$ = angle of the link between node 1 and 2 from the horizontal axis at node 2,

and $\theta 3$ = angle of the link between nodes 2 and 3 from the horizontal axis at node 3.

Then, the angle of $\theta 3$ can be determined as follows:

$$\theta 3 = 2 \cdot \tan^{-1}\left(\frac{-B \pm \sqrt{A^2 + B^2 - C^2}}{C - A}\right)$$

The position and angle of node 2 are

$$X2 = X3 + L3 \cdot \cos \theta 3$$

$$Y2 = Y3 + L3 \cdot \sin \theta 3$$

and

$$\theta 2 = \tan^{-1}\left(\frac{Y1 - Y2}{X1 - X2}\right)$$

The velocities are

$$\dot{\theta}3 = \frac{-\dot{X}1 \cdot \cos\theta2 - \dot{Y}1 \cdot \sin\theta2}{L3 \cdot \sin(\theta3 - \theta2)}$$

$$\dot{\theta}2 = \frac{\dot{X}1 \cdot \cos\theta3 + \dot{Y}1 \cdot \sin\theta3}{L2 \cdot \sin(\theta3 - \theta2)}$$

$$\dot{X}2 = -L3 \cdot \dot{\theta}3 \cdot \sin\theta3$$

and

$$\dot{Y}2 = L3 \cdot \dot{\theta}3 \cdot \cos\theta3$$

where $\dot{X}1$ and $\dot{Y}1$ are the velocity components of node 1.

Finally, the acceleration components are

$$\ddot{\theta}3 = \frac{\ddot{X}1 \cdot \cos\theta2 + \ddot{Y}1 \cdot \sin\theta2 + L3 \cdot \dot{\theta}3^2 \cdot \cos(\theta3-\theta2) + L2 \cdot \dot{\theta}2^2}{-L3 \cdot \sin(\theta3-\theta2)}$$

$$\ddot{\theta}2 = \frac{\ddot{X}1 \cdot \cos\theta3 + \ddot{Y}1 \cdot \sin\theta3 + L2 \cdot \dot{\theta}2^2 \cdot \cos(\theta3-\theta2) + L3 \cdot \dot{\theta}3^2}{L2 \cdot \sin(\theta3-\theta2)}$$

$$\ddot{X}2 = -L3 \cdot \ddot{\theta}3 \cdot \sin\theta3 - L3 \cdot \dot{\theta}3^2 \cdot \cos\theta3$$

and

$$\ddot{Y}2 = L3 \cdot \ddot{\theta}3 \cdot \cos\theta3 - L3 \cdot \dot{\theta}3^2 \cdot \sin\theta3$$

where $\ddot{X}1$ and $\ddot{Y}1$ are the acceleration components of node 1, and $\dot{\theta}2$ and $\dot{\theta}3$ are the angular velocities of the links.

A.2.3 Sliding-End Component Module (Type 3)

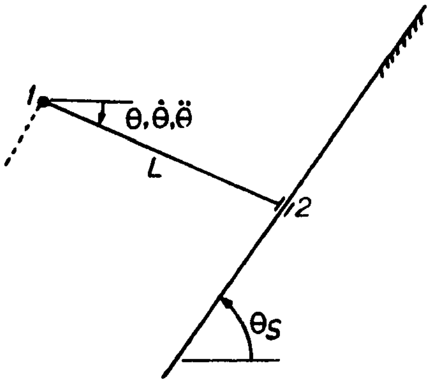

FIGURE A.3 Sliding-End Component Module

The parameters are set as follows:

$$A = L \cdot \tan \Theta s$$

$$B = -L$$

$$C = (X1 - XX) \cdot \tan \Theta s - (Y1 - YY)$$

where L = length of the link between nodes 1 and 2,

XX and YY = initial position of the slider,

and Θs = azimuth angle of the sliding axis.

Then, the angle of a link can be determined from the follow:

$$\theta = 2 \cdot \tan^{-1}\left(\frac{-B \pm \sqrt{A^2 + B^2 - C^2}}{C - A} \right)$$

The position and angle of node 2 are as follows:

$$X2 = X1 + L \cdot \cos\theta$$

$$Y2 = Y1 + L \cdot \sin\theta$$

The angular velocity of the link is

$$\dot{\theta} = \frac{\dot{X}1 \cdot \sin\theta s - \dot{Y}1 \cdot \cos\theta s}{L \cdot \cos(\theta - \theta s)}$$

and the directional velocities of node 2 are as follows:

$$\dot{X}2 = \dot{X}1 - L \cdot \dot{\theta} \cdot \sin\theta$$

$$\dot{Y}2 = \dot{Y}1 + L \cdot \dot{\theta} \cdot \cos\theta$$

where $\dot{X}1$ and $\dot{Y}1$ are the velocity components of node 1.

Finally, the accelerations of the link and of node 2 are

$$\ddot{\theta} = \frac{\ddot{X}1 \cdot \sin\theta s - \ddot{Y}1 \cdot \cos\theta s + L \cdot \dot{\theta}^2 \cdot \sin(\theta - \theta s)}{L \cdot \cos(\theta - \theta s)}$$

$$\ddot{X}2 = \ddot{X}1 - L \cdot \ddot{\theta} \cdot \sin\theta - L \cdot \dot{\theta}^2 \cdot \cos\theta$$

and

$$\ddot{Y}2 = \ddot{Y}1 + L \cdot \ddot{\theta} \cdot \cos\theta - L \cdot \dot{\theta}^2 \cdot \sin\theta$$

where $\ddot{X}1$ and $\ddot{Y}1$ are the acceleration components of node 1.

A.2.4 Solid Link Component Module (Type 4)

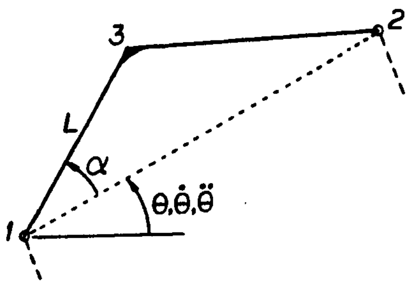

FIGURE A.4 Solid Link Component Module

The angle at node 1 from node 2 to node 3 is defined as follows:

$$\alpha = \tan^{-1}\left(\frac{Y3 - Y1}{X3 - X1}\right) - \tan^{-1}\left(\frac{Y2 - Y1}{X2 - X1}\right)$$

Then, the position of node 3 can be determined from the known kinematic properties of node 1 as follows:

$$X3 = X1 + L \cdot \cos(\theta + \alpha)$$

and

$$Y3 = Y1 + L \cdot \sin(\theta + \alpha)$$

The velocities and accelerations in each direction are

$$\dot{X}3 = \dot{X}1 - L \cdot \dot{\theta} \cdot \sin(\theta + \alpha)$$

$$\dot{Y}3 = \dot{Y}1 + L \cdot \dot{\theta} \cdot \cos(\theta + \alpha)$$

$$\ddot{X}3 = \ddot{X}1 - L \cdot \ddot{\theta} \cdot \sin(\theta + \alpha) - L \cdot \dot{\theta}^2 \cdot \cos(\theta + \alpha)$$

and

$$\ddot{Y}3 = \ddot{Y}1 + L \cdot \ddot{\theta} \cdot \cos(\theta + \alpha) - L \cdot \dot{\theta}^2 \cdot \sin(\theta + \alpha)$$

where X1 and Y1 = position components of node 1,

$\dot{X}1$ and $\dot{Y}1$ = velocity components of node 1,

$\ddot{X}1$ and $\ddot{Y}1$ = acceleration components of node 1,

θ, $\dot{\theta}$, and $\ddot{\theta}$ = slope-angle, angular velocity, and acceleration of the solid component at node 1,

and α = angle at node 1 from the line between nodes 1 and 2 to the line between nodes 1 and 3.

A.2.5 Slider-Dyad Component Module (Type 5)

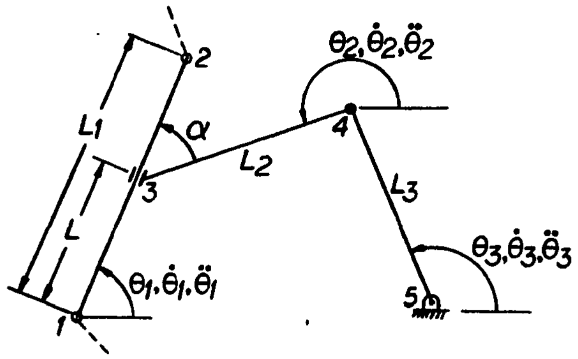

FIGURE A.5 Slider-Dyad Component Module

The value of an angle θ2 can be determined from the known θ1 and the slider-azimuth angle as follow:

$$\theta 2 = \theta 1 + \pi - \alpha$$

The parameters to determined the angle θ3 of the dyad are

$$A = L3 \cdot \sin \theta 1$$

$$B = - L3 \cdot \cos \theta 1$$

$$C = (X5 - X1) \cdot \sin \theta 1 - (Y5 - Y1) \cdot \cos \theta 1 - L2 \cdot \sin \alpha$$

where L1 = length of the link between nodes 1 and 2,

L2 = length of the link between nodes 3 and 4,

L3 = length of the link between nodes 4 and 5,

L = length to the slider from node 1,

and α = azimuth angle of the slider.

Then, the angle is calculated from the following equation:

$$\theta 3 = 2 \cdot \tan^{-1}\left(\frac{-B \pm \sqrt{A^2 + B^2 - C^2}}{C - A}\right)$$

The position of node 4 are

$$X4 = X5 + L3 \cdot \cos \theta 3$$

$$Y4 = Y5 + L3 \cdot \sin \theta 3$$

and the positions of the slider are

$$Xs = X3 = X4 + L2 \cdot \cos \theta 2$$

$$Ys = Y3 = Y4 + L2 \cdot \sin \theta 2$$

where X3 and Y3 are the positions of the node 3,
and Xs and Ys are the positions of the slider.

From the determined positions, the length to the slider from node 1 can be determined from the coordinate transformation as follow:

$$L = (X3 - X1) \cdot \cos \theta 1 + (Y3 - Y1) \cdot \sin \theta 1$$

The angular velocities in the module are

$$\dot{\theta}2 = \dot{\theta}1$$

$$\dot{\theta}3 = \frac{-\dot{X}1 \cdot \sin\theta1 + \dot{Y}1 \cdot \cos\theta1 + L \cdot \dot{\theta}1 + L \cdot \dot{\theta}2 \cdot \cos\alpha}{L3 \cdot \cos(\theta3 - \theta1)}$$

and velocities of every node are

$$\dot{X}4 = -L3 \cdot \dot{\theta}3 \cdot \sin\theta3$$

$$\dot{Y}4 = L3 \cdot \dot{\theta}3 \cdot \cos\theta3$$

$$\dot{X}3 = \dot{X}1 - L \cdot \dot{\theta}1 \cdot \sin\theta1$$

$$\dot{Y}3 = \dot{Y}1 + L \cdot \dot{\theta}1 \cdot \cos\theta1$$

Next, the velocities of the slider are as follows:

$$\dot{X}s = \dot{X}4 - L2 \cdot \dot{\theta}2 \cdot \sin\theta2$$

$$\dot{Y}s = \dot{Y}4 + L2 \cdot \dot{\theta}2 \cdot \cos\theta2$$

and

$$\dot{L} = \frac{-\dot{X}1 \cdot \cos\theta3 - \dot{Y}1 \cdot \sin\theta3 + L \cdot \dot{\theta}1 \cdot \sin(\theta1-\theta3) - L2 \cdot \dot{\theta}2 \cdot \sin(\theta2-\theta3)}{\cos(\theta1 - \theta3)}$$

The angular accelerations have the following relationships:

$$\ddot{\theta}2 = \ddot{\theta}1$$

and

$$\ddot{\theta}3 = \frac{\left[\begin{array}{c} -\ddot{X}1 \cdot \sin\theta1 + \ddot{Y}1 \cdot \cos\theta1 + 2 \cdot \dot{L} \cdot \dot{\theta}1 + L \cdot \ddot{\theta}1 + L3 \cdot \dot{\theta}3^2 \cdot \sin(\theta3 - \theta1) \\ - L2 \cdot \ddot{\theta}2 \cdot \cos(\theta2 - \theta1) + L2 \cdot \dot{\theta}2^2 \cdot \sin(\theta2 - \theta1) \end{array}\right]}{L3 \cdot \cos(\theta3 - \theta1)}$$

The directional accelerations of nodes 3 and 4 are

$$\ddot{X}4 = -L3 \cdot \ddot{\theta}3 \cdot \sin\theta 3 - L3 \cdot \dot{\theta}3^2 \cdot \cos\theta 3$$

$$\ddot{Y}4 = L3 \cdot \ddot{\theta}3 \cdot \cos\theta 3 - L3 \cdot \dot{\theta}3^2 \cdot \sin\theta 3$$

$$\ddot{X}3 = \ddot{X}1 - L \cdot \ddot{\theta}1 \cdot \sin\theta 1 - L \cdot \dot{\theta}1^2 \cdot \cos\theta 1$$

$$\ddot{Y}3 = \ddot{Y}1 + L \cdot \ddot{\theta}1 \cdot \cos\theta 1 - L \cdot \dot{\theta}1^2 \cdot \sin\theta 1$$

and the accelerationa of the slider are

$$\ddot{X}s = \ddot{X}4 - L2 \cdot \ddot{\theta}2 \cdot \sin\theta 2 - L2 \cdot \dot{\theta}2^2 \cdot \cos\theta 2$$

$$\ddot{Y}s = \ddot{Y}4 + L2 \cdot \ddot{\theta}2 \cdot \cos\theta 2 - L2 \cdot \dot{\theta}2^2 \cdot \sin\theta 2$$

A.2.6 Sliding Revolute Component Module (Type 6)

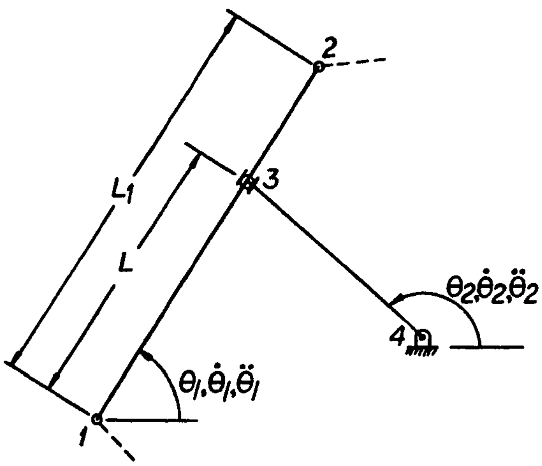

FIGURE A.6 Sliding Revolute Component Module

The parameters to determined the angle θ3 of the dyad are

$$A = L2 \cdot \sin \theta 1$$

$$B = - L2 \cdot \cos \theta 1$$

$$C = (X4 - X1) \cdot \sin \theta 1 - (Y4 - Y1) \cdot \cos \theta 1$$

where L1 = length of the link between nodes 1 and 2,

L2 = length of the link between nodes 3 and 4,

and L = distance to the slider from node 1.

Then, the angle is calculated from the following equation:

$$\theta 2 = 2 \cdot \tan^{-1} \left(\frac{- B \pm \sqrt{A^2 + B^2 - C^2}}{C - A} \right)$$

The positions of the slider are

$$Xs = X3 = X4 + L2 \cdot \cos \theta 2$$

$$Ys = Y3 = Y4 + L2 \cdot \sin \theta 2$$

where X3 and Y3 are the positions of the node 3,

and Xs and Ys are the positions of the slider.

From the determined positions, the length to the slider from node 1 can be determined from the coordinate transformation as follow:

$$L = (X3 - X1) \cdot \cos \theta 1 + (Y3 - Y1) \cdot \sin \theta 1$$

The angular velocity, $\dot{\theta}2$, of the folloer link is

$$\dot{\theta}2 = \frac{-\dot{X}1 \cdot \sin \theta1 + \dot{Y}1 \cdot \cos \theta1 + L \cdot \dot{\theta}1}{L2 \cdot \cos(\theta2 - \theta1)}$$

and the velocities of node 3 are

$$\dot{X}3 = -L \cdot \dot{\theta}1 \cdot \sin \theta1$$

$$\dot{Y}3 = L \cdot \dot{\theta}1 \cdot \cos \theta1$$

Next, the velocities of the slider can be determined as follows:

$$\dot{X}s = -L2 \cdot \dot{\theta}2 \cdot \sin \theta2$$

$$\dot{Y}s = L2 \cdot \dot{\theta}2 \cdot \cos \theta2$$

and

$$\dot{L} = \frac{-\dot{X}1 \cdot \cos \theta2 - \dot{Y}1 \cdot \sin \theta2 - L \cdot \dot{\theta}1 \sin(\theta2 - \theta1)}{\cos(\theta2 - \theta1)}$$

Finally,The angular accelerations of the follower link is

$$\ddot{\theta}2 = \frac{-\ddot{X}1 \cdot \sin \theta1 + \ddot{Y}1 \cdot \cos \theta1 + 2 \cdot \dot{L} \cdot \dot{\theta}1 + L \cdot \ddot{\theta}1 + L2 \cdot \dot{\theta}2^2 \cdot \sin(\theta2 - \theta1)}{L2 \cdot \cos(\theta2 - \theta1)}$$

The acceleration vectors of node 3 and slider are as follows:

$$\ddot{X}3 = -L \cdot \ddot{\theta}1 \cdot \sin \theta1 - L \cdot \dot{\theta}1^2 \cdot \cos \theta1$$

$$\ddot{Y}3 = L \cdot \ddot{\theta}1 \cdot \cos \theta1 - L \cdot \dot{\theta}1^2 \cdot \sin \theta1$$

$$\ddot{X}s = -L2 \cdot \ddot{\theta}2 \cdot \sin \theta2 - L2 \cdot \dot{\theta}2^2 \cdot \cos \theta2$$

and

$$\ddot{Y}s = L2\cdot\ddot{\theta}2 \cdot \cos\theta2 - L2\cdot\dot{\theta}2^2 \cdot \sin\theta2$$

A.2.7 Slider and Follower Component Module (Type 7)

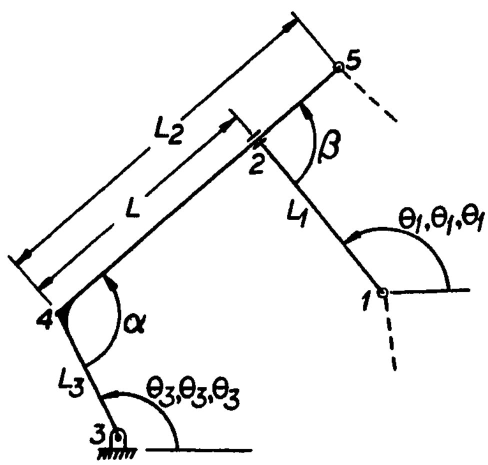

FIGURE A.7 Slider and Follower Component Module

The angles between two solid members are determined from the known initial positions

$$\alpha = \tan^{-1}\left(\frac{Y5 - Y4}{X5 - X4}\right) - \tan^{-1}\left(\frac{Y3 - Y4}{X3 - X4}\right)$$

and

$$\beta = \tan^{-1}\left(\frac{Y5 - Y2}{X5 - X2}\right) - \tan^{-1}\left(\frac{Y3 - Y2}{X3 - X2}\right)$$

where $\alpha = \pi$, when the nodes 3 and 4 are coincident.

The parameters to determine the angle of the follower link are

$$A = Y1 - Y3$$

$$B = X3 - X1$$

$$C = L3 \cdot \sin(\alpha - \pi) - L1 \cdot \sin(\beta - \pi)$$

where L1 = length of the link between nodes 1 and 2,

L2 = length of the link between nodes 4 and 5,

L3 = length of the link between nodes 3 and 4,

L = distance to the slider from node 4,

α = angle between two solid-links L2 and L3,

and β = azimuth angle of the slider.

The angle can be determined from the following equation.

$$\theta 3 = \pi - \alpha + 2 \cdot \tan^{-1}\left(\frac{-B \pm \sqrt{A^2 + B^2 - C^2}}{C - A} \right)$$

An angle of the input-link, $\theta 1$, is represented by the following equation related with the known geometric relationships:

$$\theta 1 = \theta 3 + \alpha - \beta$$

The positions of the slider are

$$Xs = X2 = X1 + L1 \cdot \cos\theta 1$$

$$Ys = Y2 = Y1 + L1 \cdot \sin\theta 1$$

where X2 and Y2 are the positions of the node 3,

and Xs and Ys are the positions of the slider.

The positions of nodes 4 and 5 are calculated as follows:

$$X4 = X3 + L3 \cdot \cos\theta 3$$

$$Y4 = Y3 + L3 \cdot \sin\theta 3$$

$$X5 = X4 + L2 \cdot \cos(\theta 3 + \alpha - \pi)$$

$$Y5 = Y4 + L2 \cdot \sin(\theta 3 + \alpha - \pi)$$

From the determined positions, the length to the slider from node 4 can be determined from the coordinate transformation as follow:

$$L = (X2 - X4) \cdot \cos(\theta 3 + \alpha - \pi) + (Y2 - Y4) \cdot \sin(\theta 3 + \alpha - \pi)$$

The angular velocities, $\dot{\theta}1$ and $\dot{\theta}3$, of the links are

$$\dot{\theta}3 = \dot{\theta}1 = \frac{-\dot{X}1 \cdot \sin(\theta 3 + \alpha - \pi) + \dot{Y}1 \cdot \cos(\theta 3 + \alpha - \pi)}{L - L1 \cdot \cos(\beta - \pi) + L3 \cdot \cos(\alpha - \pi)}$$

and the velocities of nodes are

$$\dot{X}4 = -L3 \cdot \dot{\theta}3 \cdot \sin\theta 3$$

$$\dot{Y}4 = L3 \cdot \dot{\theta}3 \cdot \cos\theta 3$$

$$\dot{X}2 = \dot{X}4 - L \cdot \dot{\theta}3 \cdot \sin(\theta 3 + \alpha - \pi)$$

$$\dot{Y}2 = \dot{Y}4 + L \cdot \dot{\theta}3 \cdot \cos(\theta 3 + \alpha - \pi)$$

$$\dot{X}5 = \dot{X}4 - L2 \cdot \dot{\theta}3 \cdot \sin(\theta 3 + \alpha - \pi)$$

$$\dot{Y}5 = \dot{Y}4 + L2 \cdot \dot{\theta}3 \cdot \cos(\theta 3 + \alpha - \pi)$$

Next, the velocities of the slider can be determined as follows:

$$\dot{X}s = \dot{X}1 - L1 \cdot \dot{\theta}1 \cdot \sin \theta 1$$

$$\dot{Y}s = \dot{Y}1 + L1 \cdot \dot{\theta}1 \cdot \cos \theta 1$$

and

$$\dot{L} = \frac{\begin{bmatrix} \dot{X}1 \cdot [- L1 \cdot \cos(\theta 3 + \alpha - \beta) + L3 \cdot \cos \theta 3 + L \cdot \cos(\theta 3 + \alpha - \pi)] \\ + \dot{Y}1 \cdot [- L1 \cdot \sin(\theta 3 + \alpha - \beta) + L3 \cdot \sin \theta 3 + L \cdot \sin(\theta 3 + \alpha - \pi)] \end{bmatrix}}{L - L1 \cdot \cos(\beta - \pi) + L3 \cdot \cos(\alpha - \pi)}$$

Finally, the angular accelerations of the links are

$$\ddot{\theta}3 = \ddot{\theta}1 = \frac{\begin{bmatrix} - \ddot{X}1 \cdot \sin(\theta 3 + \alpha - \pi) + \ddot{Y}1 \cdot \cos(\theta 3 + \alpha - \pi) \\ + L1 \cdot \dot{\theta}3^2 \cdot \sin(\beta - \pi) - L3 \cdot \dot{\theta}3^2 \cdot \sin(\alpha - \pi) - 2 \cdot \dot{L} \cdot \dot{\theta}3 \end{bmatrix}}{L - L1 \cdot \cos(\beta - \pi) + L3 \cdot \cos(\alpha - \pi)}$$

The acceleration vectors of nodes and slider are as follows:

$$\ddot{X}4 = - L3 \cdot \ddot{\theta}3 \cdot \sin \theta 3 - L3 \cdot \dot{\theta}3^2 \cdot \cos \theta 3$$

$$\ddot{Y}4 = L3 \cdot \ddot{\theta}3 \cdot \cos \theta 3 - L3 \cdot \dot{\theta}3^2 \cdot \sin \theta 3$$

$$\ddot{X}2 = \ddot{X}4 - L \cdot \ddot{\theta}3 \cdot \sin(\theta 3 + \alpha - \pi) - L \cdot \dot{\theta}3^2 \cdot \cos(\theta 3 + \alpha - \pi)$$

$$\ddot{Y}2 = \ddot{Y}4 + L \cdot \ddot{\theta}3 \cdot \cos(\theta 3 + \alpha - \pi) - L \cdot \dot{\theta}3^2 \cdot \sin(\theta 3 + \alpha - \pi)$$

$$\ddot{X}5 = \ddot{X}4 - L2 \cdot \ddot{\theta}3 \cdot \sin(\theta 3 + \alpha - \pi) - L2 \cdot \dot{\theta}3^2 \cdot \cos(\theta 3 + \alpha - \pi)$$

$$\ddot{Y}5 = \ddot{Y}4 + L2 \cdot \ddot{\theta}3 \cdot \cos(\theta 3 + \alpha - \pi) - L2 \cdot \dot{\theta}3^2 \cdot \sin(\theta 3 + \alpha - \pi)$$

$$\ddot{X}s = \ddot{X}1 - L1\cdot\ddot{\theta}1\cdot\sin\theta1 - L1\cdot\dot{\theta}1^2\cdot\cos\theta1$$

and

$$\ddot{Y}s = \ddot{Y}1 + L1\cdot\ddot{\theta}1\cdot\cos\theta1 - L1\cdot\dot{\theta}1^2\cdot\sin\theta1$$

A.2.8 Sliding Revolute and Follower Component Module (Type 8)

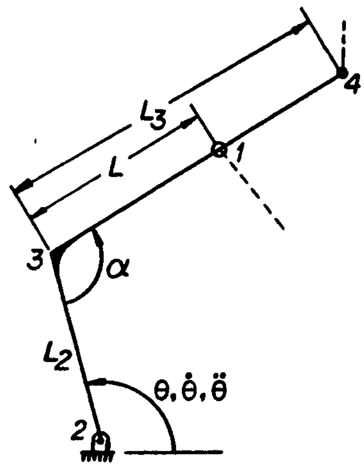

FIGURE A.8 Sliding Revolute and Follower Component Module

The angles between two solid members are determined from the known initial positions

$$\alpha = \tan^{-1}\left(\frac{Y4 - Y3}{X4 - X3}\right) - \tan^{-1}\left(\frac{Y2 - Y3}{X2 - X3}\right)$$

where $\alpha = \pi$, when the nodes 2 and 3 are coincident.

The parameters to determine the angle of the follower link are

$$A = Y2 - Y1$$

$$B = X1 - X2$$

$$C = L2 \cdot \sin(\alpha - \pi)$$

where L2 = length of the link between nodes 2 and 3,

L3 = length of the link between nodes 3 and 4,

L = distance to the slider from node 3,

and α = angle at node 3 between two solid members L2 and L3.

The angle can be determined from the following equation.

$$\theta = \pi - \alpha + 2 \cdot \tan^{-1}\left(\frac{-B \pm \sqrt{A^2 + B^2 - C^2}}{C - A}\right)$$

The positions of nodes 3 and 4 are calculated as follows:

$$X3 = X2 + L2 \cdot \cos\theta$$

$$Y3 = Y2 + L2 \cdot \sin\theta$$

$$X4 = X3 + L3 \cdot \cos(\theta + \alpha - \pi)$$

$$Y4 = Y3 + L3 \cdot \sin(\theta + \alpha - \pi)$$

From the determined positions, the length to the slider from node 3 can be determined from the coordinate transformation as follow:

$$L = (X2 - X4) \cdot \cos(\theta + \alpha - \pi) + (Y2 - Y4) \cdot \sin(\theta + \alpha - \pi)$$

The angular velocity of the link is

$$\dot{\theta} = \frac{-\dot{X}1\cdot\sin(\theta + \alpha - \pi) + \dot{Y}1\cdot\cos(\theta + \alpha - \pi)}{L + L2\cdot\cos(\alpha - \pi)}$$

and the velocities of nodes are

$$\dot{X}3 = -L2\cdot\dot{\theta}\cdot\sin\theta$$

$$\dot{Y}3 = L2\cdot\dot{\theta}\cdot\cos\theta$$

$$\dot{X}4 = \dot{X}3 - L3\cdot\dot{\theta}\cdot\sin(\theta + \alpha - \pi)$$

$$\dot{Y}4 = \dot{Y}3 + L3\cdot\dot{\theta}\cdot\cos(\theta + \alpha - \pi)$$

$$\dot{X}1 = \dot{X}3 - L\cdot\dot{\theta}\cdot\sin(\theta + \alpha - \pi)$$

and

$$\dot{Y}1 = \dot{Y}3 + L\cdot\dot{\theta}\cdot\cos(\theta + \alpha - \pi)$$

Next, the velocity of the slider in the link can be determined as follows:

$$\dot{L} = -L2\cdot\dot{\theta}\cdot\sin(\alpha - \pi) + \dot{X}1\cdot\sin(\theta + \alpha - \pi) + \dot{Y}1\cdot\cos(\theta + \alpha - \pi)$$

Finally, the angular accelerations of the links are

$$\ddot{\theta} = \frac{\left[\begin{array}{l} -\ddot{X}1\cdot\sin(\theta + \alpha - \pi) + \ddot{Y}1\cdot\cos(\theta + \alpha - \pi) \\ \qquad\qquad - L2\cdot\dot{\theta}^2\cdot\sin(\alpha - \pi) - 2\cdot\dot{L}\cdot\dot{\theta} \end{array}\right]}{L + L2\cdot\cos(\alpha - \pi)}$$

The acceleration vectors of nodes are as follows:

$$\ddot{X}3 = -L2 \cdot \ddot{\theta} \cdot \sin\theta - L2 \cdot \dot{\theta}^2 \cdot \cos\theta$$

$$\ddot{Y}3 = L2 \cdot \ddot{\theta} \cdot \cos\theta - L2 \cdot \dot{\theta}^2 \cdot \sin\theta$$

$$\ddot{X}4 = \ddot{X}3 - L3 \cdot \ddot{\theta} \cdot \sin(\theta + \alpha - \pi) - L3 \cdot \dot{\theta}^2 \cdot \cos(\theta + \alpha - \pi)$$

$$\ddot{Y}4 = \ddot{Y}3 + L3 \cdot \ddot{\theta} \cdot \cos(\theta + \alpha - \pi) - L3 \cdot \dot{\theta}^2 \cdot \sin(\theta + \alpha - \pi)$$

$$\ddot{X}1 = \ddot{X}3 - L \cdot \ddot{\theta} \cdot \sin(\theta + \alpha - \pi) - L \cdot \dot{\theta}^2 \cdot \cos(\theta + \alpha - \pi)$$

and

$$\ddot{Y}1 = \ddot{Y}3 + L \cdot \ddot{\theta} \cdot \cos(\theta + \alpha - \pi) - L \cdot \dot{\theta}^2 \cdot \sin(\theta + \alpha - \pi)$$

APPENDIX B

THE SOLUTION DETAILS FOR THE STATIC ANALYSIS OF A MECHANISM

CASDAM: COMPUTER-AIDED STATIC AND DYNAMIC ANALYSES OF MECHANISMS
CASDAM: COMPUTER-AIDED STATIC AND DYNAMIC ANALYSES OF MECHANISMS

```
 CCCCC       A        SSSSS    DDD            A       M       M
CC    C     AAA      SS    S   DD   D        AAA      MM     MM
CC         A   A     SS        DD    D      A   A     MMM   MMM
CC        A     A     SSSSS    DD    D     A     A    MM M M MM
CC       AAAAAAAAA        SS   DD    D    AAAAAAAAA   MM  M  MM
CC    C  AA      AA  S    SS   DD   D     AA     AA   MM     MM
 CCCCC   AA      AA   SSSSS    DDD        AA     AA   MM     MM
```

CASDAM: COMPUTER-AIDED STATIC AND DYNAMIC ANALYSES OF MECHANISMS
CASDAM: COMPUTER-AIDED STATIC AND DYNAMIC ANALYSES OF MECHANISMS

BY

JOONG-HO SHIN

ACADEMIC ADVISOR : GARY L. KINZEL

ADVISORS: K. J. WALDRON
H. R. BUSBY
N. BERME

DEPT. OF MECHANICAL ENGINNERING

THE OHID STATE UNIVERSITY, COLUMBUS,OHIO

1985

HIT RETURN

```
                     WELCOME TO CASDAM
                     ****************

   CASDAM - COMPUTER AIDED STATIC AND DYNAMIC ANALYSES OF MECHANISMS

                 THE PROGRAM CASDAM CAN ANALYZE
                 STATIC/DYNAMIC PROBLEMS UNDER
                 SMALL/LARGE DEFLECTIONS OF PLNAR
                 FLEXIBLE MECHANISMS/STRUCTURES

         THE PROGRAM CASDAM CONSISTS OF

         PRE-PROCESS
              MESH GENERATION OF A PLANAR MECHANISM
              WITH NODES (UP TO 200) AND LOOPS (UP TO 10)
              KINEMATIC POSITION/ACCELERATION ANALYSIS
              DATA GENERATION FOR PROCESS

         PROCESS
              STATIC AND DYNAMIC ANALYSIS FOR THE FLEXIBLE SYSTEM:
              DISPLACEMENTS, FORCES, STRESSES, AND SAFETY FACTORS

         POST-PROCESS
              GEOMETRICAL PLOTS OF DISPLACEMENTS
              GRAPHICAL PLOTS OF DISPLACEMENTS AND STRESSES


  INPUT PROBLEM TITLE (UP TO 20 CHARACTERS) =   EX1



HIT RETURN
                                    3-MAR-86   5:23:50 AM    PG 1
```

```
                    PRE-PROCESS FOR MECHANISM ANALYSIS
                    **********************************
  SELECT INPUT METHOD
  -------------------
    1 ..... KEYBOARD
    2 ..... DATA FILE
  SELECT INPUT METHOD = 1

  DATA OK ([Y]/N) ?> Y

  INPUT FILE NAME FOR ALL DATA = EX1

     ALL DATA WILL BE GIVEN IN THE FOLLOWING FILES

     XXX.DAT = GENERATED DATA FILE FOR ANALYSIS
     XXX.ANL = GENERATED DATA FILE FOR POST-PROCESS
     XXX.KIN = RESULTS FROM KINEMATIC ANALYSIS
     XXX.FLX = RESULTS FROM FLEXIBLE MECHANISM ANALYSIS
     WHERE XXX IS THE GIVEN FILE NAME

  PROBLEM TYPES ARE
  -----------------
     1 ..... STRUCTURE OR MECHANISM AT ONE POSITION
     2 ..... MECHANISM WITH CONTINUOUS POSITIONS
  SELECT PROBLEM TYPE = 1

  DATA OK ([Y]/N) ?> Y

  ANALYSIS TYPES ARE
  ------------------
    1 ..... STATIC ANALYSIS
    2 ..... QUASI-STATIC ANALYSIS
    3 ..... TIME-DOMAIN ANALYSIS
  SELECT ANALYSIS TYPE = 1

  DATA OK ([Y]/N) ?> Y

  LINK WEIGHTS ARE
  ----------------
    1 ..... NO CONSIDERED
    2 ..... CONSIDERED
  SELECT (1 OR 2) = 1

DATA OK ([Y]/N) ?> Y




  HIT RETURN
                  EX1                    3-MAR-86    5:24:24 AM    PG 2
```

```
                    MESH GENERATION FOR A MECHANISM
                    *******************************

                  MAKE NODES (UP TO 50) FOR A SYSTEM

                    AT EXTERNAL FORCE POINTS
                    AT SPRING CONNECTIONS
                    AT BRANCH POINTS
                    AT JOINTS (REVOLUTES AND SLIDES)

                  THEN, NODES ARE GENERATED


UNITS ARE 1 ...... BRITISH
          2 ...... SI

SELECT UNIT = 1

UNITS ARE
*****************************
LENGTH .......... INCHES
FORCE ........... LBS (POUNDS)
TORQUE (MOMENT).. LB-IN
STRESS .......... PSI
*****************************


FOR THE INITIAL PLOT

INPUT MIN. AND MAX. IN X-DIRECTION = 0,30
INPUT MIN. AND MAX. IN Y-DIRECTION = 0,35


HIT RETURN
```

```
ELEMENTS MUST INPUT IN SERIES
STARTING POINT OF ELEMENT 1 IS SET AS (0,0)

SELECT ELEMENT TYPE = 1

  NODE NO AT STARTING POINT = 1
   INPUT LENGTH AND ANGLE = 5,75

SELECT ELEMENT TYPE = 1

  INPUT NODE NO AT STARTING POINT = 2
   STARTING NODE =  2 DATA OK ([Y]/N) ?> Y
   INPUT LENGTH AND ANGLE = 5,30

SELECT ELEMENT TYPE = 1

  INPUT NODE NO AT STARTING POINT = 3
   STARTING NODE =  3 DATA OK ([Y]/N) ?> Y
   INPUT LENGTH AND ANGLE = 5,30

SELECT ELEMENT TYPE = 1

  INPUT NODE NO AT STARTING POINT = 4
   STARTING NODE =  4 DATA OK ([Y]/N) ?> Y
   INPUT LENGTH AND ANGLE = 7,-80

SELECT ELEMENT TYPE = 1

  INPUT NODE NO AT STARTING POINT = 5
   STARTING NODE =  5 DATA OK ([Y]/N) ?> Y
   INPUT LENGTH AND ANGLE = 7,-80

SELECT ELEMENT TYPE = 1

  INPUT NODE NO AT STARTING POINT = 5
   STARTING NODE =  5 DATA OK ([Y]/N) ?> Y
   INPUT LENGTH AND ANGLE = 5,10

SELECT ELEMENT TYPE = 1

  INPUT NODE NO AT STARTING POINT = 7
   STARTING NODE =  7 DATA OK ([Y]/N) ?> Y
   INPUT LENGTH AND ANGLE = 5,-90

SELECT ELEMENT TYPE = 4
```

```
ELEMENT TYPES ARE
-----------------
1 ..... BEAM (LINE) ELEMENT
2 ..... TRIANGULAR PLATE ELEMENT
3 ..... *** NO MORE ELEMENT
4 ..... *** PAGE CHANGE ***
```

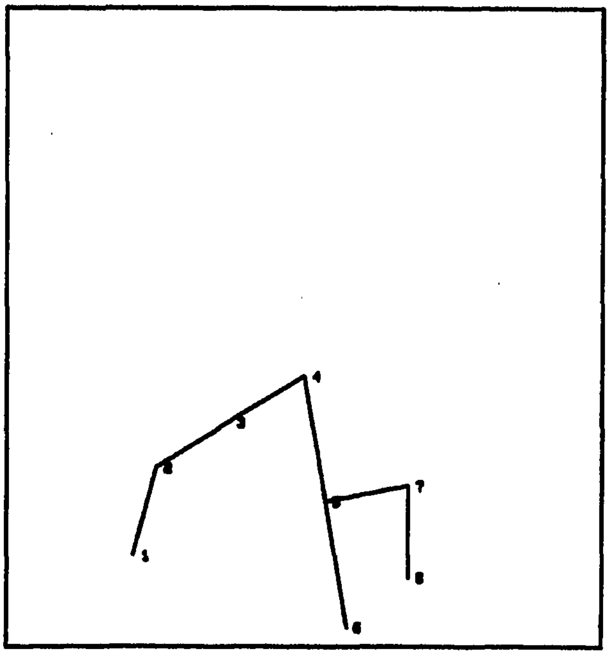

HIT RETURN

EX1 3-MAR-86 5:26:28 AM PG 4

```
SELECT ELEMENT TYPE = 2

  INPUT NODE NO AT STARTING POINT = 3
  STARTING NODE =  3 DATA OK ([Y]/N) ?> Y
  INPUT LENGTH AND ANGLE TO A VOLTEX = 7,180
  INPUT LENGTH AND ANGLE TO A VOLTEX = 10,75
  INPUT THICKNESS OF PLATE = 0.5

SELECT ELEMENT TYPE = 1

  INPUT NODE NO AT STARTING POINT = 10
  STARTING NODE = 10 DATA OK ([Y]/N) ?> Y
  INPUT LENGTH AND ANGLE = 5.225

SELECT ELEMENT TYPE = 1

  INPUT NODE NO AT STARTING POINT = 11
  STARTING NODE = 11 DATA OK ([Y]/N) ?> Y
  INPUT LENGTH AND ANGLE = 5.30

SELECT ELEMENT TYPE = 3
```

```
ELEMENT TYPES ARE
1 ...... BEAM (LINE) ELEMENT
2 ...... TRIANGULAR PLATE ELEMENT
3 ...... *** NO MORE ELEMENT
4 ...... *** PAGE CHANGE ***
```

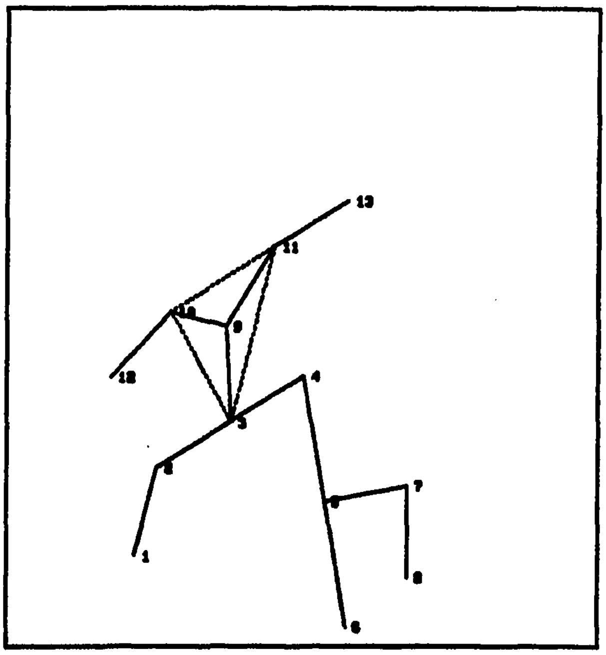


```
HIT RETURN
```

EX1 3-MAR-86 5:31:08 AM PG 5

PROCESS FOR GENERATION OF ELEMENTS

COMMANDS ARE
============
1 ..... GENERATE ELEMENT
2 ..... === GENERATE AGAIN FROM ERROR
3 ..... === NO MORE ELEMENT
4 ..... === CHANGE PAGE

```
SELECT COMMAND = 1
 FOR ELEMENT =  1  INPUT TWO NODES = 1,2

SELECT COMMAND = 1
 FOR ELEMENT =  2  INPUT TWO NODES = 2,3

SELECT COMMAND = 1
 FOR ELEMENT =  3  INPUT TWO NODES = 3,4

SELECT COMMAND = 1
 FOR ELEMENT =  4  INPUT TWO NODES = 4,5

SELECT COMMAND = 1
 FOR ELEMENT =  5  INPUT TWO NODES = 5,6

SELECT COMMAND = 1
 FOR ELEMENT =  6  INPUT TWO NODES = 5,7

SELECT COMMAND = 1
 FOR ELEMENT =  7  INPUT TWO NODES = 7,8

SELECT COMMAND = 1
 FOR ELEMENT =  8  INPUT TWO NODES = 3,9

SELECT COMMAND = 1
 FOR ELEMENT =  9  INPUT TWO NODES = 9,10

SELECT COMMAND = 1
 FOR ELEMENT = 10  INPUT TWO NODES = 10,12

SELECT COMMAND = 1
 FOR ELEMENT = 11  INPUT TWO NODES = 9,11

SELECT COMMAND = 1
 FOR ELEMENT = 12  INPUT TWO NODES = 11,13

SELECT COMMAND = 3

HIT RETURN
```

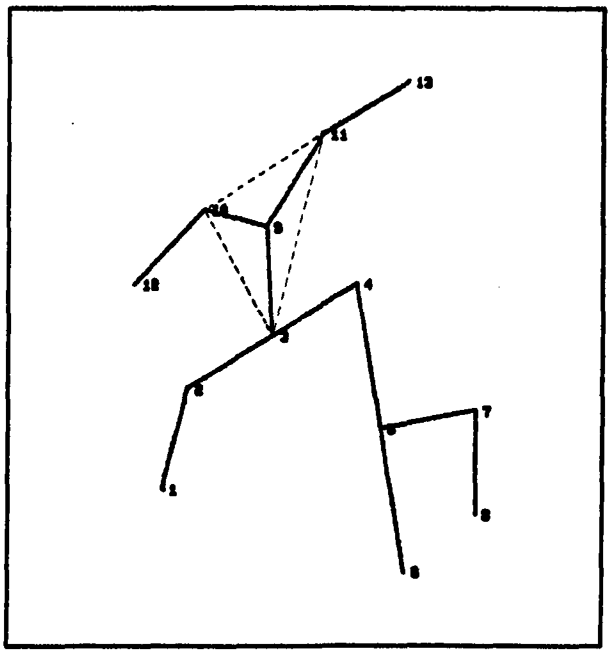

EX1 3-MAR-86 5:33:04 AM PG 6

PROCESS FOR LINK PROPERTIES

USE SAME MATERIAL FOR ALL LINKS ([Y]/N) ?> Y

MATERIAL TYPES ARE

1 ..... STEEL
2 ..... ALUMINUM
3 ..... USER SPECIFIED

SELECT MATERIAL = 1

INPUT YIELD STRENGTH = 100000

USE SAME CROSS-SECTIONS FOR ALL LINKS ([Y]/N) ?> Y

INPUT THICKNESS OF CROSS-SECTION = 0.5

INPUT HEIGHT OF CROSS-SECTION = 0.5

HIT RETURN

EX1	3-MAR-86	5:34:36 AM	PG 7

PROCESS FOR END TYPES

```
FOR MECHANISM,
..............
ONLY ONE END MUST BE FIXED FOR DRIVER LINK

 INPUT NODE NO (IF NO MORE END, HIT 0) = 1
  SELECT END TYPE = 2
  DATA OK ([Y]/N) ?> Y

 INPUT NODE NO (IF NO MORE END, HIT 0) = 6
  SELECT END TYPE = 1
  DATA OK ([Y]/N) ?> Y

 INPUT NODE NO (IF NO MORE END, HIT 0) = 8
  SELECT END TYPE = 1
  DATA OK ([Y]/N) ?> Y

 INPUT NODE NO (IF NO MORE END, HIT 0) = 12
  SELECT END TYPE = 1
  DATA OK ([Y]/N) ?> Y

 INPUT NODE NO (IF NO MORE END, HIT 0) = 13
  SELECT END TYPE = 4
  INPUT SLOPE OF SLIDE END, ANGLE(DEG.) = 0.0
  DATA OK ([Y]/N) ?> Y

 INPUT NODE NO (IF NO MORE END, HIT 0) = 0

 ====================
 SYSTEM HAS  5 ENDS. DATA OK ([Y]/N) ?> Y
```

```
END TYPES ARE
==============
1 ...... PIN END (BUSHING)
2 ...... FIXED END
3 ...... FREE END
4 ...... SLIDE END
5 ...... SIMPLE SUPPORT
```

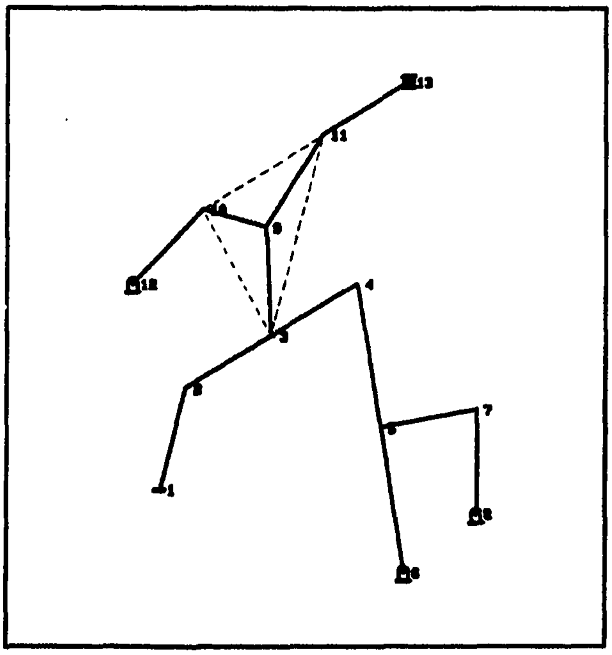

HIT RETURN

EX1 3-MAR-86 5:35:28 AM PG 8

PROCESS FOR EXTERNAL AND SPRING FORCES

NODE TYPES ARE
****
1 ...... NODE FOR EXTERNAL FORCES
2 ...... NODE FOR SPRING CONNECTION
3 ...... *** NO MORE NODE
4 ...... *** PAGE CHANGE ***

SELECT NODE TYPE = 1

INPUT NODE NO = 13

NODE = 13   DATA OK ([Y]/N) ?> Y

FORCES GIVEN BY
1 ...... DIRECTIONAL FORCES
2 ...... VECTORIAL FORCES
SELECT 1 OR 2 = 1

INPUT FORCE IN HORIZONTAL DIRECTION = -100
INPUT FORCE IN VERTICAL DIRECTION   = 0

INPUT MOMENT   = 0

SELECT NODE TYPE = 2

INPUT NODE NO = 4

NODE = 4   DATA OK ([Y]/N) ?> Y

CONNECT TO GROUND *1* OR WITH NODE *2* = 2

INPUT CONNECTED NODE NO = 11
INPUT FREE LENGTH OF SPRING = 5

SELECT NODE TYPE = 2

INPUT NODE NO = 3

NODE = 3   DATA OK ([Y]/N) ?> Y

CONNECT TO GROUND *1* OR WITH NODE *2* = 1

INPUT STIFFNESS OF SPRING = 100
INPUT LENGTH AND ANGLE TO SPRING END = 7.5,-90

SPRING END IS FIXED *1* OR SLIDING *2* = 1
INPUT FREE LENGTH OF SPRING = 5

SELECT NODE TYPE = 3

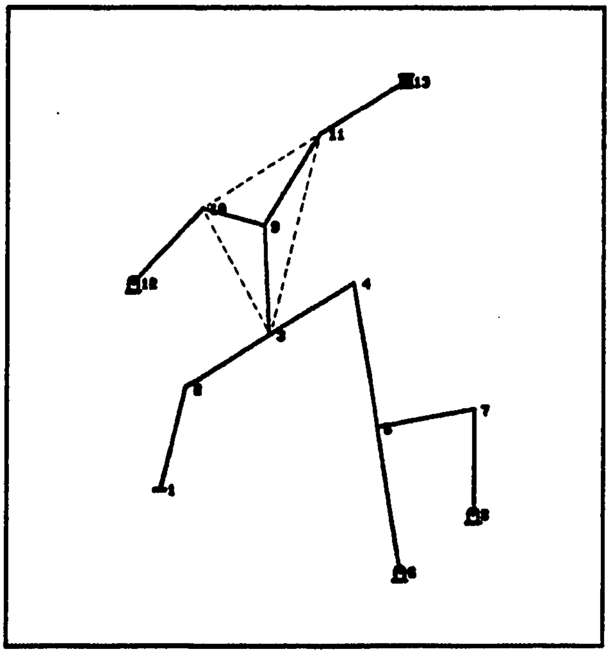

HIT RETURN

EX1   3-MAR-86   5:36:43 AM   PG 9

FOR MAIN LOOP
INPUT STARTING NODE NO IN DRIVER LINK
TO END NODE NO IN FOLLOWER LINK

TOTAL NODES IN MAIN LOOP = 6
INPUT NODE NO (TOTAL 6 NODES) = 1,2,3,4,5,6

DATA OK ([Y]/N) ?> Y
FOR SUB-LOOP
INPUT FROM BRANCH NODE NO TO END NODE NO

FOR SUB-LOOP = 2 TOTAL NODES = 4
INPUT NODE NO (TOTAL 4 NODES) = 3,9,10,12

DATA OK ([Y]/N) ?> Y

FOR SUB-LOOP = 3 TOTAL NODES = 3
INPUT NODE NO (TOTAL 3 NODES) = 9,11,13
DATA OK ([Y]/N) ?> Y

FOR SUB-LOOP = 4 TOTAL NODES = 3
INPUT NODE NO (TOTAL 3 NODES) = 5,7,8
DATA OK ([Y]/N) ?> Y

HIT RETURN

THERE ARE 4 LOOPS IN THE SYSTEM.

INPUT NODE NO FROM THE STARTING POINT
TO END POINT IN EACH LOOP

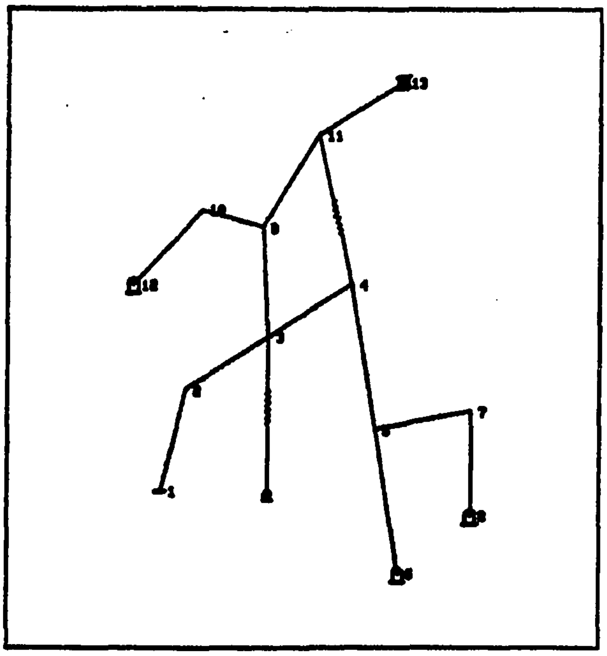

EX1 3-MAR-86 5:39:22 AM PG 10

PROCESS FOR CONNECTIVITY

MAIN LOOP

FOR REVOLUTE JOINT.....

INPUT NODE NO (IF NO MORE, HIT 0) = 2
DATA OK ([Y]/N) ?> Y

INPUT NODE NO (IF NO MORE, HIT 0) = 4
DATA OK ([Y]/N) ?> Y

INPUT NODE NO (IF NO MORE, HIT 0) = 0

NODE GENERATION

FOR SECTION BETWEEN NODES 1 AND 2
INPUT NO OF INSIDE NODES = 3

FOR SECTION BETWEEN NODES 2 AND 3
INPUT NO OF INSIDE NODES = 3

FOR SECTION BETWEEN NODES 3 AND 4
INPUT NO OF INSIDE NODES = 3

FOR SECTION BETWEEN NODES 4 AND 5
INPUT NO OF INSIDE NODES = 3

FOR SECTION BETWEEN NODES 5 AND 6
INPUT NO OF INSIDE NODES = 3

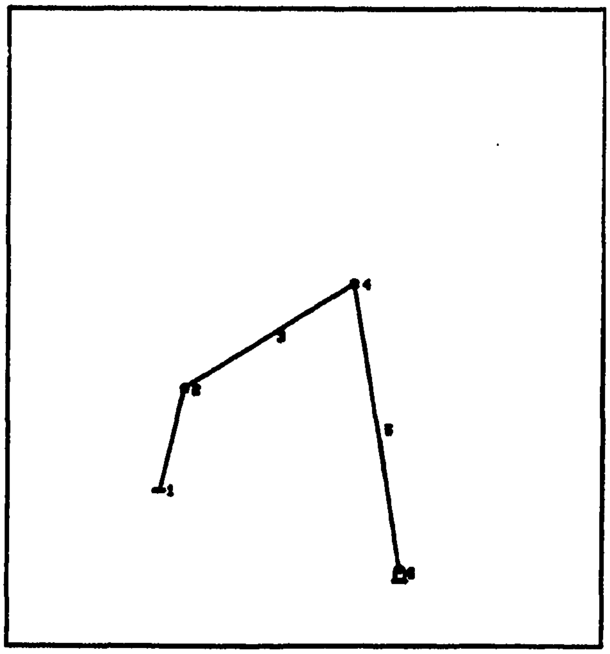

HIT RETURN

EX1 3-MAR-86 5:41:05 AM PG 11

PROCESS FOR CONNECTIVITY

SUB-LOOP = 2

CONNECTIVITIES ARE
==================
1 ..... REVOLUTE JOINT
2 ..... SLIDE JOINT

INPUT NODE NO (IF NO MORE, HIT 0) = 3
SELECT CONNECTIVITY = 1
DATA OK ([Y]/N) ?> Y

INPUT NODE NO (IF NO MORE, HIT 0) = 10
SELECT CONNECTIVITY = 1
DATA OK ([Y]/N) ?> Y

INPUT NODE NO (IF NO MORE, HIT 0) = 0

NODE GENERATION

FOR SECTION BETWEEN NODES 12 AND 10
INPUT NO OF INSIDE NODES = 3

RIGID BODY BETWEEN NODES 10 AND 9

RIGID BODY BETWEEN NODES 9 AND 3

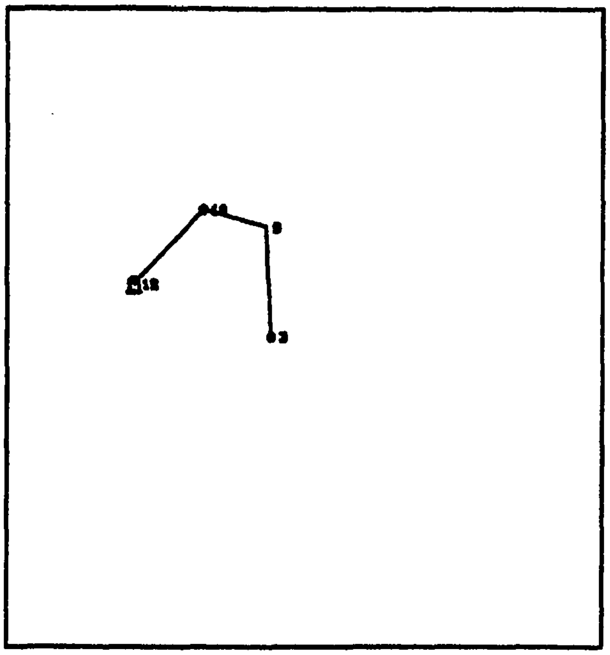

HIT RETURN

EX1 3-MAR-86 5:42:16 AM PG 12

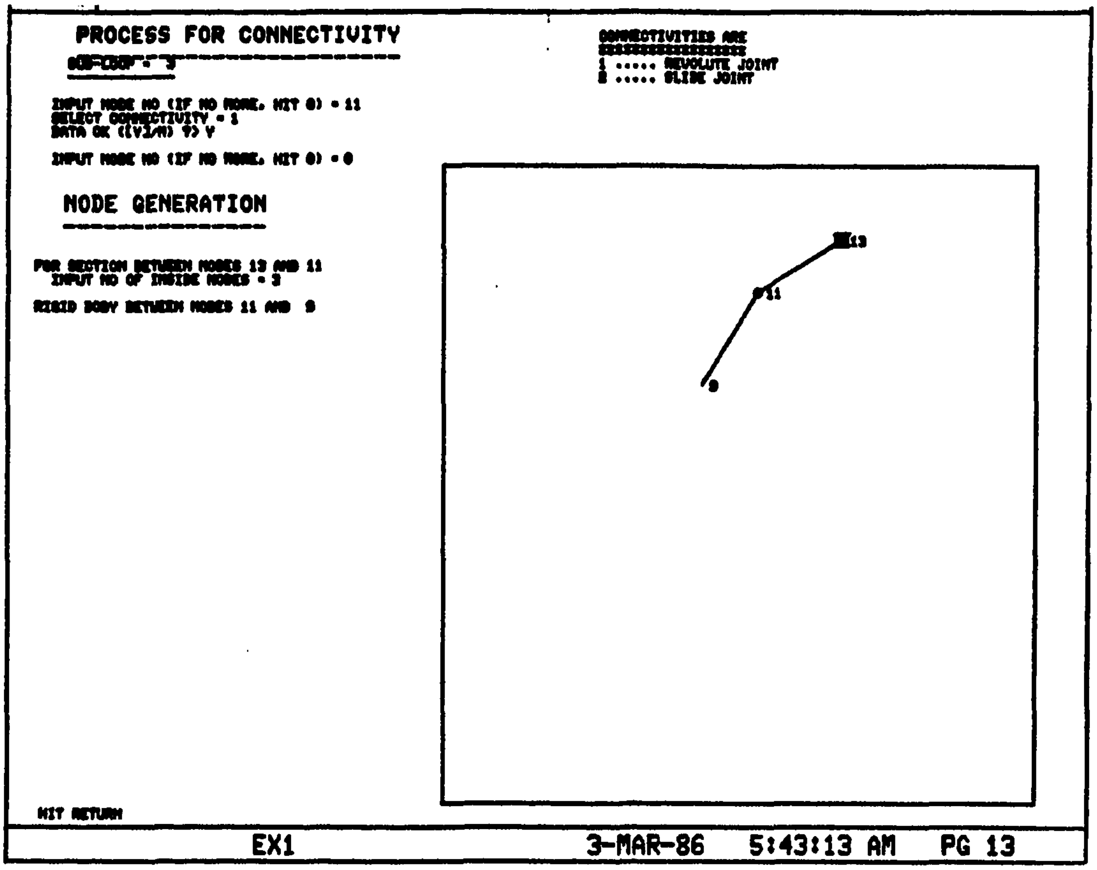
PROCESS FOR CONNECTIVITY
NODE GENERATION
13
11
EX1
3-MAR-86
5:43:13 AM
PG 13

PROCESS FOR CONNECTIVITY

SUB-LOOP = 4

```
INPUT NODE NO (IF NO MORE, HIT 0) = 8
SELECT CONNECTIVITY = 2
DATA OK ([Y]/N) ?> Y

INPUT NODE NO (IF NO MORE, HIT 0) = 7
SELECT CONNECTIVITY = 1
DATA OK ([Y]/N) ?> Y

INPUT NODE NO (IF NO MORE, HIT 0) = 0
```

CONNECTIVITIES ARE
1 ...... REVOLUTE JOINT
2 ...... SLIDE JOINT

NODE GENERATION

```
FOR SECTION BETWEEN NODES  8 AND  7
  INPUT NO OF INSIDE NODES = 3

FOR SECTION BETWEEN NODES  7 AND  5
  INPUT NO OF INSIDE NODES = 3
```

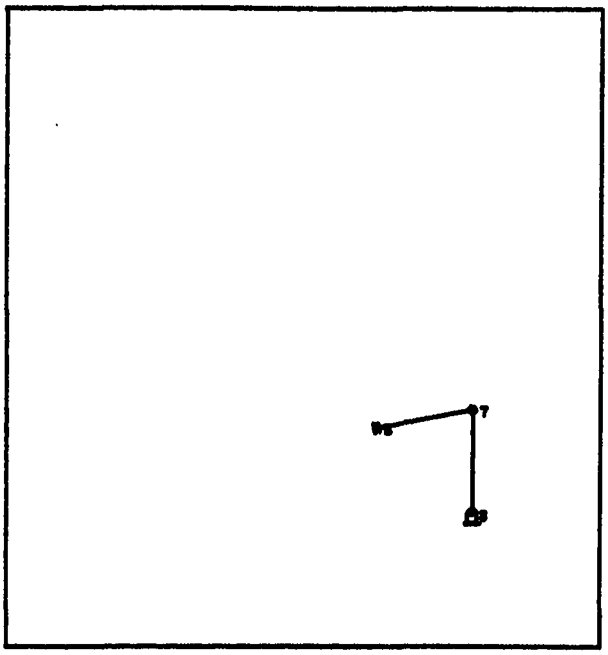

HIT RETURN :

EX1 3-MAR-86 5:44:10 AM PG 14

PROCESS FOR SYSTEM LOOPING

ANY ADDITIONAL WEIGHT OF EACH BEAM (Y/<N>) ?> N

BELL SIGNALS PROCESS COMPLETE

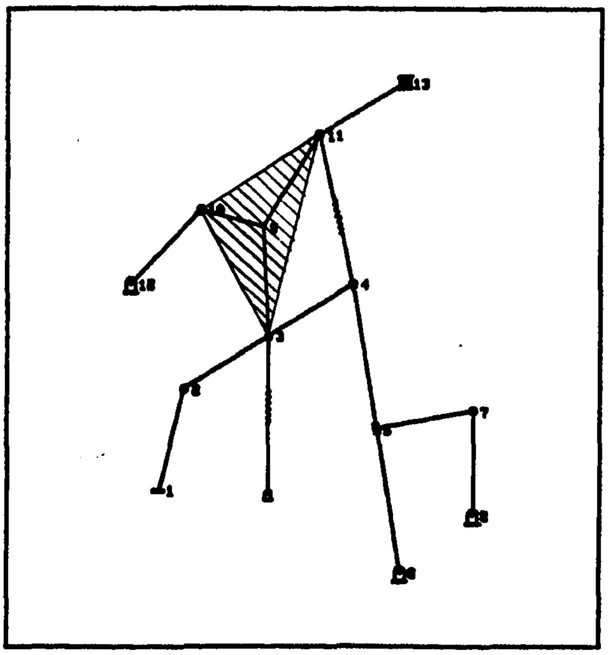

HIT RETURN

EX1 3-MAR-86 5:44:55 AM PG 15

POST-PROCESS OF ANALYSES
****

WANT OUTPUT FILE ([illegible].FLX) ([illegible]) ?) Y

DATA PROCESSING

[illegible] SIGNALS PROCESS COMPLETED

INITIAL POSITION OF MECHANISM

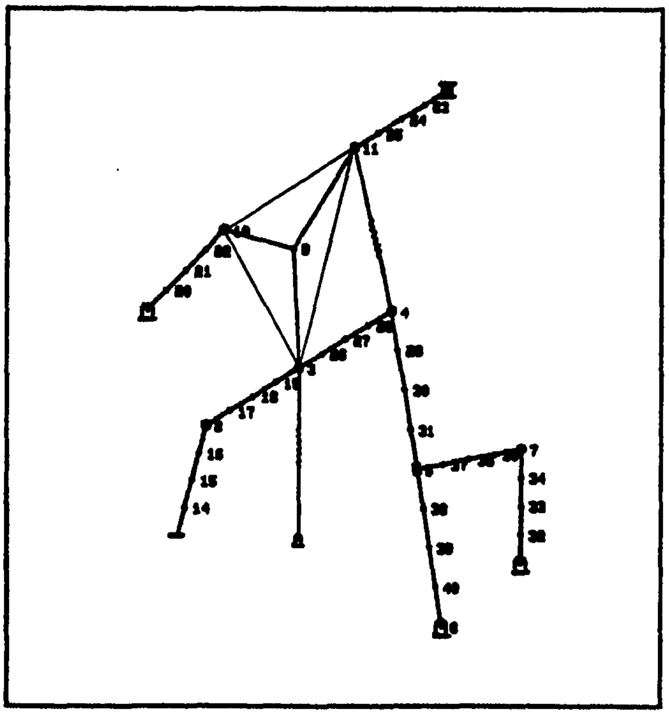

HIT RETURN

EX1 3-MAR-86 10:19:08 PM PG 3

REACTION FORCES AT SUPPORTS

NODE NO	REACTION FORCES HORZ.	VERT.	TORQUE
1	130.400	[illegible]	[illegible]
[illegible]	[illegible]	4.4[illegible]4	0.000
[illegible]	0.000	0.000	0.000
12	[illegible]	[illegible]	0.000
13	0.000	[illegible]	0.000

HIT RETURN

GEOMETRICAL PLOT
SCALE = 10.0 : 1.

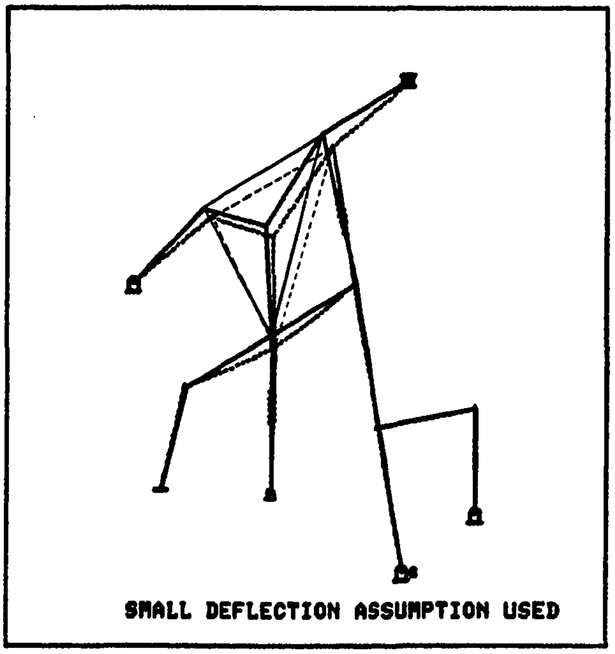

EX1 3-MAR-86 10:20:59 PM PG 4

RESULTS OF STRESS ANALYSES

NODE NO	SAFETY FACTOR	NODE NO	SAFETY FACTOR	NODE NO	SAFETY FACTOR	NODE NO	SAFETY FACTOR
1	[illegible]E+00	11	5.440E+02	21	5.[illegible]E+00	31	5.[illegible]E+03
2	1.[illegible]E+02	12	[illegible].210E+02	22	5.[illegible]E+02	32	——
3	1.[illegible]E+00	13	[illegible]E+02	23	[illegible].150E+02	33	——
4	3.170E+04	14	1.1[illegible]E+01	24	[illegible].150E+02	34	——
5	3.170E+04	15	1.[illegible]E+01	25	[illegible].150E+02	35	——
6	5.[illegible]E+03	16	[illegible]E+01	26	[illegible].470E+00	36	——
7		17	[illegible].140E+00	27	2.[illegible]E+00	37	——
8		18	3.[illegible]E+00	28	7.[illegible]E+00	38	5.[illegible]E+03
9		19	2.410E+00	29	5.[illegible]E+03	39	5.[illegible]E+03
10	3.210E+02	20	5.370E+02	30	6.[illegible]E+03	40	5.[illegible]E+03

—— FOR ZERO STRESSES

LOCATIONS OF CRITICAL POINT(S)

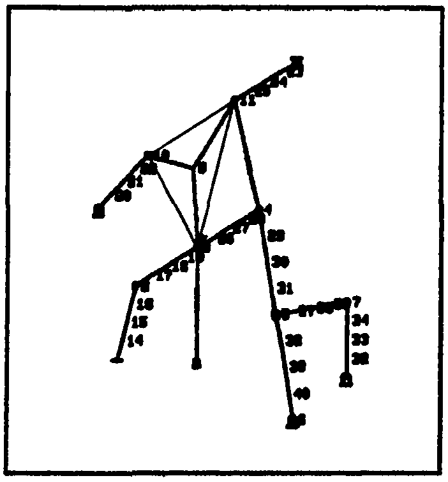

****
MIN SAFETY FACTOR FOR SYSTEM
....

1.860E+00 AT NODE 3
****

HIT RETURN

EX1 3-MAR-86 10:21:48 PM PG 5

END OF PROGRAM

HIT RETURN

3-MAR-86 10:22:40 PM PG 6

APPENDIX C

THE SOLUTION DETAILS FOR THE DYNAMIC ANALYSIS OF A MECHANISM

```
                    WELCOME TO CASDAM
                    *****************

   CASDAM - COMPUTER AIDED STATIC AND DYNAMIC ANALYSES OF MECHANISMS

                  THE PROGRAM CASDAM CAN ANALYZE
                  STATIC/DYNAMIC PROBLEMS UNDER
                  SMALL/LARGE DEFLECTIONS OF PLNAR
                  FLEXIBLE MECHANISMS/STRUCTURES

           THE PROGRAM CASDAM CONSISTS OF

           PRE-PROCESS
                MESH GENERATION OF A PLANAR MECHANISM
                WITH NODES (UP TO 200) AND LOOPS (UP TO 10)
                KINEMATIC POSITION/ACCELERATION ANALYSIS
                DATA GENERATION FOR PROCESS

           PROCESS
                STATIC AND DYNAMIC ANALYSIS FOR THE FLEXIBLE SYSTEM:
                DISPLACEMENTS, FORCES, STRESSES, AND SAFETY FACTORS

           POST-PROCESS
                GEOMETRICAL PLOTS OF DISPLACEMENTS
                GRAPHICAL PLOTS OF DISPLACEMENTS AND STRESSES

   INPUT PROBLEM TITLE (UP TO 20 CHARACTERS) =   EX2

HIT RETURN
                                   2-MAR-86   6:06:14 AM   PG 1
```

```
                    PRE-PROCESS FOR MECHANISM ANALYSIS
                    **********************************
SELECT INPUT METHOD
-------------------
  1 ..... KEYBOARD
  2 ..... DATA FILE
SELECT INPUT METHOD = 1

DATA OK ([Y]/N) ?> Y

INPUT FILE NAME FOR ALL DATA = QUASI

   ALL DATA WILL BE GIVEN IN THE FOLLOWING FILES

   XXX.DAT = GENERATED DATA FILE FOR ANALYSIS
   XXX.ANL = GENERATED DATA FILE FOR POST-PROCESS
   XXX.KIN = RESULTS FROM KINEMATIC ANALYSIS
   XXX.FLX = RESULTS FROM FLEXIBLE MECHANISM ANALYSIS
   WHERE XXX IS THE GIVEN FILE NAME

PROBLEM TYPES ARE
-----------------
   1 ..... STRUCTURE OR MECHANISM AT ONE POSITION
   2 ..... MECHANISM WITH CONTINUOUS POSITIONS
SELECT PROBLEM TYPE = 2

DATA OK ([Y]/N) ?> Y

ANALYSIS TYPES ARE
------------------
  1 ..... STATIC ANALYSIS
  2 ..... QUASI-STATIC ANALYSIS
  3 ..... TIME-DOMAIN ANALYSIS
SELECT ANALYSIS TYPE = 2

DATA OK ([Y]/N) ?> Y




HIT RETURN
```

EX2   2-MAR-86   6:07:31 AM   PG 2

```
                    MESH GENERATION FOR A MECHANISM
                    *******************************

                  MAKE NODES (UP TO 50) FOR A SYSTEM

                    AT EXTERNAL FORCE POINTS
                    AT SPRING CONNECTIONS
                    AT BRANCH POINTS
                    AT JOINTS (REVOLUTES AND SLIDES)

                  THEN, NODES ARE GENERATED

UNITS ARE 1 ...... BRITISH
          2 ...... SI

SELECT UNIT = 1

UNITS ARE
******************************
LENGTH .......... INCHES
FORCE ........... LBS (POUNDS)
TORQUE (MOMENT).. LB-IN
STRESS .......... PSI
******************************

FOR THE INITIAL PLOT

INPUT MIN. AND MAX. IN X-DIRECTION = 0,15
INPUT MIN. AND MAX. IN Y-DIRECTION = -5,10

HIT RETURN
```

EX2   2-MAR-86   6:08:38 AM   PG 3

ELEMENTS MUST INPUT IN SERIES
STARTING POINT OF ELEMENT 1 IS SET AS (0,0)

SELECT ELEMENT TYPE = 1

NODE NO AT STARTING POINT = 1
INPUT LENGTH AND ANGLE = 4,0

SELECT ELEMENT TYPE = 1

INPUT NODE NO AT STARTING POINT = 2
STARTING NODE = 2 DATA OK ((Y1/N) ?) Y
INPUT LENGTH AND ANGLE = 11, [illegible]

SELECT ELEMENT TYPE = 1

INPUT NODE NO AT STARTING POINT = 3
STARTING NODE = 3 DATA OK ((Y1/N) ?) Y
INPUT LENGTH AND ANGLE = 10.5, -78.44

SELECT ELEMENT TYPE = 3

ELEMENT TYPES ARE

1 ...... BEAM (LINE) ELEMENT
2 ...... TRIANGULAR PLATE ELEMENT
3 ...... ### NO MORE ELEMENT
4 ...... ### PAGE CHANGE ###

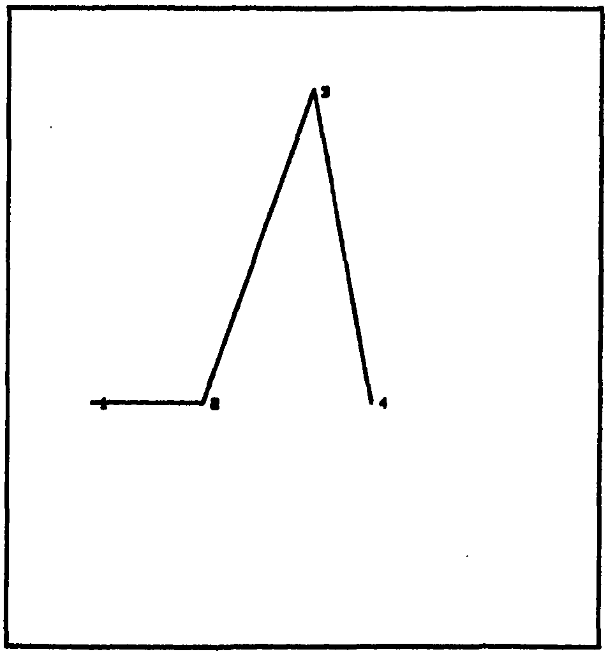

HIT RETURN

EX2 2-MAR-86 6:10:39 AM PG 4

PROCESS FOR GENERATION OF ELEMENTS

```
SELECT COMMAND = 1
 FOR ELEMENT =  1  INPUT TWO NODES = 1,2

SELECT COMMAND = 1
 FOR ELEMENT =  2  INPUT TWO NODES = 2,3

SELECT COMMAND = 1
 FOR ELEMENT =  3  INPUT TWO NODES = 3,4

SELECT COMMAND = 3
```

```
COMMANDS ARE
============
1 ..... GENERATE ELEMENT
2 ..... *** GENERATE AGAIN FROM ERROR
3 ..... *** NO MORE ELEMENT
4 ..... *** CHANGE PAGE
```

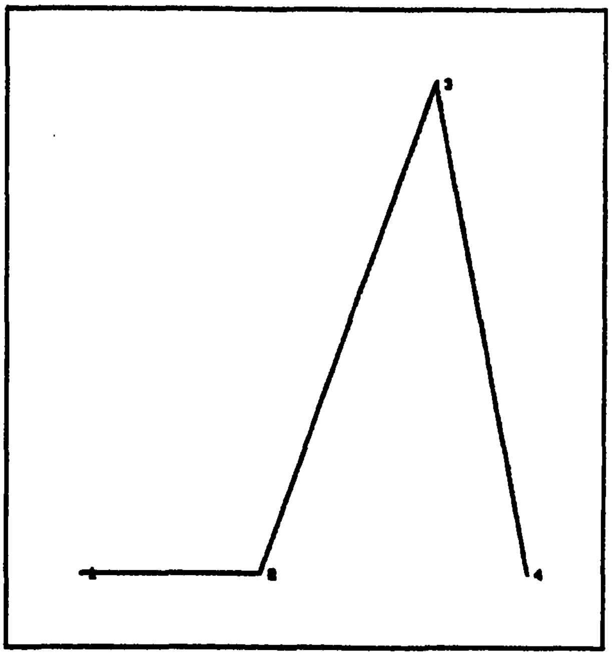

HIT RETURN

EX2	2-MAR-86	6:12:16 AM	PG 5

```
PROCESS FOR LINK PROPERTIES
---------------------------

USE SAME MATERIAL FOR ALL LINKS ([Y]/N) ?> Y
  MATERIAL TYPES ARE

    1 ..... STEEL
    2 ..... ALUMINUM
    3 ..... USER SPECIFIED

  SELECT MATERIAL = 2

  INPUT YIELD STRENGTH = [illegible]

  INPUT ENDURANCE LIMIT = [illegible]

USE SAME CROSS-SECTIONS FOR ALL LINKS ([Y]/N) ?> N

HIT RETURN
```

EX2   2-MAR-86   6:13:18 AM   PG 6

PROCESS FOR LINK PROPERTIES

FOR A ELEMENT BETWEEN NODES 1 AND 2:

INPUT THICKNESS OF CROSS-SECTION = 1.
INPUT HEIGHT OF CROSS-SECTION = 0.167

FOR A ELEMENT BETWEEN NODES 2 AND 3:

INPUT THICKNESS OF CROSS-SECTION = 1.
INPUT HEIGHT OF CROSS-SECTION = 0.083

FOR A ELEMENT BETWEEN NODES 3 AND 4:

INPUT THICKNESS OF CROSS-SECTION = 1.
INPUT HEIGHT OF CROSS-SECTION = 0.083

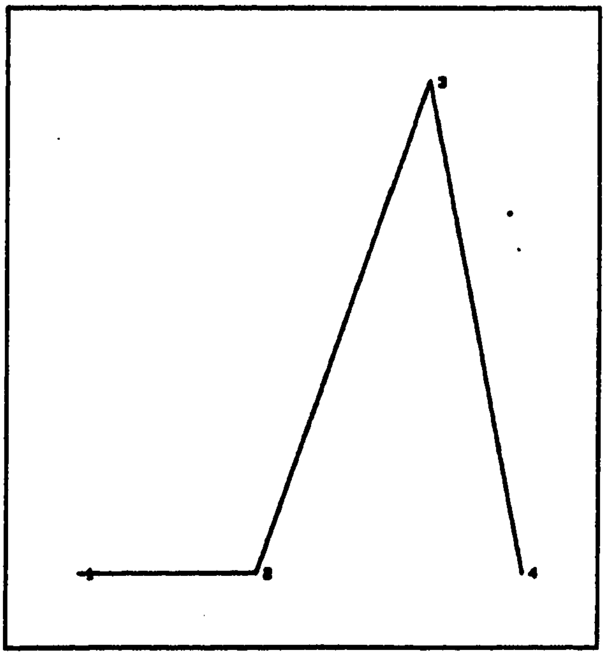

HIT RETURN

EX2 2-MAR-86 6:17:14 AM PG 7

PROCESS FOR END TYPES

```
FOR MECHANISM.
..............
ONLY ONE END MUST BE FIXED FOR DRIVER LINK

 INPUT NODE NO (IF NO MORE END, HIT 0) = 1
  SELECT END TYPE = 2
  DATA OK ([Y]/N) ?> Y

 INPUT NODE NO (IF NO MORE END, HIT 0) = 4
  SELECT END TYPE = 1
  DATA OK ([Y]/N) ?> Y

 INPUT NODE NO (IF NO MORE END, HIT 0) = 0

 ====================
 SYSTEM HAS  2 ENDS. DATA OK ([Y]/N) ?> Y
```

```
END TYPES ARE
=============
1 ...... PIN END (BUSHING)
2 ...... FIXED END
3 ...... FREE END
4 ...... SLIDE END
5 ...... SIMPLE SUPPORT
```

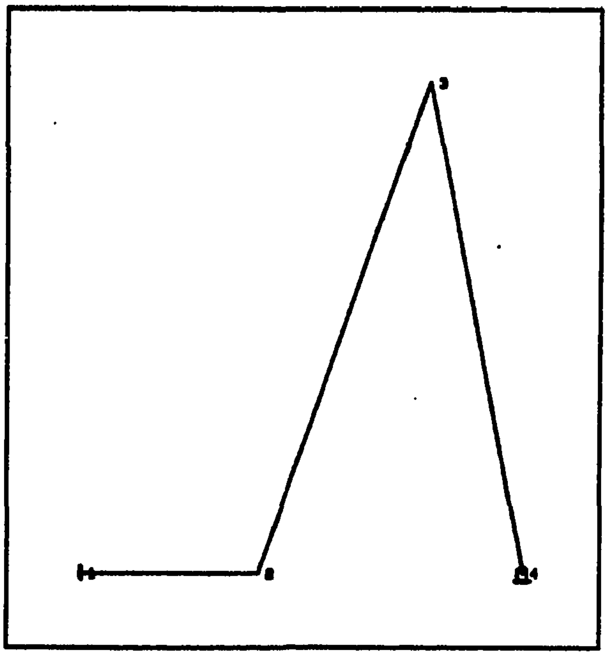

HIT RETURN

EX2 2-MAR-86 6:18:13 AM PG 8

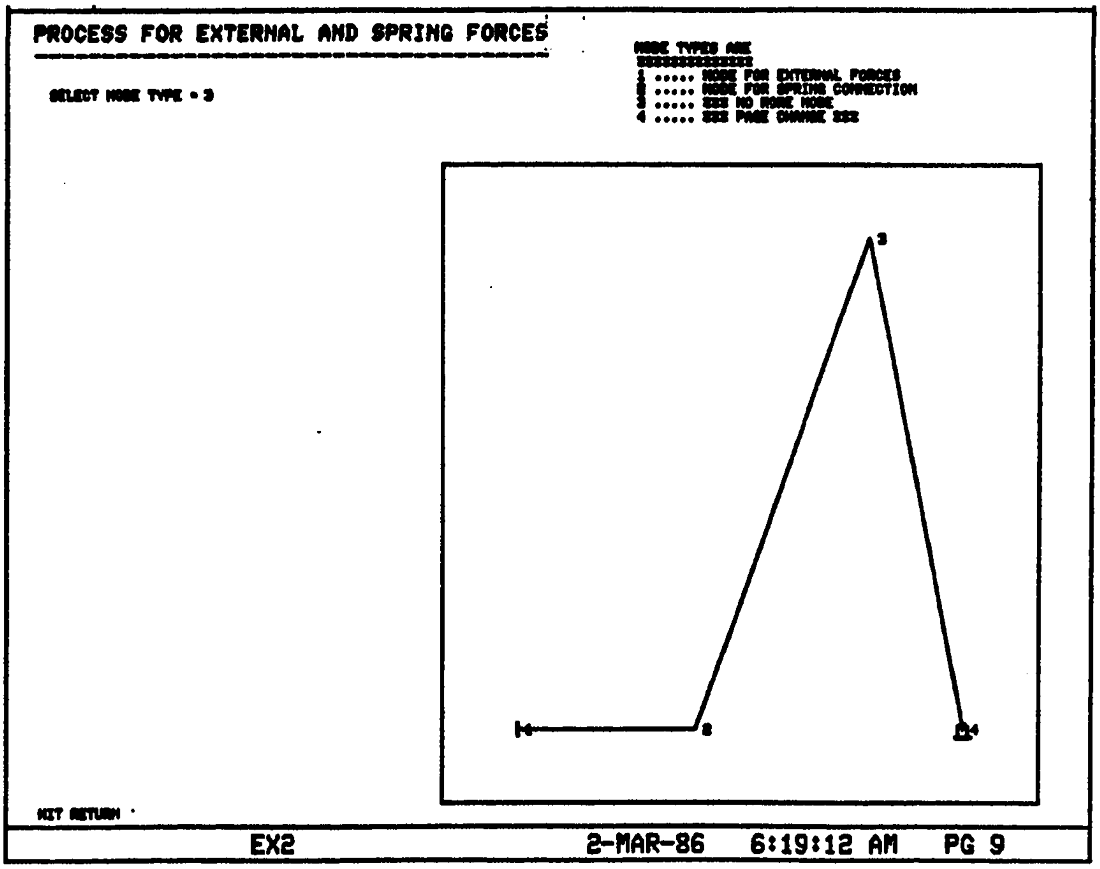
PROCESS FOR EXTERNAL AND SPRING FORCES
SELECT NODE TYPE = 3
NODE TYPES ARE
1 ..... NODE FOR EXTERNAL FORCES
2 ..... NODE FOR SPRING CONNECTION
3 ..... NO MORE NODE
4 ..... PAGE CHANGE
3
2
4
HIT RETURN
EX2
2-MAR-86
6:19:12 AM
PG 9

```
FOR MAIN LOOP
  INPUT STARTING NODE NO IN DRIVER LINK
        TO END NODE NO IN FOLLOWER LINK

  TOTAL NODES IN MAIN LOOP        = 4
  INPUT NODE NO (TOTAL  4 NODES) = 1,2,3,4

  DATA OK (Y/N) ?> Y
```

THERE ARE 1 LOOPS IN THE SYSTEM.

INPUT NODE NO FROM THE STARTING POINT
TO END POINT IN EACH LOOP

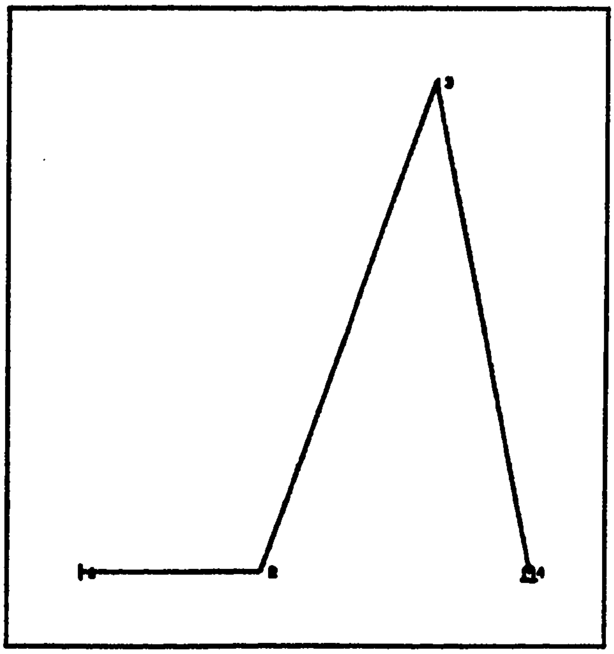

HIT RETURN

EX2 2-MAR-86 6:20:07 AM PG 10

PROCESS FOR CONNECTIVITY

MAIN LOOP

FOR REVOLUTE JOINT.....

```
  INPUT NODE NO (IF NO MORE, HIT 0) = 2
  DATA OK ([Y]/N) ?> Y
  INPUT WEIGHT OF REVOLUTE ITSELF = 0

  INPUT NODE NO (IF NO MORE, HIT 0) = 3
  DATA OK ([Y]/N) ?> Y
  INPUT WEIGHT OF REVOLUTE ITSELF = 0

  INPUT NODE NO (IF NO MORE, HIT 0) = 0
```

NODE GENERATION

```
FOR SECTION BETWEEN NODES  1 AND  2
   INPUT NO OF INSIDE NODES = 3
FOR SECTION BETWEEN NODES  2 AND  3
   INPUT NO OF INSIDE NODES = 3
FOR SECTION BETWEEN NODES  3 AND  4
   INPUT NO OF INSIDE NODES = 3
```

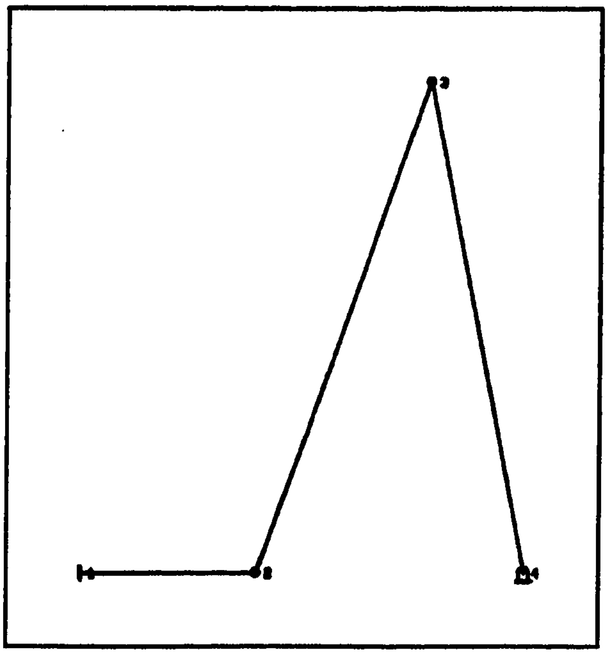

HIT RETURN

EX2   2-MAR-86   6:21:48 AM   PG 11

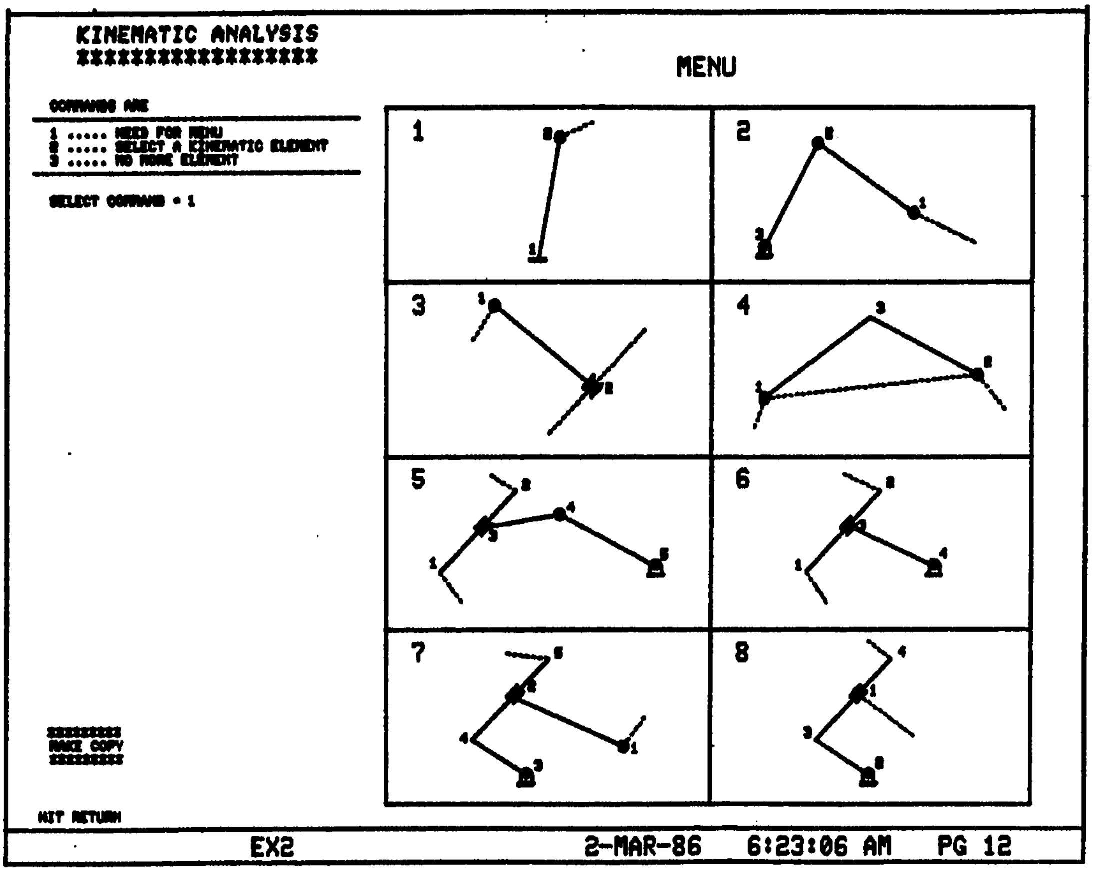

KINEMATIC ANALYSIS
MENU
1
2
3
4
5
6
7
8
EX2
2-MAR-86
6:23:06 AM
PG 12

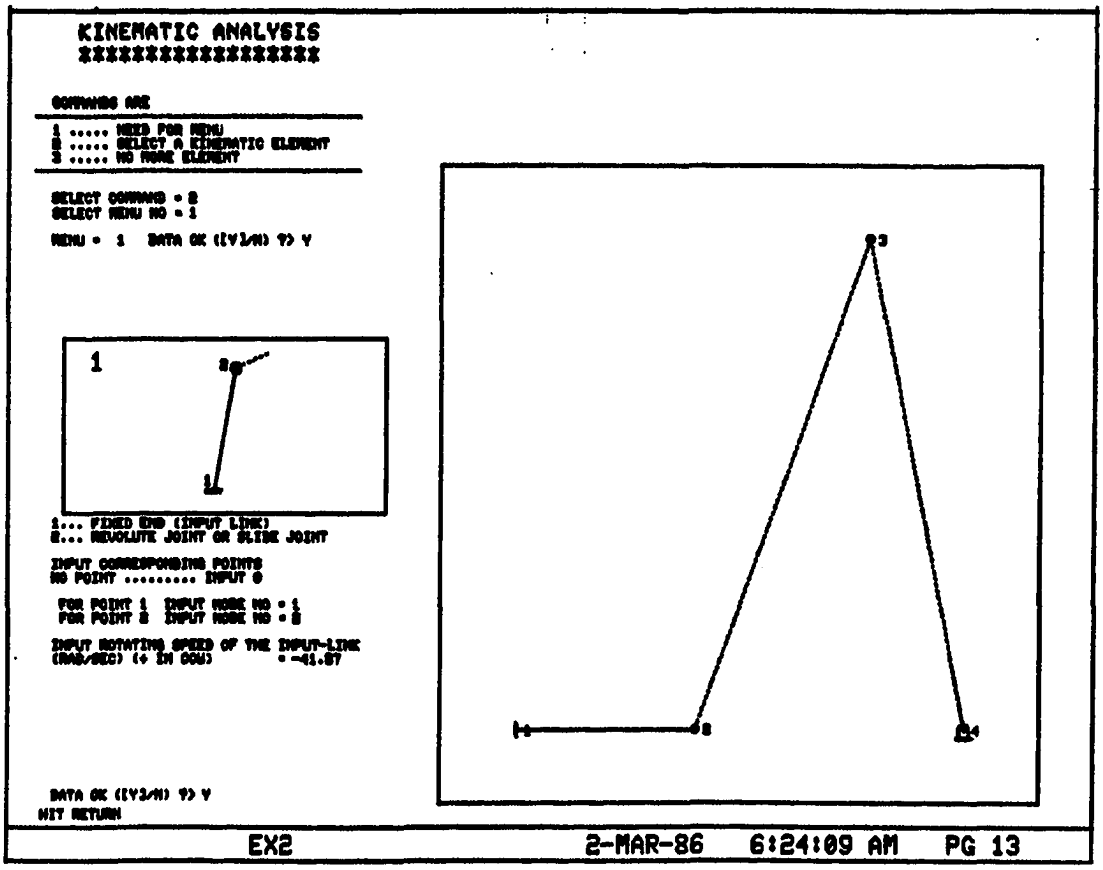
KINEMATIC ANALYSIS
COMMANDS ARE
1 ..... NEED FOR MENU
2 ..... SELECT A KINEMATIC ELEMENT
3 ..... NO MORE ELEMENT
SELECT COMMAND : 2
SELECT MENU NO : 1
MENU : 1 DATA OK ([Y]/N) ?> Y
1... FIXED END (INPUT LINK)
2... REVOLUTE JOINT OR SLIDE JOINT
INPUT CORRESPONDING POINTS
NO POINT .... INPUT 0
FOR POINT 1 INPUT NODE NO : 1
FOR POINT 2 INPUT NODE NO : 2
INPUT ROTATING SPEED OF THE INPUT-LINK
(RAD/SEC) (+ IN CCW) : -41.87
DATA OK ([Y]/N) ?> Y
HIT RETURN
EX2
2-MAR-86
6:24:09 AM
PG 13

KINEMATIC ANALYSIS
****

COMMANDS ARE

1 ..... NEED FOR MENU
2 ..... SELECT A KINEMATIC ELEMENT
3 ..... NO MORE ELEMENT

SELECT COMMAND = 2
SELECT MENU NO = 2

MENU = 2 DATA OK ([Y]/N) ?> Y

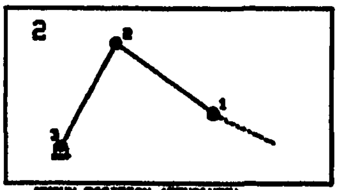

1... KNOWN POSITION (REVOLUTE)
2... REVOLUTE
3... PIN JOINT (BUSHING)

INPUT CORRESPONDING POINTS
NO POINT .... INPUT 0

FOR POINT 1 INPUT NODE NO = 2
FOR POINT 2 INPUT NODE NO = 3
FOR POINT 3 INPUT NODE NO = 4

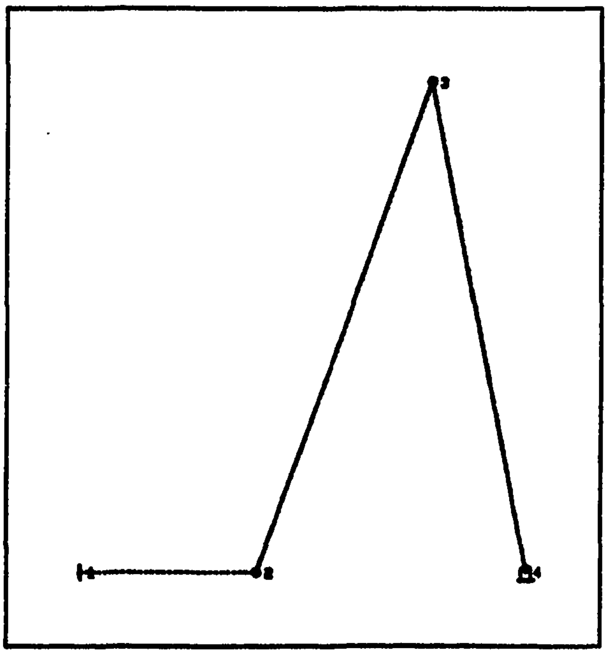

DATA OK ([Y]/N) ?> Y
HIT RETURN

EX2 2-MAR-86 6:26:16 AM PG 14

```
KINEMATIC ANALYSIS
******************

COMMANDS ARE
--------------------------------------
1 ..... NEED FOR MENU
2 ..... SELECT A KINEMATIC ELEMENT
3 ..... NO MORE ELEMENT
--------------------------------------

SELECT COMMAND = 3

          KINEMATIC ANALYSIS HAS BEGUN

         BELL SIGNALS ANALYSIS COMPLETE

HIT RETURN
         EX2                    2-MAR-86   6:27:07 AM   PG 15
```

GEOMETRICAL PLOT OF POSITION ANALYSIS

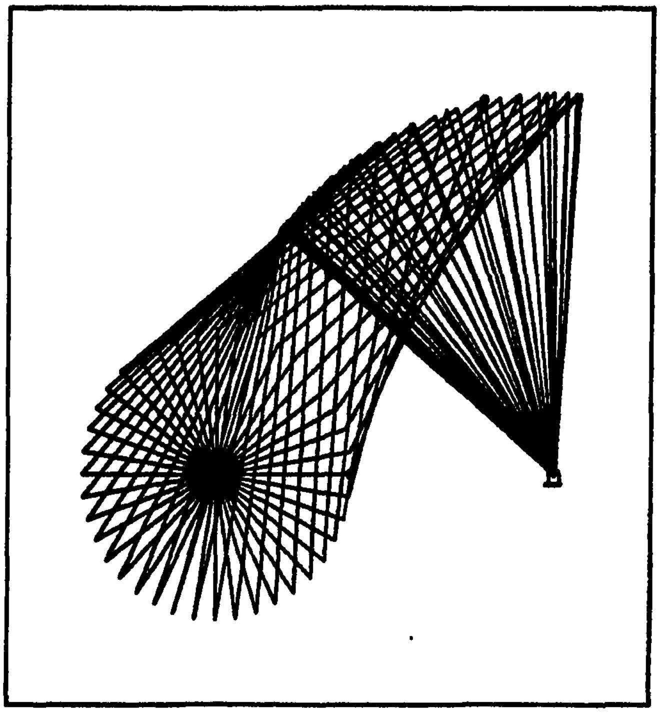

HIT RETURN

EX2 2-MAR-86 6:41:20 AM PG 16

PROCESS FOR SYSTEM LOOPING

ANY ADDITIONAL WEIGHT OF EACH BEAM (Y/(N)) ?> Y
INPUT TWO NODE NO FOR LINK : 1,2
INPUT ADDITIONAL WEIGHT : 0.06

ANY ADDITIONAL WEIGHT OF EACH BEAM (Y/(N)) ?> Y
INPUT TWO NODE NO FOR LINK : 3,4
INPUT ADDITIONAL WEIGHT : 0.06

ANY ADDITIONAL WEIGHT OF EACH BEAM (Y/(N)) ?> N

BELL SIGNALS PROCESS COMPLETE

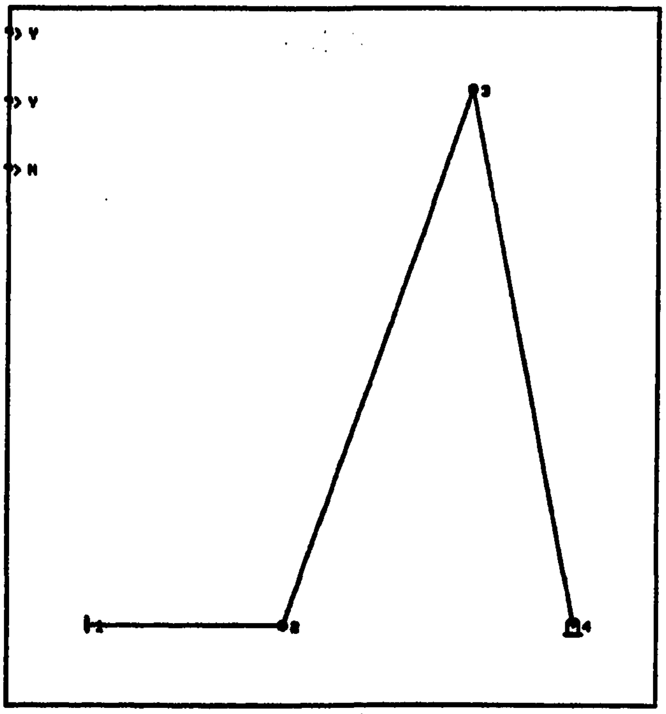

HIT RETURN

EX2 2-MAR-86 6:42:22 AM PG 17

PROCESS FOR MECHANISM ANALYSIS

POSITION OF MECHANISM

POSITION NO = 1

INPUT-LINK = 0.000E+00 DEG

ANALYSIS HAS BEGUN

BELL SIGNALS ANALYSIS COMPLETED

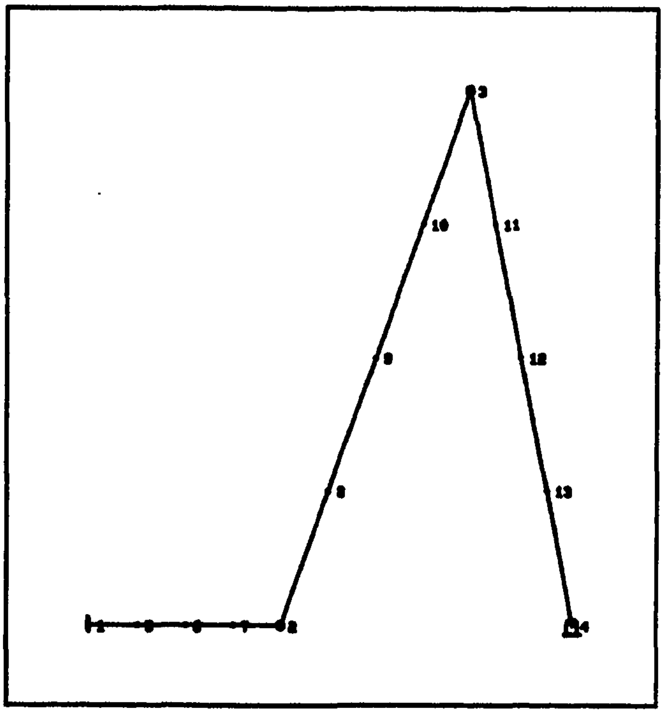

EX2 2-MAR-86 6:45:01 AM PG 18

PROCESS FOR MECHANISM ANALYSIS

POSITION OF MECHANISM

POSITION NO = 2

INPUT-LINK = -9.000E+00 DEG

ANALYSIS HAS BEGUN

BELL SIGNALS ANALYSIS COMPLETED

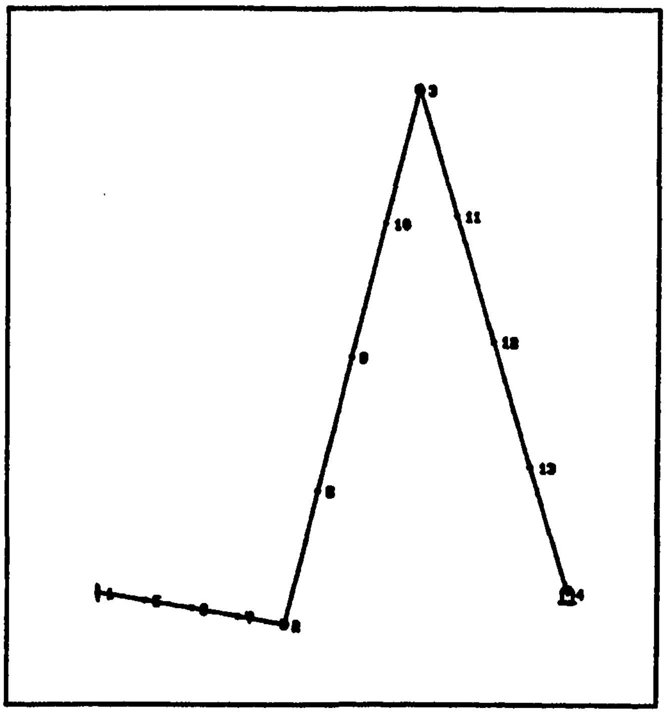

EX2 2-MAR-86 6:45:38 AM PG 19

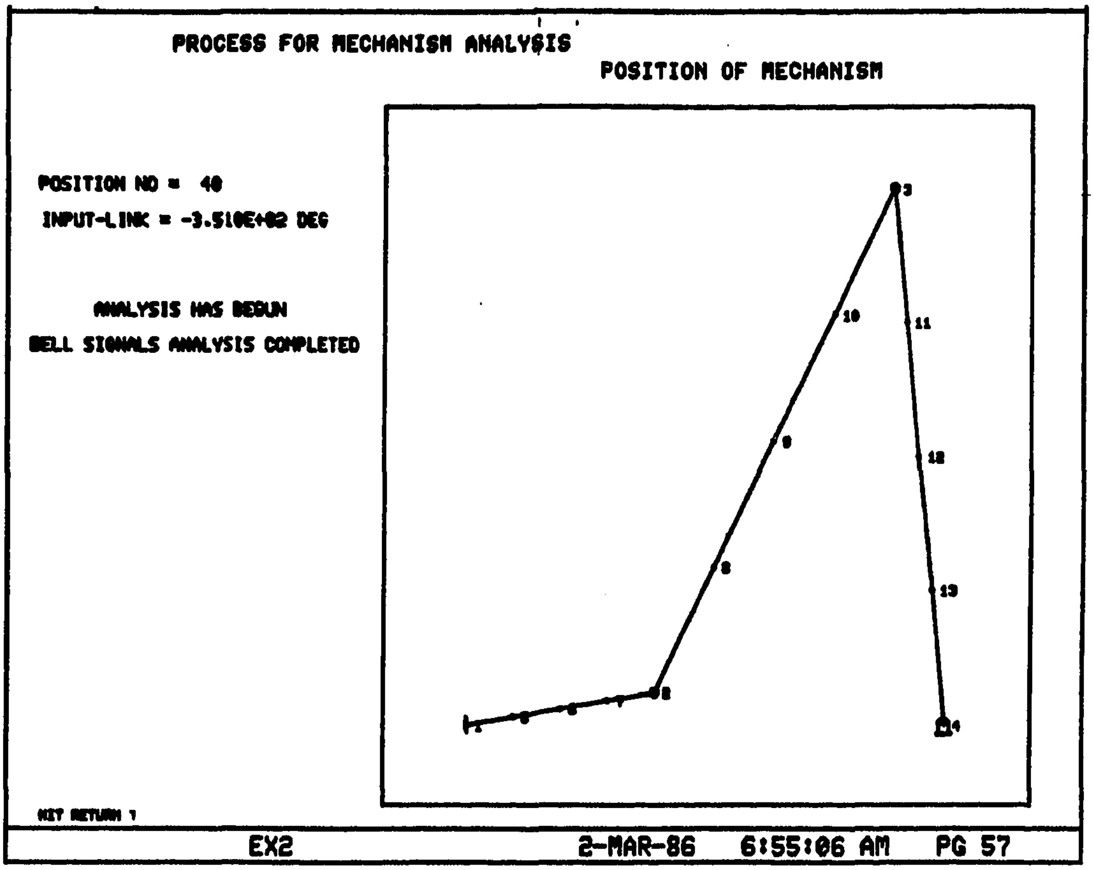
PROCESS FOR MECHANISM ANALYSIS
POSITION OF MECHANISM
POSITION NO = 40
INPUT-LINK = -3.510E+02 DEG
ANALYSIS HAS BEGUN
BELL SIGNALS ANALYSIS COMPLETED
3
10
11
9
12
8
13
2
4
HIT RETURN ?
EX2
2-MAR-86 6:55:06 AM PG 57

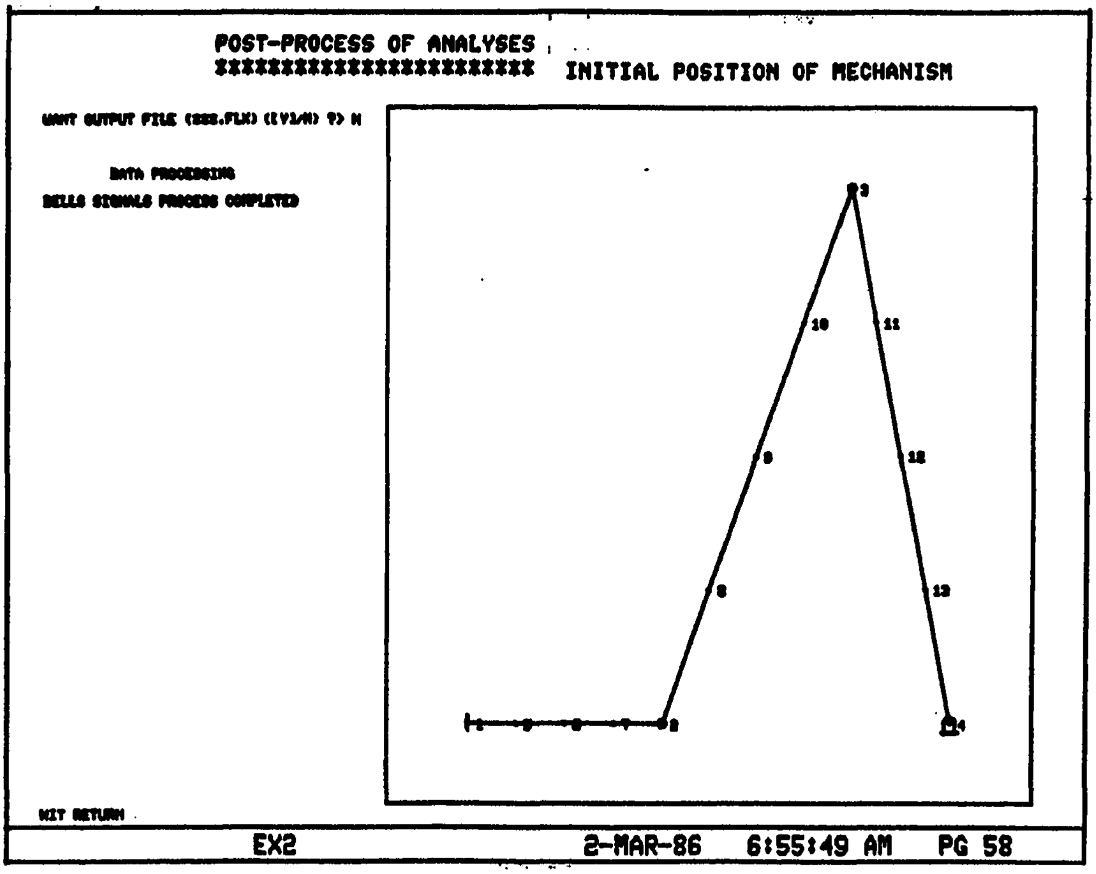
POST-PROCESS OF ANALYSES
****
INITIAL POSITION OF MECHANISM
EX2
2-MAR-86
6:55:49 AM
PG 58

```
POST-PROCESS FOR RESULTS
========================
  1 ..... GEOMETRICAL PLOT OF A SYSTEM
  2 ..... GRAPHICAL PLOT AT A NODE
  3 ..... SAFETY FACTORS
  4 ..... MAXIMUM DISTORTIONS
  5 ..... EXIT

SELECT (1, 2, 3, 4, OR 5) = 3
```

```
HIT RETURN
```

RESULTS OF STRESS ANALYSES

NODE NO	SAFETY FACTOR	NODE NO	SAFETY FACTOR	NODE NO	SAFETY FACTOR	NODE NO	SAFETY FACTOR
1	[illegible]	5	[illegible]	9	[illegible]	13	[illegible]
2	[illegible]	6	[illegible]	10	[illegible]		
3	[illegible]	7	[illegible]	11	[illegible]		
4	[illegible]	8	[illegible]	12	5.440E+00		

— FOR ZERO STRESSES

LOCATIONS OF CRITICAL POINT(S)

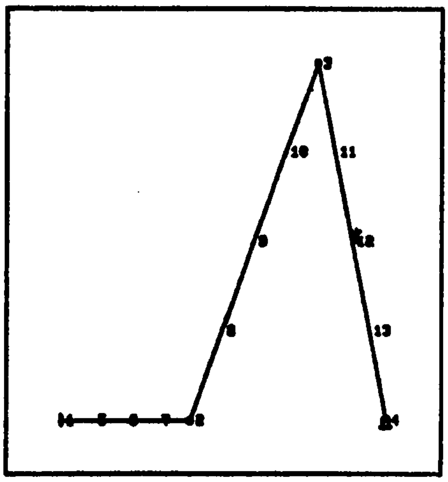

****
MIN SAFETY FACTOR FOR SYSTEM
....

5.440E+00 AT NODE 12
****

HIT RETURN

EX2	2-MAR-86	6:57:55 AM	PG 60

```
POST-PROCESS FOR RESULTS
========================
  1 ...... GEOMETRICAL PLOT OF A SYSTEM
  2 ...... GRAPHICAL PLOT AT A NODE
  3 ...... SAFETY FACTORS
  4 ...... MAXIMUM DISTORTIONS
  5 ...... EXIT

SELECT (1, 2, 3, 4, OR 5) = 4
```

```
HIT RETURN
```

RESULTS OF MAX. DISTORTIONS

NODE NO	MAX. DIST.	NODE NO	MAX. DIST.	NODE NO	MAX. DIST.	NODE NO	MAX. DIST.
1	0.0000E+00	5	[illegible]	9	[illegible]	13	[illegible]
2	[illegible]	6	[illegible]	10	[illegible]		
3	[illegible]	7	[illegible]	11	[illegible]		
4	0.0000E+00	8	[illegible]	12	3.4430E-01		

INITIAL POSITION OF SYSTEM

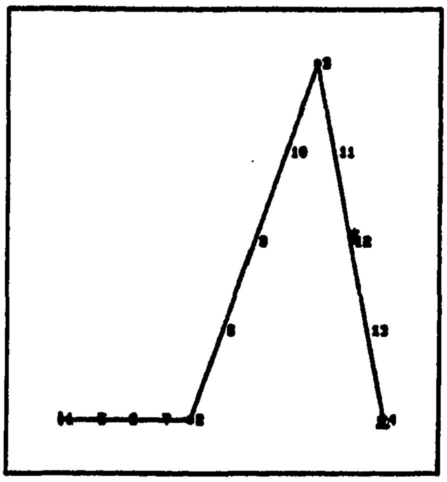

****
MAX. DISTORTION FOR SYSTEM
....

3.4430E-01 AT NODE 12
****

HIT RETURN

EX2 2-MAR-86 6:59:37 AM PG 62

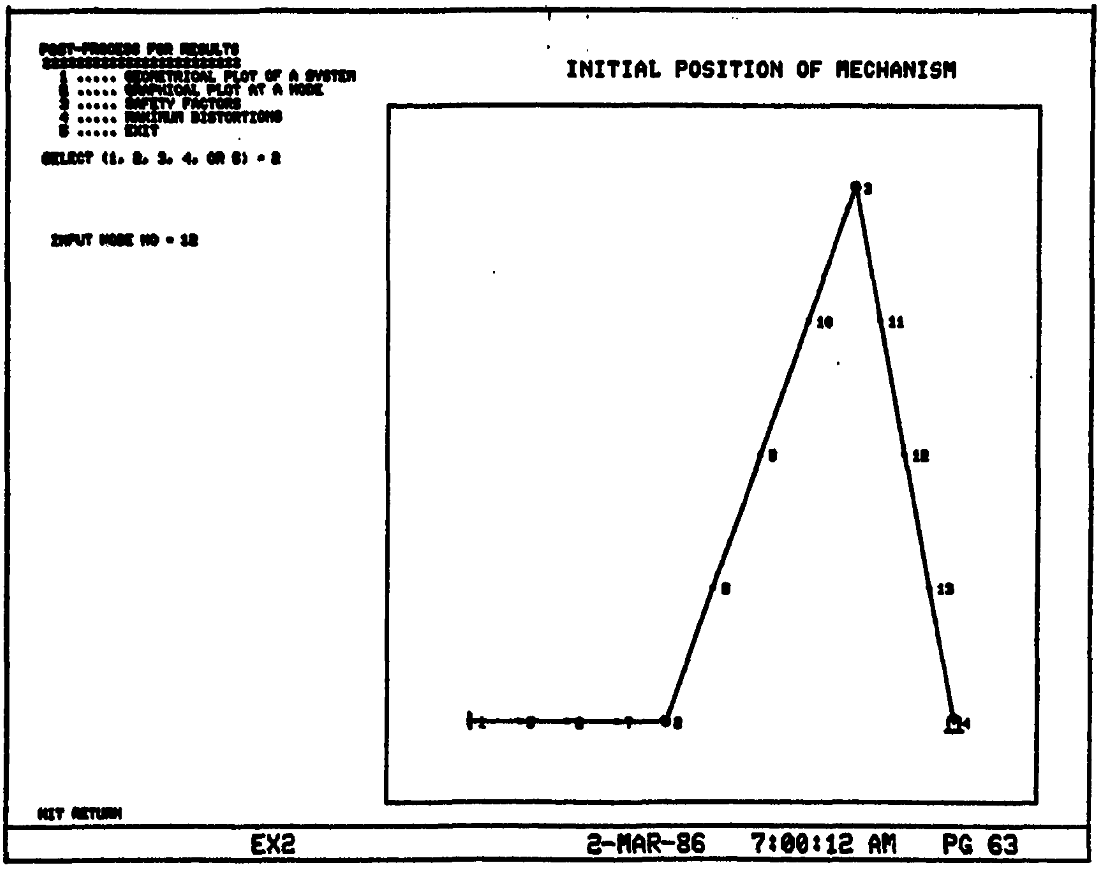
INITIAL POSITION OF MECHANISM
3
10
11
12
13
2
4
EX2
2-MAR-86
7:00:12 AM
PG 63

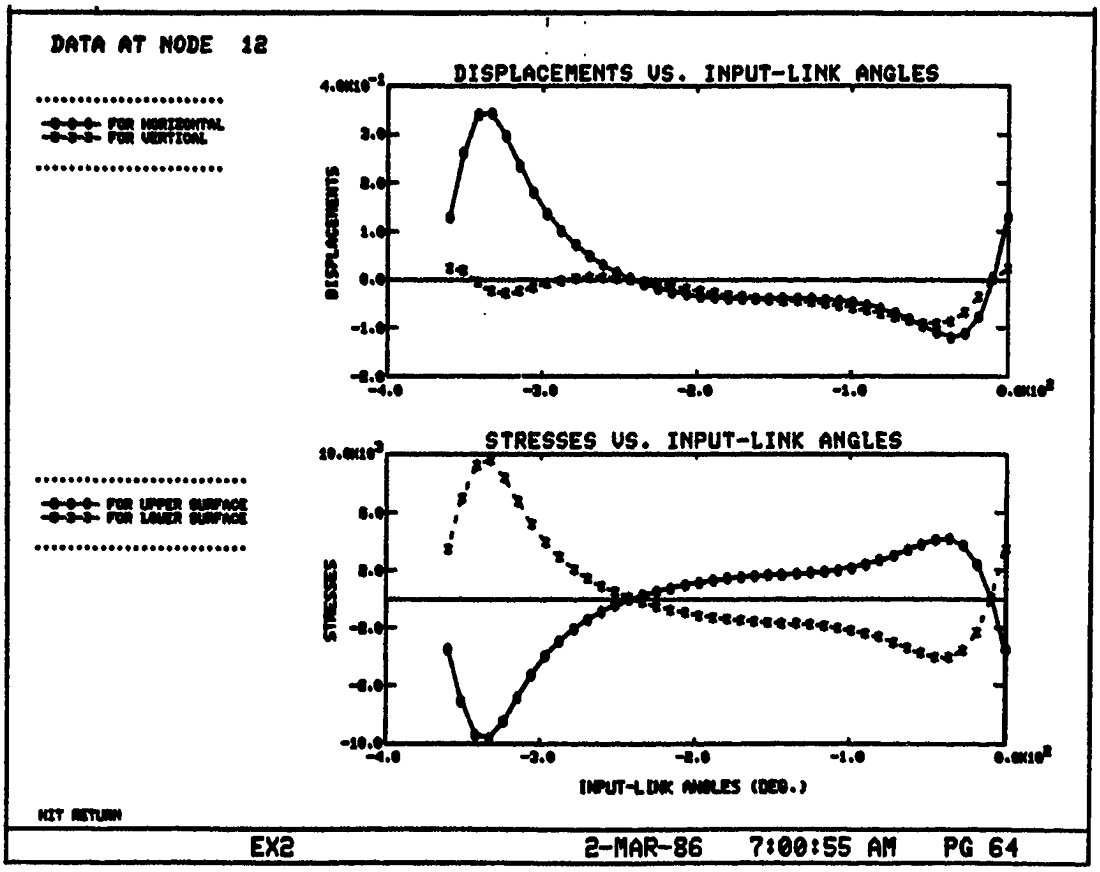
DATA AT NODE 12
DISPLACEMENTS VS. INPUT-LINK ANGLES
FOR HORIZONTAL
FOR VERTICAL
DISPLACEMENTS
STRESSES VS. INPUT-LINK ANGLES
FOR UPPER SURFACE
FOR LOWER SURFACE
STRESSES
INPUT-LINK ANGLES (DEG.)
HIT RETURN
EX2
2-MAR-86 7:00:55 AM PG 64

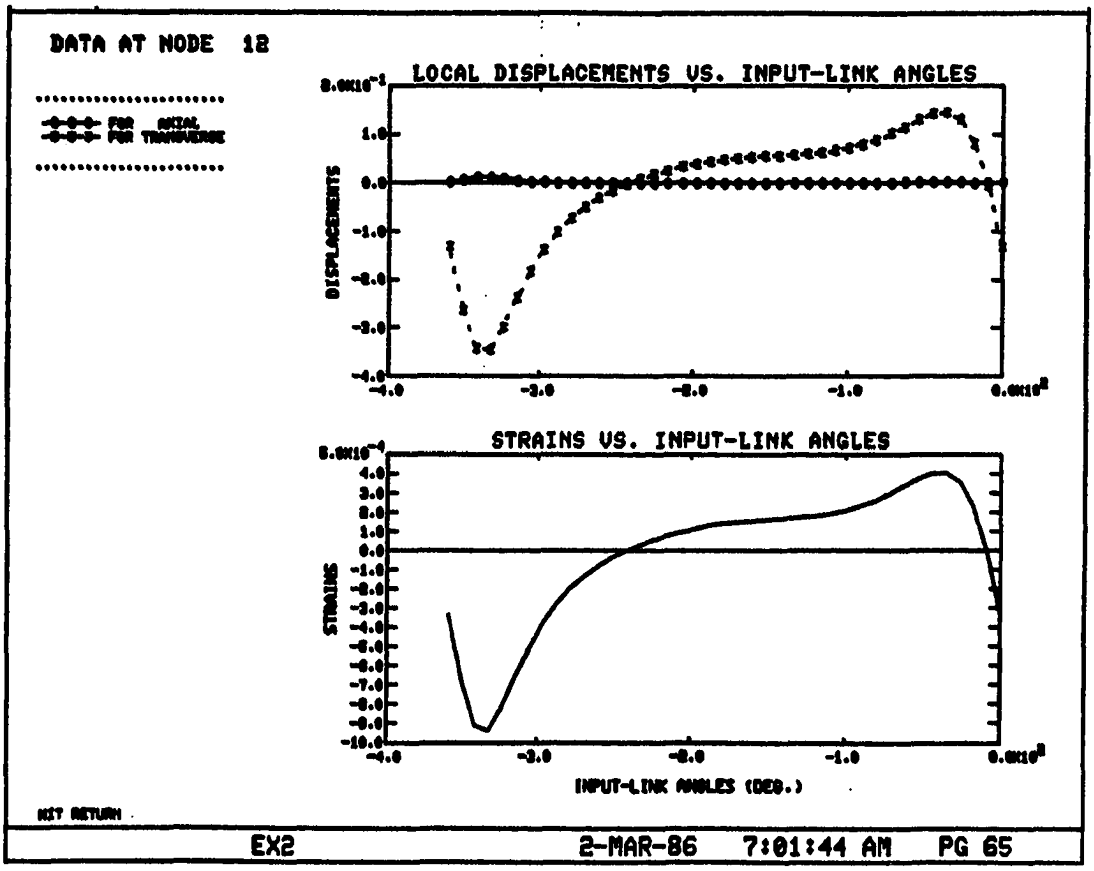
DATA AT NODE 12
LOCAL DISPLACEMENTS VS. INPUT-LINK ANGLES
DISPLACEMENTS
STRAINS VS. INPUT-LINK ANGLES
STRAINS
INPUT-LINK ANGLES (DEG.)
EX2
2-MAR-86 7:01:44 AM PG 65

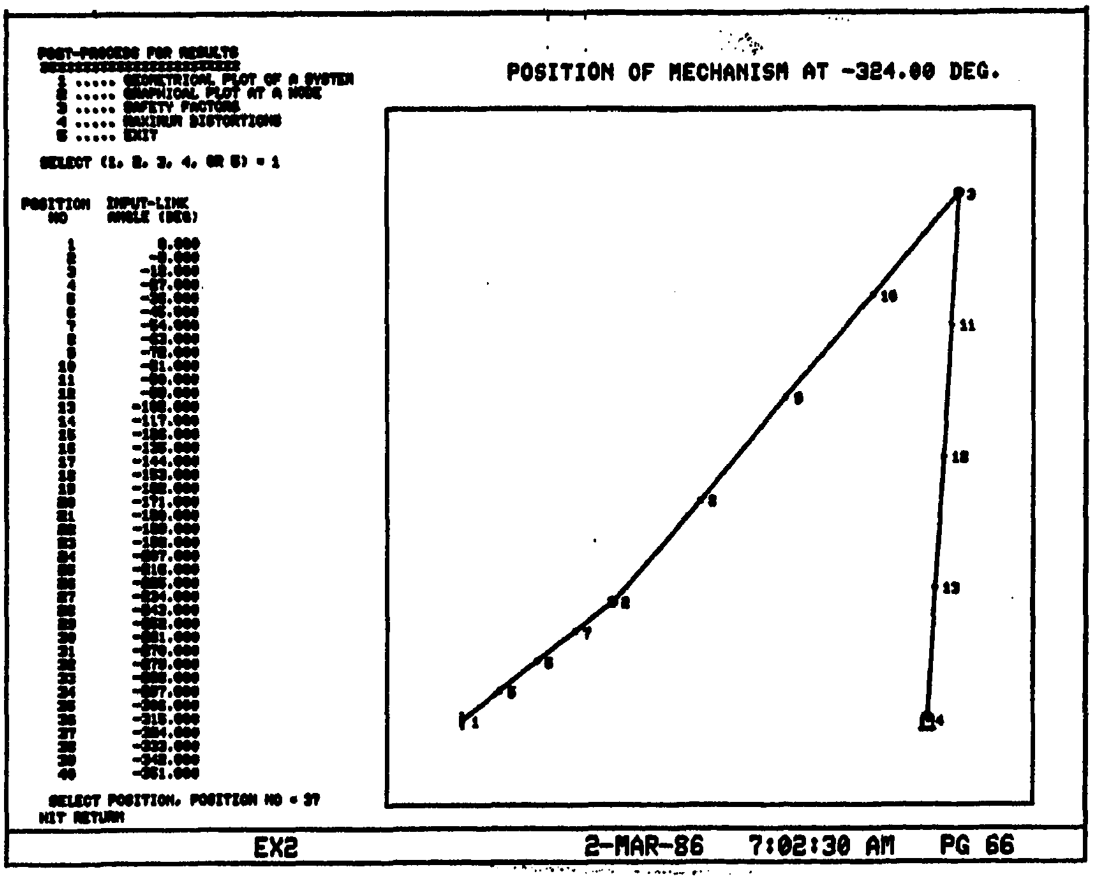
POSITION OF MECHANISM AT -324.00 DEG.
EX2
2-MAR-86 7:02:30 AM PG 66

REACTION FORCES AT SUPPORTS

NODE NO	REACTION FORCES HORZ.	VERT.	TORQUE
1	[illegible]	[illegible]	[illegible]
4	[illegible]	[illegible]	0.000

HIT RETURN :

GEOMETRICAL PLOT
SCALE = 1.0 : 1.

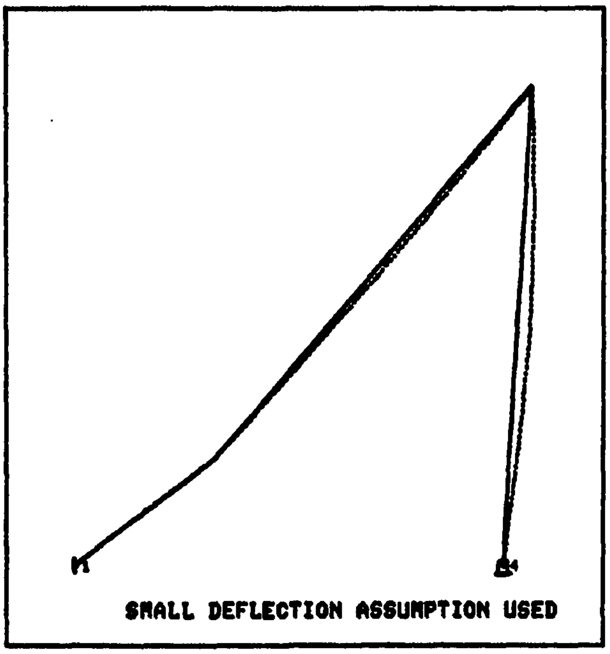

EX2 2-MAR-86 7:03:48 AM PG 67

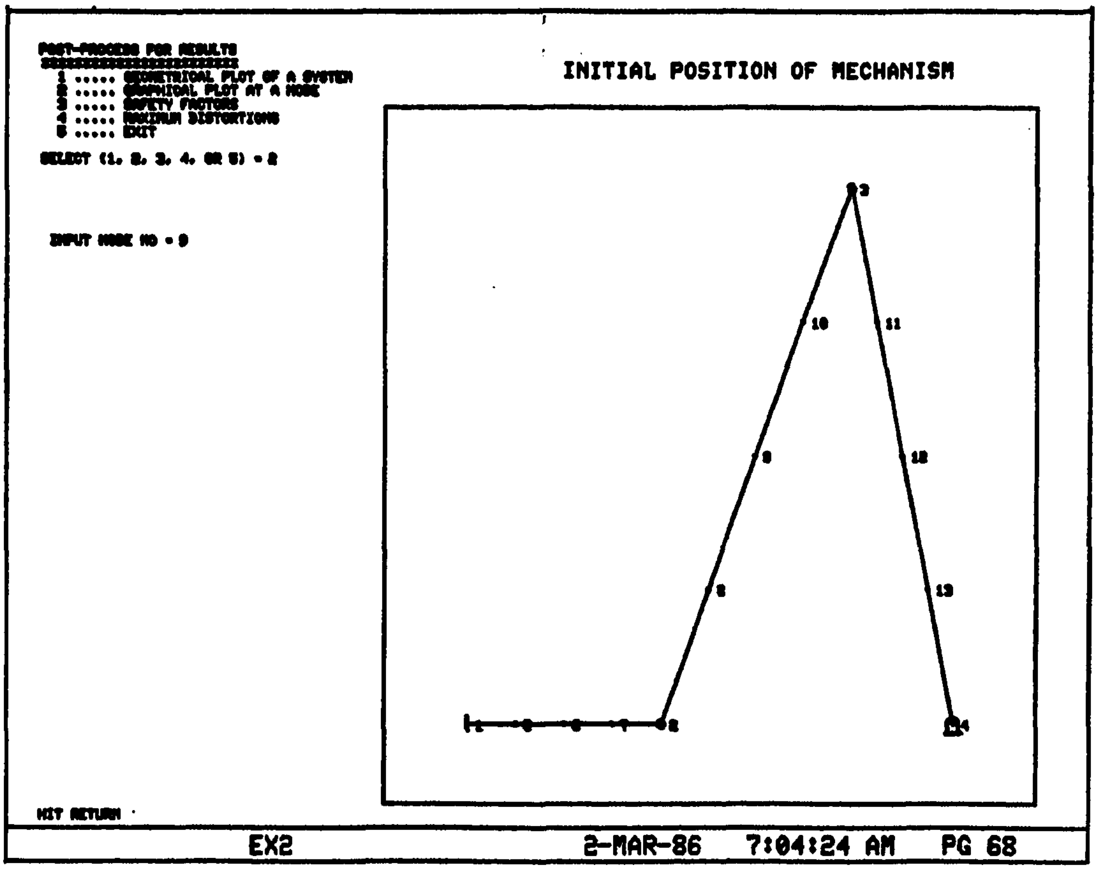
POST-PROCESS FOR RESULTS
1 ...... GEOMETRICAL PLOT OF A SYSTEM
2 ...... GRAPHICAL PLOT AT A NODE
3 ...... SAFETY FACTORS
4 ...... MAXIMUM DISTORTIONS
5 ...... EXIT
SELECT (1, 2, 3, 4, OR 5) = 2
INPUT NODE NO = 9
HIT RETURN
INITIAL POSITION OF MECHANISM
2
10
11
9
12
8
13
1
2
14
EX2
2-MAR-86
7:04:24 AM
PG 68

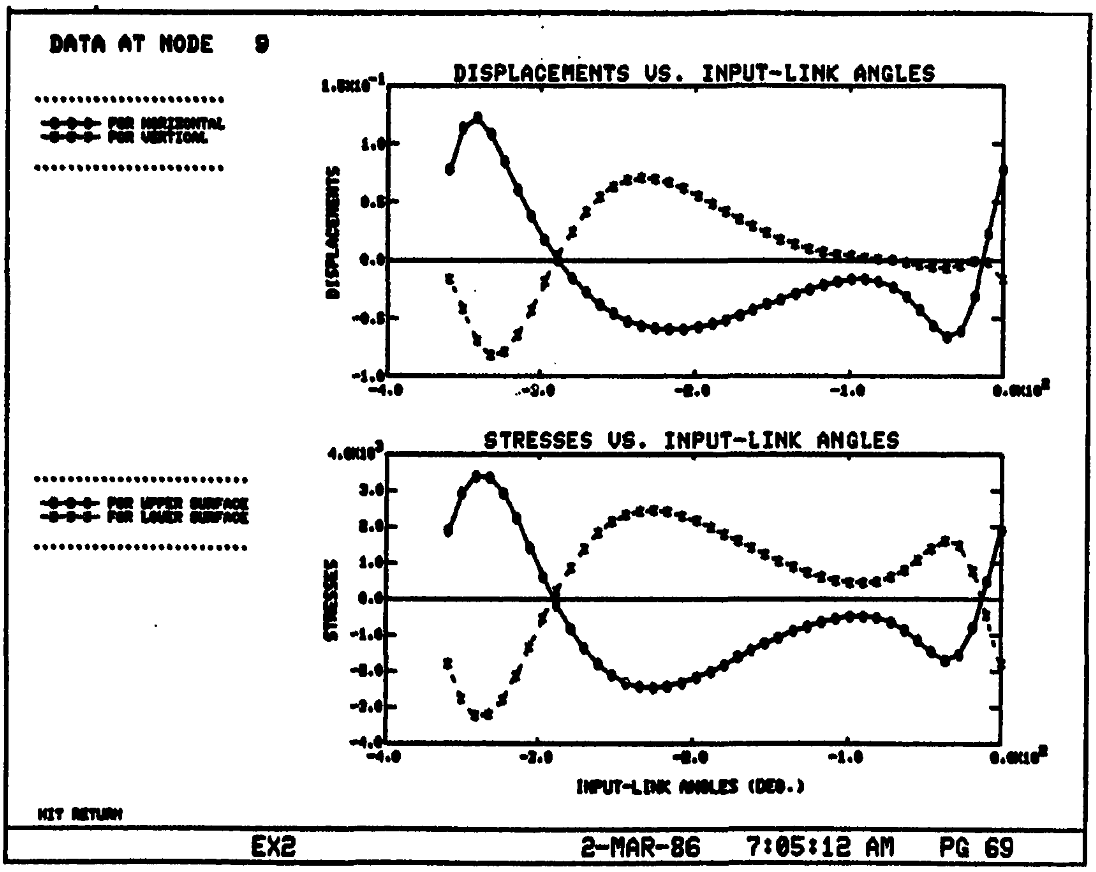
DATA AT NODE 9
DISPLACEMENTS VS. INPUT-LINK ANGLES
DISPLACEMENTS
STRESSES VS. INPUT-LINK ANGLES
STRESSES
INPUT-LINK ANGLES (DEG.)
HIT RETURN
EX2
2-MAR-86 7:05:12 AM PG 69

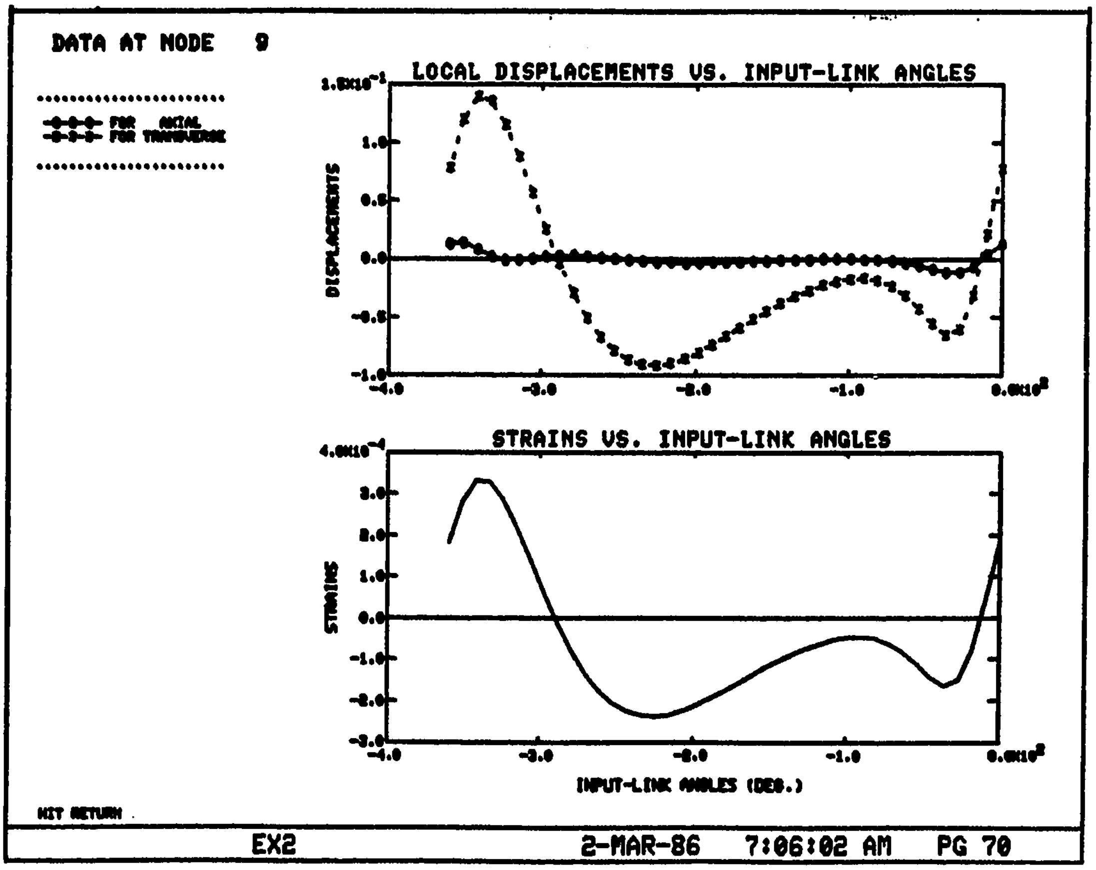
DATA AT NODE 9
FOR AXIAL
FOR TRANSVERSE
LOCAL DISPLACEMENTS VS. INPUT-LINK ANGLES
DISPLACEMENTS
STRAINS VS. INPUT-LINK ANGLES
STRAINS
INPUT-LINK ANGLES (DEG.)
HIT RETURN
EX2
2-MAR-86 7:06:02 AM PG 70

```
POST-PROCESS FOR RESULTS
========================
  1 ...... GEOMETRICAL PLOT OF A SYSTEM
  2 ...... GRAPHICAL PLOT AT A NODE
  3 ...... SAFETY FACTORS
  4 ...... MAXIMUM DISTORTIONS
  5 ...... EXIT

SELECT (1, 2, 3, 4, OR 5) = 5









HIT RETURN
```

EX2 2-MAR-86 7:06:45 AM PG 71

END OF PROGRAM

HIT RETURN

2-MAR-86 7:07:21 AM PG 72

APPENDIX D

THE SOLUTION DETAILS FOR A STEPPED BEAM ON ELASTIC SUPPORTS

```
CASDAM: COMPUTER-AIDED STATIC AND DYNAMIC ANALYSES OF MECHANISMS
CASDAM: COMPUTER-AIDED STATIC AND DYNAMIC ANALYSES OF MECHANISMS

 CCCCC        A        SSSSS    DDD          A        M        M
CC    C      AAA     SS     S   DD    D     AAA       MM      MM
CC          A   A    SS         DD     D   A   A      MMM    MMM
CC         A     A    SSSSS     DD     D  A     A     MM M M MM
CC        AAAAAAAAA       SS    DD     D AAAAAAAAA    MM  M  MM
CC    C   AA     AA  S    SS    DD    D  AA     AA    MM     MM
 CCCCC    AA     AA   SSSSS     DDD      AA     AA    MM     MM

CASDAM: COMPUTER-AIDED STATIC AND DYNAMIC ANALYSES OF MECHANISMS
CASDAM: COMPUTER-AIDED STATIC AND DYNAMIC ANALYSES OF MECHANISMS
```


BY

JOONG-HO SHIM

ACADEMIC ADVISOR : GARY L. KINZEL

ADVISORS: K. J. WALDRON
H. R. BUSBY
N. BERME

DEPT. OF MECHANICAL ENGINNERING

THE OHIO STATE UNIVERSITY, COLUMBUS,OHIO

1985

HIT RETURN

GOCAD - GRAPHICS ORIENTED COMPUTER AIDED DESIGN | CASDAM - STATIC AND DYNAMIC ANALYSES OF FLEXIBLE MECHANISM

WELCOME TO CASDAM
****

CASDAM - COMPUTER AIDED STATIC AND DYNAMIC ANALYSES OF MECHANISMS

THE PROGRAM CASDAM CAN ANALYZE
STATIC/DYNAMIC PROBLEMS UNDER
SMALL/LARGE DEFLECTIONS OF PLNAR
FLEXIBLE MECHANISMS/STRUCTURES

THE PROGRAM CASDAM CONSISTS OF

PRE-PROCESS
MESH GENERATION OF A PLANAR MECHANISM
WITH NODES (UP TO 200) AND LOOPS (UP TO 10)
KINEMATIC POSITION/ACCELERATION ANALYSIS
DATA GENERATION FOR PROCESS

PROCESS
STATIC AND DYNAMIC ANALYSIS FOR THE FLEXIBLE SYSTEM:
DISPLACEMENTS, FORCES, STRESSES, AND SAFETY FACTORS

POST-PROCESS
GEOMETRICAL PLOTS OF DISPLACEMENTS
GRAPHICAL PLOTS OF DISPLACEMENTS AND STRESSES

INPUT PROBLEM TITLE (UP TO 20 CHARACTERS) = EXAMPLE 4

HIT RETURN

DATE- 8-DEC-85 10.48.55 AM PAGE 1

PRE-PROCESS FOR MECHANISM ANALYSIS

```
SELECT INPUT METHOD
-------------------

   [1]..... KEYBOARD
   [2]..... DATA FILE

   SELECT INPUT METHOD = 1

   INPUT METHOD =  1 DATA OK, [Y/N]? Y

INPUT FILE NAME FOR ALL DATA = EX4

   ALL DATA WILL BE GIVEN IN THE FOLLOWING FILES

   ***.DAT = GENERATED DATA FILE FOR ANALYSIS
   ***.ANL = GENERATED DATA FILE FOR POST-PROCESS
   ***.KIN = RESULTS FROM KINEMATIC ANALYSIS
   ***.FLX = RESULTS FROM FLEXIBLE MECHANISM ANALYSIS
   WHERE *** IS THE GIVEN FILE NAME

PROBLEM TYPES ARE
-----------------

   [1]..... MECHANISM AT ONE POSITION
   [2]..... MECHANISM WITH CONTINUOUS POSITIONS

   SELECT PROBLEM TYPE = 1

   PROBLEM TYPE =  1 DATA OK, [Y/N]? Y

ANALYSIS TYPES ARE
------------------

   [1]..... STATIC ANALYSIS
   [2]..... DYNAMIC ANALYSIS

   SELECT ANALYSIS TYPE = 1

   ANALYSIS TYPE =  1 DATA OK, [Y/N]? Y

LINK WEIGHTS ARE
----------------

   [1]..... NO CONSIDERED
   [2]..... CONSIDERED

   SELECT (1 OR 2) = 2

   SELECT TYPE =  2 DATA OK, [Y/N]? Y

HIT RETURN
```

GOCAD - GRAPHICS ORIENTED COMPUTER AIDED DESIGN | CASDAM - STATIC AND DYNAMIC ANALYSES OF FLEXIBLE MECHANISM

MESH GENERATION FOR A MECHANISM

MAKE NODES (UP TO 50) FOR A SYSTEM

- AT EXTERNAL FORCE POINTS
- AT SPRING CONNECTIONS
- AT BRANCH POINTS
- AT JOINTS (REVOLUTES AND SLIDES)

THEN, NODES ARE GENERATED

```
UNITS ARE [1] ..... BRITISH
          [2] ..... SI

SELECT UNIT = 2

UNITS ARE
 $$$$$$$$$$$$$$$$$$$$$$$$$$$$$$
 LENGTH .......... MM
 FORCE ........... N (NEWTON)
 TORQUE (MOMENT).. N-MM
 STRESS .......... MPA
 $$$$$$$$$$$$$$$$$$$$$$$$$$$$$$

FOR THE INITIAL PLOT

  INPUT MIN. AND MAX. IN X-DIRECTION = 0,500

  INPUT MIN. AND MAX. IN Y-DIRECTION = 0,400


HIT RETURN
```

CASE TITLE- EXAMPLE 4 DATE- 2-DEC-85 10.50.31 AM PAGE 3

GOCAD - GRAPHICS ORIENTED COMPUTER AIDED DESIGN | CASDAM - STATIC AND DYNAMIC ANALYSES OF FLEXIBLE MECHANISM

ELEMENTS MUST INPUT IN SERIES
STARTING POINT OF ELEMENT 1 IS SET AS (0,0)

SELECT ELEMENT TYPE = 1

NODE NO AT STARTING POINT = 1
INPUT LENGTH AND ANGLE = 150,0

SELECT ELEMENT TYPE = 1
INPUT NODE NO AT STARTING POINT = 2
STARTING NODE = 2 DATA OK, [Y/N]? Y
INPUT LENGTH AND ANGLE = 100,0

SELECT ELEMENT TYPE = 1
INPUT NODE NO AT STARTING POINT = 3
STARTING NODE = 3 DATA OK, [Y/N]? Y
INPUT LENGTH AND ANGLE = 150,0

SELECT ELEMENT TYPE = 1
INPUT NODE NO AT STARTING POINT = 4
STARTING NODE = 4 DATA OK, [Y/N]? Y
INPUT LENGTH AND ANGLE = 100,0

SELECT ELEMENT TYPE = 3

ELEMENT TYPE ARE

[1]..... BEAM (LINE) ELEMENT
[2]..... TRIANGULAR PLATE ELEMENT
[3]..... $$$ NO MORE ELEMENT
[4]..... $$$ PAGE CHANGE $$$

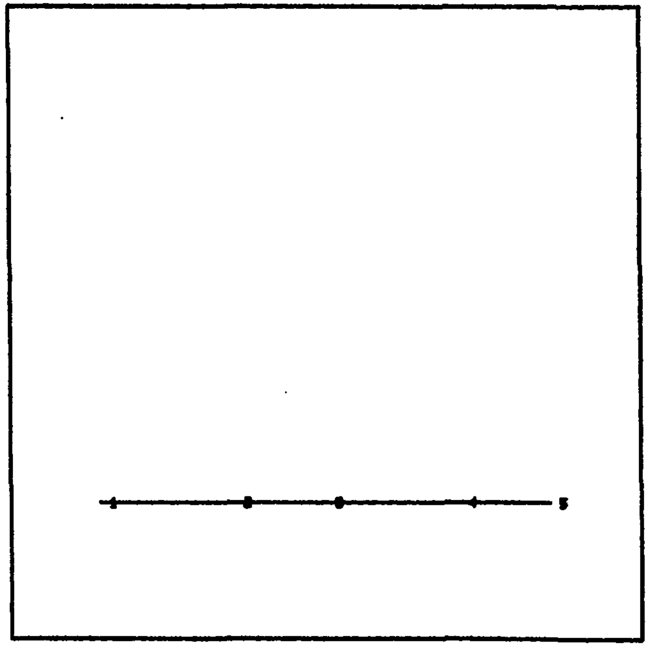

HIT RETURN

CASE TITLE- EXAMPLE 4   DATE- 2 DEC-85   10.5[illegible] AM   PAGE [illegible]

GOCAD - GRAPHICS ORIENTED COMPUTER AIDED DESIGN | CASDAM - STATIC AND DYNAMIC ANALYSES OF FLEXIBLE MECHANISM

PROCESS FOR GENERATION OF ELEMENTS

COMMANDS ARE

[1] ..... GENERATE ELEMENT
[2] ..... *** GENERATE AGAIN FROM ERROR
[3] ..... *** NO MORE ELEMENT
[4] ..... *** CHANGE PAGE

SELECT COMMAND = 1
FOR ELEMENT = 1 INPUT TWO NODES = 1,2

SELECT COMMAND = 1
FOR ELEMENT = 2 INPUT TWO NODES = 2,3

SELECT COMMAND = 1
FOR ELEMENT = 3 INPUT TWO NODES = 3,4

SELECT COMMAND = 1
FOR ELEMENT = 4 INPUT TWO NODES = 4,5

SELECT COMMAND = 3

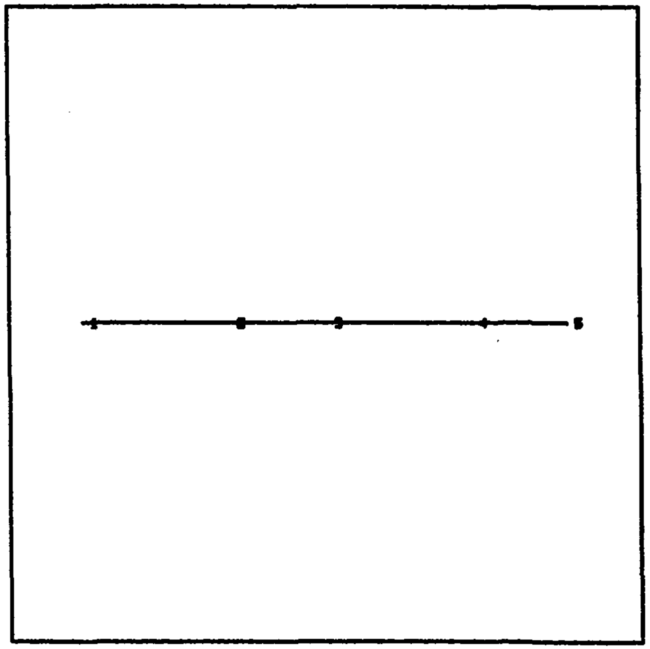

HIT RETURN

CASE TITLE- EXAMPLE 4 DATE- 2-DEC-85 10 52 49 AM PAGE 5

GOCAD - GRAPHICS ORIENTED COMPUTER AIDED DESIGN | CASDAM - STATIC AND DYNAMIC ANALYSES OF FLEXIBLE MECHANISM

PROCESS FOR LINK PROPERTIES

USE SAME MATERIAL FOR ALL LINKS, [Y/N]? Y

MATERIAL TYPES ARE

[1] ..... STEEL
[2] ..... ALUMINUM
[3] ..... USER SPECIFIED

SELECT MATERIAL = 1

INPUT YIELD STRENGTH = 689

USE SAME CROSS-SECTIONS FOR ALL LINKS, [Y/N]? N

HIT RETURN

CASE TITLE- EXAMPLE 4 DATE- 2-DEC-85 10.53.40 AM PAGE 6

GOCAD - GRAPHICS ORIENTED COMPUTER AIDED DESIGN | CASDAM - STATIC AND DYNAMIC ANALYSES OF FLEXIBLE MECHANISM

PROCESS FOR LINK PROPERTIES

FOR A ELEMENT BETWEEN NODES 1 AND 2:

INPUT THICKNESS OF CROSS-SECTION = 5
INPUT HEIGHT OF CROSS-SECTION = 5

FOR A ELEMENT BETWEEN NODES 2 AND 3:

INPUT THICKNESS OF CROSS-SECTION = 5
INPUT HEIGHT OF CROSS-SECTION = 5

FOR A ELEMENT BETWEEN NODES 3 AND 4:

INPUT THICKNESS OF CROSS-SECTION = 2.5
INPUT HEIGHT OF CROSS-SECTION = 2.5

FOR A ELEMENT BETWEEN NODES 4 AND 5:

INPUT THICKNESS OF CROSS-SECTION = 2.5
INPUT HEIGHT OF CROSS-SECTION = 2.5

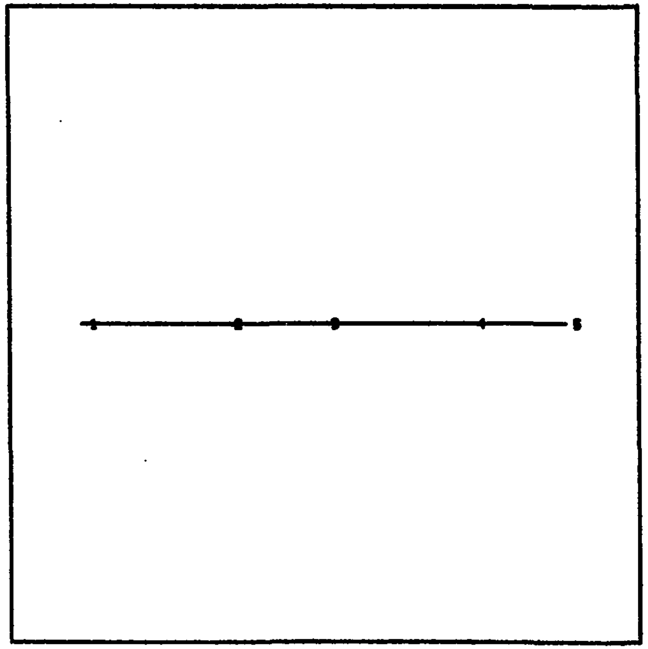

HIT RETURN

CASE TITLE- EXAMPLE 4 DATE- 2-DEC-85 10.54.34 AM PAGE 7

GOCAD - GRAPHICS ORIENTED COMPUTER AIDED DESIGN	CASDAM - STATIC AND DYNAMIC ANALYSES OF FLEXIBLE MECHANISM

PROCESS FOR END TYPES

```
FOR MECHANISM,
--------------
ONLY ONE END MUST BE FIXED FOR DRIVER LINK

 INPUT NODE NO (IF NO MORE END, HIT 0) = 1
  SELECT END TYPE = 1
  DATA OK, [Y/N]? Y

 INPUT NODE NO (IF NO MORE END, HIT 0) = 5
  SELECT END TYPE = 3
  DATA OK, [Y/N]? Y

 INPUT NODE NO (IF NO MORE END, HIT 0) = 0

 $$$$$$$$$$$$$$$$$$$$
 SYSTEM HAS  2 ENDS. DATA OK, [Y/N]? Y
```

```
END TYPES ARE
-------------
------------------------------
[1]..... PIN END (BUSHING)
[2]..... FIXED END
[3]..... FREE END
[4]..... SLIDE END
[5]..... SIMPLE SUPPORT
------------------------------
```

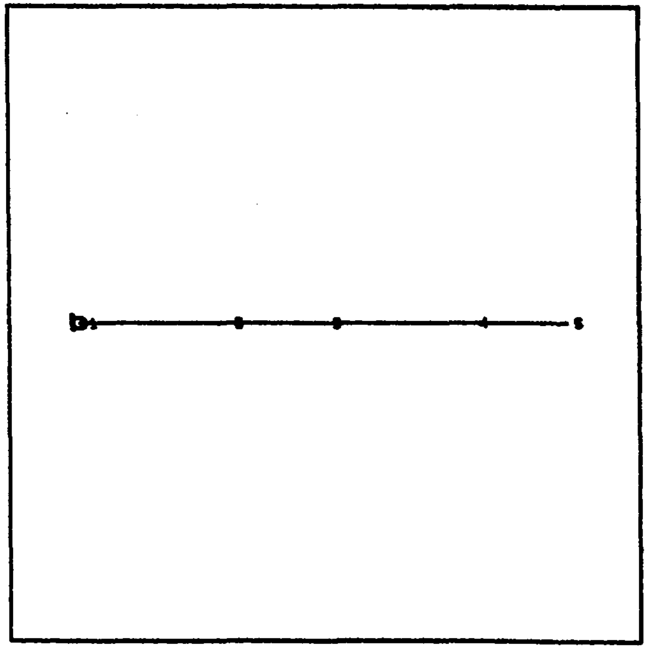

HIT RETURN

CASE TITLE- EXAMPLE 4   DATE- 2-DEC-85   10 55.[illegible] AM   PAGE 8

```
GOCAD - GRAPHICS ORIENTED COMPUTER AIDED DESIGN | CASDAM - STATIC AND DYNAMIC ANALYSES OF FLEXIBLE MECHANISM

PROCESS FOR EXTERNAL AND SPRING FORCES                  NODE TYPES ARE
-----------------------------------------               --------------
                                                        ------------------------------------
                                                        [1]..... NODE FOR EXTERNAL FORCES
                                                        [2]..... NODE FOR SPRING CONNECTION
                                                        [3]..... *** NO MORE NODE
                                                        [4]..... *** PAGE CHANGE ***
                                                        ------------------------------------
 SELECT NODE TYPE = 1

 INPUT NODE NO = 5

  NODE = 5      DATA OK, [Y/N]? Y

 FORCES GIVEN BY
  [1] ..... DIRECTIONAL FORCES
  [2] ..... VECTORIAL FORCES
  SELECT 1 OR 2 = 1

  INPUT FORCE IN HORIZONTAL DIRECTION = 0
  INPUT FORCE IN VERTICAL DIRECTION   = -15
  INPUT MOMENT                        = 0

 SELECT NODE TYPE = 2

 INPUT NODE NO = 2

  NODE = 2      DATA OK, [Y/N]? Y

 CONNECT TO GROUND [1] OR WITH NODE [2] = 1

  INPUT STIFFNESS OF SPRING = 2
  INPUT LENGTH AND ANGLE TO SPRING END = 200,90

  SPRING END IS FIXED [1] OR SLIDING [2] = 2
  TO DETERMINE SLIDING AXIS,
  INPUT NODE NO GIVEN AXIS,  NODE NO = 1
  INPUT FREE LENGTH OF SPRING = 200

 SELECT NODE TYPE = 2

 INPUT NODE NO = 4

  NODE = 4      DATA OK, [Y/N]? Y

 CONNECT TO GROUND [1] OR WITH NODE [2] = 1

  INPUT STIFFNESS OF SPRING = 2
  INPUT LENGTH AND ANGLE TO SPRING END = 400,90

  SPRING END IS FIXED [1] OR SLIDING [2] = 2
  TO DETERMINE SLIDING AXIS,
  INPUT NODE NO GIVEN AXIS,  NODE NO = 3
  INPUT FREE LENGTH OF SPRING = 400

 SELECT NODE TYPE = 3


 HIT RETURN

      EXAMPLE 4                          DATE- 2-DEC-85    11.10.24 AM      PAGE  9
```

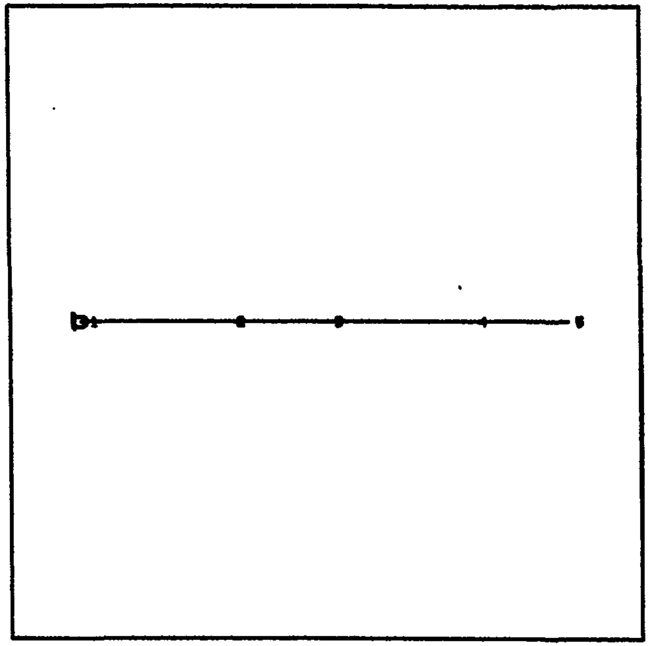

GOCAD - GRAPHICS ORIENTED COMPUTER AIDED DESIGN

CASDAM - STATIC AND DYNAMIC ANALYSES OF FLEXIBLE MECHANISM

```
FOR MAIN LOOP
  INPUT STARTING NODE NO IN DRIVER LINK
        TO END NODE NO IN FOLLOWER LINK

  NO OF TOTAL NODES IN MAIN LOOP = 5
  INPUT NODE NO (TOTAL  5 NODES) = 1,2,3,4,5
  DATA OK, [Y/N]? Y
```

THERE ARE 1 LOOPS IN THE SYSTEM.

INPUT NODE NO FROM THE STARTING POINT
TO END POINT IN EACH LOOP

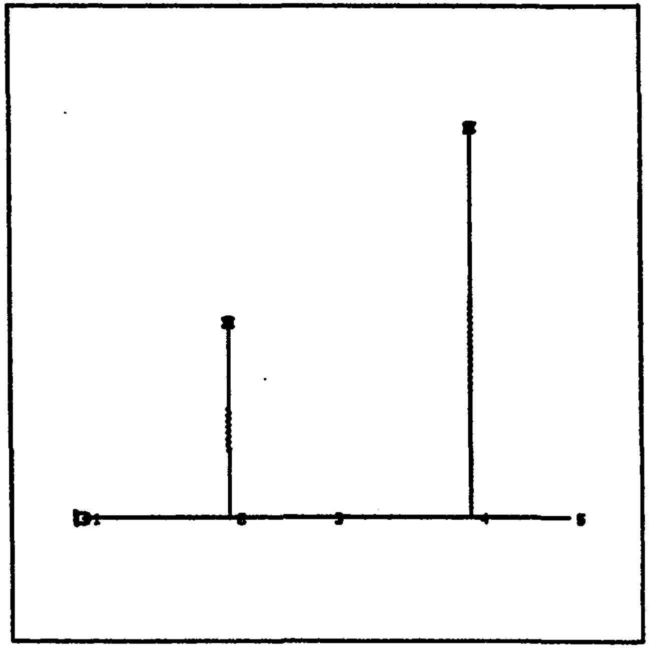

HIT RETURN

CASE TITLE- EXAMPLE 4 | DATE- 2-DEC-85 10.58.55 AM | PAGE 10

GOCAD - GRAPHICS ORIENTED COMPUTER AIDED DESIGN | CASDAM - STATIC AND DYNAMIC ANALYSES OF FLEXIBLE MECHANISM

PROCESS FOR CONNECTIVITY

MAIN LOOP

FOR REVOLUTE JOINT

INPUT NODE NO (IF NO MORE, HIT 0) = 0

NODE GENERATION

FOR SECTION BETWEEN NODES 1 AND 2
INPUT NO OF INSIDE NODES = 5

FOR SECTION BETWEEN NODES 2 AND 3
INPUT NO OF INSIDE NODES = 3

FOR SECTION BETWEEN NODES 3 AND 4
INPUT NO OF INSIDE NODES = 5

FOR SECTION BETWEEN NODES 4 AND 5
INPUT NO OF INSIDE NODES = 3

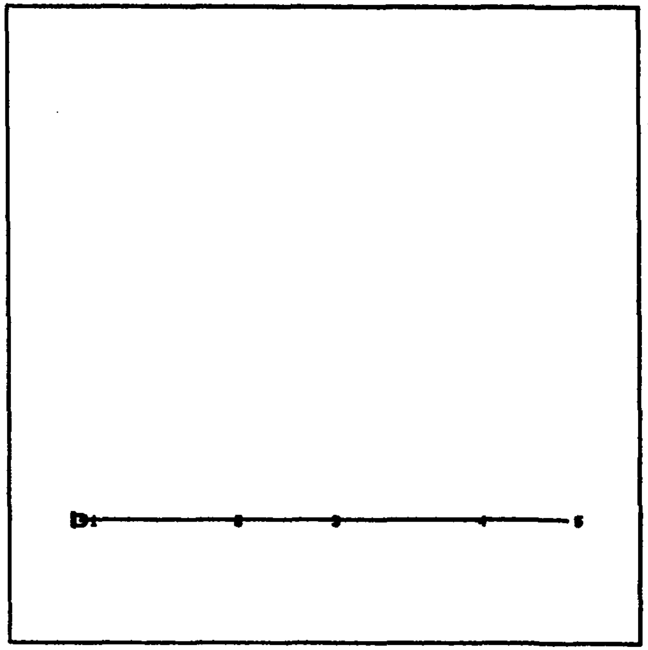

HIT RETURN

CASE TITLE- EXAMPLE 4 DATE- 2-DEC-85 10.59.48 AM PAGE 11

GOCAD - GRAPHICS ORIENTED COMPUTER AIDED DESIGN | CASDAM - STATIC AND DYNAMIC ANALYSES OF FLEXIBLE MECHANISM

PROCESS FOR SYSTEM LOOPING

BELL SIGNALS PROCESS COMPLETE

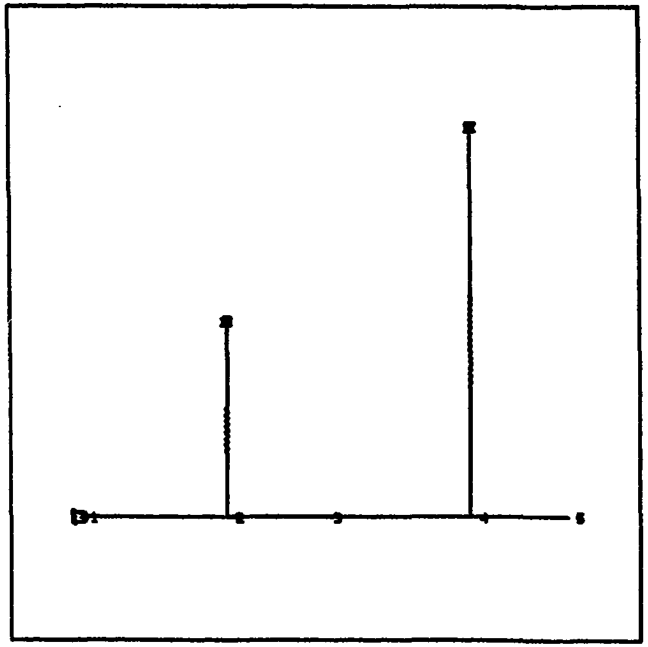

HIT RETURN

CASE TITLE- EXAMPLE 4 DATE- [illegible] [illegible] PAGE [illegible]

GOCAD - GRAPHICS ORIENTED COMPUTER AIDED DESIGN | CASDAM - STATIC AND DYNAMIC ANALYSES OF FLEXIBLE MECHANISM

PROCESS FOR MECHANISM ANALYSIS

ANALYSIS HAS BEGUN

BELL SIGNALS ANALYSIS COMPLETED

INITIAL POSITION OF MECHANISM

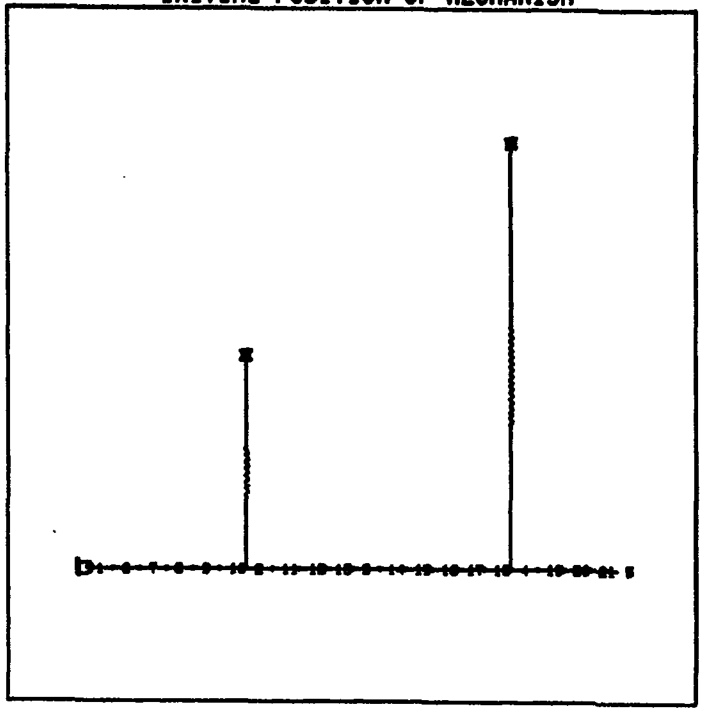

HIT RETURN

CASE TITLE- EXAMPLE 4 DATE- 2-DEC-85 11 01.45 AM PAGE 13

GOCAD - GRAPHICS ORIENTED COMPUTER AIDED DESIGN | CASDAM - STATIC AND DYNAMIC ANALYSES OF FLEXIBLE MECHANISM

POST-PROCESS OF ANALYSES

WANT OUTPUT FILE (XXX.FLX), (Y/N)? Y

DATA PROCESSING

BELLS SIGNALS PROCESS COMPLETED

INITIAL POSITION OF MECHANISM

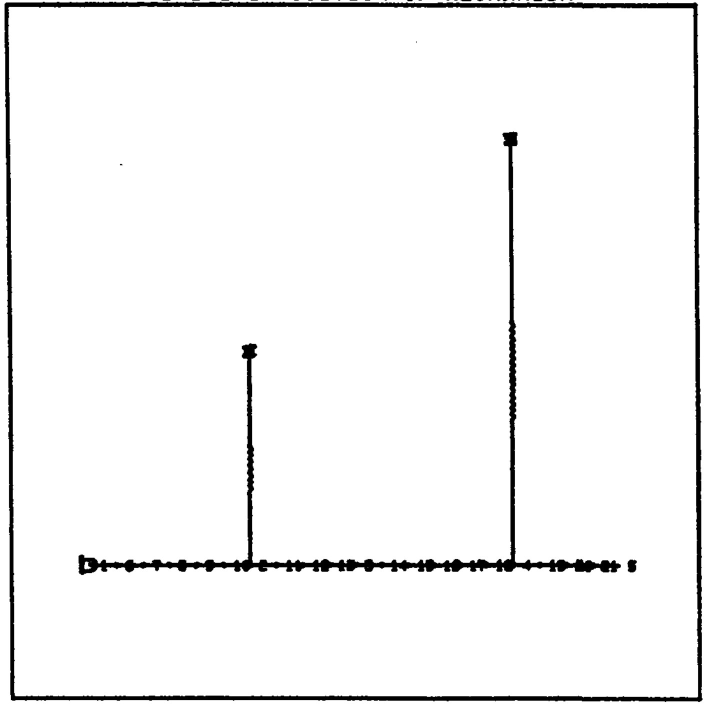

HIT RETURN

CASE TITLE- EXAMPLE 4   DATE- 2-DEC-95   11.02.12 AM   PAGE 14

GOCAD - GRAPHICS ORIENTED COMPUTER AIDED DESIGN | [illegible] - STATIC AND DYNAMIC ANALYSIS OF FLEXIBLE MECHANISM

REACTION FORCES AT SUPPORTS

NODE NO	REACTION FORCES HORZ.	REACTION FORCES VERT.	TORQUE
1	0.000	-0.004	0.000
5	0.000	0.000	0.000

GEOMETRICAL PLOT
SCALE = 1.0 : 1.

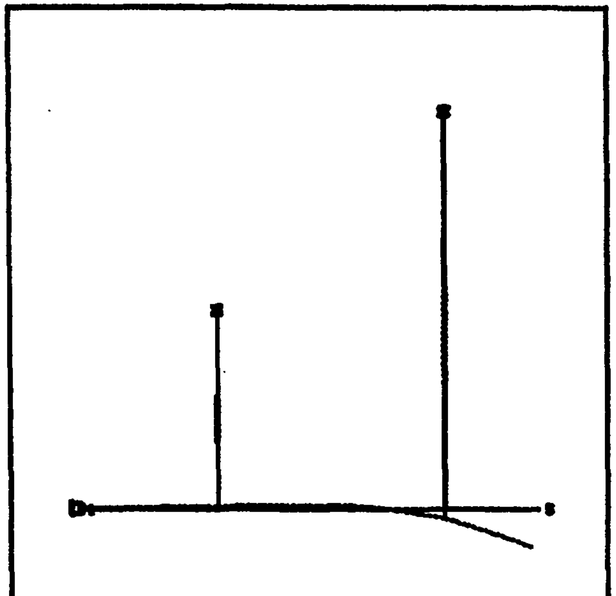

LARGE DEFLECTION ASSUMPTION USED

HIT RETURN

GOCAD - GRAPHICS ORIENTED COMPUTER AIDED DESIGN | DASSAM - STATIC AND DYNAMIC ANALYSES OF FLEXIBLE MECHANISM

RESULTS OF STRESS ANALYSES

NODE NO	SAFETY FACTOR	NODE NO	SAFETY FACTOR	NODE NO	SAFETY FACTOR	NODE NO	SAFETY FACTOR
1	---	7	[illegible]	13	[illegible]	19	[illegible]
2	[illegible]	8	[illegible]	14	[illegible]	20	[illegible]
3	[illegible]	9	[illegible]	15	[illegible]	21	[illegible]
4	0.125E+01	10	0.154E+03	16	0.172E+01		
5	---	11	[illegible]	17	[illegible]		
6	[illegible]	12	[illegible]	18	0.137E+01		

LOCATIONS OF CRITICAL POINT(S)

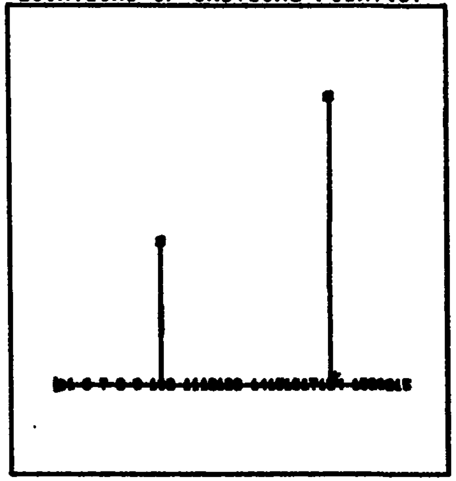

****
SAFETY FACTOR OF SYSTEM
....

0.125E+01 AT NODE 4
****

--- FOR ZERO STRESSES OR RIGID LINK

HIT RETURN

GOCAD - GRAPHICS ORIENTED COMPUTER AIDED DESIGN	CASDAM - STATIC AND DYNAMIC ANALYSES OF FLEXIBLE MECHANISM

END OF PROGRAM

HIT RETURN

DATE- 2-DEC-85 11.06.39 AM PAGE 17

APPENDIX E

OVERVIEW OF THE COMPUTER PROGRAM CASDAM

E.1 General Description

The program CASDAM is a graphics-oriented, interactive, computer-aided, static and dynamic analyses of flexible mechanisms and structures incorporated with the proposed iterative transfer-matrix method, and intended for use with a graphics terminal such as the Tektronix 4014. The program is developed on a Digital Equipment Corporation VAX 11/750 minicomputer installed in Advance Design Method Laboratory, Dept. of Mechanical Engineering, The Ohio State University. There has been considerable effort made in trying to develop the program so that the program has minimal amounts of machine dependency. The program language used is 1977 ANSI FORTRAN IV.

Section E.2 gives the subroutine descriptions briefly. Section E.3 presents the tree structure for the program, the storage requirements for the routines, and the the image synopsis of the program CASDAM on a VAX 11/750 system.

E.2 Description of Routines

This section contains the subroutine descriptions.

1. MAIN PROGRAM CASDAM - initiates and prompts the user for the information needed to analyze the flexible mechanisms and structures.

2. SUBROUTINE AFLEX - controls the analysis process and solution convergence.

3. SUBROUTINE AGAIN - solves the state vector for flexible system.

4. SUBROUTINE ANALYS - calculates the unknown variables from the system matrix equation.

5. SUBROUTINE ARIGID - solves the state vector for rigid system.

6. SUBROUTINE CALSF1 - calculates stresses and safety factors at nodes for a system at one position.

7. SUBROUTINE CALSF2 - calculates stresses and safety factors at nodes for a system in continuous motions.

8. SUBROUTINE CALSLD - calculates the state vector when a starting point in a subloop is slider.

9. SUBROUTINE CALSVE - calculates the state vector at a branch point.

10. SUBROUTINE CALSVS - calculates the state vector at supports.

11. SUBROUTINE COMPRS - determines the field matrix when compressive axial force is loaded in a element.

12. SUBROUTINE CONNEC - checks the connectivity at joints.

13. SUBROUTINE DATINT - prompts for preprocessing the program.

14. SUBROUTINE DATGEN - generates data for processing.

15. SUBROUTINE DFLEX - draws a deflected system.

16. SUBROUTINE DISPL1 - calculates distortions at nodes for a system at one position.

17. SUBROUTINE DISPL2 - calculates distortions at nodes for a system in continuous motions.

18. SUBROUTINE DOTTED - draws a dotted line.

19. SUBROUTINE DRANGE - determines range of screen window for drawing a deflected system.

20. SUBROUTINE DRAWLP - draws each loop of a system.

21. SUBROUTINE DRWALL - draws an original structure.

22. SUBROUTINE DRWBOX - draws a square for a screen window.

23. SUBROUTINE DRWDIS - draws a system and writes maximum distortions at nodes.

24. SUBROUTINE DRWDOT - draws an original system with dotted lines.

25. SUBROUTINE DRWEND - draws a support.

26. SUBROUTINE DRWINP - draws a generated system.

27. SUBROUTINE DRWORI - draws a undeflected system.

28. SUBROUTINE DRWREV - draws a revolute joint.

29. SUBROUTINE DRWSLD - draws a sliding joint.

30. SUBROUTINE DRWSF - draws a system and writes safety factors at nodes.

31. SUBROUTINE DRWSPR - draws a spring.

32. SUBROUTINE DRWSYS - draws a generated system.

33. SUBROUTINE DZERO - sets the initial values be zero for a generated system.

34. SUBROUTINE FINDPT - finds mass center and calculates total volume of a plate.

35. SUBROUTINE FLXSIS - prompts for analysis of a flexible system.

36. SUBROUTINE FORSPR - prompts for external forces and conditions of springs.

37. SUBROUTINE GENALL - sorts input data and generates data.

38. SUBROUTINE GENSEC - generates elements of an original system.

39. SUBROUTINE GETFIX - determines the three simultaneous equations for a system with a fixed end.

40. SUBROUTINE GETFRE - determines the three simultaneous equations for a system with a free end.

41. SUBROUTINE GETPIN - determines the three simultaneous equations for a system with a pinned end.

42. SUBROUTINE GETSIM - determines the three simultaneous equations for a system with a simple support.

43. SUBROUTINE GETSLD - determines the three simultaneous equations for a system with a sliding end.

44. SUBROUTINE HELLO - writes the message for the general information and description of the program CASDAM..

45. SUBROUTINE INVERS - inverses a matrix.

46. SUBROUTINE JOINTS - calculates the transfer matrix to be satisfied the joint conditions

47. SUBROUTINE KINAN1 - analyzes the 1st type of kinematic component.

48. SUBROUTINE KINAN2 - analyzes the 2nd type of kinematic component.

49. SUBROUTINE KINAN3 - analyzes the 3rd type of kinematic component.

50. SUBROUTINE KINAN4 - analyzes the 4th type of kinematic component.

51. SUBROUTINE KINAN5 - analyzes the 5th type of kinematic component.

52. SUBROUTINE KINAN6 - analyzes the 6th type of kinematic component.

53. SUBROUTINE KINAN7 - analyzes the 7th type of kinematic component.

54. SUBROUTINE KINAN8 - analyzes the 8th type of kinematic component.

55. SUBROUTINE KINANS - controls subroutines for kinematic analyses.

56. SUBROUTINE KINDR1 - draws the first type of kinematic component.

57. SUBROUTINE KINDR2 - draws the 2nd type of kinematic component.

58. SUBROUTINE KINDR3 - draws the 3rd type of kinematic component.

59. SUBROUTINE KINDR4 - draws the 4th type of kinematic component.

60. SUBROUTINE KINDR5 - draws the 5th type of kinematic component.

61. SUBROUTINE KINDR6 - draws the 6th type of kinematic component.

62. SUBROUTINE KINDR7 - draws the 7th type of kinematic component.

63. SUBROUTINE KINDR8 - draws the 8th type of kinematic component.

64. SUBROUTINE KINDRW - controls subroutines to draw the corresponding component when user indicates.

65. SUBROUTINE KININP - prompts for the input of the rotating speed of an input-link of a mechanism.

66. SUBROUTINE KINONE - draws a component from menu.

67. SUBROUTINE KINSIS - prompts for the kinematic analysis.

68. SUBROUTINE KINSYS - draws a system in the continuous motions.

69. SUBROUTINE KZERO - sets the initial values for kinematic analysis be zero.

70. SUBROUTINE LEAREQ - solves the linear simultaneous equations.

71. SUBROUTINE LIMANG - sets an angle within -180 to 180 degrees.

72. SUBROUTINE LINDOT - draws a dotted line.

73. SUBROUTINE LINSLD - draws a solid line.

74. SUBROUTINE LOOPS - determines a main loop and subloops from a system.

75. SUBROUTINE LOOPSS - checks each loop for 1 DOF system.

76. SUBROUTINE MBRAN - calculates a branch matrix.

77. SUBROUTINE MFIELD - calculates a field matrix for a flexible link.

78. SUBROUTINE MMASS - calculates a mass matrix.

79. SUBROUTINE MPOINT - calculates a point matrix.

80. SUBROUTINE MRIGID - calculates a filed matrix for a rigid link.

81. SUBROUTINE MSPRNG - calculates a spring matrix.

82. SUBROUTINE MTRANS - calculates a transformation matrix.

83. SUBROUTINE MULT74 - multiplies two matrices.

84. SUBROUTINE PLATES - calculates data for a plate element.

85. SUBROUTINE PROP1 - determines the material and geometrical properties of a link.

86. SUBROUTINE RANGEL - determines range of screen window for drawing a initial system.

87. SUBROUTINE RANGES - determines range of screen window for drawing a system in kinematic motions.

88. SUBROUTINE READIN - reads all generated data from a file.

89. SUBROUTINE RESULT - controls subroutines to calculate distortions and safety factors at nodes.

90. SUBROUTINE SECMAT - prompts for information of the properties of links.

91. SUBROUTINE SETC - sets a transfer matrix to be stored.

92. SUBROUTINE SETING - sets all state vectors determined at the previous iteration.

93. SUBROUTINE SETPNT - marks a symbol on the corresponding point.

94. SUBROUTINE SETPOS - sets position to write on screen.

95. SUBROUTINE SETWIN - sets a screen window.

96. SUBROUTINE SLIDE - calculates the corresponding state variables to a sliding end.

97. SUBROUTINE SORTS - prompts for the postprocess.

98. SUBROUTINE STARTS - calculates the initial transfer matrix from the given support conditions.

99. SUBROUTINE STATE - calculates state vectors for a rigid system.

100. SUBROUTINE STRSIS - prompts for the stress analysis.

101. SUBROUTINE SUBLP1 - generates data for an initial subloop system.

102. SUBROUTINE SUBLP2 - generates data for a double subloop system.

103. SUBROUTINE SUBLP3 - generates data for a triple subloop system.

104. SUBROUTINE SUBLP4 - generates data for a fourth subloop system.

105. SUBROUTINE SUBLP5 - generates data for a fifth subloop system.

106. SUBROUTINE SUBLP6 - generates data for a sixth subloop system.

107. SUBROUTINE TENSON - calculates field matrix when a tensile force is loaded in a link.

108. SUBROUTINE TYLOOP - generates data for the main loop system.

109. SUBROUTINE TYPEND - prompts for the end types.

110. SUBROUTINE TYPSYS - prompts for the types of analyses.

111. SUBROUTINE RESETC - resets the matrix equation.

112. SUBROUTINE RFIELD - controls subroutines to calculate a field matrix.

113. SUBROUTINE RSTATE - calculates state vectors at nodes for a flexible system.

114. SUBROUTINE WASSUM - writes the message for assumption used in the analysis.

115. SUBROUTINE WBEND - writes the generated data for a support in a subloop.

116. SUBROUTINE WBRAN - writes the generated data for a branch point.

117. SUBROUTINE WFHEAD - writes a title in a output file.

118. SUBROUTINE WFIELD - writes the generated data for a link.

119. SUBROUTINE WINABS - sets a screen window.

120. SUBROUTINE WMEND - writes the generated data for an end point in the main loop.

121. SUBROUTINE WMID - writes the generated data for an external forces.

122. SUBROUTINE WREACT - writes reaction forces on the screen.

123. SUBROUTINE WREV - writes the generated data for a revolute joint.

124. SUBROUTINE WRTABS - transforms results in the local coordinate system to those in the global coordinate system and writes them in a file for postprocessing.

125. SUBROUTINE WRTANL - writes title in a data file.

126. SUBROUTINE WRTDAT - regenerates all generated data for processing.

127. SUBROUTINE WRTFLX - writes results of displacements and stresses at nodes in an output file.

128. SUBROUTINE WRTPRO - writes title for displacements and internal forces at nodes.

129. SUBROUTINE WRTSCR - writes data on the screen.

130. SUBROUTINE WSPR - writes the generated data for a spring.

131. SUBROUTINE WSLIDE - writes the generated data for a sliding joint.

132. SUBROUTINE WSTART - writes the generated data for a starting support.

133. SUBROUTINE ZERO - sets initial values of the input system using in preprocessing.

E.3 Tree Structures of Routines

The tree structure for the program CASDAM is listed in two ways. First, all subroutines which call a given subroutine are listed in Table E.1, and then all of the subroutines called by a given subroutine are given in Table E.2. The routines are designated as either the main program (M), a subroutine in CASDAM (G), or a PLTPAK subroutine (P). The PLTPAK subroutines are the general graphics subroutines.

Table E.3 lists the storage requirements for the progeam CASDAM, and Table E.4 gives the storage requirements for the PLTPAK subroutines and the PLOT10 graphics routines. Table E.5 presents an image synopsis of the program CASDAM on a VAX 11/750 system.

TABLE E.1 CROSS REFERENCE BY CALLING ROUTINES

Routine	Type	Called by ...	
AFLEX	G	FLXSIS	
AGAIN	G	AFLEX	
ANALYS	G	AGAIN	ARIGID
ARIGID	G	AFLEX	
CALSF1	G	STRSIS	
CALSF2	G	STRSIS	

Notes on type of routine

M : Main program
G : GOCAD subroutine
P : PLTPAK subroutine

TABLE E.1 CROSS REFERENCE BY CALLING ROUTINES (CONTINUED)

Routine	Type	Called by ...
CALSLD	G	RSTATE STATE
CALSVE	G	RSTATE STATE
CALSVS	G	RSTATE STATE
CASDAM	M	
COMPRS	G	RFIELD
CONNEC	G	LOOPS
DATGEN	G	CASDAM
DATINT	G	DATGEN
DFLEX	G	DISPL1 SORTS
DISPL1	G	SORTS
DISPL2	G	SORTS
DOTTED	G	KINDR1 KINDR2 KINDR3 KINDR4 KINDR5 KINDR6 KINDR7 KINDR8
DRANGE	G	DFLEX DRWALL
DRAWLP	G	LOOPS
DRWALL	G	DRWDIS DRWINP DRWORI DRWSF FLXSIS
DRWBOX	G	DATINT DFLEX DRAWLP DRWALL DRWDOT DRWSYS
DRWDIS	G	SORTS
DRWDOT	G	GENSEC KINSIS LOOPS
DRWEND	G	DFLEX DRAWLP DRWALL DRWDOT DRWSYS KINSYS TYPEND

Notes on type of routine

M : Main program
G : GOCAD subroutine
P : PLTPAK subroutine

TABLE E.1 CROSS REFERENCE BY CALLING ROUTINES (CONTINUED)

Routine	Type	Called by ...
DRWINP	G	DISPL1
DRWORI	G	RESULT SORTS
DRWREV	G	DRWALL DRWDOT DRWSYS KINSYS LOOPS
DRWSF	G	SORTS
DRWSLD	G	DRWALL DRWDOT DRWSYS KINSYS LOOPS
DRWSPR	G	DFLEX DRWALL DRWDOT DRWSYS KINSYS
DRWSYS	G	CONNEC FORSPR GENALL SECMAT TYPEND
DZERO	G	READIN
FINDPT	G	DATINT
FLXSIS	G	CASDAM
FORSPR	G	DATGEN
GENALL	G	DATGEN
GENSEC	G	DATINT
GETFIX	G	ANALYS
GETFRE	G	ANALYS
GETPIN	G	ANALYS
GETSIM	G	ANALYS
GETSLD	G	ANALYS
HELLO	G	CASDAM

Notes on type of routine

M : Main program
G : GOCAD subroutine
P : PLTPAK subroutine

TABLE E.1 CROSS REFERENCE BY CALLING ROUTINES (CONTINUED)

Routine	Type	Called by ...
INVERS	G	MBRAN
JOINTS	G	AGAIN ARIGID
KBUSH	P	DRWEND DRWSPR KINDR1 KINDR2 KINDR3 KINDR5 KINDR6 KINDR7 KINDR8
KDING	P	AFLEX FLXSIS GENALL HELLO KINSIS RESULT
KDRWAB	P	DRWSLD DRWSPR KINDR1 KINDR2 KINDR3 KINDR4 KINDR5 KINDR6 KINDR7 KINDR8 LINSLD
KDRWRL	P	DOTTED DRWSPR KINDR5 KINDR6 KINDR7 KINDR8 LINDOT
KGRAPH	P	DISPL2
KINAN1	G	KINANS
KINAN2	G	KINANS
KINAN3	G	KINANS
KINAN4	G	KINANS
KINAN5	G	KINANS
KINAN6	G	KINANS
KINAN7	G	KINANS
KINAN8	G	KINANS
KINANS	G	KINSIS
KINDR1	G	KINDRW KINONE

Notes on type of routine

- M : Main program
- G : GOCAD subroutine
- P : PLTPAK subroutine

TABLE E.1 CROSS REFERENCE BY CALLING ROUTINES (CONTINUED)

Routine	Type	Called by ...
KINDR2	G	KINDRW KINONE
KINDR3	G	KINDRW KINONE
KINDR4	G	KINDRW KINONE
KINDR5	G	KINDRW KINONE
KINDR6	G	KINDRW KINONE
KINDR7	G	KINDRW KINONE
KINDR8	G	KINDRW KINONE
KINDRW	G	KINSIS
KININP	G	KINSIS
KINITZ	P	CASDAM
KINONE	G	KINSIS
KINSIS	G	DATGEN
KINSYS	G	KINSIS
KIQCSZ	P	DOTTED SETPOS
KLNTYP	P	CASDAM DFLEX
KLOGUN	P	AFLEX ANALYS CALSLD CALSVS CASDAM COMPRS CONNEC DATINT DFLEX DISPL1 DISPL2 DRWDIS DRWINP DRWORI DRWSF FLXSIS FORSPR GENALL GENSEC HELLO KINANS KINDR1 KINDR2 KINDR3 KINDR4 KINDR5 KINDR6 KINDR7 KINDR8 KINDRW KININP KINSIS KINSYS LINDOT LINSLD LOOPS LOOPSS RESULT SECMAT SORTS STRSIS TYPEND TYPSYS WASSUM WREACT

Notes on type of routine

M : Main program
G : GOCAD subroutine
P : PLTPAK subroutine

TABLE E.1 CROSS REFERENCE BY CALLING ROUTINES (CONTINUED)

Routine	Type	Called by ...
KMARGN	P	AFLEX CASDAM CONNEC DATINT DISPL1 DISPL2 DRWDIS DRWSF FLXSIS FORSPR GENALL GENSEC HELLO KINSIS KINSYS LOOPS SECMAT SORTS TYPEND
KMOVAB	P	DISPL2 DOTTED DRWDIS DRWSF DRWSLD DRWSPR KINDR1 KINDR2 KINDR3 KINDR4 KINDR5 KINDR6 KINDR7 KINDR8 KINDRW KINSIS LINDOT LINSLD SETPOS
KMOVRL	P	DOTTED KINDR5 KINDR6 KINDR7 KINDR8 LINDOT LINSLD
KPAUSE	P	AFLEX CASDAM CONNEC DATINT DISPL1 DISPL2 DRWDIS DRWSF FLXSIS FORSPR GENALL GENSEC HELLO KINSIS KINSYS LOOPS SECMAT SORTS TYPEND
KPGRST	P	CASDAM
KPOLGN	P	DRWALL DRWDOT DRWEND DRWREV DRWSYS KINDR1 KINDR2 KINDR3 KINDR4 KINDR5 KINDR6 KINDR7 KINDR8 KINSYS
KRECT	P	DRWBOX KINDR1 KINDR2 KINDR3 KINDR4 KINDR5 KINDR6 KINDR7 KINDR8 KINSYS
KSETTL	P	CASDAM HELLO
KSTOP	P	CASDAM
KTXSIZ	P	CASDAM CONNEC DATINT DFLEX DISPL1 DISPL2 DOTTED DRWDIS DRWEND DRWINP DRWORI DRWSF FLXSIS FORSPR GENALL GENSEC HELLO KINDR1 KINDR2 KINDR3 KINDR4 KINDR5 KINDR6 KINDR7 KINDR8 KINDRW KINSIS KINSYS LOOPS RESULT SECMAT SORTS STRSIS TYPEND WASSUM WFHEAD WREACT
KVWPAR	P	KINDR1 KINDR2 KINDR3 KINDR4 KINDR5 KINDR6 KINDR7 KINDR8 SETWIN WINABS

Notes on type of routine

M : Main program
G : GOCAD subroutine
P : PLTPAK subroutine

TABLE E.1 CROSS REFERENCE BY CALLING ROUTINES (CONTINUED)

Routine	Type	Called by ...
KWRMOD	P	AFLEX CONNEC DATINT DFLEX DISPL1 DISPL2 DOTTED DRAWLP DRWALL DRWBOX DRWDIS DRWDOT DRWEND DRWINP DRWORI DRWREV DRWSF DRWSLD DRWSPR DRWSYS FLXSIS FORSPR GENALL GENSEC HELLO KINDR1 KINDR2 KINDR3 KINDR4 KINDR5 KINDR6 KINDR7 KINDR8 KINDRW KINONE KINSIS KINSYS LINDOT LINSLD LOOPS RESULT SECMAT SETPOS SETWIN SORTS STRSIS TYPEND WASSUM WFHEAD WINABS WREACT
KZERO	G	KINANS
LEAREQ	G	GETFIX GETFRE GETPIN GETSIM GETSLD INVERS
LIMANG	G	KINAN2 KINAN3 KINAN5 KINAN6 KINAN7 KINAN8
LINDOT	G	DATINT DFLEX DRWDOT
LINSLD	G	DATINT DFLEX DRAWLP DRWALL DRWSYS GENSEC KINSIS KINSYS LOOPS
LOOPS	G	DATGEN
LOOPSS	G	LOOPS
MBRAN	G	AGAIN ARIGID
MFIELD	G	ARIGID RFIELD STATE
MMASS	G	AGAIN ARIGID RSTATE STATE
MPOINT	G	AGAIN ARIGID RSTATE STATE
MRIGID	G	AGAIN ARIGID RSTATE STATE
MSPRNG	G	AGAIN ARIGID RSTATE STATE
MTRANS	G	AGAIN ANALYS ARIGID CALSLD CALSVS RSTATE SLIDE STARTS STATE WRTABS

Notes on type of routine

M : Main program
G : GOCAD subroutine
P : PLTPAK subroutine

TABLE E.1 CROSS REFERENCE BY CALLING ROUTINES (CONTINUED)

Routine	Type	Called by ...
MULT74	G	AGAIN ANALYS ARIGID SLIDE STARTS
PLATES	G	GENALL
PROP1	G	AGAIN ARIGID RESULT RSTATE STATE
RANGEL	G	DFLEX
RANGES	G	DRWDOT DRWSYS
READIN	G	FLXSIS RESULT
RESETC	G	AGAIN ARIGID
RESULT	G	SORTS
RFIELD	G	AGAIN RSTATE
RSTATE	G	AGAIN
SECMAT	G	DATINT
SETC	G	AGAIN ARIGID
SETING	G	AFLEX
SETPNT	G	RSTATE STATE
SETPOS	G	AFLEX CONNEC DATINT DFLEX DISPL1 DISPL2 DRWDIS DRWINP DRWORI DRWSF FLXSIS FORSPR GENALL GENSEC KINSIS LOOPS RESULT SECMAT SORTS TYPEND WASSUM WREACT
SETWIN	G	DFLEX DRAWLP DRWALL DRWDIS DRWDOT DRWEND DRWREV DRWSF DRWSLD DRWSPR DRWSYS KINSYS LINDOT LINSLD
SLIDE	G	AGAIN ARIGID

Notes on type of routine

M : Main program
G : GOCAD subroutine
P : PLTPAK subroutine

TABLE E.1 CROSS REFERENCE BY CALLING ROUTINES (CONTINUED)

Routine	Type	Called by ...
SORTS	G	CASDAM
STARTS	G	AGAIN ARIGID
STATE	G	ARIGID
STRSIS	G	RESULT
SUBLP1	G	TYLOOP
SUBLP2	G	SUBLP1
SUBLP3	G	SUBLP2
SUBLP4	G	SUBLP3
SUBLP5	G	SUBLP4
SUBLP6	G	SUBLP5
TENSON	G	RFIELD
TYLOOP	G	GENALL
TYPEND	G	DATGEN
TYPSYS	G	CASDAM
WASSUM	G	DFLEX
WBEND	G	SUBLP1 SUBLP2 SUBLP3 SUBLP4 SUBLP5 SUBLP6
WBRAN	G	SUBLP1 SUBLP2 SUBLP3 SUBLP4 SUBLP5 SUBLP6
WFHEAD	G	CALSF1 CALSF2 CASDAM KINANS RESULT WRTFLX WRTPRO
WFIELD	G	SUBLP1 SUBLP2 SUBLP3 SUBLP4 SUBLP5 SUBLP6 TYLOOP

Notes on type of routine

M : Main program
G : GOCAD subroutine
P : PLTPAK subroutine

TABLE E.1 CROSS REFERENCE BY CALLING ROUTINES (CONTINUED)

Routine	Type	Called by ...
WINABS	G	CASDAM DFLEX DISPL1 DISPL2 DRAWLP DRWALL DRWBOX DRWDIS DRWDOT DRWEND DRWINP DRWORI DRWREV DRWSF DRWSLD DRWSPR DRWSYS FLXSIS KINDR1 KINDR2 KINDR3 KINDR4 KINDR5 KINDR6 KINDR7 KINDR8 KINDRW KINONE KINSYS LINDOT LINSLD SETPOS SETWIN SORTS WASSUM WREACT
WMEND	G	TYLOOP
WMID	G	SUBLP1 SUBLP2 SUBLP3 SUBLP4 SUBLP5 SUBLP6 TYLOOP
WREACT	G	DISPL1 SORTS
WREV	G	SUBLP1 SUBLP2 SUBLP3 SUBLP4 SUBLP5 SUBLP6 TYLOOP
WRTABS	G	RSTATE
WRTANL	G	AFLEX
WRTDAT	G	GENALL
WRTFLX	G	RESULT
WRTPRO	G	RESULT
WRTSCR	G	WREACT
WSLIDE	G	SUBLP1 SUBLP2 SUBLP3 SUBLP4 SUBLP5 SUBLP6
WSPR	G	SUBLP1 SUBLP2 SUBLP3 SUBLP4 SUBLP5 SUBLP6 TYLOOP
WSTART	G	SUBLP1 SUBLP2 SUBLP3 SUBLP4 SUBLP5 SUBLP6 TYLOOP
ZERO	G	CASDAM

Notes on type of routine

M : Main program
G : GOCAD subroutine
P : PLTPAK subroutine

TABLE E.2 CROSS REFERENCE BY ROUTINES CALLED

Routine	Calls to ...
AFLEX	AGAIN ARIGID KDING KLOGUN KMARGN KPAUSE KWRMOD SETING SETPOS WRTANL
AGAIN	ANALYS JOINTS MBRAN MMASS MPOINT MRIGID MSPRNG MTRANS MULT74 PROP1 RESETC RFIELD RSTATE SETC SLIDE STARTS
ANALYS	GETFIX GETFRE GETPIN GETSIM GETSLD KLOGUN MTRANS MULT74
ARIGID	ANALYS JOINTS MBRAN MFIELD MMASS MPOINT MRIGID MSPRNG MTRANS MULT74 PROP1 RESETC SETC SLIDE STARTS STATE
CALSF1	WFHEAD
CALSF2	WFHEAD
CALSLD	KLOGUN MTRANS
CALSVS	KLOGUN MTRANS
CASDAM	DATGEN FLXSIS HELLO KINITZ KLNTYP KLOGUN KMARGN KPAUSE KPGRST KSETTL KSTOP KTXSIZ SORTS TYPSYS WFHEAD WINABS ZERO
COMPRS	KLOGUN
CONNEC	DRWSYS KLOGUN KMARGN KPAUSE KTXSIZ KWRMOD SETPOS
DATGEN	DATINT FORSPR GENALL KINSIS LOOPS TYPEND
DATINT	DRWBOX FINDPT GENSEC KLOGUN KMARGN KPAUSE KTXSIZ KWRMOD LINDOT LINSLD SECMAT SETPOS
DFLEX	DRANGE DRWBOX DRWEND DRWSPR KLNTYP KLOGUN KTXSIZ KWRMOD LINDOT LINSLD RANGEL SETPOS SETWIN WASSUM WINABS
DISPL1	DFLEX DRWINP KLOGUN KMARGN KPAUSE KTXSIZ KWRMOD SETPOS WINABS WREACT
DISPL2	KGRAPH KLOGUN KMARGN KMOVAB KPAUSE KTXSIZ KWRMOD SETPOS WINABS

TABLE E.2 CROSS REFERENCE BY ROUTINES CALLED (CONTINUED)

Routine	Calls to ...
DOTTED	KDRWRL KIQCSZ KMOVAB KMOVRL KTXSIZ KWRMOD
DRAWLP	DRWBOX DRWEND KWRMOD LINSLD SETWIN WINABS
DRWALL	DRANGE DRWBOX DRWEND DRWREV DRWSLD DRWSPR KPOLGN KWRMOD LINSLD SETWIN WINABS
DRWBOX	KRECT KWRMOD WINABS
DRWDIS	DRWALL KLOGUN KMARGN KMOVAB KPAUSE KTXSIZ KWRMOD SETPOS SETWIN WINABS
DRWDOT	DRWBOX DRWEND DRWREV DRWSLD DRWSPR KPOLGN KWRMOD LINDOT RANGES SETWIN WINABS
DRWEND	KBUSH KPOLGN KTXSIZ KWRMOD SETWIN WINABS
DRWINP	DRWALL KLOGUN KTXSIZ KWRMOD SETPOS WINABS
DRWORI	DRWALL KLOGUN KTXSIZ KWRMOD SETPOS WINABS
DRWREV	KPOLGN KWRMOD SETWIN WINABS
DRWSF	DRWALL KLOGUN KMARGN KMOVAB KPAUSE KTXSIZ KWRMOD SETPOS SETWIN WINABS
DRWSLD	KDRWAB KMOVAB KWRMOD SETWIN WINABS
DRWSPR	KBUSH KDRWAB KDRWRL KMOVAB KWRMOD SETWIN WINABS
DRWSYS	DRWBOX DRWEND DRWREV DRWSLD DRWSPR KPOLGN KWRMOD LINSLD RANGES SETWIN WINABS
FLXSIS	AFLEX DRWALL KDING KLOGUN KMARGN KPAUSE KTXSIZ KWRMOD READIN SETPOS WINABS
FORSPR	DRWSYS KLOGUN KMARGN KPAUSE KTXSIZ KWRMOD SETPOS
GENALL	DRWSYS KDING KLOGUN KMARGN KPAUSE KTXSIZ KWRMOD PLATES SETPOS TYLOOP WRTDAT
GENSEC	DRWDOT KLOGUN KMARGN KPAUSE KTXSIZ KWRMOD LINSLD SETPOS
GETFIX	LEAREQ

TABLE E.2 CROSS REFERENCE BY ROUTINES CALLED (CONTINUED)

Routine	Calls to ...
GETFRE	LEAREQ
GETPIN	LEAREQ
GETSIM	LEAREQ
GETSLD	LEAREQ
HELLO	KDING KLOGUN KMARGN KPAUSE KSETTL KTXSIZ KWRMOD
INVERS	LEAREQ
KINAN2	LIMANG
KINAN3	LIMANG
KINAN5	LIMANG
KINAN6	LIMANG
KINAN7	LIMANG
KINAN8	LIMANG
KINANS	KINAN1 KINAN2 KINAN3 KINAN4 KINAN5 KINAN6 KINAN7 KINAN8 KLOGUN KZERO WFHEAD
KINDR1	DOTTED KBUSH KDRWAB KLOGUN KMOVAB KPOLGN KRECT KTXSIZ KVWPAR KWRMOD WINABS
KINDR2	DOTTED KBUSH KDRWAB KLOGUN KMOVAB KPOLGN KRECT KTXSIZ KVWPAR KWRMOD WINABS
KINDR3	DOTTED KBUSH KDRWAB KLOGUN KMOVAB KPOLGN KRECT KTXSIZ KVWPAR KWRMOD WINABS
KINDR4	DOTTED KDRWAB KLOGUN KMOVAB KPOLGN KRECT KTXSIZ KVWPAR KWRMOD WINABS
KINDR5	DOTTED KBUSH KDRWAB KDRWRL KLOGUN KMOVAB KMOVRL KPOLGN KRECT KTXSIZ KVWPAR KWRMOD WINABS
KINDR6	DOTTED KBUSH KDRWAB KDRWRL KLOGUN KMOVAB KMOVRL KPOLGN KRECT KTXSIZ KVWPAR KWRMOD WINABS

TABLE E.2 CROSS REFERENCE BY ROUTINES CALLED (CONTINUED)

Routine	Calls to ...
KINDR7	DOTTED KBUSH KDRWAB KDRWRL KLOGUN KMOVAB KMOVRL KPOLGN KRECT KTXSIZ KVWPAR KWRMOD WINABS
KINDR8	DOTTED KBUSH KDRWAB KDRWRL KLOGUN KMOVAB KMOVRL KPOLGN KRECT KTXSIZ KVWPAR KWRMOD WINABS
KINDRW	KINDR1 KINDR2 KINDR3 KINDR4 KINDR5 KINDR6 KINDR7 KINDR8 KLOGUN KMOVAB KTXSIZ KWRMOD WINABS
KININP	KLOGUN
KINONE	KINDR1 KINDR2 KINDR3 KINDR4 KINDR5 KINDR6 KINDR7 KINDR8 KWRMOD WINABS
KINSIS	DRWDOT KDING KINANS KINDRW KININP KINONE KINSYS KLOGUN KMARGN KMOVAB KPAUSE KTXSIZ KWRMOD LINSLD SETPOS
KINSYS	DRWEND DRWREV DRWSLD DRWSPR KLOGUN KMARGN KPAUSE KPOLGN KRECT KTXSIZ KWRMOD LINSLD SETWIN WINABS
LINDOT	KDRWRL KLOGUN KMOVAB KMOVRL KWRMOD SETWIN WINABS
LINSLD	KDRWAB KLOGUN KMOVAB KMOVRL KWRMOD SETWIN WINABS
LOOPS	CONNEC DRAWLP DRWDOT DRWREV DRWSLD KLOGUN KMARGN KPAUSE KTXSIZ KWRMOD LINSLD LOOPSS SETPOS
LOOPSS	KLOGUN
MBRAN	INVERS
READIN	DZERO
RESULT	DRWORI KDING KLOGUN KTXSIZ KWRMOD PROP1 READIN SETPOS STRSIS WFHEAD WRTFLX WRTPRO
RFIELD	COMPRS MFIELD TENSON
RSTATE	CALSLD CALSVE CALSVS MMASS MPOINT MRIGID MSPRNG MTRANS PROP1 RFIELD SETPNT WRTABS
SECMAT	DRWSYS KLOGUN KMARGN KPAUSE KTXSIZ KWRMOD SETPOS
SETPOS	KIQCSZ KMOVAB KWRMOD WINABS

TABLE E.2 CROSS REFERENCE BY ROUTINES CALLED (CONTINUED)

Routine	Calls to ...
SETWIN	KVWPAR KWRMOD WINABS
SLIDE	MTRANS MULT74
SORTS	DFLEX DISPL1 DISPL2 DRWDIS DRWORI DRWSF KLOGUN KMARGN KPAUSE KTXSIZ KWRMOD RESULT SETPOS WINABS WREACT
STARTS	MTRANS MULT74
STATE	CALSLD CALSVE CALSVS MFIELD MMASS MPOINT MRIGID MSPRNG MTRANS PROP1 SETPNT
STRSIS	CALSF1 CALSF2 KLOGUN KTXSIZ KWRMOD
SUBLP1	SUBLP2 WBEND WBRAN WFIELD WMID WREV WSLIDE WSPR WSTART
SUBLP2	SUBLP3 WBEND WBRAN WFIELD WMID WREV WSLIDE WSPR WSTART
SUBLP3	SUBLP4 WBEND WBRAN WFIELD WMID WREV WSLIDE WSPR WSTART
SUBLP4	SUBLP5 WBEND WBRAN WFIELD WMID WREV WSLIDE WSPR WSTART
SUBLP5	SUBLP6 WBEND WBRAN WFIELD WMID WREV WSLIDE WSPR WSTART
SUBLP6	WBEND WBRAN WFIELD WMID WREV WSLIDE WSPR WSTART
TYLOOP	SUBLP1 WFIELD WMEND WMID WREV WSPR WSTART
TYPEND	DRWEND DRWSYS KLOGUN KMARGN KPAUSE KTXSIZ KWRMOD SETPOS
TYPSYS	KLOGUN
WASSUM	KLOGUN KTXSIZ KWRMOD SETPOS WINABS
WFHEAD	KTXSIZ KWRMOD
WINABS	KVWPAR KWRMOD

TABLE E.2 CROSS REFERENCE BY ROUTINES CALLED (CONTINUED)

Routine	Calls to ...
WREACT	KLOGUN KTXSIZ KWRMOD SETPOS WINABS WRTSCR
WRTABS	MTRANS
WRTFLX	WFHEAD
WRTPRO	WFHEAD

TABLE E.3 Storage Requirements for the Main Module

MODULE NAME	BYTES
CASDAM	1050
AFLEX	70450
AGAIN	72127
ANALYS	2758
ARIGID	49638
CALSF1	2467
CALSF2	109260
CALSLD	3876
CALSVE	638
CALSVS	3940
COMPRS	814
CONNEC	4987
DATINT	18020
DATGEN	17743
DFLEX	16755
DISPL1	143047
DISPL2	110189
DOTTED	358
DRANGE	9486
DRAWLP	2986
DRWALL	13975

TABLE E.3 Storage Requirements for the Main Module (Continued)

MODULE NAME	BYTES
DRWBOX	194
DRWDIS	64648
DRWDOT	3575
DRWEND	485
DRWINP	62128
DRWORI	13666
DRWREV	174
DRWSLD	251
DRWSF	64960
DRWSPR	944
DRWSYS	3575
DZERO	48432
FINDPT	290
FLXSIS	46226
FORSPR	6254
GENALL	19506
GENSEC	14110
GETFIX	317
GETFRE	314
GETPIN	325
GETSIM	326
GETSLD	326
HELLO	3010
INVERS	610
JOINTS	1298
KINAN1	15312
KINAN2	14205
KINAN3	14673
KINAN4	13529
KINAN5	15685
KINAN6	15065
KINAN7	15977
KINAN8	15345
KINANS	20393
KINDR1	624
KINDR2	773
KINDR3	706
KINDR4	765
KINDR5	1141
KINDR6	1034
KINDR7	1154

TABLE E.3 Storage Requirements for the Main Module (Continued)

MODULE NAME	BYTES
KINDR8	1017
KINDRW	426
KININP	1028
KINONE	219
KINSIS	16143
KINSYS	4955
KZERO	3375
LEAREQ	1322
LIMANG	145
LINDOT	645
LINSLD	405
LOOPS	19195
LOOPSS	1637
MBRAN	2191
MFIELD	566
MMASS	104
MPOINT	104
MRIGID	172
MSPRNG	10074
MTRANS	171
MULT74	422
PLATES	15251
PROP1	7307
RANGEL	11147
RANGES	2074
READIN	36344
RESULT	34129
SECMAT	17005
SETC	2339
SETING	25023
SETPNT	553
SETPOS	100
SETWIN	303
SLIDE	1715
SORTS	194676
STARTS	627
STATE	50290
STRSIS	571
SUBLP1	18637
SUBLP2	18637
SUBLP3	18637

TABLE E.3 Storage Requirements for the Main Module (Continued)

MODULE NAME	BYTES
SUBLP4	18637
SUBLP5	18637
SUBLP6	18597
TENSON	818
TYLOOP	18893
TYPEND	6135
TYPSYS	1132
RESETC	2339
RFIELD	295
RSTATE	61428
WASSUM	251
WBEND	4019
WBRAN	1149
WFHEAD	2660
WFIELD	16932
WINABS	72
WMEND	4221
WMID	2784
WREACT	22366
WREV	2190
WRTABS	1013
WRTANL	432
WRTDAT	2423
WRTFLX	16979
WRTPRO	577
WRTSCR	155
WSPR	3210
WSLIDE	4706
WSTART	2368
ZERO	16409

TABLE E.4 Storage Requirements for the Library Module

MODULE NAME	BYTES
KBUSH	742
KDING	64
KDRWAB	361
KDRWRL	185
KGRAPH	4901
KINITZ	2007
KIQCSZ	273
KIQLTY	137
KIQMAG	27
KIQROT	27
KIQTMD	196
KIQTRT	135
KIQTSZ	135
KIQVWP	147
KIQWIN	147
KLNIDX	1137
KLNTYP	162
KLOGUN	11
KMAGFY	27
KMAPID	1060
KMARGN	2455
KMOVAB	271
KMOVCA	342
KMOVRL	185
KPAUSE	580
KPBUFF	80241
KPGRST	530
KPLOT	2554
KPOLGN	286
KPSTMV	90
KRECT	229
KROTAT	190
KSCALE	1345
KSELTM	5456
KSETTL	175

TABLE E.4 Storage Requirements for the Library Module (Continued)

MODULE NAME	BYTES
KSTART	184
KSTOP	237
KTEXT	1827
KTIME	1485
KTMCTL	268
KTXMOD	205
KTXMRG	143
KTXROT	408
KTXSIZ	785
KVWPAR	245
KVWPRT	729
KWINDO	729
KWRMOD	104
KYES	22
KALFNM	1580
KAXIS	3871
KBGIDX	1054
KCHARC	1066
KCLEAR	1915
KCLIPW	878
KCVCHR	691
KDATE	189
KDRWCA	350
KFINSH	86
KFORMT	2186
KGRID	264
KINCHG	208
KINICO	1863
KIQEQP	294
KLEXDT	30
KLINFD	637
KMAPTB	2222
KMKPLT	2075
KNO	22
KPGTCH	51
KPGTDR	96
KPGTMV	83
KPGTRT	51
KPGTSZ	51
KPGTTY	264
KPLCTL	148

TABLE E.4 Storage Requirements for the Library Module (Continued)

MODULE NAME	BYTES
KPLT10	4787
KPLT21	1456
KPSTCH	55
KPSTDR	100
KPSTRT	55
KPSTSZ	55
KREGIS	1743
KUPDAT	64
KXANMD	285
KXBELL	295
KXCHAR	334
KXCHSZ	412
KXCWSD	305
KXDRWA	351
KXDSHA	306
KXERAS	68
KXFINT	59
KXINIT	358
KXIOWT	48
KXMOVA	292
KXNWLN	17
KXNWPG	370
KXOUT	42
KXOUTS	342
KXPNTA	301
KXRECV	392
KXREST	536
KXSCUR	452
KXSTBF	336
KXTERM	282
KXTKDH	1245
KXTKPT	333
KXTSND	37
KXVCMD	339
KXWAIT	152
KXXYCV	682
KCHDAT	6210
KDCBGN	783
KDCCHR	117
KDCDMP	267
KDCDNG	57

TABLE E.4 Storage Requirements for the Library Module (Continued)

MODULE NAME	BYTES
KDCDRW	422
KDCDSH	279
KDCERS	142
KDCLOC	567
KDCMOV	422
KDCOUT	714
KDCPNT	80
KDCSTP	71
KDCWRT	503
KKCLPF	869
KKCSZA	950
KKDRAW	907
KKDSLN	1492
KKLIMT	1401
KKLOCT	1029
KKMOVE	907
KKMPUU	986
KKNMP	996
KKNPEN	970
KKPLOF	960
KKPLON	904
KKPLT	2100
KKPLTS	2672
KKPUMU	929
KKSTIN	870
KKSTUU	870
KKSYMB	2154
KKWHER	923
KOUTKI	239
KREAD	203
KXAFMD	305
KXBFPK	1598
KXCRTN	343
KXDSHM	387
KXINS	790
KXLINF	375
KXPLCH	580
KXPNTM	332
KXQSUB	23
KDCINC	102
KKADRW	949

TABLE E.4 Storage Requirements for the Library Module (Continued)

MODULE NAME	BYTES
KKAGP	1151
KKAMOV	942
KKARTL	977
KKAXY	1463
KKCDIR	1004
KKCFNT	1063
KKCHNG	969
KKCLP	1086
KKCLPR	1354
KKCPLT	976
KKCSZ	1256
KKDATO	973
KKDELT	1057
KKGUPU	927
KKHPOU	164
KKHSHK	1316
KKINPU	927
KKIPL1	1401
KKLBOF	918
KKLBTM	1043
KKMUPU	929
KKOUC1	1113
KKOUE	1155
KKOUR1	1091
KKOUR3	1113
KKOUR4	1145
KKPDIR	1004
KKPNSP	997
KKPNUP	870
KKPUUN	969
KKUUPU	987
KXADIN	187
KXADOU	372
KKANG	1272
KKHPIN	189
KKIDRW	947
KKIMOV	948
KKIXY	1210
KKPUGU	927
KKPUIN	929
KKPUUU	987

TABLE E.5 Image Synopsis

Virtual memory allocated:	(660480. bytes, 1290. pages)
Number of files:	8.
Number of modules:	336.
Number of program sections:	84.
Number of global symbols:	1082.
Number of image sections:	20.
User transfer address:	00081C00
Debugger transfer address:	7FFEDF68
Number of code references to shareable images:	56.
Image type:	EXECUTABLE.